Rhenium, osmium and nitrogen uptake in Phaephyceae macroalgae, Fucus vesiculosus

RACIONERO-GOMEZ, BLANCA

Rhenium, osmium and nitrogen uptake in Phaephyceae macroalgae, *Fucus vesiculosus*

- Rhenium uptake and distribution in Phaephyceae macroalgae, *Fucus vesiculosus*
- Osmium uptake, distribution and isotope composition in Phaephyceae macroalgae, *Fucus vesiculosus*: implications for determining the Os isotope composition of seawater
- Nitrogen uptake in Phaeophyceae macroalgae, *Fucus vesiculosus*. An understanding of ^{15}N isotope changes due to different nitrogen sources in River Tees and Staithes

Blanca Racionero Gómez

Masters Research in Geology
Earth Sciences Department, May 2016

A story has no beginning or end; arbitrarily one chooses that moment of experience from which to look back or from which to look ahead. – Graham Greene, The End of the Affair (1951)

Masters Research in Geology, Department of Earth Sciences, Durham University (U.K.)

LaTEX template

This research was done under the supervision of Dr. Chris Hugh Greenwell and Darren Gröcke with the financial support of OEA Labs Ltd.

First release, May 2016

Abstract

Despite rhenium (Re) and osmium (Os) having no known biological role, living macroalgae concentrate Re and Os. Moreover, macroalgae nitrogen isotopes (δ^{15}N) are a powerful tool for monitoring water eutrophication, sewage influence and pollution. This study utilizes *Fucus* sp., brown macroalgae (Phaephyceae) to assess, on the one hand, Re and Os localization and uptake in the macroalgae biomass and, on the other hand, to understand the source of N of the river Tees and Staithes. The current study demonstrates that Os is evenly distributed within the macroalgae, but Re concentration varies within macroalgae structures. The uptake and tolerance of Re and Os was evaluated *via Fucus* sp. cultures grown in seawater of different Re or Os concentrations. A positive correlation between Re or Os concentration in doped seawater and the abundance of Re or Os accumulated in the tips of the macroalgae is shown. Moreover, it was observed that metabolically inactivated *Fucus* sp. does not accumulate Re in oxic conditions, indicating that Re uptake is *via* syn-life bioadsorption/bioaccumulation. Thus, macroalgae may provide a source for Re phytomining and/or bioremediation. Furthermore, the strong correlation of Os isotopic composition in *Fucus* sp. and in the culture medium, strongly confirms the possible use of macroalgae as a biological proxy for the Os isotopic composition of seawater. The source of N in the River Tees and Staithes was evaluated via *in situ* and *ex situ* tip cultures. *Ex situ* cultures were performed in seawater with different nitrate or ammonia concentrations and show a positive relation between the δ^{15}N of macroalgae and the δ^{15}N of the seawater doped. Therefore, a confirmation of the usefulness of *Fucus* sp. as an eutrophication or pollutant tracker is achieved. Thus, deciphering that River Tees most probable source of N is NO_3^- from chemical plants nearby and Staithes most probable source of N is sewage waste.

Contents

Acknowledgements

I would really like to express my gratitude to Durham University for offering the facilities required for these studies and to OEA (organic elemental analysis) Labs Ltd and Durham University for the funding of the project and scholarship.

I would really like to thank my supervisors, Prof. Chris Greenwell and Prof. Darren Gröcke for their guidance and advice in this project.

Many thanks to Prof. David Selby and Adam Sproson, for their support, advice, guidance, help and demonstrations of Re-Os procedures and TritonX MS. Thanks also to Dr Joanna Hesselink, Dr Chris Ottley and Dr Emily Unsworth for their help with the ICP-MS. Special thanks also to Dr Hilary Redden, for her support, and key advice. Thanks to Prof. Nigel Robinson and Dr Carl Patterson for his help with the protein extraction.

I am very grateful to Emma Kate Prout, Josie Mahony, Jack Rowbotham, Rikan Kareem, Munira Raji, Dr Valentina Erastova, Ali Riza, Dr Mussarrat Mohammed, Tom Underwood and Dr Manohara Gudiyor-Veerabhadr for making a nice and happy environment to work.

Thanks to all the people I had around me during these years and have helped to create the right atmosphere for me to feel at home.

Finally, I would like to acknowledge my relatives and close individuals for their support and help.

1. Introduction

The current thesis investigates the uptake of rhenium (Re), osmium (Os) and nitrogen (N) by *Fucus* sp. macroalgae. This section introduces key issues for the understanding of the subsequent chapters. The elements and specific macroalgae under study as well as the different mechanisms and functional groups that could be involved in metal binding and the factors affecting heavy metal binding are detailed here. Moreover, a brief review of the current knowledge of Re, Os and N uptake and accumulation by macroalgae is also provided. And finally, the instruments used to study the elements concentrations and ratios as well as the general structure of the thesis are explained in this section.

It is important to notice that all the concentrations are expressed in ppb and ppt, when the concentrations refer to a solution (i.e. seawater or river water), ppb corresponds to μg/L and ppt corresponds to ng/L, whereas when the concentrations refer to a solid (i.e. macroalgae or rock), ppb corresponds to μg/kg and ppt to ng/kg.

1.1 Research general objectives

As previously said, the current project seeks to examine how and where macroalgae store Re and Os, as well as assess the usefulness of δ^{15}N measurements in macroalgae as an eutrophication and pollution recorder. The experimental work has five specific objectives:

1. To culture *F. vesiculosus* in the presence of different concentrations of Re(VII) (Re metal in HNO_3 ($HReO_4$), Sodium perrhenate ($NaReO_4$), Ammonium perrhenate (NH_4ReO_4) and potassium perrhenate ($KReO_4$)), Os (DROsS (Durham Romil Osmium Standard)), nitrate and ammonia.

Using this approach will help to establish:

- *The limit on uptake of the metals.*

- *The form which Re and Os are taken up (nanoparticle, chelates etc).*
- *The isotopic change in N.*

2. To culture *F. vesiculosus* in the presence of different concentrations of Re and changing conditions, such as; different phosphate concentrations, light intensities (without light, medium and high light), pH (7, 8 and 9), salinities (25%, 50%, 75% and 100%), previously heated at 100 °C, 30 °C dried and frozen with nitrogen liquid.

Using this approach will help to gain knowledge on:

- *The uptake mechanism of Re (i.e. bioaccumulation or bioadsorption).*
- *The factors affecting the uptake mechanism.*

3. To separate the macroalgae into different parts: holdfast, stipe, fertile tips, non-fertile tips, leaves, veins and blades.

Using this approach will help to establish:

- *The location and relative concentrations of Re and Os within macroalgae parts.*

4. To divide and separate the macroalgae cells from macroalgae sub-parts (i.e. alginate, mitochondria, chloroplasts and others) that exhibit higher concentrations (from Obj. 3).

Using this approach will help to establish:

- *The location of Re and Os within the cells.*

5. To culture *in vivo Fucus* species at different sites of in the river Tees while looking at the height in the water column.

Using this approach will help to establish:

- *The source of nitrogen in the river.*
- *The usefulness of $\delta^{15}N$ measurements in macroalgae as an eutrophication recorder (i.e., pollution).*
- *The differences in $\delta^{15}N$ of macroalgae growing at different tidal levels (e.g., high tide versus low tide).*

1.2 Elements under investigation

1.2.1 Rhenium

Rhenium is a silvery metallic element in Group 7 of the periodic table. Re is rarely encountered in the environment owing to its scarceness of 1 part per billion (ppb) on Earth (Wedepohl, 1995). Discovered by Ida Tacke-Noddack and Otto Carl Berg in 1925, in the minerals columbite, gadolinite and molybdenite (Loren, 1933), Re has an atomic number of 75 and two naturally occurring isotopes,

^{185}Re and ^{187}Re, with 37.4% and 62.6% of abundance respectively. Re shows a wide variety of oxidation states, ranging from -1 to +7 and it is similar chemically to technetium, a radioactive element. Re and Tc are so similar chemically that Re is often used as a proxy for ^{99}Tc.

Re is an important component in super alloys for jet turbine engines and is also used as a catalyst for petroleum-reforming (Survey, 2010). Furthermore, within oil exploration, Re and osmium are used as petroleum geochronometers to date crude oil generation from source rocks (Cohen *et al.*, 1999; Lillis and Selby, 2013). In addition, Re is now being studied in medicine to be used for treatments of liver cancer (Sundram *et al.*, 2004). Re has been shown to react with the nucleus of tumoral cells but not the benignal cells (Collery *et al.*, 2014).

Re does not occur in isolation, but exists always as pegmatites, molybdenites and rocks altered by pneumatolysis (Sutulov, 1967). The behaviour of Re in seawater is marked by the low reactivity (i.e. low interaction with other reactants) of the perrhenate ion (ReO_4^-), which is the only significant Re species found in ocean waters (Koide *et al.*, 1986). The concentration of Re in the open ocean (0.0074–0.009 ppb; parts per billion; Anbar *et al.* (1992); Helz and Dolor (2012)) is slightly higher compared to that of rivers (~0.005 ppt; Miller *et al.* (2011)) and much lower compared to terrestrial environments (continental crust values of 0.2-2 ppb; organic-rich sedimentary rocks values 0.2–100 ppb; Selby and Creaser (2003) and references therein) and sulphide minerals (low ppb to hundreds of ppm; Stein (2014) and references therein).

1.2.2 Osmium

Osmium is a transition metallic element in Group 8 of the periodic table with the atomic number 76. Os and iridium were discovered at the same time by the chemist Smithson Tennant in 1803 (Venetskii, 1974). Os is the densest and least abundant stable naturally occurring element, with an average mass fraction of 50 parts per trillion (ppt) on Earth crust (Wedepohl, 1995). Os shows a wide variety of oxidation states, ranging from -2 to +8, and has six stable naturally occurring isotopes; ^{184}Os, ^{187}Os, ^{188}Os, ^{189}Os, ^{190}Os with the most abundant being ^{192}Os.

Os alloys with platinum and iridium have many applications, such as pen tips or electrical contacts (Cramer and Covino, 2005). Moreover, Os tetroxide (OsO_4) is used for Transmission Electron Microscopy (TEM) fixation and staining (Hayat, 2000), for fingerprint detection (MacDonell, 1960) and for the treatment of arthritis (H. Sheppeard and Ward, 1980).

Os exists in natural alloys, mainly iridium-osmium alloys although it can also be found in nature as an uncombined element (Emsley, 2011). Os in seawater has been shown to exhibit both conservative and non-conservative behaviour (Chen and Sharma, 2009; Gannoun and Burton, 2014), with the present day seawater Os isotope (^{187}Os/^{188}Os) composition inferred to reflect Earth surface processes, i.e. the balance of inputs from radiogenic continental-derived and unradiogenic mantle-derived sources (Peucker-Ehrenbrink and Ravizza, 2000; Cohen *et al.*, 2003; Banner, 2004). Thermodynamic

data predict that Os in seawater likely exists as the species; $OsO_4{}^0$, $HOsO_5$ and H_3-OsO_6 (Palmer *et al.*, 1988; Yamashita *et al.*, 2007), with all speciated forms present in the highest oxidation state available to Os. However, chloride complexing is also possible ($OsCl_6$, Cotton and Wilkinson, 1988), and it has also been suggested that Os exists as an organo-complex (Levasseur *et al.*, 1998). The concentration of Os in seawater is of 0.01 ppt (Sharma *et al.*, 1997; Levasseur *et al.*, 1998;Chen and Sharma, 2009; Gannoun and Burton, 2014), similar to that of rivers (values of 84 – 3 ppq (Chen *et al.*, 2006; Sharma and Wasserburg, 1997) and much lower compared to that of terrestrial environments (upper continental crust osmium concentration of 30-50 ppt and terrigenous sediments of 15–90 ppt (Esser and Turekian, 1993; Wedepohl, 1995; Peucker-Ehrenbrink and Jahn, 2001).

1.2.3 Technetium

Technetium (Tc) is a radioactive element. Re has been used as a Tc surrogate as they are very similar chemically (Harvey *et al.*, 1991; Lide, 2000). The common oxidation states of Tc range from 0 to +7, and has three isotopes; ^{97}Tc, ^{98}Tc and ^{99}Tc.

^{99}Tc isotope is widely used for medical diagnostic studies (Emsley, 2001) and in concentrations of about 5 ppm it acts as an inhibitor of corrosion (Cartlege, 1955).

Almost all Tc is synthetically produced, although very small amounts can be produced in uranium and molybdenum ores as a spontaneous fission product (Kenna and Kuroda, 1964) or by neutron capture (Robson, 1974) respectively. Under oxidizing aqueous conditions Tc(VII) will exist as pertechnetate ion (TcO_4^-) which is considered one of the most mobile radionuclides in the environment (Wildung *et al.*, 2004).

1.2.4 Nitrogen

Nitrogen is a chemical element in Group 15 of the periodic table with the atomic number 7. N is a very abundant element on Earth (~78% of Earth atmosphere). It was formally discovered before Re and Os, in 1772 by Daniel Rutherford (Elvira, 1932). N shows a large variety of oxidation states, ranging from -3 to +5, and has two stable naturally occurring isotopes; ^{14}N and ^{15}N, being ^{14}N, by far, the most abundant (i.e. 99.6%). However, N concentration and composition can change depending on the metabolic routes that the molecule follows. To express the isotopic ratios of natural substances, a delta notation is used (Robinson, 2001):

$$\delta\ ^{15}\mathrm{N}\ ‰ = (\mathrm{R}_{sample}{:}\mathrm{R}_{standard} - 1) \times 1000$$

R is the relation between the light and heavy isotopes (i.e. ^{14}N: ^{15}N) of a substance. The standard is atmospheric dinitrogen (N_2), which has $\delta\ ^{15}$N of 0‰. Both biological cycles and water/rock reactions often change isotopic ratios of N.

N exists in many different forms such as ammonia, organic nitrates, cyanides or nitric acid,

and is found many industrially important compounds (i.e. fertilizers, antibiotics, drugs and others). Moreover, N occurs in all organisms in nucleic acids (RNA and DNA), in amino acids (proteins) and in the energy transfer molecule (ATP; adenosine triphosphate).

All organic and inorganic forms of N undergo many different transformations in the ecosystem (i.e. N cycle) (Bernhard, 2010). The major transformations of N are represented in Figure 1.1: nitrification, N fixation, denitrification, anammox and ammonification. Human activities, such as making fertilizers and burning fossil fuels, have significantly altered the amount of fixed nitrogen in the Earth's ecosystems, thus organisms living in them have been affected.

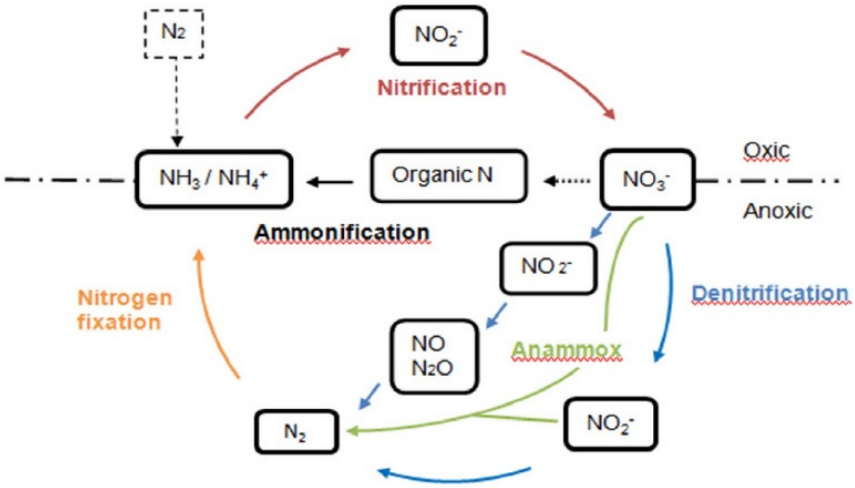

Figure 1.1 Representation of the major transformations in the nitrogen cycle. Modified after Bernhard (2010).

1.3 Brown macroalgae (Phaeophyceae)

Macroalgae (seaweeds) are plant-like organisms generally marine and attached to rocks of coastal areas. They belong to three different phyla: brown, red and green algae (Guiry, 2000).

Brown macroalgae (Phaeophyceae) contain about 265 genera, around 2200 species and have the most complex and largest members of the algae division, there are no unicellular representatives found (Guiry, 2000). The brown colour of these macroalgae results from the dominance of the carotenoid fucoxanthin in their chloroplasts, which masks the other pigments (i.e. chlorophyll a and c, β-carotene and other xanthophylls) (Guiry, 2000). Brown macroalgae appear in sub-polar to temperate regions.

Phaeophyceae division is subdivided into 13 orders which are divided into families and subse-

quently divided to genus and species (Graham and Wilcox, 2000).

The complete body of the macroalgae is known as the thallus. Its main parts are; the holdfast, which holds the algae to the surface, the stipe and the blades or fronds, which are the principal locations of nutrient uptake and photosynthesis. Figure 1.2 illustrates the different structures that a macroalgae has.

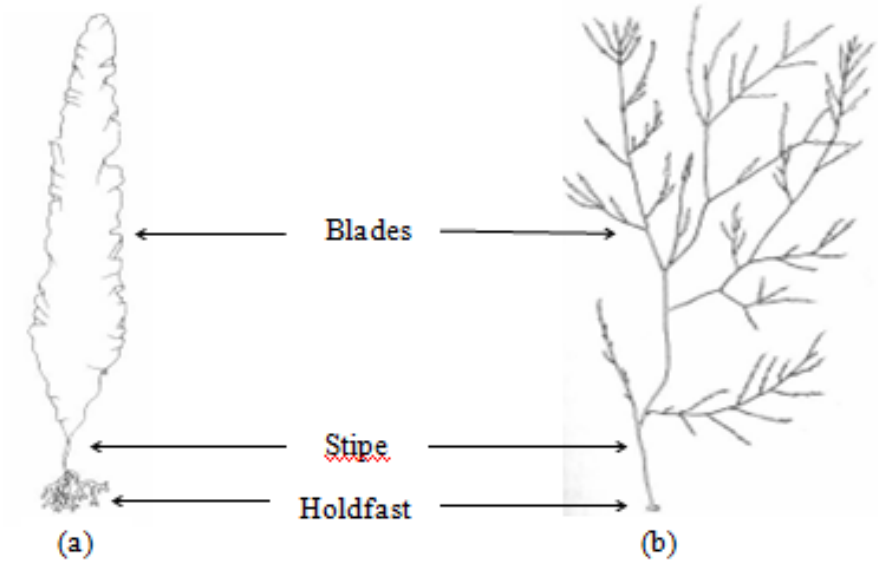

Figure 1.2 Brown macroalgae structure representation of two species; a) Laminaria b) Desmarestia (Bold and Wynne, 1986).

A typical algal cell is detailed in Figure 1.3. Depending on the genus, there may be from one to many plastids (P) in each cell. The most common plastid structure is the chloroplast, which stores energy and food material and contains chlorophyll a, c1 and c2. Chloroplasts have three thylakoids (an interconnected set of disc-like sacs) per band and are enclosed into an envelope surrounded by two membranes that interconnect with the membranes of pirenoids, which are responsible for CO_2 fixation (Markey and Wilce, 1975).

The physodes (Ps) are inclusions of uncertain constitution and function. Production and secretion of the polysaccharides take place in the golgi bodies (G). Vacuoles (V) are the organelles responsible for storage and transport of various macromolecules within and to the exterior of the cell. The principal function of mitochondria (M) is cellular respiration and they are bounded by a double membrane. Nucleus (N) function is to control the genetic expression and cellular division as it contains almost all the DNA (DNA is also found in mitochondria and chloroplasts). Finally, cells are interconnected by plasmodesma pit fields (pores) (F).

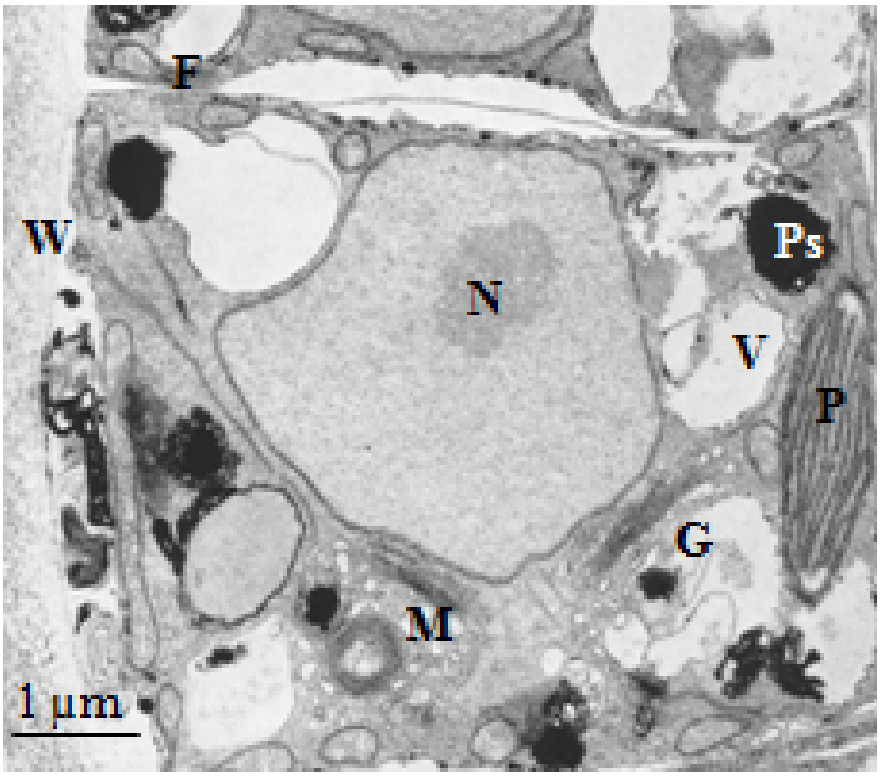

Figure 1.3 Ultrastructural features of a Brown macroalgae which includes; irregular electron-opaque structures that contain tannins, known as physodes (Ps), the nucleus (N), golgi bodies (G), vacuoles (V), mitochondria (M), cell wall (W) and plastids (mainly Chloroplasts) (P) (Markey and Wilce, 1975).

The cell wall structure is comprised of two different layers: an amorphous embedding matrix and a fibrillar skeleton, it is illustrated in Figure 1.4.

1.3.1 *Fucus vesiculosus*

Fucus vesiculosus is a common brown macroalgae of the order *Fucales*, family *Fucaceae* (Figure 5) found along sheltered shores of the North Sea, Baltic Sea, Atlantic and Pacific Ocean.

F. vesiculosus is a tethered macroalgae with air bladders that are produced annually allowing the individual fronds to float. The growth rate ranges between 0.05–0.8 cm/day (Carlson, 1991; Strömgren, 1977) and they have a life span in the order of 3 to 5 years (White, 2008). The species is annually episodic, gonochoristic and highly fecund (i.e. prolific) (White, 2008). Gametes are released into the seawater and the eggs are fertilized externally to form a zygote that starts to develop as soon as it settles into a substrate (Graham and Wilcox, 2000). The gametes are released from receptacles, which are found in the fertile tips of the macroalgae. However, *F. vesiculosus* also has non-fertile tips without these structures. Non-fertile tips are composed by a parenchymatous thallus

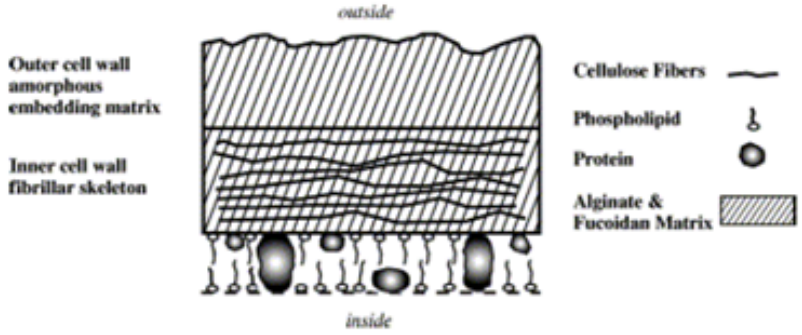

Figure 1.4 Cell wall structure in Phaeophyta (Davis *et al.*, 2003).

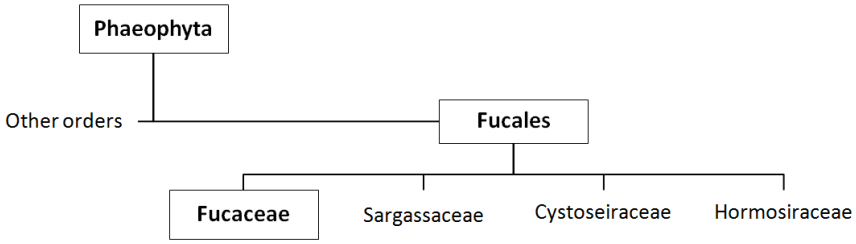

Figure 1.5 Classification scheme of Phaeophyta division (Graham and Wilcox, 2000).

(i.e. tissue like structure) which is produced by the division of an apical cell or a group of several apical initials (Graham and Wilcox, 2000; Hiscock, 1991; White, 2008). Figure 1.3 illustrates the different structures that *F. vesiculosus* has.

1.3.2 *F. vesiculosus* uses

Many uses of *F. vesiculosus* have been reported, such as body creams, antioxidant (Wang *et al.*, 2012) or health supplements (kelp) (White, 2008). *Fucus* sp. have been reported to have a direct effect on the human body metabolism by controlling the weight, cellulite deposits and thyroid problems remediation (Moro and Basile, 2000). The polysaccharides of *Fucus* sp. have been shown to have beneficial properties in hyperoxaluria treatment, because they enhance the antioxidant properties, thus preventing membrane damage and alleviating the microenvironment favourable for stone formation (Veena *et al.*, 2005). Furthermore, as other macroalgae, *Fucus* sp. might also have uses as fertilizers and insecticides, as it has deterrent compounds for herbivores (Yang, 1991).

Moreover, brown macroalgae appear to be useful in heavy metal removal (Davis *et al.*, 2003) and have recorded the highest Re and Tc accumulation of all macroalge, while *F. vesiculosus* has the highest Re concentrations measured to date, about hundreds of ppb (J. Kučera *et al.*, 2006; Mas *et al.*, 2004).

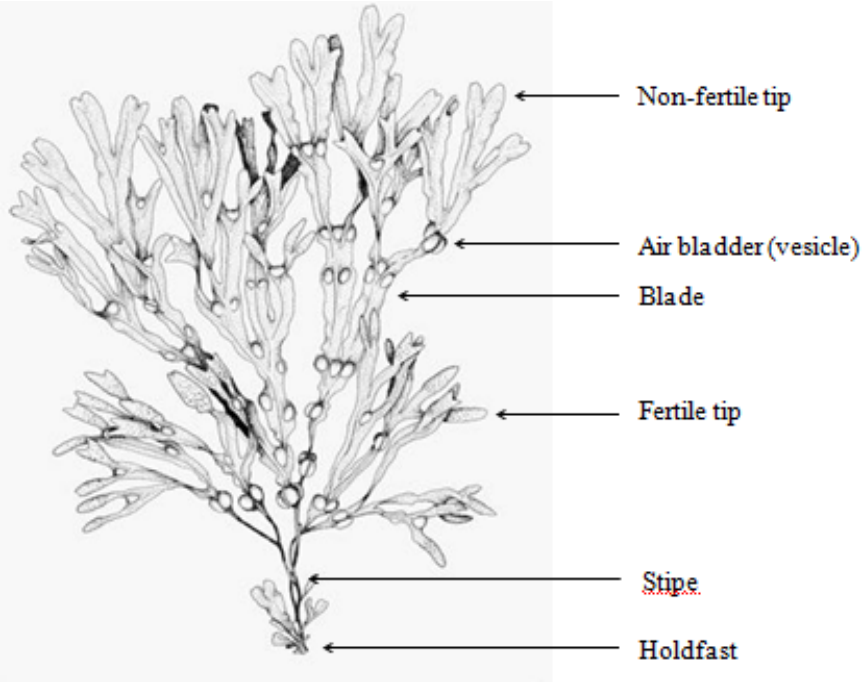

Figure 1.6 *F. vesiculosus* structures representation (Guiry and Nic Dhonncha, 2001).

1.4 Mechanisms of metal binding in macroalgae

There are two important classifications of metal binding mechanisms depending on the observation level; by looking at the mechanism in a micro level (i.e. ions) or macro level (i.e. organism or cell). The first classification (micro level) has mainly two mechanisms of metal binding:

- **Ion-exchange** which describes the binding site as already occupied by a proton that can take part in ion-exchange with a metal cation. Ion-exchange explains many of the observations made during heavy metal uptake (Davis *et al.*, 2003).
- **Complexation** which is the donation of electrons from a complexing ligand to a metal forming a metal complex. Basically, complexation is a Lewis acid - Lewis base neutralization process (Volesky, 1990).

The second classification (macro level) also has two mechanisms of metal binding (**bioaccumulation** and **biosorption**) which are discussed below.

1.4.1 Bioaccumulation by living macroalgae

The term bioaccumulation refers to an active metal removal process which is metabolically controlled by the living organism. The metals absorbed are transferred onto and/or within the cellular surface. The parameters that affect bioaccumulation are listed below:

- The age of the cells.

- The physiological state of the organism.
- The availability of micronutrients during their growth.
- The environmental conditions during uptake, such as pH, temperature, light intensity, salinity and others.

Metal accumulation by macroalgae has been shown to happen in a rapid surface reaction followed by a much slower metal uptake over a period of hours (Crist *et al.*, 1992). The rapid phase uptake corresponds to extracellular and/or passive intracellular uptake. The slower uptake corresponds to an active incorporation into the cell. Thus, the rapid uptake is metabolism-independent and the slower uptake is metabolism-dependent (Crist *et al.*, 1992).

1.4.2 Biosorption by dead macroalgae biomass

The term biosorption describes a passive (i.e. does require little energy) heavy metal removal by binding to non-living biomass from an aqueous solution. Metals are adsorbed onto the cellular structure and the amount of metals adsorbed is dependent on the kinetic equilibrium and composition of the cellular surface sorbents. The parameters that affect biosorption are listed below:

- Concentration of biomass
- pH
- Metallic ions interactions
- Redox potential

Nowadays there are sorption columns used for industrial biosorption of heavy metals using marine algae (Silvaprakash *et al.*, 2010).

The sorption rate is faster and can produce higher concentrations in biosorption uptakes rather than bioaccumulation sequestrations, thus biosorption is preferable to bioaccumulation (Velásquez and Dussan, 2009). Moreover, due to the binding of metals onto the cellular surface, biosorption is a reversible process whereas bioaccumulation is only partially reversible (Velásquez and Dussan, 2009).

1.5 Key functional groups in Phaeophyta division

The factors that affect the functional group in binding metals are as follows (Davis *et al.*, 2003):

- Number of sites on the biosorbent material.
- Accessibility and chemical state (i.e. availability).
- Affinity between site and metal (i.e. binding strength).

The different key structures and functions are described below.

1.5.1 Alginic acid

Alginates (i.e. alginic acid) comprise up to 40% of the brown macroalgae dry matter, 90% is present in the matrix of the cell wall and the other 10% is found in the intercellular spaces (Black, 1954; Mabeau and Kloareg, 1986). Alginates are formed by (1→ 4) linked β-mannuronic acid (M) and α-L-guluronic acid (G) of extensively varying composition and sequence. Three fractions can be distinguished (Haug, 1964) (Figure 1.7):

1) Fraction of almost homopolymeric G molecules.
2) Fraction of almost homopolymeric M molecules.
3) Fraction of nearly equal proportions of both monomers.

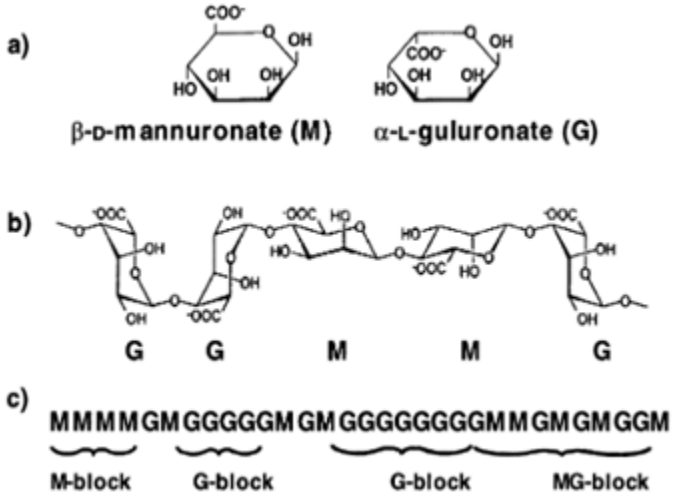

Figure 1.7 Structural alginate characteristics: a) alginate monomers, b) chain conformation and c) block distribution (Steinbüchel and Rhee, 2005).

In order to understand the polymer properties of alginates, the monomer ring conformation has to be known (Figure 1.7), to give an example, G/M ratio has an important effect in rigidity (Haug *et al.*, 1967). Thus, alginate composition in macroalgae does vary throughout the organism: GG dimers are found mostly in the holdfast and stipe, in order to provide strength and rigidity, while the majority MM dimers are found in the blades, providing flexibility to float (Andresen *et al.*, 1977; Haug *et al.*, 1974).

Physiologically, the function of alginate, as it is a structure-forming component, is to give strength as well as flexibility to the macroalgae.

Physically, the properties of alginate are the selective binding of multivalent cations (i.e. Ca^{2+} or Mg^{2+}) which is the basis of gel formation, not influenced by temperature. Free hydroxyl, carboxylic acid groups, the space between uronic acid molecules and the position of the oxygen on C1 in G

contribute to favourable ionic interactions with a metal cation (Cathell and Schauer, 2007; Schweiger, 1962). G polymer forms a rod-like shape made by two chains that pass each other with two hydroxyl groups and two carboxylic acid groups, creating an ideal binding site for metals (Davis *et al.*, 2003). This metal binding model is called the egg-box model (Figure 1.8). The more cations bound to the chains, fewer chains are able to move freely, and thus the solution becomes a gel.

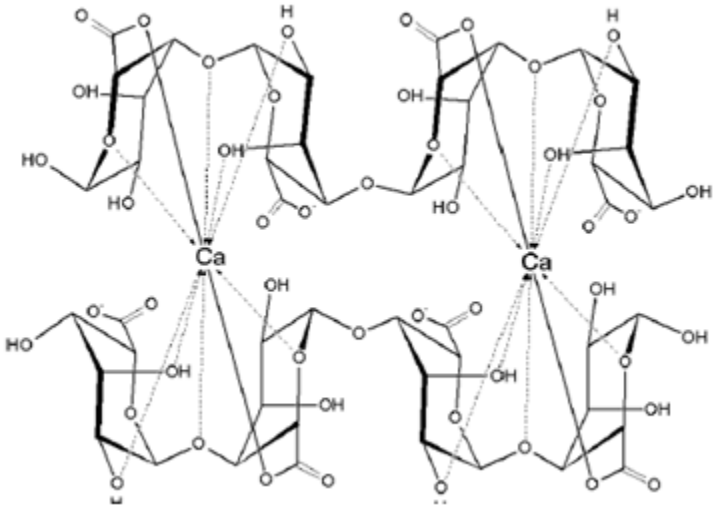

Figure 1.8 Egg-box model of calcium binding two alginate chains (Grant *et al.*, 1973).

1.5.2 Fucoidan

The fucoidan is a fucose-containing sulphated polysaccharide present through the fibrillar wall and the intercellular spaces of brown macroalgae (Mabeau and Kloareg, 1986). The fucoidan structure is represented in Figure 1.9. Sulphate groups are responsible for metal adsorption (Chapman and Chapman, 1980) without having different selectivities for divalent or monovalent cations (Kloareg *et al.*, 1986). Brown macroalgae contain three types of fucoidan: glycuronofucoglycans, ascophyllans and homofucans, although all of them are believed to regulate cell contents passively through cation binding (Mabeau and Kloareg, 1986).

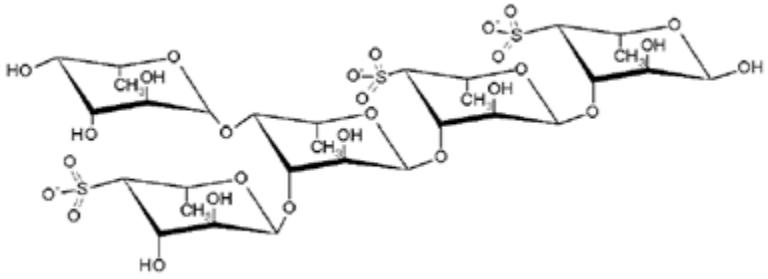

Figure 1.9 Representation of fucoidan structure (Patankar *et al.*, 1993).

1.5.3 Proteins

Brown macroalgae proteins constitute between 8-15% of the dry matter (Goñi *et al.*, 2002). Protein amino groups are responsible for metal ions binding (Raize *et al.*, 2004). It has been observed that cadmium binds to amino groups in the brown macroalgae, *Padina tetrastromatica* (D'Souza *et al.*, 2008).

1.5.4 Other

- **Polyphenols** in macroalgae are phlorotannins (i.e. polymers of phloroglucinol) (Ragan and Glombitza, 1986) which can chelate divalent metal cations (Ragan *et al.*, 1979).
- **Phytochelatins** are cysteine-rich metallothionein proteins produced to allow macroalgae to survive in highly metal contaminated areas (Morris *et al.*, 1999).

1.6 Factors affecting heavy metal uptake

There are many biological, chemical and physical variables affecting the uptake of chemical elements such as; pH, ionic strength, salinity, temperature, light, competition between metal ions and many others. Most of these factors are discussed below.

1.6.1 pH

Dependence of metal uptake on pH is related to metal chemistry in solution and to the surface functional groups. Thus, as carboxylic and sulphonate groups are acidic, the optimum pH in solution for a maximum metal uptake is related to the pK_a of these surface groups. Therefore, at low pH, both carboxylic and sulphonate groups are protonated and thereby become less available for the binding of heavy metals (Greene *et al.*, 1987; Ramelow *et al.*, 1992). Algal biomass may have an overall negative charge, which increases with increasing pH (i.e. more sites are deprotonated), therefore the binding of most metals increases with increasing pH (Schiewer and Volesky, 1995).

1.6.2 Ionic strength

Ionic strength or background electrolyte concentration changes influence metal binding by changing the competition of the electrolyte ion (i.e. metal of interest) and adsorbing ions for sorption sites (i.e. Na^+) and by altering the interfacial potential, thus the activity of the electrolyte ions. It has been observed that an increase in metal binding with decreasing ionic strength occurs in green (*Ulva lactuca*) and brown macroalgae (*Sargassum hemiphyllum, Petalonia fascia* and *Colpomenia sinuosa*) (Schiewer and Wong, 2000).

1.6.3 Salinity

The amount of dissolved salt content in seawater affects the photosynthesis and growth of the organisms living in it. Thus, it could have an effect on metal absorption. It has been observed that in

some macroalgae (i.e. *Ascophyllum nodosum*) metal uptake decreased with low salinity whereas in some other macroalgae (i.e. *F. vesiculosus* or *Ulva lactuca*) metal content increased, suggesting different uptake mechanisms between species (Connan and Stengel, 2011; Turner *et al.*, 2008).

1.6.4 Temperature

Temperature affects water chemistry and the metabolic rate of macroalgae, thus their heavy metal uptake could be affected (Lemus and Chung, 1999). However, in some cases it has been observed that enhanced temperature increased the uptake of metals like Zn^{+2} and Mn^{+2} in macroalgae (Munda and Hudnik, 1988), whereas in other species it has been observed that the metal uptake has little change under temperature treatments (Zhao *et al.*, 1994).

1.6.5 Light

Light also controls the metabolic rate of macroalgae, hence their heavy metal uptake could be affected as well. Heavy metal uptake has been shown to increase in some macroalgae with increasing light (Hu *et al.*, 1996).

1.6.6 Competition between metal ions

Some metal binding decreases in the presence of multi-metallic systems while some other metals are totally unaffected (Kuyucak and Volesky, 1989). Hence, biosorption of metals in a multi-metallic solution depends on two things, a) the physicochemical nature of the solution and b) the interaction between metals. For instance, iron and manganese (oxihydr)oxides can adsorb some metals like niquel, form surface complexes or co-precipitate them. Thus, decreasing the overall binding to macroalgae surface (Hatje *et al.*, 2001).

1.6.7 Redox potential, E_h

Metal geochemistry as well as the availability of ligands for sorption, precipitation or complexation are affected by redox conditions. Moreover, the distribution between metal species depends to a large extent on redox conditions and is a critical factor to understand the role of interaction of metals with macroalgae (Du Lain, 2011).

1.6.8 Other

- **Growth rate**: It has been observed that metal accumulation in macroalgae increase or decrease as the specific growth rate increases, which might indicate a metabolic regulation of metal uptake (Rice, 1984) or an increase in the metal-to-biomass ratio (Göthberg *et al.*, 2004; Greger *et al.*, 1991; Wang and Dei, 1999).

- **Humic substances**: The presence of humic substances in the aquatic environment has been observed to reduce the bioavailability and toxicity of heavy metals by complexation of the

metals and other elements with the dissolved organic matter, hence, reducing the concentration of free ionic metals in the aquatic environment (Guo *et al.*, 2001; Kim *et al.*, 1999; Tubbing *et al.*, 1994).

- **Nutrient concentration**: Some nutrient concentrations are reported to affect metal bioavailability. In rich nutrient environments, metal uptake can be inhibited as a result of complex formation between the ion metal and the nutrient (Göthberg *et al.*, 2004; Haglund *et al.*, 1996).
- **Seasonal variation**: Changes in macroalgae physiology and metabolism are observed throughout the year (Kang *et al.*, 2011). Seasonal variation in growth could be affecting macroalgae element binding; it has been observed that seasonal variation in temperature does not affect heavy metal accumulation (Zumdahl, 1992).
- **Heights and tidal levels**: Changes in height and tide levels affect many of the factors mentioned above, such as nutrient concentrations, humic substances, light and temperature. As such, the metal or element uptake might be influenced by the height where the macroalgae grow.

1.7 Re, Os and Tc uptake and accumulation by macroalgae

Although the Re concentration in seawater is low (i.e. 0.0074-0.009 ppb) in comparison to the terrestrial realm (i.e. 0.2-2 ppb), marine macroalgae, especially brown macroalgae, are known to bind Re up to several tens of ppb (J. Kučera *et al.*, 2006; Mas *et al.*, 2004; Prouty *et al.*, 2014; T. Ishii *et al.*, 2003; Yang, 1991), in addition to many other positive and negative charged metals through a variety of mechanisms, i.e. alginate, proteins, polysaccharides of the cell wall, fucans, etc. (Davis *et al.*, 2003), despite there being no known biological use for Re. To date, positively charged metals associated with macroalgae have been extensively studied such as Pb^{2+}, Cd^{2+} or Ni^{2+} (Chapman and Chapman, 1980; Lobban and Harrison, 1994; Ragan *et al.*, 1979; Raize *et al.*, 2004). However, little is known about the mechanisms by which macroalgae uptake negatively charged metals such as the perrhenate ion. Experiments have shown that Re is most likely stored within algal cells, rather than on the algal cell surface or within the intercellular matrix (Xiong *et al.*, 2013; Yang, 1991). Specifically, it has been proposed that protonated amino or amine groups could be involved, forming ion pairs with perrhenate (Meilián *et al.*, 2000; T. Ishii *et al.*, 2003; Xiong *et al.*, 2013). Moreover, Kim *et al.* (2004) showed that ReO_4^- had a high interaction with chitosan which is basically a polymer of glucosamine. Chitosan is only reported in nature in some fungi, crustacea and termite queen's abdominal wall. However, Nishino *et al.* (1994) isolated and characterized a novel polysaccharide containing an appreciable amount of glucosamine in *F. vesiculosus*.

Assuming that this evidence proposing Re being stored inside the cells is true, a mechanism for Re uptake into the cells should exist. Tagami and Uchida (2005) showed that there is a positive correlation between the K^+ and the Re accumulated in three plant species and explained this as

a result of ReO_4^- being similar to Cl^- as a counter ion for K^+ uptake. Moreover, macroalgae could inadvertently take up Re by using the same mechanism as for phosphate (PO_4^{3-}). A similar mechanisms has been proposed for arsenate uptake by macroalgae (AsO_4^{3-}) (Klumpp, 1980).

To our knowledge there is no data available of Os concentrations in macroalgae, Os concentrations and ratios have been analysed in plants, lichens, mosses, pine needles, tree leaves and mushrooms (Rodushkin *et al.*, 2007). Moreover, Rodushkin *et al.* (2011) observed that *Myodes glareolus* (common herbivore in boreal forests) uptake Os, as lichens are their main food source, it is stated that lichens are the pre-concentrators of Os.

However, if observed an accumulation of Os in *F. vesiculosus*, an idea of where it is found could be approached, as there is evidence of the biological elements in which OsO_4 binds to in staining and fixation for TEM (i.e. Transfer Electron Microscopy) and SEM (i.e. Scanning Electron Microscopy). It has been shown that OsO_4 mainly binds to phospholipid head regions of the cell membranes while reducing to Os metal (Hayes *et al.*, 1963).

As it is thought with Re, Tc is believed to have no known biological role. However, it has been also observed that Tc can be concentrated in macroalgae (Birks, 1975). The distribution of Tc in the brown macroalgae *Ascophyllum nodosum* has been analysed and showed an increase of Tc concentration from the youngest to the oldest growth segments of the macroalgae (Heldal and Sjøtun, 2010). Moreover, it has been reported that biological reduction of Tc in aquifers and sediments (N. Ishii *et al.*, 2003) and it was stated that bacteria were responsible for the formation of insoluble Tc. However, no similarity was observed with Re.

1.8 Eutrophication and N accumulation by macroalgae

Eutrophication is commonly caused by water pollution (industrial or fertilizers) in modern water masses. As a consequence of the nutrient enrichment, excessive floral growth is produced (i.e., macroalgae – seaweed), which subsequently makes it difficult for other plants and/or animals to survive and take up nutrients. In addition, the death of these macroalgal blooms promotes oxygen depletion in the water column causing anoxia, again restricting the environment in which other flora and/or animals can live. To monitor such changes in water mass eutrophication nitrogen isotopes of organic matter have been used (de Carvalho, 2008; Fernandes *et al.*, 2012; Maier *et al.*, 2009).

The utilization of nitrogen isotope analysis of macroalgae has been used to trace eutrophication on this premise. The levels of $\delta^{15}N$ in seaweed are significantly altered due to the enrichment of nitrates in a river. These variations in seaweed were initially documented by Minagawa and Wada (1984), and more recently there have been further studies (Savage and Elmgren, 2004; Viana *et al.*, 2011). Viana *et al.* (2011) measured $\delta^{15}N$ signatures in macroalgal tissues in coastal areas between 1990 and 2007 and found a decrease in $\delta^{15}N$ over the successive analyses, which the authors related

to eutrophication. Savage and Elmgren (2004) reported the same conclusion, i.e. decreases of δ^{15}N values in *F. vesiculosus* are found under sewage influence.

1.9 Instrumental analysis for isotope ratios and element concentrations

There are many techniques used to study elements in natural organisms, however this work uses mass spectrometry (MS). Mass spectrometry is an analytical technique that identifies the type and amount of chemical elements and isotope ratios present in a sample by measuring the abundance and mass-to-charge ratio of gas-phase ions. The sample, which can be solid, liquid or gas, is ionized (i.e. bombarding it with electrons). As a result of this, the sample breaks into charged fragments (ions) that are separated according to their mass-to-charge ratio, mainly by subjecting the sample to acceleration and electromagnets. The molecules or atoms in the sample can be identified by correlating the known masses with the identified masses.

There are different mass spectrometer techniques and configurations, in this work inductively plasma-mass spectrometry (ICP-MS), thermal ionization mass spectrometry (TRITON) and Thermo Scientific Delta V Advantage isotope ratio mass spectrometer (IRMS) are used.

1.9.1 Thermal ionization mass spectrometry (Thermo Scientific TRITON)

Thermal ionization mass spectrometry is a very sensitive mass spectrometry technique, which consists in placing the sample into a filament that is heated to high temperatures in order to ionize the atoms of the sample which are then separated according to their mass-to-charge ratio. The technique is used mainly in isotope geochemistry, geochronology and cosmochemistry.

1.9.2 Inductive coupled plasma mass spectrometry (Thermo Scientific X-Series ICP-MS)

Inductive coupled plasma mass spectrometry is a mass spectrometry technique capable of detecting metals and several non-metals at concentrations as low as one part per quadrillion (ppq). ICP-MS is used largely in the medical forensic field, industrial and biological monitoring, geochemistry dating and pharmaceutical industry. The sample is ionized with inductive coupled plasma (i.e. ionized plasma obtained by inductively heating the gas with an electromagnetic coil) and the atoms ionized are separated by their mass-to-charge ratio.

1.9.3 Thermo Scientific Delta V Advantage isotope ratio mass spectrometer (IRMS)

Thermo Scientific Delta V Advantage isotope ratio mass spectrometer systems combine outstanding sensitivity with excellent linearity and stability to tackle many different applications, mainly to analyse the stable isotopes of carbon and nitrogen.

1.10 Applications

1.10.1 Re and Os perspective

As mentioned previously Re and Os are used as a geochronometer to date crude oil generation from source rocks based on the beta decay of the isotope ^{187}Re to ^{187}Os (Cohen *et al.*, 1999; Lillis and Selby, 2013). Isochron dating is the methodology used in order to date using Re-Os, which consists in plotting the ratio of radiogenic ^{187}Os to non-radiogenic ^{188}Os against the ratio of the parent isotope ^{187}Re to the non-radiogenic isotope ^{188}Os, thus obtaining the approximate age of sample. This method is explained by the following equation (Cohen *et al.*, 1999):

$$\left(\frac{^{187}Os}{^{188}Os}\right)_{present} = \left(\frac{^{187}Os}{^{188}Os}\right)_{initial} + \left(\frac{^{187}Os}{^{188}Os}\right) \times (e^{\lambda t} - 1)$$

Where, λ is the decay constant of ^{187}Re, t the age of the sample and ($e^{\lambda t}$-1) is the slope of the isochron which defines the age of the system.

An understanding of Re and Os biogeochemical processes is important, as if Re is taken up actively by organisms, it changes the way that may account for the presence of Re and Os in organic-rich sedimentary rocks, source rocks and crude oil. Therefore, the models used within source rock geochronology, as well as our understanding of Re and Os biogeochemical cycles in marine systems will need to be re-evaluated. In order to improve our understanding of the Re and Os cycles, it is necessary to understand where, and in what form and oxidation state, both Re and Os concentrates within macroalgae.

Furthermore, a better knowledge on the uptake of Re will help to elucidate the uptake of Tc, which could raise the possibility to use macroalgae as bioconcentrators of Re and Tc, thus bioremediation of Tc contaminated waters, phytomining of Re and environmental monitoring could be achieved by the use of *F. vesiculosus*.

Owing to the high value of Re, recovery of this element has both economic and environmental benefits.

1.10.2 N perspective

The utilization of N isotope analysis of macroalgae can be used to trace eutrophication. It has been observed that the levels of δ^{15}N in macroalgae are significantly altered due to the enrichment of nitrates in a river. And, as seawater is more difficult to analyse directly for N levels than macroalgae, the usage of *Fucus* sp. as a N recorder would be a solution. Moreover, macroalgae could be used as a tool for cleaning contaminated areas with nitrates or ammonia.

1.11 General structure of the thesis

The analysis of all the data obtained to fulfill the objectives explained in section 1.1, is divided into 5 different chapters that are structured as follows:

The second chapter focuses on the uptake and distribution of Re in *F. vesiculosus*; objectives 1, 2, 3 and 4 are applied here. A better understanding of the distribution of Re, the factors affecting the uptake mechanism and uptake mechanism itself are very important, from a simple biology point of view, to know how these organisms work. This knowledge is also valuable to assess if *F. vesiculosus* can be used as a source of phytomining or bioremediation.

The third chapter aims to study the uptake and distribution of Os in *F. vesiculosus*, thus, assessing if macroalgae is a good proxy of seawater Os isotopic values. Mainly objectives 1 and 3 are answered here.

In the fourth chapter we seek to understand the source of nitrogen in river Tees using δ^{15}N measurements in *Fucus* sp. *In vivo* cultures are made to assess the usefulness of δ^{15}N macroalgae signatures as a N pollution recorder. *In vitro* culture experiments are performed in order to understand and relate the changes in δ^{15}N signature in macroalgae with different N conditions (nitrates or ammonia). Experiments explained in objectives 1 and 5 are shown here.

Finally, the fifth chapter presents a general discussion as well as with common conclusion and further research that could be done in this topic.

In chapters 2, 3 and 4, the tables and figures are placed at the end of the each respective section.

1.12 References

Anbar A.D. Creaser D. Papanastassiou A. and Wasserburg G.J. (1992) Rhenium in seawater: Confirmation of generally conservative behaviour. Geochim. Cosmochim. Ac. 56, 4099-4103.

Andresen I.-L. Skipnes O. Smidsrød O. Ostgaard K. and Hemmer P. (1977) Some biological functions of matrix components in benthic algae in relation to their chemistry and the composition of seawater. Cell. Chem. Technol. 48, 361-381. DOI 10.1021/bk-1977-0048.ch024

Banner J.L. (2004) Radiogenic isotopes: systematics and applications to earth surface processes and chemical stratigraphy. Earth-Science Reviews 65, 141-194. DOI 10.1016/S0012-8252(03)00086-2

Bernhard A. (2010) The Nitrogen Cycle: Processes, Players, and Human Impact. Nature Education Knowledge 3(10), 25.

Birks J.L. (1975) Medical radionuclides in marine environment. Nature 255, 621-622. DOI 10.1038/255621a0

Black W.A.P. (1954) The seasonal variation in the combined L-fucose content of the common

British Laminariaceae and fucaceae. J. Sci. Food Agr. 5, 445-448. DOI 10.1002/jsfa.2740050909

Bold H.C. Wynne M.J. (1986) Introduction to the Algae, New Jersey.

Carlson L. (1991) Seasonal variation in growth, reproduction and nitrogen content of *Fucus vesiculosus* in the Öresund, Southern Sweden. Bot. Mar. 34, 447-453. DOI 10.1515/botm.1991.34.5.447

Cartlege G.H. (1955) The pertechnetate ion as an inhibitor of the corrosion. J. Am. Chem. Soc. 335-342. DOI 10.1021/ja01614a103

Cathell and M.D. Schauer C.L. (2007) Structurally colored thin films of Ca^{2+}-cross-linked alginate. Biomacromolecules 8, 33-41. DOI 10.1021/bm060433f

Chapman V. and Chapman D. (1980) Seaweeds and their Uses, London New York.

Chen C. and Sharma M. (2009) High Precision and High Sensitivity Measurements of Osmium in Seawater. Anal. Chem. 81, 5400-5406. DOI 10.1021/ac900600e

Chen C. Sharma M. and Bostick B.C. (2006) Lithologic controls on osmium isotopes in the Rio Orinoco. Earth and Planetary Science Letters 252, 138-151. DOI 10.1016/j.epsl.2006.09.035

Cohen A.S. Coe A.L. Bartlett J.M. and Hawkesworth C.J. (1999) Precise Re-Os ages of organic-rich mudrocks and the Os isotope composition of Jurassic seawater. Earth and Planet. Sc. Lett. 197, 159-173. DOI 10.1016/S0012-821X(99)00026-6

Collery P. Bastian G. Santoni F. Mohsen A. Wei M. Collery T. Tomas A. Desmaele D. and D'angelo J. (2014) Uptake and efflux of Rhenium in Cells exposed to Rhenium Diseleno-Ether and Tissue Distribution of Rhenium and Selenium after Rhenium Diseleno-Ether treatment in mice. Anticancer Res. 34, 1679-1690.

Connan S. and Stengel D.B. (2011) Impacts of ambient salinity and copper on brown algae: 1. Interactive effects on photosynthesis, growth, and copper accumulation. Aquatic Toxicology 104, 94-107. DOI 10.1016/j.aquatox.2011.03.015

Cotton F.G. Wilkinson G. (1998) Advanced Inorganic chemistry, 5th edition, J. Wiley and Sons.

Cramer S.D. and Covino B.S. (2005) ASM Handbook Corrosion Material.

Crist R.H. Oberholser K. McGarrity J. Crist D.R. Johnson J.K. and Michael J. (1992) Interaction of metals and protons with algae. 3. Marine algae, with emphasis on lead and aluminum. Environ. Sci. Technol. 26, 496-502. DOI 10.1021/es00027a007

Davis T.A. Volesky B. and Mucci A. (2003) A review of the biochemistry of heavy metal biosorption by brown algae. Water Res. 37, 4311-4330. DOI 10.1016/S0043-1354(03)00293-8

de Carvalho M.C. (2008) Uso dos isotopos estaveis de carbono, nitrogeno e enxofre em estudios de ecologia costeira. Oecologia Bras 12, 694-705.

D'Souza L. Devi P. Shridhar D.M.P. and Naik C.G. (2008) Use of Fourier Transform Infrared (FTIR) spectroscopy to study cadmium-induced changes in *Padina tetrastromatica* (Hauck). Anal.

Chem. Insights 2008, 135-143.

Du Laing G. (2011) Redox Metal Processes and Controls in Estuaries. In: Wolanski E and McLusky DS (eds.) Treatise on Estuarine and Coastal Science, Vol 4, pp. 115–141. Waltham: Academic Press.

Elvira M. (1932) The discovery of the elements. IV. Three important gases. J. Chem. Educ. 9, 215.DOI 10.1021/ed009p215

Emsley J. (2001) Nature's building blocks: an A-Z guide to the elements, New York.

Esser B.K. and Turekian K.K. (1993) The osmium isotopic composition of the continental crust. Geochim. Cosmochim. Acta 57, 3093-3104.DOI 10.1016/0016-7037(93)90296-9

Fernandes M. Benger S. Sharma S.K. Gaylard S. Kildea T. Hoared S. Braley M. and Irving A.D. (2012) The use of δ^{15}N signatures of translocated macroalgae to map coastal plumes; improving species selection and spatial analysis of metropolitan datasets. J. Environ. Monitor. 14, 2399- 2410. DOI 10.1039/C2EM10997B

Gannoun A. and Burton K.W. (2014) High precision osmium elemental and isotope measurements of North Atlantic seawater. J. Anal. Atom. Spectrom. 29, 2330-2342. DOI 10.1039/c4ja00265b

Goñi I. Gudiel-Urbano M. and Saura-Calixto F. (2002) *In vitro* determination of digestible and unavailable protein in edible seaweeds. J. Agric. Food Chem. 82, 1850-1854. DOI 10.1002/jsfa.1270

Göthberg A. Greger M. Holm K. and Bengtsson B. (2004) Influence of nutrients on uptake and effects of Hg, Cd and Pb in *Ipomoea aquatica*. J. Environ. Qual. 33, 1247-1255. DOI 10.2134/jeq2004.1247

Graham L.E. and Wilcox L.W. (2000) Algae. United States of America.

Grant G.T. Morris E.R. Rees D.A. Smith P.J.C. and Thom D. (1973) Biological interactions between polysaccharides and divalent cations: The egg-box model. FEBS Lett. 32, 195-198. DOI 10.1016/0014-5793(73)80770-7

Greene B. McPherson R. and Darnall D. (1987) Algal sorbents for selective metal ion recovery.In Metals Speciation, Separation and Recovery, Lewis Publishers Inc., Chelsea, MI, USA.

Greger M. Brammer E. Lindberg S. Larsson G. and Idestam-Almquist J. (1991) Uptake and physiological effects of cadmium in sugar beet (*Beta vulgaris*) related to mineral provision. J. Exp. Bot. 42, 729-737. DOI 10.1093/jxb/42.6.729

Guiry M.D. (2000) What are seaweeds, The seaweed site: information on marine algae, www.seaweed.ie. Accessed January 2015

Guiry M.D. and Nic Dhonncha E. (2001) AlgaeBase, World wide web electronic publication. Accessed January 2015

Guo L. Hunt B.J. Santschi P.H. and Ray S.M. (2001) Effect of Dissolved Organic Matter on

the Uptake of Trace Metals by American Oysters. Environ. Sc. Technol. 35, 885-893. DOI 10.1021/es001758l

Hatje V. Birch G.F. Hill D.M. (2001) Spatial and temporal variability of particulate trace metals in Port Jackson estuary, Australia. Estuarine, Coastal and Shelf Science. 53: 63–77.

Haglund K. Björklund M. Gunnare S. Sandberg A. Olander U. and Pedersén M. (1996) New method for toxicity assessment in marine and brackish environments using the macroalga *Gracilaria tenuistipitata* (Gracilariales, Rhodophyta). Hydrobiologia 326-327, 317-325. DOI 10.1007/BF00047825

Harvey B.R. Ibbett R.D. Williuams K.J. and Lovett M.B. (1991) Determination of Technetium-99 in Environment Materials. Ministry of Agriculture, Fisheries and Food Directorate of Fisheries Research Lowestoft, p. 22.

Haug A. (1964) Composition and Properties of Alginates. N.T.H. Trykk.

Haug A. Larsen B. and Smidsrød O. (1974) Uronic acid sequence in alginate from different sources. Carbohyd. Res. 32, 217-225. DOI 10.1016/S0008-6215(00)82100-X

Haug A. Myklestad S. Larsen B. and Smidsrød O. (1967) Correlation between chemical structure and physical properties of alginates. Acta chem. scand. 21, 768-778. DOI 10.3891/acta.chem.scand.21-0768

Hayat M.A. (2000) Principles and techniques of electron microscopy. Biological applications, University of Cambridge.

Hayes T.L. Lindgren F.T. and Gofman J.W. (1963) A quantitative determination of the osmium tetroxide-lipoprotein interaction. J. Biol. Chem. 1, 251-255. DOI 11/1963; 19(1):251-5

Heldal H.E. and Sjøtun K. (2010) Technetium-99 (^{99}Tc) in annual growth segments of knotted wrack (*Ascophyllum nodosum*). Sci. Total Environ. 408, 5575-5582. DOI 10.1016/j.scitotenv.2010.07.068

Helz G.R. and Dolor M.K. (2012) What regulates rhenium deposition in euxinic basins? Chemical Geology 304-395, 131-141. DOI 10.1016/j.chemgeo.2012.02.011

Hiscock S. (1991) Brown seaweeds. A field key to the british., Shrewsbury, Montford Bridge.

Hu S. Tang C.H. and Wu M. (1996) Cadmium accumulation by several seaweeds. Sci. Total Environ. 187, 65-71. DOI 10.1016/0048-9697(96)05143-1

Ishii T. Hirano S. and Watabe T. (2003) Hyperaccumulation of radioactive isotopes by marine algae, Japan Atomic Energy Research Institute, Japan, pp. 187-191.

Ishii N. Tagami K. Enomoto S. and Uchida S. (2003) Influence of microorganisms on the behaviour of technetium and other elements in paddy soil surface water. J. Environ. Radioactiv. 77, 369-380. DOI 10.1016/j.jenvrad.2004.04.006

Kang J.C. Choi H.G. and Kim M.S. (2011) Macroalgal species composition and seasonal

variation in biomass on Udo, Jeju Island, Korea. Algae 26, 333-342.DOI 10.4490/algae.2011.26.4.333

Kenna B.T. and Kuroda P.K. (1964) Technetium in nature. J. Inorg. Nucl. Chem. 26, 493-499. DOI 10.1016/0022-1902(64)80280-3

Kim E. Benedetti M.F. and Boulègue J. (2004) Removal of dissolved rhenium by sorption onto organic polymers: study of rhenium as an analogue of radioactive technetium. Water Res. 38, 448-454. DOI 10.1016/j.watres.2003.09.033

Kim S.D. Ma H. Allen H.E. and Cha D.K. (1999) Influence of dissolved organic matter on the toxicity of copper to *Ceriodaphnia dubia*: effect of complexation kinetics. Environ. Toxicology Chem. 18, 2433-2437. DOI 10.1002/etc.5620181108

Kloareg B. Demarty M. and Mabeau S. (1986) Polyanionic characteristics of purified sulfated homofucans from brown algae. Int. J. Biol. Macromol. 8, 380-386. DOI 10.1016/0141-8130(86)90060-7

Klumpp D.W. (1980) Characteristics of Arsenic accumulation by the seaweeds *Fucus spiralis* and *Ascophyllum nodosum*. Mar. Biol. 58, 257-264.

Koide M. Hodge V.F. Yang J. Stallard M. and Goldberg E.G. (1986) Some comparative marine chemistries of Rhenium, Gold, Silver and Molybdenum. Appl. Geochem. 1, 705-714. DOI 10.1016/0883-2927(86)90092-2

Kučera J. Byrne A.R. Mizera J. Lučaníková M. and Řanda Z. (2006) Development of a radiochemical neutron activation analysis procedure for determination of rhenium in biological and environmental samples at ultratrace level. J. Radioanal. Nucl. Ch. 269, 251-257. DOI 10.1007/s10967-006-0331-2

Kuyucak N. and Volesky B. (1989) Accumulation of gold on algal biosorbent. Biorecovery 1.

Lemus M.J. and Chung K.S. (1999) Effect of temperature on copper toxicity, accumulation and purification in tropical fish juveniles *Petenia Kraussii* (Pisces: Cichlidae). J. Caribbean Hist. 35, 64-69.

Levasseur S. Birck J.-L. and Allègre J. (1998) Direct Measurement of femptomoles of Osmium and the $^{187}Os/^{186}Os$ Ratio in seawater. Science 282, 272-274. DOI 10.1126/science.282.5387.272

Lide D.R. (2000) CRC Handbook of Chemistry and Physics.

Lillis P.G. and Selby D. (2013) Evaluation of the rhenium-osmium geochronometer in phosphoria petroleum system Bighorn Basin of Wyoming and Montana. Geochim. Cosmochim. Acta 118, 312-330. DOI 10.1016/j.gca.2013.04.021

Lobban C.S. and Harrison P.J. (1994) Seaweed Ecology and Physiology. Press syndicate of the university of Cambridge, Cambridge University.

Loren C.H. (1933) The Discovery of Rhenium. J. Chem. Educ. October 1933, 605-608.

Mabeau S. and Kloareg B. (1986) Isolation and analysis of the cell walls of brown algae: *Fucus*

spiralis, F. ceranoides, F. vesiculosus, F. serratus, Bifurcaria bifurcata and *Laminaria digitata*. J. Exp. Bot. 38, 1573-1580. DOI 10.1093/jxb/38.9.1573

MacDonell H.L. (1960) The use of hydrogen fluoride in the development of latent fingerprints found on glass surfaces. J. Crim. Law Criminol. 51, 465-470. DOI 10.2307/1140672

Maier G. Nimmo-Smith R.J. Glegg G.A. Tappin A.D. and Worsford P.J. (2009) Estuarine eutrophication in the UK: current incidence and future trends. Aquat. Conserv. 19, 43-56. DOI 10.1002/aqc.982

Markey D.R. and Wilce R.T. (1975) The Ultrastructure of Reproduction in the brown alga *Pylaiella littoralis*. Protoplasma 85, 219-241.DOI 10.1007/BF01567948

Mas J.L. Tagami K. and Uchida S. (2004) Rhenium measurements on North Atlantic seaweed samples by ID-ICP-MS: An observation on the Re concentration factors. J. Radioanal. Nucl. Ch. 265, 361-365. DOI 10.1007/s10967-005-0833-3

Meilián C. Kremer C. Suescun L. Mombrú A. Mariezcurrena R. and Krémer E. (2000) Re(V) complexes with amino acids based on the '3+2' approach. Inorg. Chim. Acta 306, 70-77.

Miller C.A. Peucker-Ehrebrink B. Walker B.D. and Marcantonio F. (2011) Re-assessing the surface cycling of molybdenum and rhenium. Geochim. Cosmochim. Acta 75, 7146-7179. DOI

Minagawa M. and Wada E. (1984) Stepwise enrichment of ^{15}N along food chains: further evidence and the relation between δ^{15}N and animal age. Geochim. Cosmochim. Acta 48, 1135-1140. DOI 10.1016/0016-7037(84)90204-7

Moro C.O. and Basile G. (2000) Obesity and medicinal plants. Fitoterapia 71, S73-S82.DOI 10.1016/S0367-326X(00)00177-5

Morris C.A. Nicolaus B. Sampson V. Harwood J.L. and Kille P. (1999) Metal-specific synthesis of two metallothioneins and gamma-glutamyl peptides in *Candida glabrata*. Biochem. J. 85, 8815-8819. DOI 10.1073/pnas.85.23.8815

Munda I.M. and Hudnik V. (1988) The effects of Zn, Mn and Co accumulation on growth and chemical composition of *Fucus vesiculosus* L. under different temperature and salinity conditions. Mar. Ecol. 9, 213-225.DOI 10.1016/j.aquatox.2011.03.015

Nishino T. Nishioka C. Ura H. and Nagumo T. (1994) Isolation and partial characterization of a novel amino sugar-containing fucan sulfate from commercial *Fucus vesiculosus* fucoidan. Carbohyd. Res. 255, 213-224. DOI 10.1016/S0008-6215(00)90980-7

Palmer M.R. Falkner K.K. Turekian K.K. and Calvert S.E. (1988) Sources of osmium isotopes in manganese nodules. Geochim. Cosmochim. Acta 52, 1197-1202. DOI 10.1016/0016-7037(88)90274-8

Patankar M.S. Oehninger S. Barnett T. Williams R.L. and Clark G.F. (1993) A revised structure

for fucoidan may explain some of its biological activities. J. Biol. Chem. 268, 21770-21776.

Peucker-Ehrenbrik B. and Ravizza G. (2000) The marine osmium isotope record. Terra Nova 12, 205-219. DOI 10.1046/j.1365-3121.2000.00295.x

Prouty N.G. Roark E.B. Koenig A.E. Demopoulos A.W.J. Batista F.C. Kocar B.D. Selby D. McCarty M.D. Mienis F. and Ross S.W. (2014) Deep-sea coral record of human impact on watershed quality in the Mississippi River Basin. Global Biogeochem. Cy. 28, 29-43. DOI 10.1002/2013GB004754

Ragan M.A. and Glombitza K. (1986) Phlorotannins, brown algal polyphenols, Bristol.

Ragan M.A. Smidsrod O. and Larsen B. (1979) Chelation of divalent metal ions by brown algal polyphenols. Mar. Chem. 7, 265-271. DOI 10.1016/0304-4203(79)90043-4

Raize O. Argaman Y. and Yannai S. (2004) Mechanisms of biosorption of different heavy metals by brown marine macroalgae. Biotechnol. Bioeng. 87, 451-458. DOI 10.1002/bit.20136

Ramelow G.J. Fralick D. and Zhao Y. (1992) Factors affecting the uptake of aqueous metal ions by dried seaweed biomass. Microbios 72, 81-93.

Rice D.L. (1984) A simple mass transport model for metal uptake by marine macroalgae growing at different rates. J. Exp. Mar. Biol. Ecol. 821, 175-182. DOI 10.1016/0022-0981(84)90102-3

Robinson D. (2001) δ^{15}N as an integrator of the nitrogen cycle. Trends Ecol. Evol. 16(3), 153-162. DOI /10.1016/S0169-5347(00)02098-X

Robson J. (1974) Process for the production of technetium-99m from neutron irradiated molybdenum trioxide, in: Australia, A.E.o. (Ed.)

Rodushkin I. Engström E. Sörlin D. Baxter D. Hörnfeldt B. Nyholm E. and Ecke F. (2011) Uptake and accumulation of anthropogenic Os in free-living bank voles (*Myodes glareolus*). Water Air Soil Pollut. 218, 603-610. DOI 10.1007/s11270-010-0671-y

Rodushkin I. Engström E. Sörlin D. Pontèr C. and Baxter D.C. (2007) Osmium in environmental samples from Northeast Sweden Part I. Evaluation of background status. Sci. Total Environ. 386, 145-158.

Savage C. and Elmgren R. (2004) Macroalgal (*Fucus vesiculosus*) δ^{15}N values trace decrease in sewage influence. Ecol. Appl. 14, 517-526. DOI 10.1890/02-5396

Schiewer S. and Volesky B. (1995) Modeling of the proton-metal ion exchange in biosorption. Environ. Sci. Technol. 29, 3049-3058. DOI 10.1021/es00012a024

Schiewer S. and Wong M.H. (2000) Ionic strenth effects in biosorption of metals by marine algae. Chemosphere 41, 271-282. DOI 10.1016/S0045-6535(99)00421-X

Schweiger R.G. (1962) Acetylation of alginic acid. II. Reaction of algin acetates with calcium and other divalent ions. J. Org. Chem. 27, 1789-1791. DOI 10.1021/jo01052a073

Selby D. and Creaser R.A. (2003) Re-Os geochronology of organic rich sediments: an evaluation

of organic matter analysis methods. Chem. Geol. 200, 225-240. DOI 10.1016/S0009-2541(03)00199-2

Sharma M. and Wasserburg G.J. (1997) Osmium in rivers. Geochim. Cosmochim. Acta 61, 5411-5416.

Sheppeard H. and Ward D.J. (1980) Intra-articular osmic acid in rheumatoid arthritis: five years' experience. Rheumatol. Rehabil. 19, 25-29. DOI 10.1093/rheumatology/19.1.25

Silvaprakash B. Rajamohan N. and Sadhik A.M. (2010) Batch and column sorption of heavy metal from aqueous solution using a marine alga *Sargassum tenerrimum*. Int. J. ChemTech Res. 2, 155-162.

Stein H.J. (2014) Dating and tracing the history of ore formation. 2nd ed, Oxford: Elsevier.

Steinbüchel A. and Rhee S.K. (2005) Polysaccharides and polyamides in the food industry.

Strömgren T. (1977) Short-term effect of temperature upon the growth of intertidal Fucales. J. Exp. Mar. Biol. Ecol. 29. DOI 10.1016/0022-0981(77)90047-8

Sundram F. Chau T.C. Onkhuundai P. Bernal P. and Padhy A. (2004) Preliminary results of transarterial rhenium-188 HDD lipiodol in the treatment of inoperable primary hepatocellular carcinoma. Eur. J. Nucl. Med. Mol. I. 31, 250-257. DOI 10.1007/s00259-003-1363-2

Survey U.S.G. (2010) Metals and minerals: U.S. Geological Survey Minerals Yearbook.

Sutulov A. (1967) Molybdenum and Rhenium Conception. University of Concepcion.

Tagami K. and Uchida S. (2005) A comparison of concentration ratios for technetium and nutrient uptake by three plant species. Chemosphere 60, 714-717. DOI 10.1016/j.chemosphere.2005.03.087

Tubbing D.M.J. Admiraal W. Cleven R.F.M.J. Iqbal M. van de Meent D. and Verweij W. (1994) The contribution of complexed copper to the metabolic inhibition of algae and bacteria in synthetic media and river water. Water Res. 28, 37-44. DOI 10.1016/0043-1354(94)90117-1

Turner A. Pedroso S.S. and Brown M.T. (2008) Influence of salinity and humic substances on the uptake of trace metals by marine macroalga, *Ulva lactuca*: experimental observations and modelling using WHAM. Mar. Chem. 110, 176-184. DOI 10.1016/j.marchem.2008.04.003

Veena K.C. Josephine A. Preetha S.P. and Varalakshmi P.(2005) Beneficial role of sulphated polysaccharides from edible seaweed *Fucus vesiculosus* in experimental hyperoxaluria. Food Chem. 100(2007), 1552-1559

Velásquez L. and Dussan J. (2009) Biosorption and bioaccumulation of heavy metals on dead and living biomass of *Bacillus sphaericus*. J. Hazard. Mater. 167, 713-716. DOI 10.1016/j.jhazmat.2009.01.044

Venetskii S.I. (1974) Osmium. Metallurgist 18, 155-157.

Viana I.G. Fernandez J.A. Aboal J.R. and Carballeira A. (2011) Measurement of δ^{15}N in macroalgae stored in an environmental specimen bank for regional scale monitoring of eutrophication

in coastal areas. Ecol. Indic. 11, 888-895. DOI 10.1016/j.ecolind.2010.12.004

Volesky B. (1990) Removal and recovery of heavy metals by biosorption, in: Press, C. (Ed.), Biosorption of Heavy Metals, Boca Raton, FL, pp. 7-44.

Wang T. Jonsdottir R. Liu H. Gu L. Kristinsson H.G. Raghvan S. and Olafdottir G. (2012) Antioxidant capacities of phlorotannins extracted from the brown algae *Fucus vesiculosus*. J. Agr. Food Chem. 60, 5874-5883. DOI 10.1021/jf3003653

Wang W.X. and Dei R.C.H. (1999) Kinetic measurements of metal accumulation in two marine macroalgae. Mar. Biol. 135, 11-23. DOI 10.1007/s002270050596

Wedepohl K.H. (1995) The composition of continental crust. Geochim. Cosmochim. Acta 59, 1217-1232. DOI 10.1016/0016-7037(95)00038-2

White N. (2008) *Fucus vesiculosus*. Bladder wrack., in: [on-line]., M.L.I.N.B.a.S.K.I.S.-p. (Ed.), Plymouth: Marine Biological Association of the United Kingdom. Accessed January 2015

Wildung R.E. Li S.W. Murray C.J. Krupka K.M. Xie Y. Hess N.J and Roden E.E. (2004) Technetium reduction in sediments of a shallow aquifer exhibiting dissimilatory iron reduction potential. FEMS Microbiol. Ecol. 49, 151-162.

Xiong Y. Xu J. Shan W. Lou Z. Fang D. Zang S. and Han G. (2013) A new approach for rhenium(VII) recovery by using modified brown algae *Laminaria japonica* absorbent. Bioresource Technol. 127, 464-472. DOI 10.1016/j.biortech.2012.09.099

Yamashita Y. Takahashi Y. Haba H. Enomoto S. Shimizu H. (2007) Comparison of reductive accumulation of Re and Os in seawater–sediment systems. Geochim. Cosmochim. Acta 71, 3458–3475. DOI 10.1016/j.gca.2007.05.003

Yang J.S. (1991) High rhenium enrichment in brown algae: a biological sink of rhenium in the sea? Hydrobiologia 211, 165-170. DOI 10.1007/BF00008532

Zhao Y. Hao Y. and Ramelow G.J. (1994) Evaluation of treatment techniques for increasing the uptake of metal ions from solution by nonliving seaweed algal biomass. Environ. Monit. Assess 33, 61-70. DOI 10.1007/BF00546662

Zumdahl S.S. (1992) Chemical Principles D.C., Canada.

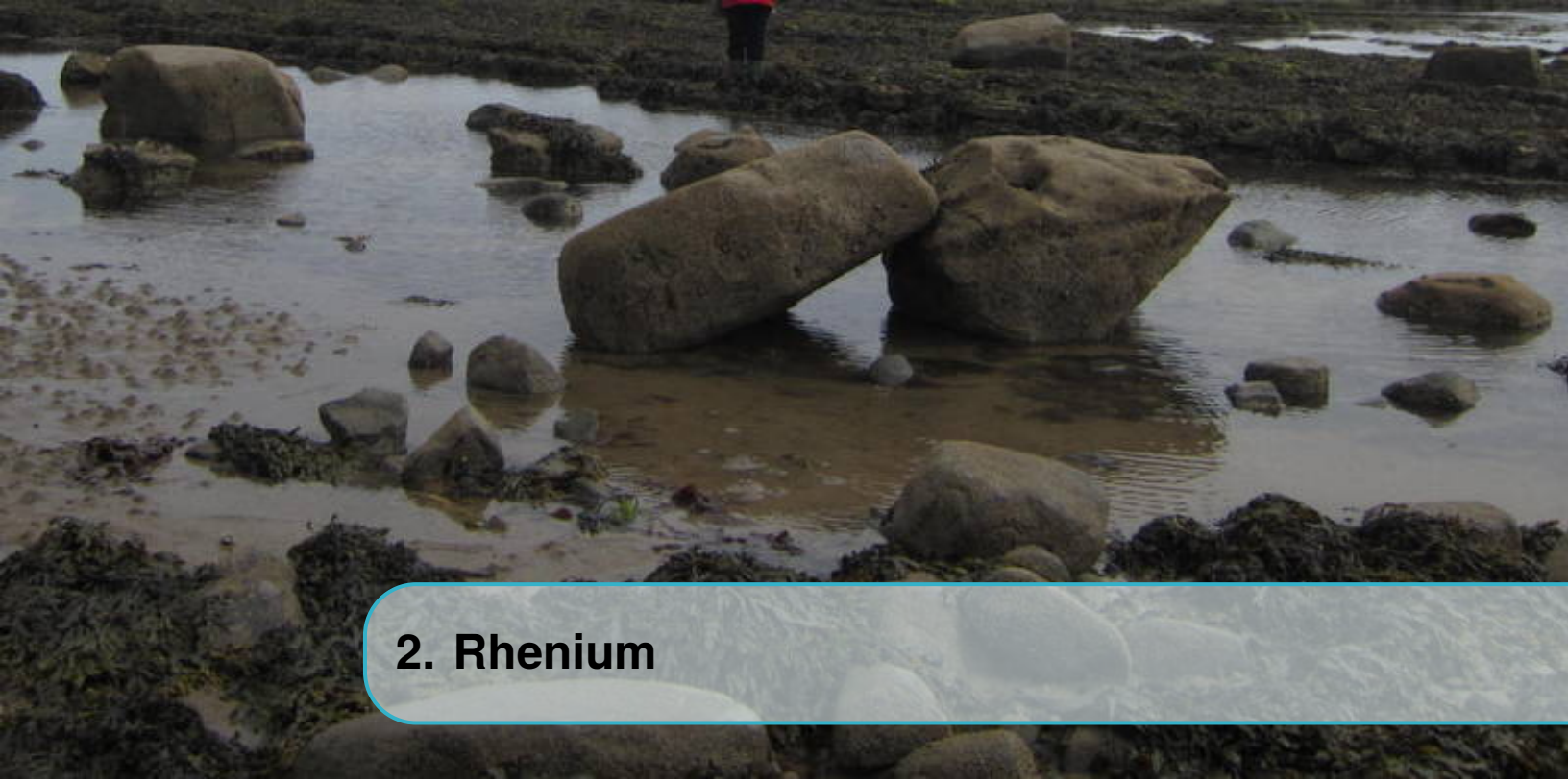

2. Rhenium

From manuscript published in Royal Journal of Open Science, 2016, enclosed in appendix E.

Rhenium uptake and distribution in Phaephyceae macroalgae, *Fucus vesiculosus*

B. Racionero-Gómez[1], A.D. Sproson[1], D. Selby[1], D.R. Gröcke[1], H. Redden[1,2] and H.C. Greenwell[1,2]

[1] Department of Earth Sciences, Durham University, Durham, DH1 3LE, UK.

[2] Department of Chemistry, Durham University, Durham, DH1 3LE, UK.

Correspondence to:

B. Racionero Gómez (blancaraci@gmail.com telephone: +34646976656)

H. C. Greenwell (chris.greenwell@durham.ac.uk telephone: +441913342324)

Keywords Rhenium, macroalgae, uptake, distribution, phytomining, bioremediation

Abstract

Owing to Re having no known biological role, it is not fully understood how Re is concentrated in oil kerogens. A commonly held assumption is that Re is incorporated into decomposing biomass under reducing conditions. However, living macroalgae also concentrates Re to several orders of magnitude greater than that of seawater. This study utilizes *Fucus vesiculosus* to assess Re uptake and its subsequent localization in the biomass. It is demonstrated that the Re abundance varies within the macroalgae and that Re is not located in one specific structure. In *F. vesiculosus*, the uptake and tolerance of Re was evaluated *via* tip cultures grown in seawater of different Re(VII) compound concentrations (0 to 7450 ng/g). A positive correlation is shown between the concentration of Re doped seawater and the abundance of Re accumulated in the tips. However, significant differences between Re(VII) compounds are observed. Although the specific cell structures where the Re is localized is not known, our findings suggest that Re is not held within chloroplasts or cytoplasmic proteins. In addition, metabolically inactivated *F. vesiculosus* does not accumulate Re, which indicates that Re uptake is *via* syn-life bioadsorption/bioaccumulation and that macroalgae may provide a source for Re phytomining and/or bioremediation.

2.1 Introduction

The behaviour of rhenium (Re) in seawater is explained in page 14, third paragraph (section 1.2.1) and the interaction of Re with macroalgae is explained in page 27, first paragraph (section 1.7).

Assuming that Re is being stored inside the macroalgae cells, a mechanism for Re uptake into the cells should be identifiable. Macroalgae could inadvertently take up ReO_4^- (ionic radius of 2.60 Å) by confusing it for phosphate (PO_4^{3-}) (ionic radius of 2.38 Å). A similar mechanism is proposed for arsenate (AsO_4^{3-}) (Klumpp, 1980). Sulphate (SO_4^{2-}), nitrate (NO_3^-) and chloride (Cl^-) aslo have similar ionic radius to ReO_4^- (i.e. 2.58 Å, 1.96 Å and 1.81 Å, respectively). Thus these ions could also compete with ReO_4^-. For instance (Tagami and Uchida, 2005) showed that there is a positive correlation between K^+ and technetium (Tc) accumulated in three plant species (*Cucumis sativus L., Raphanus sativus L.* and *Brassica chinensis L.*) and explained this as a result of TcO_4^- being taken up following the same mechanism as for Cl^-, as a counter ion for K^+ uptake. As Re is a Tc analogue (Harvey *et al.*, 1991; Tagami and Uchida, 2005; Yang, 1991), ReO_4^- might be taken up in a similar manner. In addition, competitive incorporation between ReO_4^- and NO_3^- in sodalites has also been found (Dickson *et al.*, 2014), however, as sodalite is a mineral, ReO_4^- incorporation cannot be compared with ReO_4^- concentration in biologically active organisms.

Importantly, understanding the uptake of Re will help to elucidate the uptake of Tc, which is produced in nuclear power stations. Moreover, a better knowledge on the uptake mechanism could open the possibility to use macroalgae as bioconcentrators of Re and Tc, thus bioremediation of

Tc contaminated waters and phytomining of Re could be achieved using *F. vesiculosus*, as well as potentially providing an alternative hypothesis for the high concentration of Re within oil forming kerogens.

This study uses a brown macroalgae (Phaeophyceae) to establish: (i) where Re is stored; (ii) the limit of Re uptake; and (iii) the uptake mechanism of Re (i.e. active concentration in which the transport requires energy to oppose the concentration gradient, or passive concentration, with transport requiring no energy and entirely correlated with the concentration). The Re abundance data for the different structures of *F. vesiculosus*: holdfast, stipe, fertile tips, non-fertile tips, vesicles and blades (Figure 2.1), and isolated cytoplasmic proteins and chloroplasts is investigated. The uptake limit of Re in macroalgae is determined *via* cultures of *F. vesiculosus* under different ReO_4^- concentrations and using different ReO_4^- chemical compounds (i.e. $HReO_4$ (Re metal dissolved in HNO_3), $KReO_4$, $NaReO_4$ and NH_4ReO_4). Cultured versus dead macroalgae were used to provide insight into the uptake mechanism of ReO_4^- by macroalgae.

2.2 Materials and methods

2.2.1 Macroalgae used in the study: *Fucus vesiculosus*

Explained in page 19 (section 1.3.1).

2.2.2 Macroalgae collection sites

Five specimens of *F. vesiculosus* were collected from Staithes, North Yorkshire, UK (54°33'N 00°47'W) in May, 2014. These samples were used to determine the Re abundance of specific structures of the macroalgae. An additional six samples were collected each month at Boulmer Beach, Northumberland, UK (55º25'N 1º34'W) in May, June, October and November in 2014, and January to June in 2015, for fertile and non-fertile tip separation, all the culture experiments, chloroplast isolation and protein purification.

2.2.3 Rhenium abundance and distribution in macroalgae structures

Prior to analysis all specimens were kept individually in plastic sample bags for transport, and stored in a freezer (-10 ºC) for 48 h. Each specimen was washed and soaked in deionised (Milli-Q^{TM}) water to remove any attached sediment and salt. To establish the abundance and distribution of Re in the macroalgae the sample was divided into different structural components; fertile tips, non-fertile tips, vesicles, stipe, holdfast, blades (Figure 2.1). In addition, all the algae components were mixed to assess an average Re abundance. Each structure was dried in an oven at 60 ºC for 12 h.

2.2.4 Rhenium uptake of macroalgae

To investigate the uptake of Re by macroalgae, non-reproductive apical thallus tips of nine *F. vesiculosus* specimens (length = > 1.5 cm; wet weight (WW) = 0.12–0.15 g), without visible

microalgae (i.e. epiphytes), from Boulmer Beach were cultured in seawater (modified after Gustow *et al.* (2014)) with a known concentration of Re. In brief, the culture experiments were performed using a 250 mL glass jar containing two mesh shelves. Three tips were placed in the bottom of the jar and three tips to each mesh, having in total nine tips, with each set of tips taken from a different specimen (Figure 2.2). All jars were filled with sterile filtered (0.7 μm) seawater from Boulmer Beach. A huge diversity of macroalgae grow naturally at Boulmer Beach, thus water obtained at Boulmer is expected to be nutrient replete as it permits the growth of a wide variety of species. Each set of three jar replicates were doped using a known volume of ReO_4^- from different Re compounds: an already prepared solution of Re metal with nitric acid ($HReO_4$) (i.e. 83787 Sigma Aldrich) or commercially obtained Re(VII) salts ($KReO_4$, NH_4ReO_4 and $NaReO_4$).

HNO_3 dissolves Re metal forming $HReO_4$, (Gaines, 2014). For the cultures using $HReO_4$, Boulmer seawater ReO_4^- concentration was analysed. The Re abundance in the seawater was determined by isotope dilution ICP-MS (details below). The seawater possessed a Re abundance of 0.007 ng/g (6.95 ± 0.19 pg/g) consistent with the concentrations reported by Anbar *et al.* [2]. The seawater culture experiments were conducted in Re concentrations are equal to that of seawater, and 10×, 50×, 100×, 500×, 1000×, 2667×, 10000×, 133333× and 266667× that of the concentration of seawater (i.e. 0.007 ng/g, 0.075 ng/g, 0.373 ng/g, 0.745 ng/g, 3.725 ng/g, 7.450 ng/g, 20 ng/g, 75 ng/g, 1000 ng/g and 2000 ng/g, respectively). In addition, three jars were filled with artificial seawater that was not doped with Re, and one jar was doped with a concentration a million times that of the Re seawater concentration in order to reach an extreme concentration of 7450 ng/g.

For the cultures using Re(VII) (perrhenate) salts, the same approach was used, where the doped Re concentrations of seawater in the cultures were 10×, 50×, 100× and 1000× that of seawater (i.e. 0.075 ng/g, 0.373 ng/g, 0.745 ng/g and 7.45 ng/g, respectively).

To reduce evaporation, while allowing gaseous exchange with the atmosphere, all the jars were loosely covered with lids. No additional nutrients were added into the seawater or artificial seawater. The algae tips inside the bottles were transferred into an incubator with a set light/dark rhythm of 16:8, light intensity of 125 μmol photons/m^2s^2 and a temperature of 11ºC. The wet weight (WW) of the algal tips, per jar, was measured every 2–3 days during 25 days of the culturing period for all cultures except the cultures of June 2015, which only lasted 15 days. At the same time, the media was changed (between 4 and 7 times for all cultures) to avoid accumulation of metabolites and replenish nutrients. The salinity (~35 ppt) of the Re doped seawater did not appreciably change from that of natural seawater collected from Boulmer and remained constant throughout the culture experiments. The pH (~9.0), however, changed from that of the natural seawater collected from Boulmer (~8.2) due to the metabolic activity of the macroalgae (photosynthesis)and remained constant throughout the culture experiments.

Two additional sets of culture experiments were conducted to establish if ReO_4^- is taken up by

syn-life bioabsorption/bioaccumulation or passive processes. Understanding syn-life bioaccumulation and bioabsorption as the biological sequestration of substances or chemicals through any route at a higher concentration than that at which it occurs in the surrounding environment/medium when macroalgae is metabolically active (i.e. alive) (U.S. Geological Survey, 2007). Therefore, in order to assess bioaccummulation, non-reproductive thallus tips were killed through either boiling, drying or freezing. Specifically, non-reproductive thallus tips (n = 81) from Boulmer Beach were heated for 2 h at 100 ºC, and a further 21 tips were heated at 100 ºC for only 5 min. Additionally, 21 non-reproductive thallus tips were air dried for 72 h and another 21 tips were frozen with liquid nitrogen. In total, 18 jars were filled with sterile (i.e. autoclaved at 121 ºC for 30 min) and filtered (0.7 μm) seawater from Boulmer Beach. The jars containing boiled tips were divided into three subgroups composed of three replicates of each with the following treatments: seawater and seawater doped with 7.45 ng/g of $HReO_4$. The other set of three replicates containing dried, boiled (5 min) or frozen non-reproductive thallus tips, respectively, were only treated with seawater spiked with 7.45 ng/g $HReO_4$.

In order to re-confirm the uptake mechanism, four tips were placed in the bottom of the jar and four tips to each mesh, having in total 12 tips of different specimens in each jar. All jars were filled with sterile filtered (0.7 μm) seawater from Boulmer Beach and doped with 7.45 ng/g $NaReO_4$. After 3 days the media solution was changed and set to 0.075 ng/g of $NaReO_4$ and, finally, after another 3 days the media solution was changed and not doped. Prior to each change of the media four sample tips were taken for Re analysis.

2.2.5 Chloroplast isolation

A procedure modified from Popovic *et al.* (1983) was used for the isolation of chloroplasts. Approximately 10 g of non-reproductive thallus tips were cut into 2 mm^2 pieces using scissors. These were washed by stirring with 2 L of filtered seawater with 75 mL of grinding medium added. The grinding medium consisted of 1 M sorbitol, 2 mM $MnCl_2$, 1 mM $MgCl_2$, 0.5 mM K_2HPO_4, 5 mM EDTA, 2 mM $NaNO_3$, 2 mM ascorbate, 2 mM cysteine, 0.2% (w/v) BSA and 50 mM of MES buffer (pH 6.1). All the subsequent steps were undertaken in ice water. The washed tissue was divided into two portions, each ground with a mortar and pestle, increasing gradually the volume to 50 mL. Then, each portion was diluted into 100 mL of medium and passed through a stainless steel strainer and four layers of cheese cloth. Chloroplasts were isolated by centrifugation for 7 min at 5500 G. The pellet was re-suspended with 10 mL of a reaction medium containing 1 M sorbitol, 1 mM $MnCl_2$, 1 mM $MgCl_2$, 2 mM EDTA, 0.5 mM K_2HPO_4 and 50 mM HEPES (pH 8.1). Another centrifugation at 5500 G for 7 min was performed and chloroplasts were re-suspended with 2 mL of HEPES buffer. To test the isolation, the absorbance spectrum of the last solution obtained was observed under a light microscope. The extracted chloroplasts were preserved using HEPES (as it does not contain Re) and stored in a fridge for 3 days. In order to remove HEPES from the chloroplasts the HEPES-chloroplast

mixture was centrifuged. The chloroplast pellet was white-brown and the HEPES solution was green-brown. The observation showed that the pigments had released and were free in the solution.

2.2.6 Cytoplasmic proteins isolation

A procedure modified from Boer *et al.* (1986) was employed for the isolation of cytoplasmic proteins. Approximately 2 g of freshly ground non-reproductive thallus tips were used for protein extraction. The tips were mixed with 9 mL of 10 mM HEPES (pH 7.8) buffer, vortexed and centrifuged twice at 1000 G for 1 min. The homogenate was sonicated for 1 min, 10 times and centrifuged at 4500 G for 5 min. The supernatant was centrifuged at 14000 G for 10 min. A 60 mM saturated $CaCl_2$ solution was used to re-suspend the pellet, which was agitated and then centrifuged at 14000 G for 5 min. The supernatant was then separated *via* gel filtration (i.e. size exclusion column chromatography). A PD-10 Desalting Column containing Sephadex G-25 Medium as matrix was used to separate molecules from the supernatant by their molecular size. Larger molecules than the Sephadex matrix pores are eluted first and smaller molecules than the matrix pores are eluted later, depending on the molecular size, the molecules will penetrate the matrix pores to varying extent. The separation was carried out following the gravity protocol detailed in PD-10 Desalting Colums Instructions (GE Healthcare, 2007) using the same buffer described above. 1 mL elution fractions obtained were analysed by ICP-MS (Inductively Coupled Plasma Mass Spectrometry) after being diluted 10 times with 0.8 N HNO_3. Protein content of the fractions was analysed based on the absorbance shift of the dye Coomassie Brilliant Blue G-250.

2.2.7 Re abundance determinations and data treatment

Rhenium abundance determinations for all samples were obtained at the Durham Geochemistry Centre in the Laboratory for Sulphide and Source Rock Geochronology and Geochemistry. Each sample of *F. vesiculosus* was oven-dried at 60 ºC for 24 h and ground into a powder with an agate mortar and pestle. Approximately 100 mg of the sample powder was spiked. Abundances were obtained by both direct calibration and isotope-dilution methodologies (Table 1, 2, 3, 4 and 5). For the latter samples were doped with a known amount of ^{185}Re tracer solution (isotope dilution methodology). The sample and if used, the tracer solution, were digested in a mix of 3 ml of 12 N HCl and 6 ml of 16 N HNO_3 at 120 ºC overnight in a PFA Savillex 22 mL vial. The dissolved sample solution was evaporated to dryness at 80 ºC. The rhenium abundance of seawater from Boulmer Beach was determined by isotope dilution-ICP-MS. Approximately 30 mL of seawater was doped with a known amount of ^{185}Re tracer solution and evaporated. The rhenium fraction was further purified using standard anion chromatography methodology. Rhenium for all macroalage samples was isolated from the dried sample using 5 mL 5 N NaOH 5 mL acetone solvent extraction procedure (Cumming *et al.*, 2013; Prouty *et al.*, 2014). The Re-bearing acetone was evaporated to dryness at 60 ºC. For ICP-MS the dried Re fraction was dissolved in 1.2 mL of 0.8 N HNO_3. For thermal ionization mass spectrometry in negative ion mode (N-TIMS) analysis the purified Re fraction was loaded onto

a Ni wire filament, with the Re isotope compositions determined using Faraday cup measurements on a Thermo Scientific TRITON mass spectrometer. Total procedural blanks are 1 ± 0.1 pg (n = 6). For samples analysed by isotope dilution to determine absolute Re abundance, all sources of uncertainty (e.g., standard measurement, isotope measurement, calibration of the tracer solution, fractionation correction and blank values) are propagated to yield a final uncertainty. For direct calibration, prior to each analysis, an instrument performance check confirm satisfactory performance of the ICP-MS. Five freshly prepared standards were made each time and formed calibration lines with an R value > 0.999 and < 2% RSD uncertainty. Moreover, all the samples had a reproducibility of < 5% RSD.

Statistical analysis, t-test and Tukey's HSD tests, using a significance level of 0.05, were performed using R Studio software. For testing the statistical hypothesis, p-values are used. The p-value is defined as the probability of obtaining a result more extreme or equal to what was actually observed, thus, if p-value is smaller or equal to the significance level, it suggests that the observed data are consistent with the hypotheses.

2.3 Results

2.3.1 Location of Re within *F. vesiculosus* structures

All analyzed structures of *F. vesiculosus* are naturally enriched in Re by approximately one thousand times the concentration found in seawater (Figure 2.1). The contents of Re range from 23 to 313 ng/g (Figure 2.1). Significant differences were observed (p-value: 0.02) between the five samples of macroalgae tips (~126 ng/g) and the sample representing a mix of the plant components (~74 ng/g). Further, significant differences were also observed (p-value: 0.003) between fertile (~123 ng/g) and non-fertile tips (~313 ng/g) (Figure 2.1).

2.3.2 Uptake of Re by *F. vesiculosus* culture tips

The natural Re abundance of the seawater collected from Boulmer Beach and utilized for the culture experiments is 6.95 ± 0.19 pg/g (~0.007 ng/g), which is in agreement with previous studies of coastal waters (Anbar *et al.*, 1992). The results shown in Figures 2.3, 2.4 and 2.5 indicate that, in 25 days, the Re content of the macroalgae increased proportionally to the amount of Re species doped in the seawater. However, variation in the uptake capacity by *F. vesiculosus* of the different ReO_4^- compounds doped in seawater is observed. Moreover, a significant variation (p-value < 0.05) in uptake capacity between months of collection (i.e. February, March, May and June cultures with Re(VII) salts) was observed only after 0.37 ng/g of doped Re(VII) in the media. March cultures accumulated ~7000 ng/g more Re than February, May and June culture tips (Table 2.6). Moreover, cultures doped with $HReO_4$ and Re(VII) salts also show different amounts of accumulation. The accumulation of Re in *F. vesiculosus* grown with all Re(VII) salts is significantly lower (p-value < 0.05) than the accumulation obtained with cultures made with $HReO_4$, also only after 0.37 ng/g of doped Re to the media (Figure 2.3). It is observed that cultures in Re doped solution made from

$HReO_4$ take up 50% of the amount of Re in seawater, in contrast to only 0.03–15% for solution doped with Re from Re(VII) salts (Table 2.6). Because of this, cultures with high concentrations of ReO_4^- in the media were made only with $HReO_4$. A linear correlation is observed between the amount of Re doped in the cultures and the accumulation of Re in the alive cultured macroalgae until an accumulation of 63284 ng/g of Re was reached, after which Re uptake ceased as the macroalgae died (Figure 2.4). We also observed that there is a limit on the uptake of Re in the cultured macroalage between 75 and 1000 ng/g of $HReO_4$ in the seawater media. Furthermore, visually the macroalgae tips grown in high concentrations (2000 and 7450 ng/g) did not seem as metabolically active as those in lower concentrations. In total, macroalgae tips extracted up to ~60000 ng/g of Re in 25 days (see Figure 2.4 and 2.5).

F. vesiculosus non-fertile tips under 7.45 ng/g of $NaReO_4$ in the media, after 3 days were capable of accumulating ~150 ng/g more than the background Re concentration in them (Figure 2.6). These tips were then transferred to subsequent lower concentrations of $NaReO_4$ (0.075 and 0.007 ng/g) and exhibited accumulations of ~100 ng/g more than the background concentration of Re. Therefore, a release of 50 ng/g was found after transference (Figure 2.6).

In comparison to living organism samples, *F. vesiculosus* non-fertile thallus tips metabolically deactivated by boiling, freezing with liquid nitrogen or drying showed appreciably little to no accumulation of Re (between 36 and 19 ng/g) compared to the concentration reached in fresh tips (i.e. alive) (~16000 ng/g) with same $HReO_4$ concentrations in the media of 7.45 ng/g (see Figure 2.7). Also, the majority of the Re content in the macroalage was released in the media within the first 2–3 days of the experiment and the media turned brown.

2.3.3 Chloroplast isolation

Chloroplasts were isolated from *F. vesiculosus* non-fertile tips. The non-fertile tips as a whole contain between 100 and 200 ng/g of Re. Chloroplasts are found throughout the whole macroalgae organism, although exist in greater abundance in the non-fertile tips. Both the HEPES solution and the chloroplast pellet were analyzed. 1 ng/g of Re was detected in the chloroplast extract, and 3 ng/g of Re detected in the HEPES solution in which the chloroplasts were stored (Table 2.7). Regardless of the difficulty in isolating the chloroplast, less than 1% of the Re is present in the chloroplast relative to the host structure (non-fertile tips) which posses ~150 ng/g.

2.3.4 Cytoplasmic proteins purification

Cytoplasmic proteins (~48 μg) were purified from 2 g of wet (i.e. 0.6 g dry) *F. vesiculosus* non-fertile tips. Proteins possess sizes in excess of 5 kDa, and were only found in fractions 4 to 6 eluting (1 ml fractions were collected with a G25 column). No Re was observed in the elutions containing the proteins (Figure 2.8). However, a total amount of ~200 ng of Re was eluted from the chromatography from cycles 10 to 14 with other unknown particles smaller than 5 kDa. Given the total volume

of macroalgae used for the isolation of the protein (i.e. 0.6 g of dry weight) this equates to a concentration of ~300 ng/g Re, as it is between the range of Re expected to be in the non-fertile tips, it can be stated that all Re from the tips structures was eluted.

2.4 Discussion

2.4.1 Localization of Re within *F. vesiculosus* structures

The apical growth in the Phaeophyceae family is thought to occur by division of cells in cylindrical directions, with daughter cells generating a parenchymatous tissue construction (Graham and Wilcox, 2000). Parenchyma tissue cells are capable of cell division if stimulated and can differentiate into specialized cells for photosynthesis, reproduction, growth and nutrient uptake. In Phaeophyceae, it is possible to distinguish five types of cells: epidermal cells, primary cortical cells, secondary cortical cells, medullary cells and hyphae (Davy de Virville and Feldmann, 1961). The non-fertile tips are the apical meristems of *F. vesiculosus*. Therefore, it is composed of cells that can divide and differentiate, including photosynthetic cells. Although there is variability between the different macroalgae specimens collected, the relative levels of Re vary significantly within the macroalgae structures. There are significant differences (p-value < 0.05) between the amount of Re stored in the tips (~126 ng/g) *versus* Re stored in the remainder of the macroalgae (~74 ng/g) (Figure 2.1). Furthermore, significant concentration of Re is found in the non-fertile tips which suggests a link between Re and the meristematic and photosynthetic specialized cells. More specifically, an average concentration of 313 ng/g of Re was found in the non-fertile tips, 122 ng/g Re in the fertile tips, 67 ng/g Re in the blades, 66 ng/g Re in the vesicles, 23 ng/g Re in the stipe and 21 ng/g Re in the holdfast. This suggests that Re is most likely to be stored in the photosynthetic structures and it is not involved in the reproductive structures (receptacles). In herbaceous plants, the distribution of Re is also higher in photosynthetic structures, with 86% of the plant Re reported to be at the leaves (Bozhkov *et al.*, 2006). Bozhkov and Borisova (2002) stated that, in plants, Re is accumulated in chlorophylls forming $Mg(ReO_4)_2$. However, no Re was found in the chloroplasts of *F. vesiculosus*, thus our study suggests that Re is not strongly bound by/to chlorophylls. The concentrations of Re in the chloroplast extraction and the HEPES solution where the chloroplasts were stored are 1 and 3 ng/g of Re, respectively (See Table 2.7). These concentrations are very low, much lower than the concentrations expected given the observed concentration on the tip structures (~100 ng/g).

It should be emphasized that the data in Table 2.1 shows that there is Re in all parts of *F. vesiculosus*, i.e. Re is not locally concentrated into a single structure, or a small number of structures, which means that Re is present in all cell types. In previous studies, it was demonstrated that the cell surface is not the main accumulation site of Re in the brown macroalgae *Pelvetia fastigiata* (Yang, 1991). As a result it would be expected that Re enters into the cell and remains in the cytoplasmic or a cell compartment. Moreover, Xiong *et al.* (2013) made a macroalgae cell gel by chemically modifying brown macroalgae with sulphuric acid obtaining a gel of the macroalgae alginate and

fucoidan matrix. The resulting gel had a high Re affinity and it was stated that amino acids were taking part in Re absorption, as it was observed in the IR spectroscopy that the intensity of the peaks corresponding to amino $–NH_2$ groups decreased after adsorption. Moreover, this fact was supported by removal of the amino acids of the gel (i.e. previously boiling the brown algae) which showed no adsorption of Re. Thus, this could mean that Re is not found in the cell wall in macroalgae, but interacts with cell membrane proteins or other molecules that contain $–NH_2$ groups in the cell, while not interacting with cytoplasmic proteins (see Figure 2.8). As in this present study, no disruption of the membranes was done it cannot be assumed that membrane bound proteins were simultaneously extracted. Moreover, the method for protein detection used does not detect free amino acids, peptides (i.e. glutathione, metallothioneins and phytochelatins) and proteins smaller than 3 kDa. Thus, it cannot be stated absolutely that Re is not protein bound because we cannot be sure to have isolated all the proteins. However, it can be stated that it is not related to cytoplasmic proteins larger than 3 kDa or, if it is, the Re binding of the protein is sufficiently weak that the analytical protocol for protein isolation is capable of breaking any Re protein associated bond.

2.4.2 Comparison of perrhenate compounds ($HReO_4$, $NaReO_4$, $KReO_4$ and NH_4ReO_4) uptake by cultured *F. vesiculosus* tips

A sorption study of Re onto organic polymers was undertaken by Kim *et al.* (2004), who concluded that negatively charged perrhenate ions interacted with protonated amine groups in chitosan. The authors explain the adsorption by a combination of a Langmuir-Freundlich type mechanism and the electric diffuse double layer model. Our experiments show that all perrhenate salts have the same linear trendline (Figure 2.3A) which strongly differs from perrhenate obtained from $HReO_4$ (Figure 2.3B). This unexpected result highlights the importance of the chemical species of Re compound used for doping, which we further discuss below.

Perrhenate salts ($NaReO_4$, $KReO_4$ and NH_4ReO_4) are highly soluble in water with solubilities around 1.1 g/mL. It has been observed that cations are used as a symport for perrhenate uptake in animal cells (Tagami and Uchida, 2005). Our results seem to show that H^+ is the best counter ion for perrhenate uptake, therefore a greater uptake is observed when $HReO_4$ is used. Moreover, H^+ could be increasing the conversion of $–NH_2$ groups of the macroalgae to $–NH_3{}^+$, thus allowing perrhenate to bind. Therefore more polymers of glucosamine and amino groups in *F. vesiculosus* (Nishino *et al.*, 1994; Xiong *et al.*, 2013) could be positively charged allowing more perrhenate binding, as it has been observed that perrhenate interacts strongly with polymers of glucosamine [17] and amino groups (Xiong et. al., 2013). Although the difference of such discrepancy cannot be resolved here, uptake of $ReO_4{}^-$ is observed no matter the what form of perrhenate compound used. The mechanisms that control Re entry into the cells of macroalgae have not been identified. There are many reports studying cation metal transporters, (Cobbett *et al.*, 2003; Mäser *et al.*, 2001; Williams *et al.*, 2000), but little is known about anion transporters (pumps) of macroalgae. Phosphate, chloride,

sulphate, nitrate and molybdate transporters are all anion transporters reported in cells. Macroalgae could take up Re as perrhenate instead of other substrates of these transporters. Other trace metals in seawater exist, rather than as the free metal ion, as oxo-anions (e.g., perrhenate, chromate, vanadate, molybdate, arsenate). The existing active transport pumps (e.g. sulphate, nitrate, phosphate) could be taking up such metal oxo-anions or there could be metal-specific pumps (Dallinger and Rainbow, 1993). It has been observed that arsenate and phosphate have a common mechanism of uptake in bacteria and yeast (Rothstein and Donovan, 1963), but not in phytoplankton (Andrae and Klumpp, 1979) and brown macroalgae (Klumpp, 1980), although high concentrations of phosphate inhibit the uptake of arsenate. Nitrate could be also competing with perrhenate. However, this has only been observed for the mineral sodalite, and not in living organisms (Dickson *et al.*, 2014).

The seasonal Re(VII) salt uptake variation of cultures (Table 2.6) suggest that perrhenate uptake is biologically influenced. Riget *et al.* (1995), observed that zinc obtained maximum concentrations in macroalgae in March and a minimum in September, and it was similarly observed, albeit less clearly, with lead and copper. Macroalgae growth is the most likely cause for seasonal variations in metal uptake (Fuge and James, 1973; Riget *et al.*, 1995). Although our studies seem to support this theory, a monthly perrhenate uptake research should be done in order to confirm it more strongly and decipher if it is simply a dilution effect or if perrhenate has a real metabolic role in the macroalgae. Here we did not perform any seasonal experiments using $HReO_4$.

Our study also shows that when non-fertile thallus tips start dying they do not accumulate more Re and start to degrade, thus Re is released to the media (Table 2.6; Figure 2.4). Therefore, less accumulation of Re in those cultured macroalgae tips that started dying is expected. This happened in the macroalgae tips cultured with 2000 and 7450 ng/g of $HReO_4$ in the seawater. In addition, it is worth emphasizing that the more time the dying tips are left in the water, the more Re is released in the seawater by macroalgae (i.e. the less accumulation of Re). Thus, this explains the results obtained in Figure 2.4, where non-fertile thallus tips grown with a concentration of 2000 ng/g of $HReO_4$ accumulate less Re than the ones cultured with 7450 ng/g, because the firsts sets were cultured for 15 more days than the tips grown with 7450 ng/g of $HReO_4$.

Therefore, a good linear correlation fit between $HReO_4$ doped in seawater and Re taken up by *F. vesiculosus* is observed up to 75 ng/g Re in seawater, but with higher concentrations (i.e. 1000, 2000 and 7450 ng/g) there is no linear correlation (Figure 2.4 and 2.5) due to the probable metabolically inactivation of the tips. This indicates that the limit of uptake by the tips occurs when the tips are grown in a media of between 75 and 1000 ng/g of Re.

Phytoaccumulation (or phytoextraction) of metals by plants and algae is widely known (Lasat, 2002), and refers to the concentration of metals from the environment into plant tissues. Plants absorb substances through the root, and then they transport and store these substances into the stems or leaves. There are two types of phytoextraction species: accumulator species and hyperaccumulator species.

The main difference between those two types is stated in Rascio *et al.* (2011). Hyperaccumulator species are able to extract higher concentrations of metals and have a faster root-to-shoot transport system compared to non-hyperaccumulators species without showing phytotoxic effects. However, from the data obtained in this study it cannot be stated that *F. vesiculosus* is a hyperaccumulator species, because the thallus tips grown with the highest concentrations of ReO_4^- started to decrease in growth and die; although they were at concentrations not typical of any environmental setting.

2.4.3 An understanding of Re uptake: active or passive

Figure 2.6 and 2.7 show that Re uptake is not by simple diffusion, as it is observed that only living *F. vesiculosus* tips concentrate Re. Re levels in tips with high Re media concentration (7.45 ng/g) do not decrease when subsequently placed in media with lower Re concentrations. This suggests that the uptake is not driven by simple equilibria. If Re was taken up by simple diffusion we would expect the same uptake of Re after boiling, freezing or drying the tips, as the membranes are not affected, and a direct correlation between the concentration of Re in the solution and in the macroalgae tips would be expected. Although Re could be taken up through passive mediated transport (facilitated diffusion) because, after metabolically inactivating the macroalgae tips, the transport proteins of the membranes are expected to be denatured (as happens when tips are boiled). Thus no uptake is observed. However, this seems unlikely, due to the high Re uptake observed in living *F. vesiculosus* tips relative to the Re concentration in seawater. In addition, our results show that the uptake mechanism is syn-life, therefore Re is bioabsorbed. It can also be concluded that Re is not taken up by simple diffusion, at least for the perrhenate compounds used here. And, finally, Figure 2.6, shows that the uptake mechanism of the macroalgae is unidirectional, not a simple partition, as we observe that once living *F. vesiculosus* has accumulated Re, it does not release it back to the media.

2.4.4 Implications of bioaccumulation of Re

Our results show little to no Re accumulation by metabolically inactivated *F. vesiculosus*. Thus, if this is the case for macroalgae preserved in sediments as organic matter, using Re as a paleo redox may not strictly apply. However, we do suggest that once *F. vesiculosus* has died we may see release back to the water column as the macroalgae breaks down. Thus anoxia may be how the Re is stabilized, through prevention of macroalgae degradation.

Despite *F. vesiculosus* being a non-hyperaccumulator macroalgae, it is seen that until a limit, *F. vesiculosus* can accumulate up to 50000 ng/g when $HReO_4$ was present in the media, recovering the metal from the media. Thus, *F. vesiculosus* could be used as a source of phytomining of Re. Although differences in Re uptake are associated with the form of the perrhenate compounds, all ReO_4^- compounds used here permit the uptake of Re by *F. vesiculosus*. Moreover, as Re is also a Tc analogue (Kim *et al.*, 2004), *F. vesiculosus* could be used for bioremediation of water contaminated with Tc residues, as it has been found in ocean waters near to the Fukushima nuclear accident

(Steinhauser, 2014).

2.5 Conclusions

The observation that macroalgae concentrates Re, an element with no known biological use, raises interesting questions. This study documents the first detailed examination of the relative proportions of Re in the structures of the macroalgae. The following conclusions are drawn from the present study:

i. Re is not solely concentrated into a single macroalgae structure; all the cells possess Re. There is a distribution of Re that increases from the holdfast to the tips. Non-reproductive thallus tips exhibit the most Re accumulation, even more than reproductive thallus tips. As the only difference between them is the reproductive structures (receptacles), we can say that Re is not bound in the reproductive structures.

ii. Our data shows that Re is bioadsorbed by *F. vesiculosus*, rather than bioaccumulated, and does not follow a simple diffusion uptake mechanism. The uptake is unidirectional, not a simple partition. However the data conclusively, *F. vesiculosus* uptakes and stores Re.

iii. Re recovery is observed from the seawater enriched with ReO_4^-, opening the possibility of using *F. vesiculosus* as a source of phytomining.

iv. A difference in the uptake of Re between pherrenate salts and $HReO_4$ is observed. However the cause has yet to be established.

v. The seasonal differences in Re uptake associated with pherrenate salts are a function of *F. vesiculosus* growth.

vi. There is a limit on the uptake of Re in the cultured macroalage between 75 and 1000 ng/g of $HReO_4$ in the seawater media, and beyond that a deleterious effect is observed.

vii. Re is not accumulated in the cytoplasmic proteins or chloroplasts.

Acknowledgements

We wish to express special thanks to Dr Carl Patterson, Dr Deenah Osman and Prof. Nigel Robinson for their help with the protein column preparation, protein analysis and discussions, and to Dr Chris Ottley, Dr Joanna Hesselink and Dr Emily Unsworth for their help with the ICP-MS. We are very grateful to OEA Labs Ltd for funding the project. We thank the School of Biological and Biomedical Sciences of Durham University for the culture experiment facilities. Finally, we acknowledge the constructive remarks by Bernhard Peucker-Ehrenbrink and an anonymous reviewer, which have improved this manuscript.

2.6 References

Anbar A.D. Creaser D.A. Papanastassiou and Wasserburg G.J. (1992) Rhenium in seawater: Confirmation of generally conservative behaviour. Geochimica et cosmochimica Acta 56, 4099-4103. DOI 10.1016/0016-7037(92)90021-A

Andrae M.O. and Klumpp D.W. (1979) Biosynthesis and release of organoarsenic compounds by marine algae. Environ. Sci. Technol. 13, 738–741. DOI 10.1021/es60154a001

Bozhkov O. and Borisova L. (2002) Extraction and determination of trace amounts of Rhenium in plants. Int. J. Environ. An. Ch. 83, 135–141. DOI 10.1080/0306731021000048627

Bozhkov O. Christina T. Borisova L. Ernakov V. and Ryabukhin V. (2006) Study of rhenium accumulation in plants. Trends in Inorganic Chemistry 9, 1–9.

Cobbett C.S. Hussain D. and Haydon M.J. (2003) Structural and functional relationships between type 1B heavy metal-transporting P-type ATPases in Arabidopsis. New Phytol. 159, 315–321. DOI 10.1046/j.1469-8137.2003.00785.x

Cumming V.M. Poulton S.W. Rooney A.D. and Selby D. (2013) Anoxia in the terrestrial environment during the late Mesoproterozoic. Geology 41, 583–586. DOI 10.1130/G34299.1

Dallinger R and Rainbow P.S. (1993) Ecotoxicology of Metals in Invertebrates. CRC Press. Florida.

Davy de Virville A. and Feldmann J. (1961) IV International Symposium on Seaweed. Pergamon Press. Biarritz.

de Boer E. Tromp M.G.M. Plat H. Krenn G.E. and Wever R. (1986) Vanadium(V) as an essential element for haloperoxidase activity in marine brown algae: purification and characterization of a vanadium(V)-containing bromoperoxidase from *Laminaria saccharina*. Bioch. Biophys. Acta 872, 104–115. DOI 10.1016/0167-4838(86)90153-6

Dickson J.O. Harsh J.B. Flury M. Lukens W.W. and Pierce E.M. (2014) Competitive incorporation of perrhenate and nitrate into a soladite Environ. Sci. Technol. 48, 12851-12857. DOI 10.1021/es503156v

Fuge R. and James K.H. (1973) Trace metal concentrations in brown seaweeds, Cardigan Bay, Wales. Mar. Chem. 1, 281–293. DOI 10.1016/0304-4203(73)90018-2

Gaines P. (1985-2014) Sample Preparation Guide [online]. Inorganic Ventures. Christiansburg, Virginia USA. Accessed on December 2015. Available from: http://www.inorganicventures.com/samples-containing-rhenium

GE Healthcare (2007) PD-10 Desalting Columns. Instructions 52-1308-00-88. Uppsala, Sweeden.

Graham L.E. and Wilcox L.W. (2000) Algae. Prentice Hall. New Jersey.

Gustow L. Rahman M.M. Bartl K. Saborowski R. Bartsch I. and Wiencke C. (2014) Ocean

acidification affects growth but not nutritional quality of the seaweed *Fucus vesiculosus* (Phaeophyceae, Fucales). J. Exp. Mar. Biol. Ecol. 453, 84–90. DOI 10.1016/j.jembe.2014.01.005

Harvey B.R. Williams K.J. Lovett M.B. and Ibbett R.D. (1991) Determination of technetium-99 in environmental material with rhenium as a yield monitor. J. Radioanal. Nucl. Ch. 158, 417–436. DOI 10.1007/BF02047127

Kim E, Benedetti M.F. and Boulègue J. 2004 Removal of dissolved rhenium by sorption onto organic polymers: study of rhenium as an analogue of radioactive technetium. Water Res. 38, 448–454. DOI 10.1016/j.watres.2003.09.033

Klumpp D.W. (1980) Characteristics of arsenic accumulation by the seaweeds *Fucus spiralis* and *Ascophyllum nodosum*. Mar. Biol. 58: 257–264. (doi: 10.1007/BF00390774)

Lasat M.M. (2002) Phytoextraction of Toxic Metals: A Review of Biological Mechanisms. J. Environ. Qual. 31, 109–120. DOI 10.2134/jeq2002.1090

Mäser P. Thomine S. Schroeder J.I. Ward J.M. Hirschi K. Sze H. Talke I.N. Amtmann A. Maathuis F.J.M. Sanders D. Harper J.F. Tchieu J. Gribskov M. Persans M.W. Salt D.E. Kim S.A. and Guerinot M.L. (2001) Phylogenetic Relationships within Cation Transporter Families of Arabidopsis. Plant Physiol. 126, 16461–667. DOI 10.1104/pp.126.4.1646

Nishino T. Nishioka C. Ura H. and Nagumo T. (1994) Isolation and partial characterisation of a novel amino sugar-containing fucan sulfate from commercial *Fucus vesiculosus* fucoidan. Carbohyd. Res. 255, 213–224. DOI 10.1016/S0008-6215(00)90980-7

Popovic R. Colbow K. Vidaver W. and Bruce D. (1983) Evolution of O_2 in Brown Algal Chloroplasts. Plant Physiol. 73, 889–892. DOI 10.1104/pp.73.4.889

Prouty N.G. Roark E.B. Koenig A.E. Demopoulos A.W.J. Batista F.C. Kocar B.D. Selby D. McCarty M.D. Mienis F. and Ross S.W. (2014) Deep-sea coral record of human impact on watershed quality in the Mississippi River Basin. Global Biogeochem. Cy. 28, 29–43. DOI 10.1002/2013GB004754

Rascio N. and Navarri-Izzo F. (2011) Heavy metal hyperaccumulating plants: How and why do they do it? And what makes them so interesting? Plant Sci. 180, 169–181. DOI 10.1016/j.plantsci.2010.08.016

Riget F. Johansen P. and Asmund G. (1995) Natural Seasonal Variation of Vadmium, Copper, Lead and Zinc in Brown Seaweed (*Fucus vesiculosus*). Mar. Pollut. Bull. 30, 409–413. DOI 10.1016/0025-326X(95)99847-W

Rothstein A. and Donovan K. (1963) Interactions of Arsenate with the Phosphate-Transporting System of Yeast. J. Gen. Physiol. 46, 1075–1085. DOI 10.1085/jgp.46.5.1075

Steinhauser G. (2014) Fukushima's forgotten radionuclides: a review of the understudied

radioactive emissions. Environ. Sci. Technol. 48, 4649–4663. DOI 10.1021/es405654c

Tagami K. and Uchida S. (2005) A comparison of concentration ratios for technetium and nutrient uptake by three plant species. Chemosphere 60, 714–717. DOI 10.1016/j.chemosphere.2005.03.087

U.S. Geological Survey (2007) Glossary–Bioaccumulation: U.S. Geological Survey. Accessed February 2016 http://water.usgs.gov/water-basicsglossary.html

Williams L.E. Pittman J.K. and Hall J.L. (2000) Emerging mechanisms for heavy metal transport in plants. Biochim. Biophys. Acta 1465, 104–126. DOI 10.1016/S0005-2736(00)00133-4

Xiong Y. Xu J. Shan W. Lou Z. Fang D. Zang S. and Han G. (2013) A new approach for rhenium(VII) recovery by using modified brown algae *Laminaria japonica* absorbent. Bioresource Technol. 127, 464–472. DOI 10.1016/j.biortech.2012.09.099

Yang J.S. (1991) High rhenium enrichment in brown algae: a biological sink of rhenium in the sea? Hydrobiologia 211, 165–170. DOI 10.1007/BF00008532

2.7 Tables and Captions

Table 2.1 Re abundance for *F. vesiculosus* structures analysed with Thermo Scientific X-Series ICP-MS isotope dilution methodology. (*) samples analysed with Thermo Scientific Triton Mass Spectrometer

Sample		Re (ng/g)	2σ (±)
Macroalgae 1			
	Control	69.8	0.1
	Tips 1	163.4	0.1
	Leaves	28.4	0.1
	Stipe	23.0	0.2
	Holdfast	21.0	0.2
	Blades	67.3	0.1
	Veins	33.8	0.1
	Blades without veins	65.8	0.1
Macroalgae 2			
	Fertile tips	117.4	<0.1
	Non-Fertile tips	383.2	<0.1
	Tips	76.0	0.1
	Control	51.0	0.1
Macroalgae 3			
	Fertile tips	145.0	<0.1
	Non-Fertile tips	363.2	<0.1
	Tips	144.1	<0.1
	Control	103.4	0.1
Macroalgae 4			
	Fertile tips	106.4	0.1
	Non-Fertile tips	273.5	<0.1
	Tips	158.5	0.1
	Control	61.0	0.1
Macroalgae 5			
	Fertile tips	120.7	0.1
	Non-Fertile tips	229.1	<0.1
	Tips	147.2	0.1
	Control	84.3	0.1
Macroalgae 6			
	Non-Fertile tips	382.5	<0.1
	Tips	129.5	0.1
	Control	105.1	0.1
Macroalgae 7			
	*Control**	64.0	0.7
	*Tips**	138.0	0.7
	*Blades**	56.8	0.3
	*Stipe**	22.5	0.2
	*Holdfast**	21.6	0.2
	*Blades2**	58.9	0.4

Table 2.2 Re concentrations of the media utilized for Re uptake experiments for boiled (2 h and 5 min) and dried and freezed with liquid nitrogen *F. vesiculosus* tips. Re abundances determined with Thermo Scientific X-Series ICP-MS isotope calibration methodology.

Non-reproductive thallus tips treatment	Re (ng/g) doped in seawater media	Re (ng/g) uptaken by *F. vesiculosus*	2σ (±)
Boiled			
2h	7.5	7.1	0.0
5 min	7.5	7.1	0.1
Dried 72 h	7.5	2.6	0.0
Freezed with N_2 liquid	7.5	6.6	0.0
Non-treated macroalgae (control)	7.5	0.3	0.0

Table 2.3 Re concentrations of the boiled (2 h and 5 min) and dried and freezed with liquid nitrogen *F. vesiculosus* tips following Re uptake experiments. Re abundances determined with Thermo Scientific X-Series ICP-MS isotope calibration methodology.

Non-reproductive thallus tips treatment	Re (ng/g) doped in seawater media	Re (ng/g) uptaken by *F. vesiculosus*	2σ (±)
Boiled			
2h	7.5	36.2	0.1
2h	0.0075	1.1	1.0
2h	0.0	0.5	1.0
5 min	7.5	20.9	<0.1
Dried 72 h	7.5	24.1	<0.1
Freezed with N_2 liquid	7.5	20.0	<0.1

Table 2.4 Re concentration of Macroalgae tips cultured under the different concentrations of $HReO_4$ in the media. Re abundances determined with Thermo Scientific X-Series ICP-MS with isotope calibration methodology.

Replicate number	$HReO_4$(ng/g) Seawater	Re (ng/g) uptake by *F. vesiculosus*	2σ (±)	Replicate average	SD (±)
1	0.0075	187.0	0.4	168.2	9.5
2	0.0075	149.4	0.2		
1	0.07	549.6	0.2		
2	0.07	391.0	0.1	415.4	50.6
3	0.07	305.7	1.0		
1	0.4	995.2	16.0		
2	0.4	1190.0	1.3	1275.6	135.2
3	0.4	1641.7	52.0		
1	0.8	1668.1	0.3		
2	0.8	2007.3	3.0	1769.6	84.4
3	0.8	1633.3	2.4		
1	3.7	8575.0	18.1		
2	3.7	10505.9	2.9	9218.6	455.1
3	3.7	8575.0	12.8		
1	7.5	15961.8	37.9		
2	7.5	16387.0	5.0	16208.7	90.1
3	7.5	16277.3	50.2		
1	20.0	48738.7	69.0		
2	20.0	52521.9	74.0	48007.2	2009.2
3	20.0	42760.9	68.0		
1	75.0	51477.0	72.0		
2	75.0	59611.8	16.5	63283.4	5718.7
3	75.0	78761.5	99.0		
1	1000.0	53009.5	45.0		
2	1000.0	61752.1	85.5	55588.2	2188.9
3	1000.0	52003.1	99.5		
1	2000.0	23488.8	4.0		
2	2000.0	21070.8	26.5	22472.5	512.0
3	2000.0	22857.8	16.0		
1	7450.0	33061.0	50.0	33061.0	

Table 2.5 Re concentration of macroalgae tips cultured under the different concentrations of Re(VII) salts and $HReO_4$ in the media. Re abundances determined with Thermo Scientific X-Series ICP-MS with isotope calibration methodology.

Replicate number	$NaReO_4$ (ng/g) Seawater (March)	Re (ng/g) uptake by *F. vesiculosus*	2σ (±)	Replicates average	SD (±)
2	0.074	206.3	0.2	219.6	6.6
3	0.074	232.9	0.5		
2	0.373	624.5	0.8	629.5	2.5
3	0.373	634.5	1.0		
2	0.745	986.7	2.3	1033.6	23.4
3	0.745	1080.4	2.1		
2	7.450	8421.4	6.3	8064.2	178.6
3	7.450	7706.9	11.5		
Replicate number	$NaReO_4$ (ng/g) Seawater (May)	Re (ng/g) uptake by *F. vesiculosus*	2σ (±)	Replicates average	SD (±)
2	0.0074	95.3	<0.1	86.1	4.6
3	0.0074	76.9	<0.1		
2	0.074	175.0	<0.1	132.9	21.0
3	0.074	90.9	<0.1		
2	0.373	214.3	0.1	200.3	7.0
3	0.373	186.4	0.1		
2	0.745	227.9	0.3	225.7	1.1
3	0.745	223.5	0.2		
2	7.450	1268.0	1.1	2103.9	32.0
3	7.450	1139.9	1.7		
Replicate number	NH_4ReO_4 (ng/g) Seawater (May)	Re (ng/g) uptake by *F. vesiculosus*	2σ (±)	Replicates average	SD (±)
2	0.074	230.6	<0.1	226.1	2.2
3	0.074	221.6	<0.1		
2	0.373	128.6	<0.1	129.4	9.4
3	0.373	130.1	<0.1		
2	0.745	283.6	<0.1	268.9	7.3
3	0.745	254.3	<0.1		
2	7.450	1244.6	0.3	1208.1	18.2
3	7.450	1171.6	2.1		

Replicate number	$KReO_4$ (ng/g) Seawater (May)	Re (ng/g) uptake by *F. vesiculosus*	2σ (±)	Replicates average	SD (±)
2	0.074	88.0	0.1	91.9	7.0
3	0.074	95.9	0.1		
2	0.373	143.6	<0.1	138.4	2.6
3	0.373	133.2	1.0		
2	0.745	166.5	<0.1	176.1	4.8
3	0.745	185.8	0.3		
2	7.450	1260.3	0.5	1251.1	4.4
3	7.450	142.2	0.6		
Replicate number	NH_4ReO_4 (ng/g) Seawater (June)	Re (ng/g) uptake by *F. vesiculosus*	2σ (±)	Replicates average	SD (±)
2	0.074	81.0	0.2	82.3	0.7
1	0.074	83.7	<0.1		
2	0.745	125.4	0.2	129.2	1.9
1	0.745	133.0	<0.1		
2	7.450	689.2	3.3	732.8	21.8
1	7.450	776.4	0.2		
Replicate number	$KReO_4$ (ng/g) Seawater (June)	Re (ng/g) uptake by *F. vesiculosus*	2σ (±)	Replicates average	SD (±)
2	0.074	51.9	0.1	58.3	3.2
1	0.074	64.6	<0.1		
2	0.745	233.8	0.6	272.4	2.2
1	0.745	242.6	1.0		
2	7.450	587.0	0.4	564.9	10.7
1	7.450	544.4	<0.1		
Replicate number	$HReO_4$ (ng/g) Seawater (June)	Re (ng/g) uptake by *F. vesiculosus*	2σ (±)	Replicates average	SD (±)
2	0.074	125.6	<0.1	128.6	1.5
1	0.074	131.8	<0.1		
2	0.745	733.8	0.2	722.5	5.6
1	0.745	711.3	41.0		
2	7.450	5924.3	33.5	6741.4	408.6
1	7.450	7558.6	56.5		

Table 2.6 Seasonal uptake percentage variation of Re(VII) salts (i.e. NH_4ReO_4, $KReO_4$ and $NaReO_4$) cultures done in 2015 versus uptake rate of $HReO_4$ cultures performed in June 2014 and 2015. (*) Total Re in seawater / average dry weight of macroalgae tips (0.5 g)

	Re(VII) salts				$HReO_4$	
	February 2015	March 2015	May 2015	June 2015	June 2014	June 2015
Number of media changes	5	5	7	4	5	4
Total ReO_4 (ng) in seawater [doped ng × num. of media changes]	12500	12500	17500	10000	9300	7440
Possible Re (ng/g) accumulation by *F. v.**	~25000	~25000	~35000	~20000	~18600	~14880
Real Re (ng/g) accumulation by *F.v.*	~1700	~8000	~1200	~800	~9300	~7400
Uptake [Real/Possible accumulation]	6.8%	32.0%	3.4%	4.0%	50.0%	49.7%

Table 2.7 Concentration of Re (ng/g) in chloroplasts and in HEPES solution where chloroplasts were stored.

Sample	Re concentration (ng/g)
Chloroplast pellet	~1
HEPES solution	~3

Figure 2.1 Average (2-5 samples) concentration of rhenium (ng/g) in the different structures of *F. vesiculosus*. Round marker symbolizes Re abundance in each particular structure and square marker symbolizes Re abundance of a mixture of all the structures (control). All the samples had a reproducibility of < 5% RSD, in some cases, graph symbol size is greater than uncertainties. The concentrations shown are in dry mass, and although the concentration of each structure might change when wet mass, the differences of Re concentration are greater than the differences in water loss.

Figure 2.2 Culture representation of non-reproductive *F. vesiculosus* thallus tips. 21 tips of each *F. vesiculosus* specimen were cut and a tip from each specimen was displaced into one of the 21 jars (**A**). Two meshes were put inside each jar ending up with three levels that store three non-fertile tips each (**B**). **C**) Real culture jar picture.

Figure 2.3 A) Rhenium (ng/g) accumulation in *F. vesiculosus* under different Re(VII) salts concentrations. Cultures made with NH_4ReO_4 represented with a round marker, $KReO_4$ shown in square marker and $NaReO_4$ in triangle marker. **B**) Rhenium (ng/g) accumulation in *F. vesiculosus* under different Re(VII) salts (round marker) and $HReO_4$(square marker) plotted in logarithmic scale. All the samples had a reproducibility of <5% RSD, in some cases, graph symbol size is greater than uncertainties.

Figure 2.4 Rhenium (ng/g) accumulation in *F. vesiculosus* under different $HReO_4$ doped seawater concentrations. It follows a logarithmic trend line. All the samples had a reproducibility of < 5% RSD, in some cases, graph symbol size is greater than uncertainties.

Figure 2.5 Rhenium (ng/g) accumulation in *F. vesiculosus* under different $HReO_4$ doped seawater concentrations. All the samples had a reproducibility of <5% RSD, in some cases, graph symbol size is greater than uncertainties.

Figure 2.6 Re (ng/g) accumulation in *F. vesiculosus* under changing concentrations of Re(VII) salts in the media. Day 1 to 3 Re concentration of 7.45 ng/g, from day 3 to 6; 0.075 ng/g and from day 6 to 9; 0.0075 ng/g. Day 0 measure is the background concentration of Re found in the seaweed cultured. All the samples had a reproducibility of <5% RSD.

Figure 2.7 Accumulation of ReO_4^- in *F. vesiculosus* under different treatments (previously heated at 100 ºC for 5 min, liquid nitrogen freezed and 30 ºC dryed) and 7.45 ng/g $HReO_4$ media concentration. All the samples had a reproducibility of < 5% RSD.

Figure 2.8 A) Concentration of proteins (μg/mL) in each elution (i.e. fraction eluted, corresponding to 1 mL). There are two protein peaks in elution 6 and 8-9. **B**) Concentration of rhenium (ng/g) in each elution. The peak is in the elution 12.

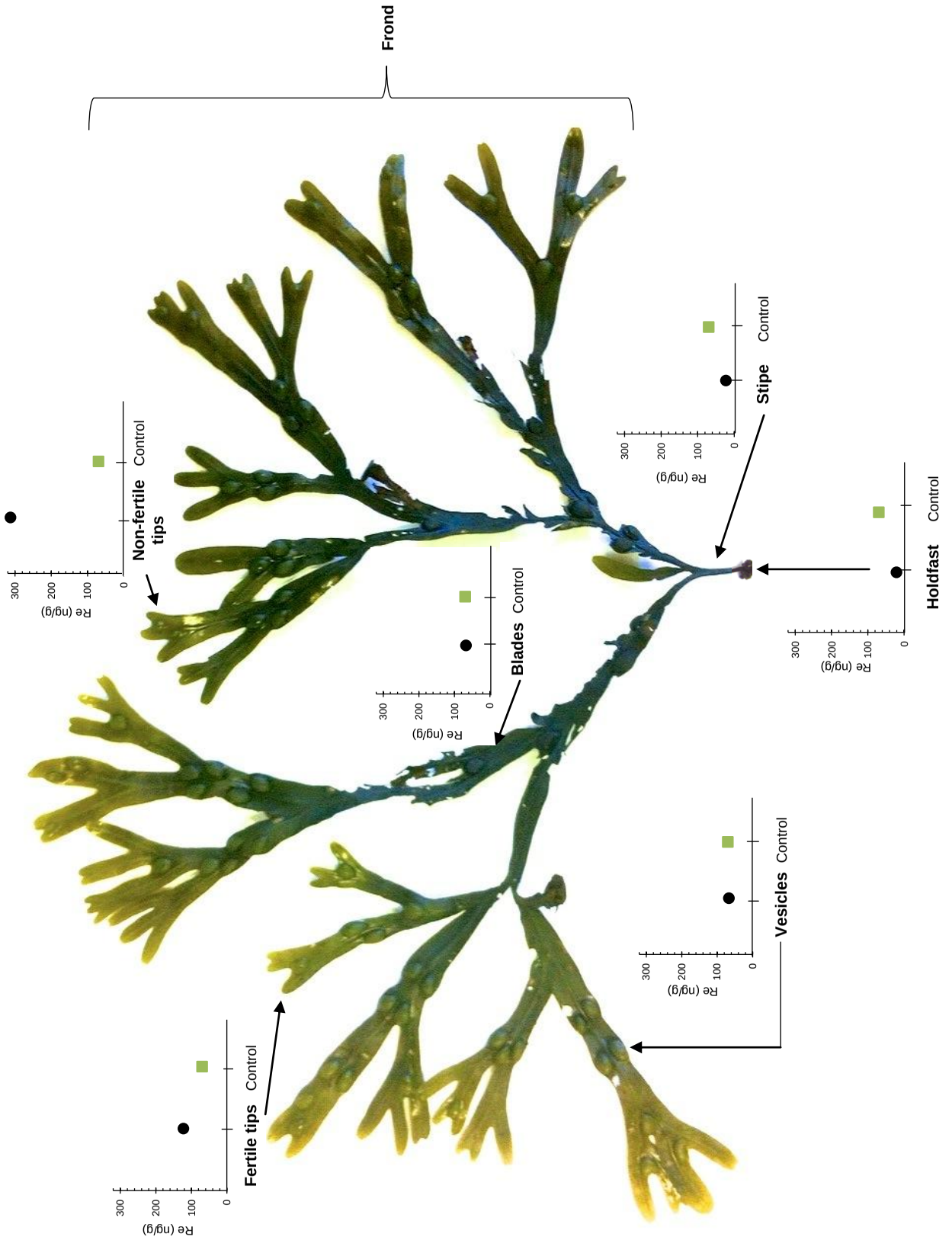

Figure 2.1 Average (2-5 samples) concentration of rhenium (ng/g) in the different structures of *F. vesiculosus*. Round marker symbolizes Re abundance in each particular structure and square marker symbolizes Re abundance of a mixture of all the structures (control). All the samples had a reproducibility of < 5% RSD, in some cases, graph symbol size is greater than uncertainties. The concentrations shown are in dry mass, and although the concentration of each structure might change when wet mass, the differences of Re concentration are greater than the differences in water loss.

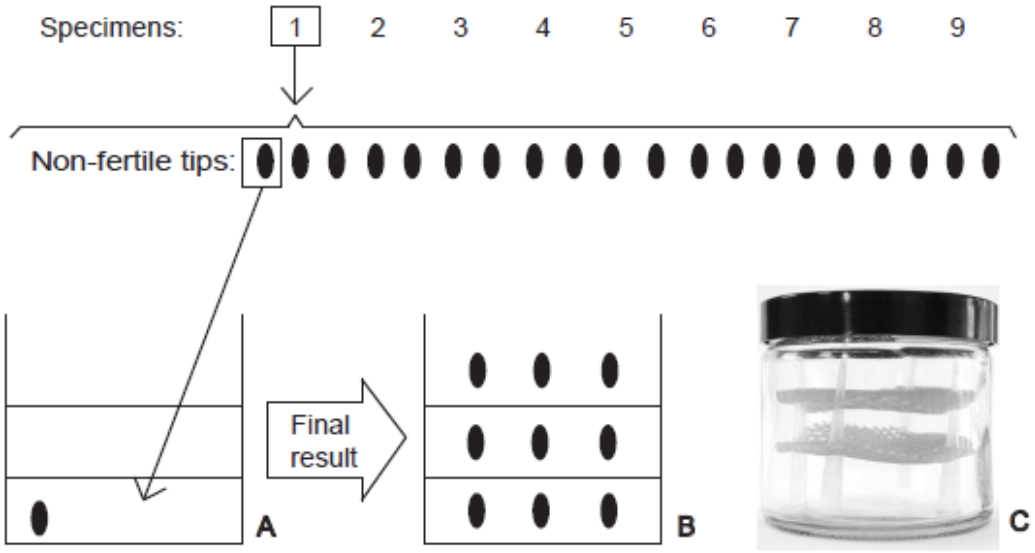

Figure 2.2 Culture representation of non-reproductive *F. vesiculosus* thallus tips. 21 tips of each *F. vesiculosus* specimen were cut and a tip from each specimen was displaced into one of the 21 jars (**A**). Two meshes were put inside each jar ending up with three levels that store three non-fertile tips each (**B**). (**C**) Real culture jar picture.

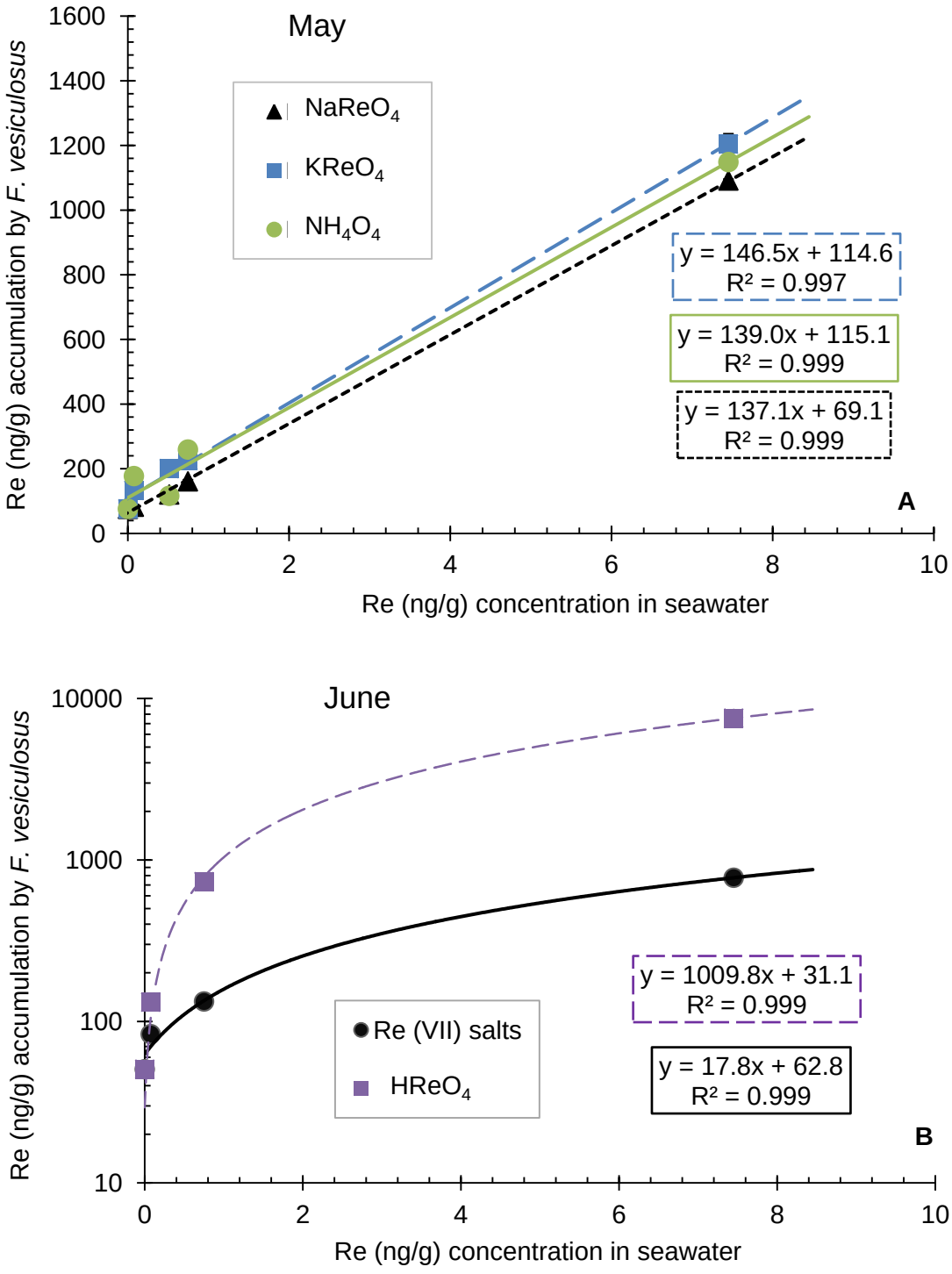

Figure 2.3 (**A**) Rhenium (ng/g) accumulation in *F. vesiculosus* under different Re(VII) salts concentrations. Cultures made with NH_4ReO_4 represented with a round marker, $KReO_4$ shown in square marker and $NaReO_4$ in triangle marker. (**B**) Rhenium (ng/g) accumulation in *F. vesiculosus* under different Re(VII) salts (round marker) and $HReO_4$ (square marker) plotted in logarithmic scale. All the samples had a reproducibility of <5% RSD, in some cases, graph symbol size is greater than uncertainties.

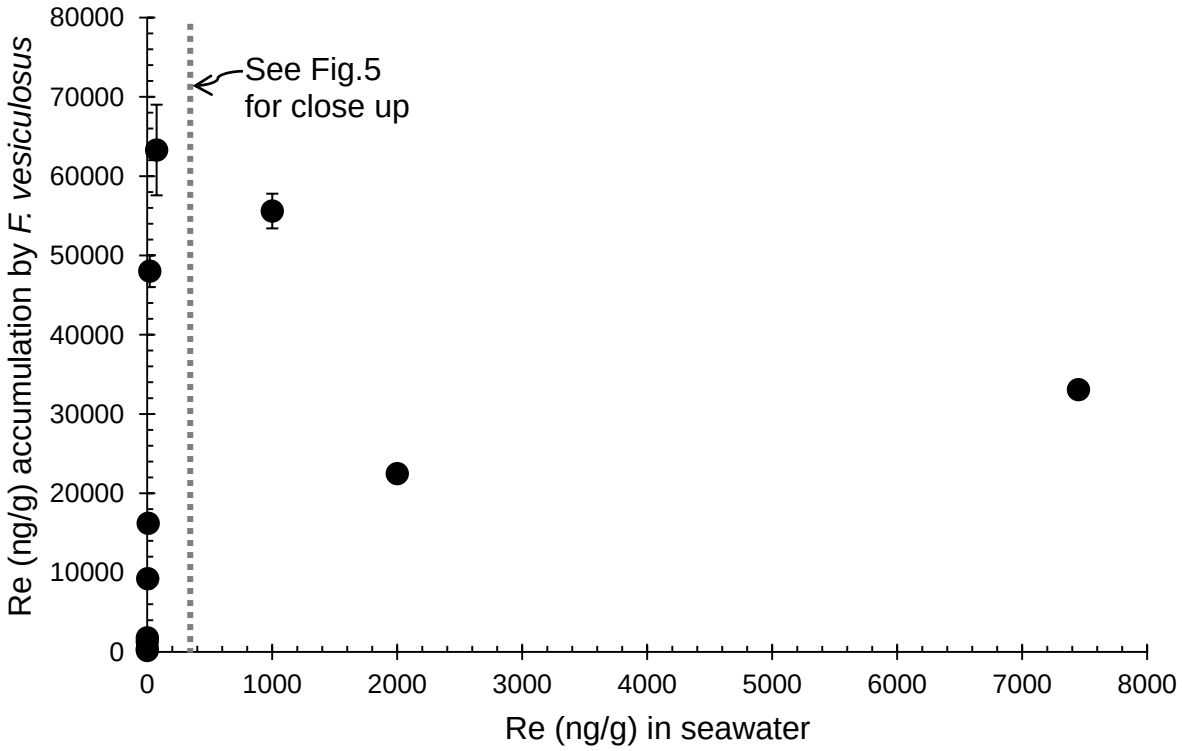

Figure 2.4 Rhenium (ng/g) accumulation in *F. vesiculosus* under different $HReO_4$ doped seawater concentrations. It follows a logarithmic trend line. All the samples had a reproducibility of < 5% RSD, in some cases, graph symbol size is greater than uncertainties.

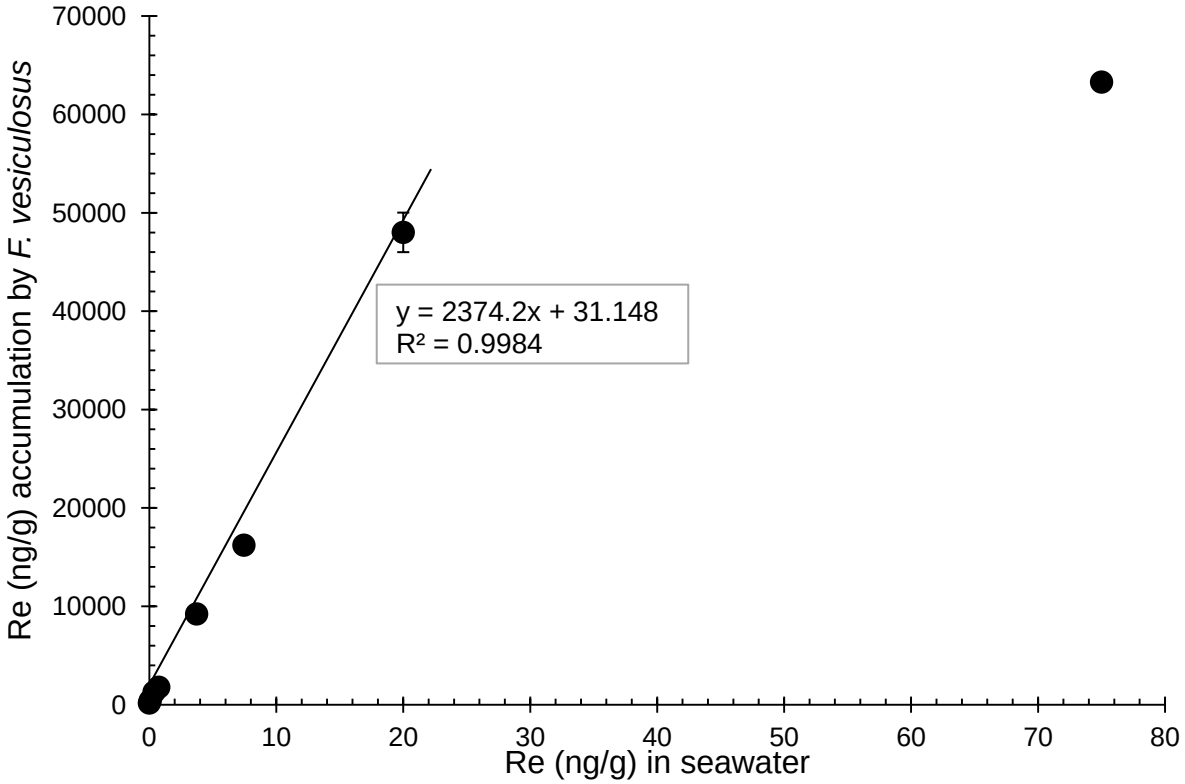

Figure 2.5 Rhenium (ng/g) accumulation in *F. vesiculosus* under different $HReO_4$ doped seawater concentrations. All the samples had a reproducibility of <5% RSD, in some cases, graph symbol size is greater than uncertainties.

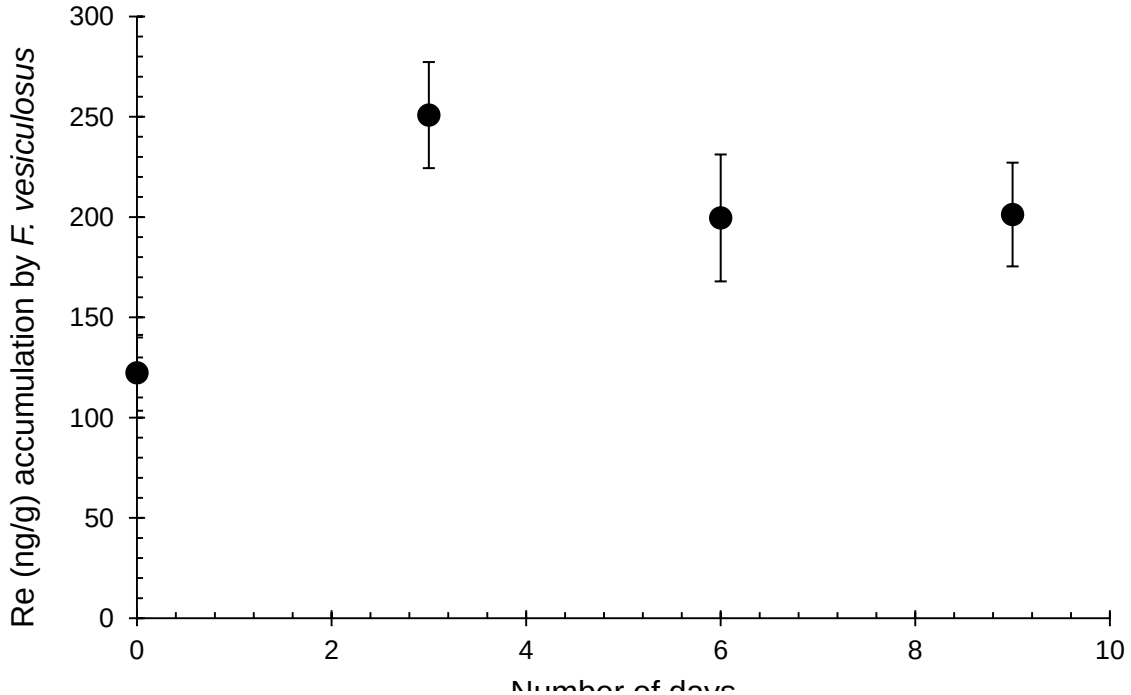

Figure 2.6 Re (ng/g) accumulation in *F. vesiculosus* under changing concentrations of Re(VII) salts in the media. Day 1 to 3 Re concentration of 7.45 ng/g, from day 3 to 6; 0.075 ng/g and from day 6 to 9; 0.0075 ng/g. Day 0 measure is the background concentration of Re found in the seaweed cultured. All the samples had a reproducibility of <5% RSD.

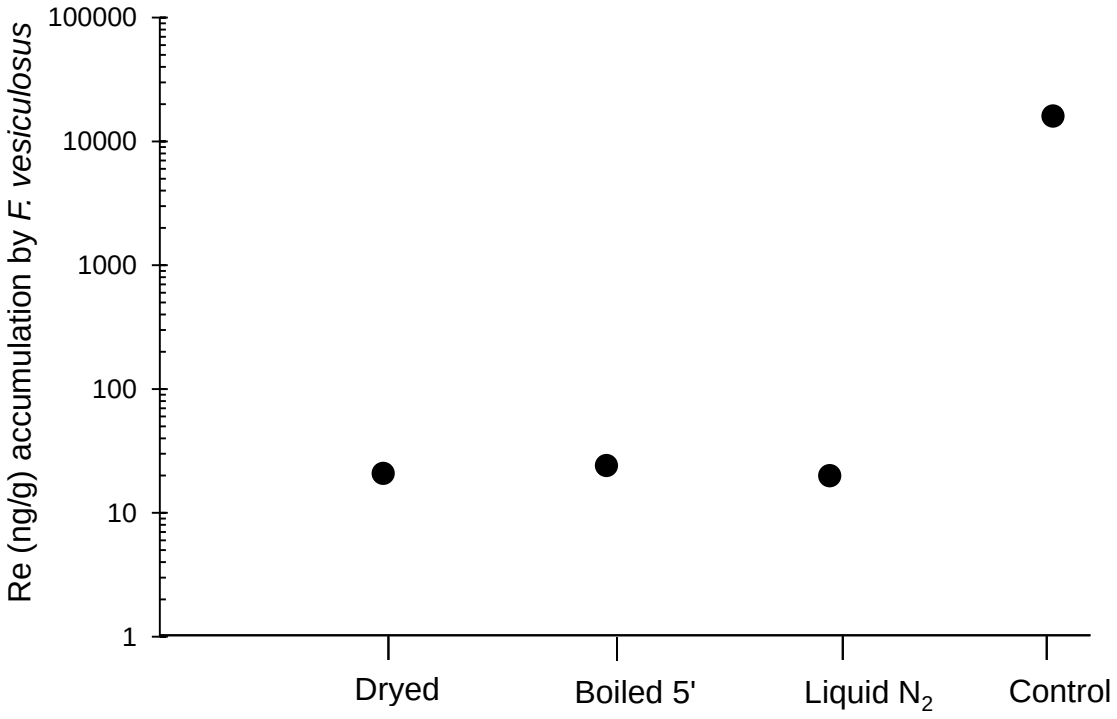

Figure 2.7 Accumulation of ReO_4^- in *F. vesiculosus* under different treatments (previously heated at 100 ºC for 5 min, liquid nitrogen freezed and 30 ºC dryed) and 7.45 ng/g $HReO_4$ media concentration. All the samples had a reproducibility of < 5% RSD.

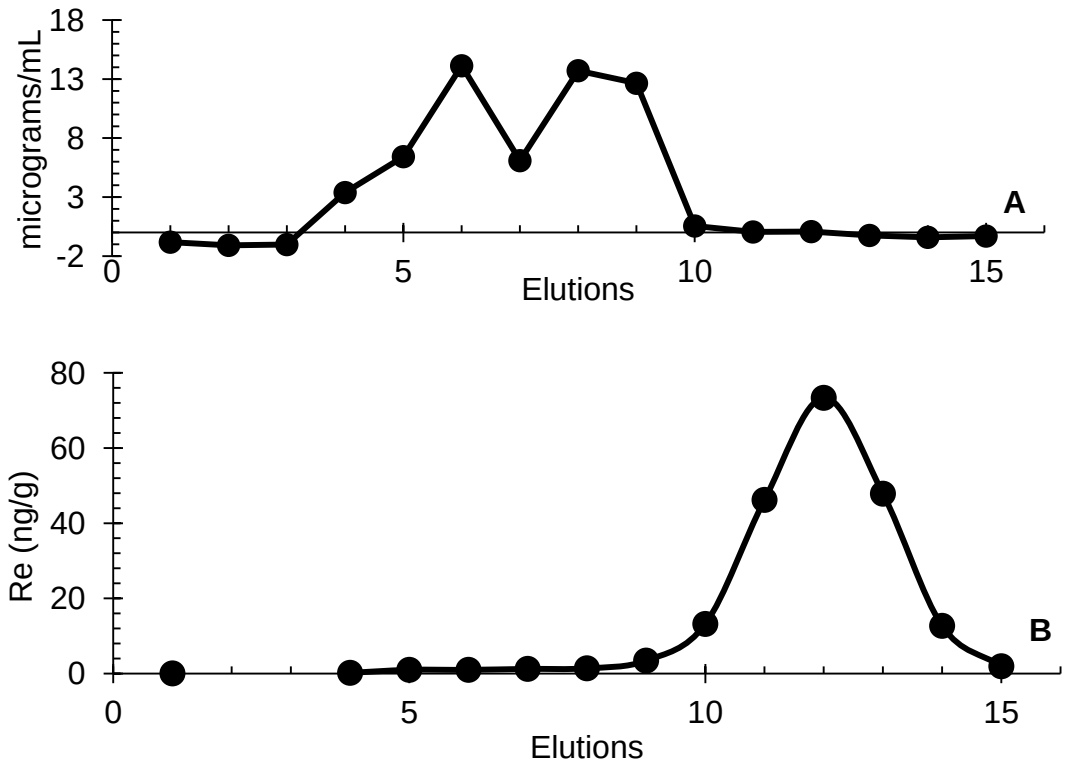

Figure 2.8 (**A**) Concentration of proteins (µg/mL) in each elution (i.e. fraction eluted, corresponding to 1 mL). There are two protein peaks in elution 6 and 8-9. (**B**) Concentration of rhenium (ng/g) in each elution. The peak is in the elution 12.

3. Osmium

From manuscript published in Geochimica et Cosmochimica Acta, 2016, enclosed in appendix E.

Osmium uptake, distribution and isotope composition in Phaephyceae macroalgae, *Fucus vesiculosus*: Implication for determining the Os isotope composition of seawater

B. Racionero-Gómez[1], A.D. Sproson[1], D. Selby[1], A. Gannoun[2], D.R. Gröcke[1], H.C. Greenwell[1] and K.W. Burton[1]

[1] Department of Earth Sciences, Durham University, Durham, DH1 3LE, UK.

[2] Campus Universitaire des Cezeaux, 6 Avenue Blaise Pascal TSA 60026, Cedex, France.

Correspondence to:

B. Racionero Gómez (blancaraci@gmail.com telephone: +34646976656)

D. Selby (david.selby@durham.ac.uk telephone: +441913342294)

Keywords Osmium, macroalgae, uptake, distribution, isotope composition

Abstract

The osmium isotopic composition ($^{187}Os/^{188}Os$) of seawater reflects changes in the Earth's surface. This study, utilizes the Phaeophyceae, *Fucus vesiculosus*, to analyze its Os abundance and uptake, and to assess if macroalgae records the Os isotope composition of the medium it lives in; i.e seawater. Our data demonstrates that Os is not located in one specific structure within macroalgae, but is found throughout the organism. Osmium uptake was measured by culturing *F. vesiculosus* non-fertile tips with different concentrations of Os with a known $^{187}Os/^{188}Os$ composition (~0.16), which is significantly different from the background isotopic composition of local seawater (~0.8). The Os abundance of cultured non-fertile tips show a positive correlation to the concentration of the Os doped seawater. Moreover, the $^{187}Os/^{188}Os$ composition of the seaweed equaled that of the culture medium, which strongly confirms the possible use of macroalgae as a biological proxy for the Os isotopic composition of seawater.

3.1 Introduction

Osmium (Os) concentration and behaviour in seawater is explained in page 15, third paragraph (section 1.2).

Brown macroalgae (i.e. seaweed) are known to concentrate many metal cations and anions in a variety of complexes, e.g. alginate, proteins, polysaccharides of the cell wall, fucans, etc. (Davis *et al.*, 2003). To date, positively charged metals associated with macroalgae have been extensively studied (e.g., Ragan *et al.*, 1979; Chapman and Chapman, 1980; Karez *et al.*, 1994; Lobban and Harrison, 1994; Raize *et al.*, 2004). However, relatively little is known about the mechanisms by which macroalgae uptake negatively charged metal anions. To our knowledge, there have been no studies on the uptake of Os by any macroalgae species. Although, it is known that Os, in addition to Re can accummulate in seaweed (Scadden *et al.*, 1969; Yang, 1991; Mas *et al.*, 2005; Racionero-Gómez *et al.*, 2016; Rooney *et al.*, 2016). As such, this study uses the brown macroalgae (Phaeophyceae), *F. vesiculosus*, as it has been observed to be one of the greatest accumulators of metals (Scadden *et al.*, 1969; Morries and Bale, 1975; Bryan, 1983; Yang, 1991; Rainbow and Phillips, 1993; Karez *et al.*, 1994; Mas *et al.*, 2005; Racionero-Gómez *et al.*, in press) to establish specific sites and mechanisms of Os accumulation, and its importance in recording the direct Os isotope composition of seawater. We present Os abundance data for different structures of *F. vesiculosus*: holdfast, stipe, tips, vesicles and blades (Figure 3.1) and we determine the uptake rate of Os in macroalgae *via* cultures of *F. vesiculosus* under different Os concentrations. We also demonstrate experimentally that macroalgae record the Os isotope composition of the medium that live in (i.e. seawater), indicating that seaweed has the ability to record the interaction between the ocean and the Earth's surface, a mechanism proposed for brown algae based on samples collected from the west coast of Greenland and the Gulf of Mexico (Rooney *et al.*, 2016). In addition, given the analytical approach applied here (isotope

dilution negative ion mass spectrometry), we also present the rhenium (Re) abundance, and the $^{187}Os/^{188}Os$ composition of the studied macroalgae.

3.2 Materials and methods

3.2.1 Macroalgae used in this study: *Fucus vesiculosus*

Explained in page 19 (section 1.3.1).

The *F. vesiculosus* samples were collected from Staithes Beach near Roxby Beck, North Yorkshire, UK (54º33'N 00º47'W) in May, 2014 and June, 2015. The Lower Pliensbachian Staithes Sandstone Formation comprises the geology of the harbour, beach and village of Staithes, with the cliffs of the surrounding the area coinsisting of the Upper Pliensbachian Cleveland Ironstone Formation (Rawson and Wright, 2000). The May 2014 F. vesiculosus collection (5 *F. vesiculosus* specimens growing in the same rock) was utilised to determine the Os abundance of specific structures of the macroalgae, with the additional samples collected in June 2015 utilised for culture experiments (~100 non-fertile tips from *F. vesiculosus* specimens growing in the same rock to avoid genetic variation).

3.2.2 Analytical protocol

Prior to analysis, all collected specimens were kept individually in plastic sample bags for transport, and stored in a freezer (-10 ºC) for 48 h. Each specimen was washed and rinsed in deionised (Milli-Q^{TM}) water to remove any attached sediment and salt. To establish the abundance and distribution of Os in the macroalgae the sample was divided into different structural components: fertile tips, non-fertile tips, vesicles, stipe, holdfast, and blades (Figure 3.1). In addition, a mixture of the above components was created to determine an average Os abundance of the macroalgae. Each structure was dried in an oven at 60 ºC for 12 h, prior to powdering in an agate pestle and a mortar. In addition, to investigate the uptake of Os by macroalgae, culture experiments were conducted in seawater (modified after Gustow *et al.* (2014)) in the school of Biological and Biomedical Sciences at Durham University. In total, three separate culture experiments were conducted, with each experiment replicated a total of three times. For each experiment, non-reproductive apical thallus tips were taken from separate *F. vesiculosus* specimens of the same area (length > 1.5 cm; wet weight (WW) = 0.12–0.15 g) without visible microalgae (i.e. epiphytes). The apical thallus tips were placed into a 250 mL glass jars containing two plastic mesh shelves. Three tips were placed in the bottom of the jar and three tips to each mesh, having in total nine tips of different specimens in each jar (see Figure 3.2). All culture experiments were carried out using filtered (0.7 μm) seawater from Staithes, North Yorkshire, UK (54º33'N 00º47'W) collected in June 2015. The seawater was collected and stored in cleaned PFA Teflon bottles (following the method of Chen and Sharma, 2009). The source of Os used to dope the natural seawater for the culture experiments is DROsS (Durham Romil Osmium Standard; Nowell *et al.*, 2008). DROsS is the in-house Os solution reference material and possesses a $^{187}Os/^{188}Os$ composition of 0.1609 (Nowell *et al.*, 2008). The DROsS solution

utilized in this study is in chloride form. The filtered seawater was doped with DROsS to create a seawater Os concentration 10× (0.1 ppt), 100× (1 ppt) and 1000× (10 ppt) to that of seawater. The modelled $^{187}Os/^{188}Os$ composition of the doped seawater (Table 3.2) is based on the natural Os abundance (10 fg/g; Chen *et al.*, 2009; Gannoun and Burton, 2014), and $^{187}Os/^{188}Os$ composition of seawater (~0.8; based on the $^{187}Os/^{188}Os$ values of the tips collected May 2014 and June 2015; Table 1). The modelled $^{187}Os/^{188}Os$ composition for the 10×, 100×, and 1000× Os doped seawater are ~0.22, ~0.17, ~0.16, respectively (Table 3.2). The $^{187}Os/^{188}Os$ compositions for the cultured tips were calculated assuming that between 5 and 30% of the Os provided by DROsS is taken up by the *F. vesiculosus* tips and that the background Os concentration already present in the tips (~7 and 21 ppt) is not exchanged the culture media.

To reduce evaporation and to allow gaseous exchange with the atmosphere all the jars were loosely sealed. No nutrients were added to the Os doped seawater. The jars, plus tips were placed into an incubator with a set light/dark rhythm of 16:8, light intensity of 125 μmol photons/m^2s^2 and a temperature of 11 ºC. The wet weight (WW) of the algal tips in each jar was measured every 2–3 days during the 14 day culturing period. At the same time, the seawater medium was changed (5 times in total) to avoid accumulation of metabolites. The pH (~9) and salinity (~16 ppt) of the Os doped seawater did not appreciably change from that of the natural seawater collected from Staithes, and remained constant throughout the culture experiments. Following the culture experiment, each sample was oven-dried at 60 ºC for 24 h and ground into a powder with an agate mortar and pestle.

The Re-Os abundance and isotope composition determinations for all samples were obtained by isotope-dilution negative ion mass spectrometry (ID-NTIMS) at the Durham Geochemistry Centre in the Laboratory for Sulphide and Source Rock Geochronology and Geochemistry. Approximately 80 to 100 mg of sample powder was utilised for the Re-Os analysis. The powdered sample was added to a Carius tube with a known amount of a mixed ^{185}Re + ^{190}Os tracer solution. To prevent any sample reaction prior to sealing, the Carius tubes were placed into an ethanol/dry ice bath and 3 mL of 11 N HCl and 6 mL of 15.5 N HNO_3 were added. After sealing, the Carius tubes were placed into an oven and heated to 220 ºC for 24 h. The Os was isolated from the acid medium using $CHCl_3$ solvent extraction, with the Os back extracted into HBr. The Os was further purified using a CrO_3-H_2SO_4 – HBr micro-distillation methodology (Birck *et al.*, 1997; Cohen and Waters, 1996). The resultant Re-bearing acid medium was evaporated to dryness at 80 ºC, with the Re isolated and purified using both NaOH-acetone solvent extraction and HNO_3-HCl anion chromatography (Cumming *et al.*, 2013).

The purified Re and Os fractions were loaded onto Ni and Pt filaments respectively and measured using ID-NTIMS (Creaser *et al.*, 1991; Völkening *et al.*, 1991) on a Thermo Scientific TRITON mass spectrometer using Faraday collectors in static mode, and an electron multipler in dynamic mode. The Re and Os abundances and isotope compositions are presented with 2s absolute uncertainties

which include full error propagation of uncertainties in the mass spectrometer measurements, blank, spike and sample and spike weights. Full analytical blank values are 2.4 ± 0.04 pg for Re, 0.05 ± 0.02 pg for Os, with a $^{187}Os/^{188}Os$ composition of 0.25 ± 0.15 (n = 3).

3.3 Results

3.3.1 Re and Os abundances and isotope compositions within *F. vesiculosus* structures

The natural total Os abundance within all structures of *F. vesiculosus* collected directly from Staithes and not cultured, is between 1600 and 3700 times greater than the concentration found in seawater (Figure 3.1). The Os abundance in the *F. vesiculosus* structures ranges from 16 to 38 ppt. (Figure 3.1; Table 3.1). The structure that contains the least amount of Os is the holdfast (16 ppt), with the blades possessing the highest Os abundance (38 ppt). The remaining structures (tips, stipe and vesicles) possess similar concentrations (24 and 25 ppt Os). The mixture of all the *F. vesiculosus* structures possesses ~34 ppt Os.

The natural total abundance and distribution of Re in *F. vesiculosus* has been previously reported (Racionero-Gómez *et al.*, 2016). In this study, we see that the Re abundance is highly variable throughout *F. vesiculosus*, with Re abundances ranging from ~22 to 138 ppb, being between 3100 to 19700 times greater than that found in seawater (Table 3.1). Similar to Os, the holdfast (and stipe) possess the least amount of Re (~22 ppb). However, in contrast to Os, the tips possess the greatest enrichment of Re (~138 ppb). The distribution of Re in these specimens of *F. vesiculosus* in this study is in agreement with that of Racionero-Gómez *et al.* (2016).

The variability in Re and Os abundance means that the $^{187}Re/^{188}Os$ values for the *F. vesiculosus* structures is highly variable (Table 3.1). The $^{187}Re/^{188}Os$ values range between ~4672 (stipe) and 30558 (tips), with the holdfast and blades possessing similar values to those of the stipe. The $^{187}Os/^{188}Os$ values for the *F. vesiculosus* structures, with the exception of the holdfast, possesses a composition of 0.82 ± 0.03 (1 SD) that reflects a moderately radiogenic composition. This is identical, within uncertainty, to the mixture of all the structures (0.81 ± 0.04).

3.3.2 Uptake of Osmium by *F. vesiculosus* culture tips

The Os abundance of tips from a specimen of *F. vesiculosus* collected in June 2015 possesses significantly less Os and Re (7.8 ppt; Table 3.1) than that of the same structure from a specimen collected in May 2014 (23.5 ppt; Table 3.1). The same is observed for rhenium (138 ppb for May 2014 versus 47 ppb for June 2015; Table 3.1). This difference can be due to many different factors; yearly, monthly or daily changes, ocean sediment turbulence, age of the specimen and other presently unknown conditions (Horta-Puga *et al.*, 2013; Lyngby and Brix, 1982). However, to our knowledge the impacts that each specific factor produces to the flux of Re to the nearshore have not been determined. Although the Re and Os abundances are different between the samples collected in May

2014 and June 2015, the isotope compositions are similar within uncertainty ($^{187}Re/^{188}Os$ = ~30558 ± 2046 (May 2014) versus ~31983 ± 4311 (June 2015); $^{187}Os/^{188}Os$ = 0.75 ± 0.05 (May 2014) vs 0.86 ± 0.12 (June 2015); Table 3.2).

The tips of the *F. vesiculosus* collected June 2015 were used for the culture experiments. For all the culture experiments the Re abundance of the tips (~67 to 79 ppb) is greater than that from specimen tips analysed directly from the ocean (~47 ppb) (Table 3.1). We note that the only Re present in the culture media is that present in the natural seawater (~7 pg/g; Racionero *et al.*, 2016) because the Re abundance of the Os solution (DROsS) used to dope the natural seawater is negligible (e.g., 1 pg/g Os solution contains ~7 x 10^{-6} fg/g Re (Nowell *et al.*, 2008). The Re abundance of the cultured tips shows a decrease from ~79 ppb for the 10× experiment, to ~71 ppb for the 100× experiment, and ~67 ppb for the 1000× experiment (Table 3.1).

For osmium, the abundance increases proportionally to the amount of Os doped in the seawater (10× = ~20 ppt, 100× = ~30 ppt, 1000× = ~200 ppt; Table 3.1; Figure 3.3). Coupled with this increase in Os abundance is a trend to less radiogenic $^{187}Os/^{188}Os$ compositions (10× = ~0.35, 100× = ~0.28, 1000× = ~0.18; Table 3.1; Figure 3.3). Additionally, as a direct result of the overall increase of Os in the cultured tips with a relatively similar Re abundance, the $^{187}Re/^{188}Os$ composition significantly decreases (natural sample = ~32000; 10× = ~18000, 100× = ~12000, 1000× = ~1600; Table 3.1).

3.4 Discussion and implications

3.4.1 Localization and uptake of Os within *F. vesiculosus*

In brown macroalgae, it is possible to distinguish five types of cells: epidermal cells, primary cortical cells, secondary cortical cells, medullary cells and hyphae (Davy de Virville and Feldmann, 1961). Previous studies distinguished different Re accumulation in *F. vesiculosus* depending on the structure measured indicating that there were some cells/structures more specialized for the uptake of Re (Racionero-Gómez *et al.*, 2016). In the case of Os, its abundance does not signifcantly vary between structures, with the exception of the holdfast, suggesting that there is no specific cell specialization for the uptake of Os (Figure 3.1 and Table 3.1). The holdfast does not serve as the primary organ for water or nutrient uptake. Instead, it serves to anchor the macroalgae to the substrate. Therefore, lower Os abundances in the holdfast are expected. Moreover, it is suggested that Re could be biologically influenced (Racionero-Gómez *et al.*, 2016), with uptake controlled by the growing season, as observed for zinc, lead and copper (Riget *et al.*, 1995, Fuge and James, 1973). As such, this may also be the case for Os. However, we cannot conclusively state that Os uptake is biologically controlled, given that our samples were collected principally in the same growing season. Although, this may explain the variability in Re and Os abundance between the May 2014 and June 2015 samples as noted above. Nevertheless, the uptake of Os by *F. vesiculosus* is similar to that of Re, in

the sense that, it is currently known to have no biological role.

The measured Os abundance in the cultured *F. vesiculosus* tips show a positive correlation to the concentration of Os doped seawater (see Table 3.1, 3.2; Figure 3.3). The culture experiment with the highest Os concentration (1000× (10 ppt Os) seawater), resulted in tips possessing an Os abundance of ~200 ppt, which is ~25 times higher than the background concentration of Os in the specimens collected (Table 3.1).

Coincident with the increase in Os abundance with the culture experiments is the decrease in Re (Table 3.1), indicating possible similar cell binding sites or uptake pathways between Re and Os. However, the uptake pathways and binding sites of Re have not been identified. Thus it is currently not known where Os is accumulating in *F. vesiculosus*.

3.4.2 Implications of the $^{187}Os/^{188}Os$ isotope composition of *F. vesiculosus*

The $^{187}Os/^{188}Os$ composition of *F. vesiculosus* in a natural setting (i.e. from Staithes Beach) is ~0.8 (Table 3.1 and Figure 3.3) based on results from specimens collected in May 2014 and June 2015. Using this value to reflect the isotope composition of seawater at Staithes Beach, together with the range in Os abundance in the tips (~7 to 23 ppt; Table 3.1), with the concentration of the doped seawater and its $^{187}Os/^{188}Os$ composition, we calculate a range for the expected $^{187}Os/^{188}Os$ composition of the cultured tips (~0.22-0.48 for 10×; ~0.17-0.37 for 100×; ~0.16-0.20 for 1000×; Table 3.2; Figure 3.3). For each culture experiment the measured $^{187}Os/^{188}Os$ composition of the tips coincides with the range of the expected value (Tables 3.1, 3.2; Figure 3.3), indicating that the $^{187}Os/^{188}Os$ composition of seaweed reflects the media in which it grows, and thus directly supports the use of *F. vesiculosus* (and macroalgae) as a biological proxy for the $^{187}Os/^{188}Os$ composition in seawater (Rooney *et al.*, 2016).

The $^{187}Os/^{188}Os$ composition for three floating macroalgaes (*Sargassum fluitans* and *S. natans*) collected from three different locations ~300 miles offshore in the Gulf of Mexico (1.05 ± 0.01; Rooney *et al.*, 2016) are coincident with that of the present day open oceanic $^{187}Os/^{188}Os$ value of 1.06 (1.04 for the North Atlantic and Central Pacific; 1.06 for the Eastern Pacific and Indian Ocean) determined from direct analyses of seawater and of hydrogenetic Fe-Mn crusts (see Peucker-Ehrenbrink and Ravizza, 2012 and references therein; Gannoun and Burton, 2014 and references therein). In contrast, macroalgae from the coast of the Disko Bugt and Uummannaq regions of the west coast of Greenland show deviations from the $^{187}Os/^{188}Os$ composition of the open ocean (~0.9 and ~1.9) which directly relate to Os flux (abundance and isotope compositon) into the coastal region (Rooney *et al.*, 2016). The latter together with the slightly lower $^{187}Os/^{188}Os$ composition (~0.8; Table 3.1) of the macroalgae from Staithes, in comparison to that of the open ocean, may suggest that the Os isotope composition of macroalgae is strongly controlled by its proximity to the coast, riverine input and regional variations in the Os flux (i.e., abundance and isotope composition) into

the ocean, as also shown along the transects of estuaries (e.g., Levasseur *et al.*, 2000; Martin *et al.*, 2001; Sharma *et al.*, 2007). For example, the Fly River Estuary reflects the input of unradiogenic Os and shows an increasing $^{187}Os/^{188}Os$ composition oceanward from 0.61 to 0.91 (Martin *et al.*, 2001). In contrast the Lena River Estuary and the Godavari Delta reflects the input of radiogenic Os, with the $^{187}Os/^{188}Os$ value decreasing oceanward from 1.55 to 1.13, and 1.30 to 0.90, respectively (Levasseur *et al.*, 2000; Sharma *et al.*, 2007). Therefore macroalgae from distinct oceanic settings (e.g., coastal, estuarine versus open ocean) provides the ability to record the $^{187}Os/^{188}Os$ composition of seawater in addition to direct seawater and sediment analysis to further access the factors (e.g., geological and anthroprogenic) controlling the $^{187}Os/^{188}Os$ composition of seawater.

3.4.3 Implications of the $^{187}Re/^{188}Os$ isotope composition of *F. vesiculosus*

In addition to the $^{187}Os/^{188}Os$ composition of macroalgae, the $^{187}Re/^{188}Os$ values of macroalgae (this study; Rooney et al., 2016) may provide insight into the variability of the $^{187}Re/^{188}Os$ in sediments as organic matter. The $^{187}Re/^{188}Os$ values for Staithes seawater (2790.6 ± 49.7) falls somewhere between open ocean (4270; Anbar *et al.*,1992; Colodner *et al.*, 1993a; Sharma *et al.*, 1997; Levasseur *et al.*, 1998; Woodhouse *et al.*, 1999; PeuckerEhrenbrink and Ravizza, 2000) and riverine (227; Colodner *et al.*, 1993b; Sharma and Wasserburg, 1997; Levassuer *et al.*, 1999; Peucker-Ehrenbrink and Ravizza, 2000) estimates, as expected for estuarine conditions. However, the $^{187}Re/^{188}Os$ values of macroalgae from this study (34794.1 ± 2074.4) are far higher suggesting that the $^{187}Re/^{188}Os$ ratios in macroalgae are not proportional to the seawater in which they live, but controlled by the uptake mechanism(s) of macroalgae that are currently unknown.

To date, it is known that the Re abundance in macroalgae can be highly variable (sub ppb to tens of ppb;Scadden,1969; Yang, 1991; Mas *et al.*, 2005; Prouty *et al.*, 2014;Racionero-Gómez *et al.*, 2016; Rooney *et al.*, 2016). For osmium, the results thus far also indicate that the Os abundance in macroalgae can also be highly variable (this study;Rooney *et al.*, 2016). Further, in addition to macroalgae that are components of sediment organic matter, microorganisms can also accumulate Re (Mashkani *et al.*, 2009; Ghazvini and Mashkani, 2009; Prouty *et al.*, 2014), although to date, no data exists for osmium. Given the variability of Re and Os uptake by macroalgae, the $^{187}Re/^{188}Os$ composition of macroalgae is seen to range from 10 to 35,000 (this study;Rooney $^{187}Re/^{188}Os$, 2016). Metabolically inactive (i.e. dead) macroalgae (*F. vesiculosus*) does not appreciably accumulate rhenium (Racionero-Gómez *et al.*, 2016). If Os in metabolically inactive macroalgae and/or microorganisms is not accumulated or released, then the Re and Os abundance, and isotope composition could be dominantly controlled by the abundance, variability, and the structural type of the organisms preserved in a sediment as organic matter rather than purely sequestration at the sediment–water interface (Yamashita *et al.*, 2007 and references therein). As such, organic matter and organic type, in addition to the depositional setting conditions (Yamashita *et al.*, 2007; Georgiev *et al.*, 2011), maybe important factors in controlling

Re/Os fractionation observed in organic-rich sediments (Cumming *et al.*, 2012; Harris *et al.*, 2012).

A further implication of the uptake of Re and Os by organisms could be its effect on Re-Os organic-rich sedimentary geochronology. In addition to the Re-Os isotope system remaining undisturbed and for the samples to possess a range in $^{187}Re/^{188}Os$ values, the stratigraphic interval must possess similar initial $^{187}Os/^{188}Os$ values to provide reliable (accurate and precise) dates of sediment deposition (Cohen *et al.*, 1999; Selby and Creaser, 2003). As such the heterogenous mixing of organisms with variable $^{187}Os/^{188}Os$ compositions in a sedimentary rock could hamper the ability to yield precise Re-Os dates. This could be particularly problematic in nearshore depositional settings of organic-rich sediments. For example, in a estuarine or deltaic sedimentary system, the $^{187}Os/^{188}Os$ composition is variable along its transect (Levasseur *et al.*, 2000; Martin *et al.*, 2001; Sharma *et al.*, 2007). As such, organisms along the transect will also have variable $^{187}Os/^{188}Os$ compositions. Therefore any heterogeneous mixing of organisms that are preseved as organic matter within a sediment with different $^{187}Os/^{188}Os$ compositions could impact on the precision of Re-Os organic-rich sedimentary geochronology.

3.5 Conclusions

Culture experiments indicate that macroalgae acquires the $^{187}Os/^{188}Os$ composition of the media in which it grows. As a result suggests that macroalgae is a viable biological proxy to determine the $^{187}Os/^{188}Os$ composition of seawater in various oceanographic settings. Specifically in coastal settings the the $^{187}Os/^{188}Os$ composition of macroalgae could be used to assess the $^{187}Os/^{188}Os$ composition of continental input in to the ocean.

Acknowledgements

We wish to express special thanks to Dr Joanna Hesselink for technical support and to John Bothwell and the Faculty of Biological Sciences of Durham for the laboratory support. We are very grateful to OEA Labs Ltd for funding the project. Nancy Prouty is thanked for her constructive comments.

3.6 References

Anbar A.D. Creaser R.A. Papanastassiou D.A. and Wasserburg G.J. (1992) Rhenium in seawater: confirmation of generally conservative behavior. Geochim. Cosmochim. Acta56, 4099–4103.

Birck J.L. Roy-Barman M. and Capmas F. (1997) Re–Os isotopic measurements at the femtomole level in natural samples. Geostand Newstett 20, 19-27. DOI 10.1111/j.1751-908X.1997.tb00528.x

Bryan G.W. (1983) Brown seaweed, *Fucus vesiculosus*, and the gastropod, *Littorina littoralis*, as indicators of trace-metal availability in estuaries. Sci. Total Environ. 28, 91-104. DOI

10.1016/S0048-9697(83)80010-2

Chapman V. and Chapman D. (1980) Seaweeds and their Uses, 3rd ed, New York.

Chen C. and Sharma M. (2009) High precision and high sensitivity measurements of Osmium in seawater. Anal. Chem. 81, 5400-5406. DOI 10.1021/ac900600e

Cohen A.S. Coe A.L. Barlett J.M. Hawkesworth C.J. (1999) Precise Re-Os ages of organic-rich mudrocks and the Os isotope composition of Jurassic seawater. Earth Planet Sc. Lett. 167, 159–173. DOI 10.1016/S0012-821X(99)00026-6

Cohen A.S. and Waters F.C. (1996) Separation of osmium from geological materials by solvent extraction for analysis by thermal ionization mass spectrometry. Anal. Chim. Acta 332, 269-275. DOI 10.1016/0003-2670(96)00226-7

Colodner D. Sachs J. Ravizza G. Turekian K. K. Edmond J. and Boyle E. (1993) The geochemical cycle of rhenium: a reconnaissance.Earth Planet. Sci. Lett.117, 205–221.

Creaser R.A. Papanastassiou D.A. and Wasserburg G.J. (1991) Negative thermal ion mass spectrometry of osmium, rhenium and iridium. Geochim. Cosmochim. Acta 55, 397-401. DOI 10.1016/0016-7037(91)90427-7

Cumming V. M. Selby D. and Lillis P.G. (2012) Re-Os geochronology of lacustrine organic-rich sedimentary rocks: insights into direct depositional dating of lacustrine successions. Re-Os systematics and paleocontinental weathering. Earth Planet. Sc. Lett. 359–360, 194–205. DOI 10.1016/j.epsl.2012.10.012

Cumming V.M. Poulton S.W. Rooney A.D. Selby D. (2013) Anoxia in the terrestrial environment during the Late Mesoproterozoic. Geology. DOI 10.1130/G34299.1

Davis T.A. Volesky B. and Mucci A. (2003) A review of the biochemistry of heavy metal biosorption by brown algae. Water Res. 37, 4311-4330. DOI 10.1016/S0043-1354(03)00293-8

Davy de Virville A. and Feldmann J. (1961) IV International Symposium on Seaweed. Pergamon press, Biarritz.

Fuge R. and James K.H. (1973) Trace metal concentrations in brown seaweeds, Cardigan Bay, Wales. Mar. Chem. 1, 281-293. DOI 10.1016/0304-4203(73)90018-2

Gannoun A. and Burton K.W. (2014) High precision osmium elemental and isotope measurements of North Atlantic seawater. J. Anal. Atom. Spectrom. 29, 2330-2342. DOI 10.1039/c4ja00265b

Greorgiev S. Stein H.J. Hannah J.L. Bingen B. Weiss H.M. and Piasecki S. (2011) Hot acidic Late Permian seas stifle life in record time: Earth Planet. Sc. Lett. 310:389-400. DOI 10.1016/j.epsl.2011.08.010

Ghazvini P.T.M. Mashkani S.G. (2009) Screening of bacterial cells for biosorption of oxyanions: Application of micro-PIXE for measurement of biosorption. Hydrometallurgy 96, 246-252. DOI

10.1016/j.hydromet.2008.10.012

Gustow L. Rahman M.M. Bartl K. Saborowski R. Bartsch I. and Wiencke C. (2014) Ocean acidification affects growth but not nutritional quality of the seaweed *Fucus vesiculosus* (Phaeophyceae, Fucales). J. Exp. Mar. Biol. Ecol 453, 84-90. DOI 10.1016/j.jembe.2014.01.005

Harris N.B. Mnich C.A. Selby D. Korn D. (2012) Minor and Trace Element and Re-Os Chemistry of the Upper Devonian Woodford Shale, Permian Basin, West Texas: Insights into Metal Abundance and Basin Processes. Chem. Geol. 356,76–93. DOI 10.1016/j.chemgeo.2013.07.018

Horta-Puga G. Cházaro-Olvera S. Winfield I. Avila-Romero M. and Moreno-Ramírez M. (2013) Cadmium, copper and lead in macroalgae from Veracruz Reef System, Gulf of Mexico: Spatial distribution and rainy season variability. Mar. Pollut. Bull. 68, 127-133. DOI 10.1016/j.marpolbul.2012.12.008

Karez C.S. Magalhaes V.F. Pfeiffer W.C. and Amado Filho G.M. (1994) Trace metal accumulation by algae in Sepetiba Bay, Brasil. Environ. Pollut. 83, 351-356. DOI 10.1016/0269-7491(94)90157-0

Koide M. Goldberg E.D. and Walker R. (1996) The analysis of seawater osmium. Deep Sea Reasources 43, 53-55. DOI 10.1016/0967-0645(95)00082-8

Levasseur S. Birck J.-L. Allegre C.J. (1998) Direct measurement of femtomoles of osmium and the $^{187}Os/^{186}Os$ ratio in seawater. Science 282, 272-274. DOI 10.1126/science.282.5387.272

Levassuer S. Birck J.-L. and Allegre C. J. (1999) The osmium riverine flux and the oceanic mass balance of osmium. Earth Planet. Sci. Lett. 174, 7–23.

Levasseur S. Rachold V. Birck J.L. and Allegre C.J. (2000) Osmium behavior in estuaries: the Lena River example. Earth Planet. Sci. Lett.177(3–4), 227–235. DOI dx.doi.org/10.1016/S0012-821X(00)00049-2.

Lobban C.S. and Harrison P.J. (1994) Seaweed Ecology and Physiology. Press syndicate of the university of Cambridge, Cambridge University.

Lyngby J.E. and Brix H. (1982) Seasonal and environmental variation in cadmium, copper, lead and zinc concentrations in eelgrass (*Zostera marina L.*) in the Limfjor,k Denmark. Aquat. Bot. 14, 59-74. DOI 10.1016/0304-3770(82)90086-9

Martin C.E. Peucker-Ehrenbrink B. Brunskill G. and Szymczak R. (2001) Osmium isotope geochemistry of a tropical estuary. Geochim. Cosmochim. Acta65(19), 3193–3200.

Mas J.L. Tagami K. Uchida S. (2005) Rhenium measurements on North Atlantic seaweed samples by ID-ICP-MS: An observation on the Re concentration factors. J. Radioanal. Nucl. Ch. 265: 361–365. DOI 10.1007/s10967-005-0833-3

Mashkani S.G. Ghazvini P.T.M. Aligol D.A. 2009. Uptake of Re(VII) from aqueous solutions by Bacillus sp. GT-83-23. Bioresource Technol. 100, 603-608. DOI 10.1016/j.biortech.2008.06.065

Morries A.W. and Bale A.J. (1975) The accumulation of cadmium, copper, manganese and

zinc by Fucus vesiculosus in the Bristol Channel. Estuar. Coast. Mar. Sci. 3, 153-163. DOI 10.1016/0302-3524(75)90018-3

Nowell G.M. Luguet A. Pearson D.G. and Horstwood M.A. (2008) Precise and accurate $^{186}Os/^{188}Os$ and $^{187}Os/^{188}Os$ measurements by Multi- Collector Plasma Ionisation Mass Spectrometry (MC-ICP-MS) part I: solution analyses. Chem. Geol. 248, 363-393. DOI 10.1016/j.chemgeo.2007.10.020

Peucker-Ehrenbrik B. and Ravizza G. (2000) The marine osmium isotope record. Terra Nova 12, 205-219. DOI 10.1046/j.1365-3121.2000.00295.x

Prouty N.G. Roark E.B. Koenig A. Demopoulos A.W. Batista F.C. Kocar B.D. Selby D. McCarthy M.D. and Mienis F. (2013) Deep-sea coral record of human impact on watershed quality in the Mississippi River Basin. Global Biochem. Cy. 28 DOI 10.1002/ 2013GB004754.

Racionero-Gómez B. Sproson A.D. Selby D. Gröcke D.R. Redden H. and Greenwell H.C. (2016) Rhenium uptake and distribution in Phaeophyceae macroalgae, *Fucus vesiculosus*. Royal journal of interface. Royal Society Open Science, in press

Ragan M.A. Smidsrod O. and Larsen B. (1979) Chelation of divalent metal ions by brown algal polyphenols. Mar. Chem. 7, 265-271. DOI 10.1016/0304-4203(79)90043-4

Rainbow P.S. and Phillips D.J.H. (1993) Cosmopolitan biomonitors of trace metals. Mar. Pollut. Bull. 26, 593-601. DOI 10.1016/0025-326X(93)90497-8

Raize O. Argaman Y. and Yannai S. (2004) Mechanisms of biosorption of different heavy metals by brown marine macroalgae. Biotechnol. Bioeng. 87, 451-458. DOI 10.1002/bit.20136

Rawson P.F. and Wright J.K. (2000) The Yorkshire Coast. Geologists' Association Guide No. 34. The Geologists' Association, Burlington House, Piccadilly, London. 130pp. With contributions by Starmer I.C. Whitham F. and Hemingway J.E. The Third Revised Edition, edited by Greensmith J.T.

Riget F. Johansen P. Asmund G. (1995) Natural Seasonal Variation of Vadmium, Copper, Lead and Zinc in Brown Seaweed (*Fucus vesiculosus*). Mar. Pollut. Bull. 30, 409–413. DOI 10.1016/0025-326X(95)99847-W

Rooney A.D. Selby D. Lloyd J.M. Roberts D.H. Lückge A. Sageman B.B. and Prouty N.G. (2016) Using Osmium isotopes to track millennial-scale Holocene glacial advance and retreat: Insights from the Greenland Ice Sheet. Quaternary Sci. Rev. 138, 49-61. DOI 10.1016/j.quascirev.2016.02.021

Scadden E. M. (1969) Rhenium: its concentration in Pacific Ocean surface waters. Geochim. Cosmochim. Acta 33, 5: 633-637. DOI 10.1016/0016-7037(69)90019-2

Selby D. and Creaser R.A. (2003) Re-Os geochronology of organic rich sediments: An evaluation of organic matter analysis methods. Chem. Geol. 200, 225-240. DOI 10.1016/S0009-

2541(03)00199-2

Sharma M. Papanastassiou D.A. and Wasserbug G.J. (1997) The concentration and isotopic composition of osmium in the oceans. Geochim. Cosmochim. Acta 61, 3287-3299. DOI 10.1016/S0016-7037(97)00210-X

Sharma M. Balakrishna K. Hofmann A.W. Shankar R. (2007) The transport of Osmium and Strontium isotopes through a tropical estuary. Geochim. Cosmochim. Acta 71, 4856-4867. DOI 10.1016/j.gca.2007.08.004

Sharma M. and Wasserburg G.J. (1997) Osmium in the rivers. Geochim. Cosmochim. Acta6, 5411–5416.

Völkening J. Walczyk T. and Heumann K.G. (1991) Osmium isotope ratio determinations by negative thermal ion mass spectrometry. Int. J. Mass Spectrom. 105, 147-159.

Woodhouse O.B. Ravizza G. Kenison Falker K. Statham P.J. and Peucker-Ehrenbrik B. (1999) Osmium in seawater: vertical profiles of concentration and isotopic composition in the eastern Pacific Ocean. Earth Planet. Sc. Lett. 173, 223-233.

Yang J.S. (1991) High rhenium enrichment in brown algae: a biological sink of rhenium in the sea? Hydrobiologia 211, 165–170. DOI 10.1007/BF00008532

Yamashita Y. Takahashi Y. Haba H. Enomoto S. Shimizu H. (2007) Comparison of reductive accumulation of Re and Os in seawater–sediment systems. Geochim. Cosmochim. Acta 71, 3458–3475. DOI 10.1016/j.gca.2007.05.003

3.7 Tables and captions

Table 3.1 Rhenium (ppb), Osmium (ppt) and Re-Os isotope compositions in *F. vesiculosus* structures and following culture experiment. The Re-Os abundances are based on the dry mass of the macroalgae

Sample	Re (ppb)	Os (ppt)	$^{187}Re/^{188}Os$	$^{187}Os/^{188}Os$
May 2014 collection				
Tips	138.0 ± 0.7	23.5 ± 0.7	30558.8 ± 2046.6	0.75 ± 0.05
Blades	56.8 ± 0.3	37.6 ± 0.7	7902.1 ± 336.9	0.78 ± 0.04
Stipe	22.5 ± 0.2	25.2 ± 0.7	4672.6 ± 299.8	0.81 ± 0.05
Holdfast	21.6 ± 0.2	16.0 ± 0.7	7223.4 ± 736.2	0.95 ± 0.10
Vesicles	59.0 ± 0.4	24.8 ± 0.7	12476.6 ± 805.9	0.80 ± 0.05
Mix of structures	64.0 ± 0.7	33.8 ± 0.7	9930.3 ± 469.9	0.81 ± 0.04
June 2015 collection				
Tips	47.4 ± 0.1	7.8 ± 0.4	31983.8 ± 4311.5	0.86 ± 0.12
Culture experiment				
1- 10× seawater[1]	79.3 ± 0.2	21.2 ± 0.4	18585.9 ± 866.6	0.35 ± 0.02
2- 10× seawater[1]	77.7 ± 0.2	20.5 ± 0.1	18819.6 ± 757.5	0.34 ± 0.01
1- 100× seawater[1]	71.3 ± 0.2	28.6 ± 0.5	12235.8 ± 421.2	0.28 ± 0.01
2- 100× seawater[1]	71.1 ± 0.2	32.7 ± 0.5	10696.6 ± 323.4	0.28 ± 0.01
1- 1000× seawater[1]	67.1 ± 0.2	201.6 ± 0.8	1615.0 ± 12.7	0.18 ± 0.00
2- 1000× seawater[1]	66.8 ± 0.2	194.3 ± 0.8	1668.6 ± 13.4	0.18 ± 0.00

[1] Culture experiment uses tips from specimens collected June 2015

Table 3.2 Osmium (ppt) and $^{187}Os/^{188}Os$ compositions expected (calculated) in *F. vesiculosus* under different Os seawater (SW) concentrations assuming that there is complete exchange of background macroalgae internal Os abundance

Sample	Seawater [Os] (ppt)	$^{187}Os/^{188}Os$ or seawater culture experiment	Expected (calculated) cultured seaweed [Os] (ppt)
Natural SW	0.01[1]	0.81-0.86[2]	~7- 23[3]
10× SW	0.1	0.22-0.23	~20-50
100× SW	1	0.17	~30-90
1000× SW	10	0.16	~ 190-300
Sample	Seawater [Os] (ppt)	Expected (calculated) cultured seaweed $^{187}Os/^{188}Os$	Measured $^{187}Os/^{188}Os$ of seaweed culture experiment
Natural SW	0.01[1]	-	0.81-0.86[2]
10× SW	0.1	0.22-0.48	0.34-0.35[2]
100× SW	1	0.17-0.37	0.28[2]
1000× SW	10	0.16-0.20	0.18[2]

[1] Chen *et al.*, 2009; Gannoun and Burton, 2014

[2] based on the seaweed $^{187}Os/^{188}Os$ composition (see Table 3.1)

[3] measured in tip structures from specimens taken directly from the ocean

Figure 3.1 Photograph exhibiting the key structures of *F. vesiculosus*. Also shown are the Re and Os abundances, and Re-Os isotope compositions. (Data including uncertainties are shown in Table 3.1).

Figure 3.2 Culture representation of non-reproductive *F. vesiculosus* thallus tips. (**A**) Two meshes were put inside each jar generating three levels that each hold three non-fertile tips each. (**B**) Photo of the culture jar used.

Figure 3.3 Osmium (ppt) accumulation in *F. vesiculosus* under different Os seawater concentrations (filled circles). *F. vesiculosus* $^{187}Os/^{188}Os$ compositions under different Os seawater concentrations and $^{187}Os/^{188}Os$ composition (filled squares). Also plotted are the predicted (calculated) range of Os accummulation (dotted line) and $^{187}Os/^{188}Os$ compositions (box) in *F. vesiculosus* (see Table 3.2).

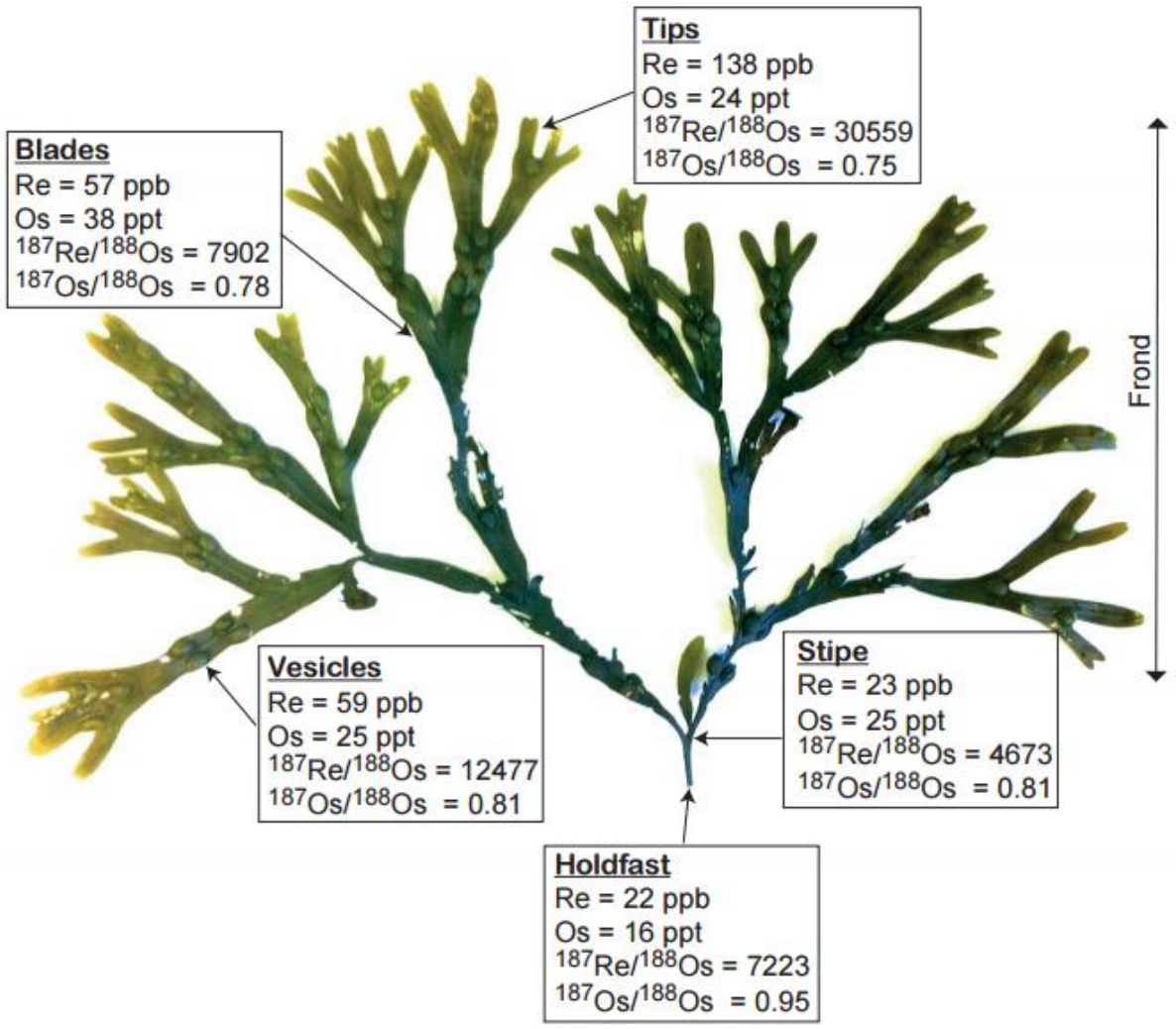

Figure 3.1 Photograph exhibiting the key structures of *F. vesiculosus*. Also shown are the Re and Os abundances, and Re-Os isotope compositions. (Data including uncertainties are shown in Table 3.1)

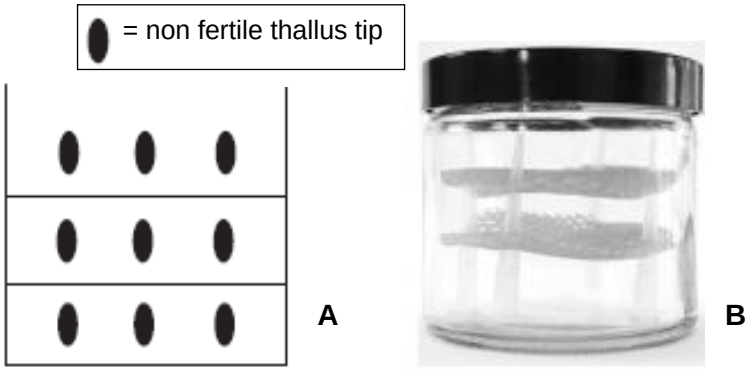

Figure 3.2 Culture representation of non-reproductive *F. vesiculosus* thallus tips. (**A**) Two meshes were put inside each jar generating three levels that each hold three non-fertile tips each. (**B**) Photo of the culture jar used.

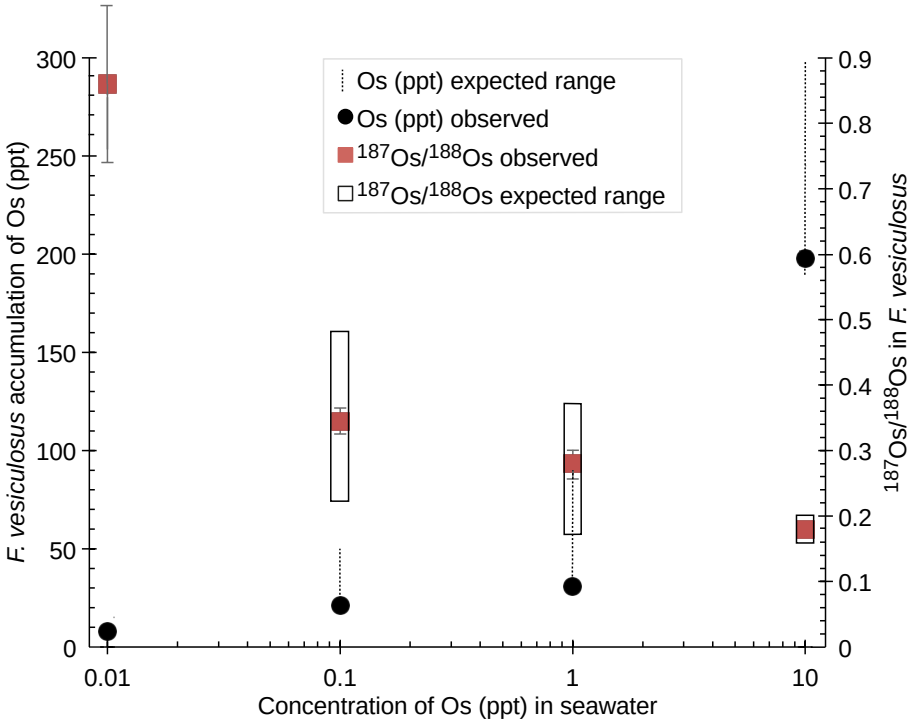

Figure 3.3 Osmium (ppt) accumulation in *F. vesiculosus* under different Os seawater concentrations (filled circles). *F. vesiculosus* $^{187}Os/^{188}Os$ compositions under different Os seawater concentrations and $^{187}Os/^{188}Os$ composition (filled squares). Also plotted are the predicted (calculated) range of Os accummulation (dotted line) and $^{187}Os/^{188}Os$ compositions (box) in *F. vesiculosus* (see Table 3.2).

4. Nitrogen

Modified from manuscript submitted to Journal of Applied Phycology, enclosed in Appendix E.

Nitrogen uptake in Phaephyceae macroalgae, *Fucus vesiculosus*. An understanding of δ^{15}N isotope changes due to different nitrogen sources in river Tees and Staithes

Key words

Macroalgae, nitrogen, uptake, eutrophication, isotopes

Abstract

Macroalgae are a powerful tool for monitoring water mass eutrophication, sewage influence and pollution. This study measures δ^{15}N in *Fucus* sp., brown macroalgae (Phaephyceae) to assess the source of N of the river Tees and Staithes by performing *in-situ* and *ex-situ* tip culture experiments. *Ex-situ* cultures were performed in seawater with different nitrate or ammonia concentrations and show a positive relation between the δ^{15}N of macroalgae and the δ^{15}N of the seawater doped. Therefore, a confirmation of the usefulness of *Fucus* sp. as an eutrophication or pollutant tracker is achieved, deciphering that River Tees most probable source of N is NO_3^- from chemical plants nearby and Staithes most probable source of N is sewage waste.

4.1 Introduction

The behaviour of nitrogen (N), it's isotopes (i.e. ^{14}N and ^{15}N) and it's isotope ratio (i.e. δ ^{15}N) are explained in page 16 (section 1.2.4).

Previous studies by Mariotti *et al.* (1981) have shown that in biological reactions the substrates are enriched in ^{15}N (i.e., a more positive δ ^{15}N signature), whereas the products are subsequently depleted in ^{15}N (i.e., δ ^{15}N signatures that are near zero or negative). Moreover, industrialization, sewage, groundwater and other wastes are normally more enriched in ^{15}N than seawater (Vizzini and Mazzola, 2004), although agricultural waste products are normally more depleted in ^{15}N (Heaton, 1986).

Industry and fertilizers can cause eutrophication, which is explained in page 28 (section 1.8).

The River Tees and Estuary, Borough of Teeside, UK, is a clear example of eutrophication. Intensive industrialization in the river began in 1830's. The railway and Tees port construction influenced iron manufacture, ship building, engineering and chemical industries and human population growth. These factors led to the mouth of River Tees becoming one of the most heavily industrialized in Britain and the river was used for the disposal of liquid effluents. Consequently, the lower river became heavily polluted with excessive growth of macroalgae in specific locations of the river. Fortunately since the 1970's there have been major reductions in the quantity of pollutants emitted to the river (e.g. 70% ammonia emissions reductions).

Another current example of eutrophication caused by a different source of nitrogen is Staithes, North Yorkshire, UK. There was a spillage of sewage from Hinderwell Waste Water Treatment Works into Dales beck at Dalehouse, whose watercourse enters Staithes beck reported on the 10th of July 2015 by the Department of Environment Food and Rural Affairs.

To monitor such changes in water mass eutrophication and sewage influence, nitrogen isotopes of organic matter and nitrogen isotope analysis of macroalgae have been used (de Carvalho, 2008; Fernandes *et al.*, 2012; Maier *et al.*, 2009). The levels of δ^{15}N in macroalgae are significantly altered due to the enrichment of nitrates in a river. These variations in macroalgae were initially documented by Minagawa and Wada (1984), and more recently there have been further studies (Savage, 2005; Savage and Elmgren, 2004; Viana *et al.*, 2011). Viana *et al.* (2011) measured δ^{15}N signatures in macroalgal tissues in coastal areas between 1990 and 2007 and found a decrease in δ^{15}N (from ~8‰to ~5‰) over the successive analyses, which the authors related to changes in the source of contamination or environmental factors. Savage (2005); Savage and Elmgren (2004) reported increases of δ^{15}N values (>7‰) in *Fucus* sp. are found under sewage influence. Background δ^{15}N in *Fucus* sp. are reported to be ~6‰(Riera, 1998; Riera *et al.*, 2000). However, in other studies, δ^{15}N values in *Fucus* sp. used as uncontaminated control sites were between 4 and 5‰(Savage and Elmgren, 2004). In the current study, we aim to assess the usefulness of δ^{15}N measurements in

macroalgae as an eutrophication or pollutant recorder; thus to understand the source of nitrogen of the river Tees and Staithes.

4.2 Materials and methods

4.2.1 Macroalgae used in the study: *Fucus*

Fucus sp. belong to Phaeophyceae macroalgae (brown macroalgae) family. The natural localization of this species in the river and the previous analysis done of eutrophication measuring δ^{15}N in this macroalgae (Savage and Elmgren, 2004; Viana *et al.*, 2011) are the reasons of the usage of this macroalgae in our studies.

Fucus characteristics correspond to that of *F. vesiculosus* explained in page 19 (section 1.3.1). Non-fertile tips of *Fucus* have a significant greater uptake of N than the rest of *Fucus* structures (Savage and Elmgren, 2004; Viana *et al.*, 2015), thus tips are used in this study.

4.2.2 Study area and collection sites

Fucus non-fertile tips were collected from Staithes, North Yorkshire, UK (54º33'N 00º47'W) in July, August and September, 2015 and June 2014 (Figure 4.1). A part of year 2015 samples were used to culture *in vivo* the macroalgae in four specific sites and heights of the River Tees, Borough of Teeside, UK (54º35'N 1º11'W) (Figure 4.1) and another part of the samples were used for *in vitro* culturing using different concentrations of nitrate and ammonia. Moreover, in order to have a background level, *Fucus* sp. growing in the surroundings of the river Tees where the *in vivo* cultures were done, were collected.

4.2.3 *in vivo Fucus* culture in the River Tees

In order to analyse changes in δ^{15}N from *Fucus* depending of the contamination of the area, *Fucus* tips from Staithes (with δ^{15}N values in *Fucus* sp. ~10‰) were transferred and cultured *in vivo* in 4 buoys locations in the River Tees (See Figure 4.1). All non-fertile apical thallus tips specimens were kept in a plastic container filled with seawater from Staithes for transportation. Once in the River Tees, tips were placed in fruit bags which were holding from a chain attached to a river channel navigation buoy, previously agreed with PD ports. Four buoys in total were used and each buoy had two heights (0.4 and 1.2 m) for fruit bag attachment. Two *in vivo* simultaneous experiments were undertaken in the same buoy locations and heights. The first experiment used 200 non-fertile tips in total (i.e. 25 tips per fruit bag) and 5 tips were collected every week for analysis (3 collections in total). 40 non-fertile tips were transferred in total for the second experiment every week (i.e. 5 tips per fruit bag). After a week of *in vivo* culturing all the tips of each bag were collected and replaced for new fresh tips from Staithes. Because of the natural difference between both experiments, the first experiment explained will be referred as the long term experiment, and the second will be referred as the short term one. The long term experiment aims to understand the rate of accumulation of the N

source and the short term experiment measures the changes that take place every week in the River Tees.

4.2.4 *in vitro Fucus* culture

To investigate N uptake by macroalgae, non-reproductive apical thallus tips of *Fucus* specimens (length > 1.5 cm; wet weight (WW) = 0.12–0.15 g), without visible microalgae (i.e. epiphytes), from Staithes, were cultured in seawater (modified after; Gustow *et al.* (2014)). In brief, ten tips were placed into separate 250 mL glass jars containing two mesh shelves. Four tips were placed in the bottom of the jar and three tips to each mesh, having in total ten tips of different specimens in each jar (See Figure 4.2 and 4.3). All jars were filled with sterile filtered (0.7 μm) seawater from Staithes. Each set of three jar replicates were doped using a known volume of nitrate (HNO_3) or ammonia (NH_4OH). Doped N (nitrate or ammonia) concentrations in the seawater cultures were 0 μM, 10 μM, 50 μM, 100 μM and 500 μM.

To reduce evaporation all the jars were loosely covered with lids, while allowing gaseous exchange with the atmosphere. No nutrients were added into the seawater. The algae tips inside the bottles were transferred into an incubator with a set light/dark rhythm of 16:8, light intensity of 125 μmol photons/m^2s^2 and a temperature of 11ºC. The WW of the algal tips, per jar, was measured every 2–3 days during 13 days. At the same time, the medium was changed (2 times for all cultures) to avoid accumulation of metabolites. The pH and salinity of each jar was measured once. Tips samples were taken after 3 days and 13 days.

4.2.5 N isotope determinations and data treatment

N isotope measurements for all samples were obtained at the Durham Stable Isotope Biogeochemistry Laboratory (SIBL) at Durham University. Each sample was oven-dried at 60 ºC for 24 h and ground into a powder with an agate mortar and pestle. Aliquots of the powder, weighing between 1.3 and 1.5 mg, were placed into tin capsules and stored in a desiccator until analysis. δ^{15}N, δ^{13}C, %C, %N and C/N ratio were analyzed using a Costech Elemental Analyser (ECS 4010) connected to a ThermoFinnigan Delta V Advantage Isotope Ratio Mass Spectrometer.

Carbon-isotope ratios are corrected for ^{17}O contribution. Carbon and nitrogen isotope ratios are reported in standard delta (δ) notation in per mil (‰) relative to the VPDB (Vienna PDB) standard and AIR (atmospheric air) scale respectively. Data accuracy is monitored through routine analyses of in-house standards, which are stringently calibrated against international standards (e.g., USGS 40, USGS 24, IAEA 600, IAEA N1, IAEA N2). Analytical uncertainty for δ^{13}C and δ^{15}N measurements is typically ± 0.1‰ for replicate analyses of the international standards and typically < 0.2‰ on replicate sample analysis. Total organic carbon and total nitrogen data was obtained as part of the isotopic analysis using an internal standard (i.e., glutamic Acid, 40.82% C and 9.52% N).

Statistical analysis t-tests using a significance level of 0.05 were performed using R Studio software (Pruim, 2011). For testing the statistical hypothesis, p-values are used. The p-value is defined as the probability of obtaining a result more extreme or equal to what was actually observed, thus, if p-value is smaller or equal to the significance level, it suggests that the observed data are consistent.

4.3 Results

4.3.1 δ^{15}N values of *Fucus* long term *in vivo* cultures from Saithes to Tees

All *Fucus* δ^{15}N measurements from River Tees (n= 29) have negative isotopic values in average (-2.9‰) which are significantly different (p-value < 0.01) than *Fucus* from Staithes (n=15) (10.1‰ ± 1.0) (see Table 4.1). Moreover, tips collected from Staithes (10.0‰ ± 1.0) are significantly different (p-value < 0.05) from all the tips transferred from Staithes to River Tees buoys (~4.9‰ ± 1.0), although they do not reach the background levels of natural *Fucus* growing in the River (-2.2‰ ± 4.3) (Figure 4.4). After one week, all the tips δ^{15}N values decrease and stay without significant differences (p-value > 0.9) over the rest of the weeks. Significant differences (p-value < 0.01) are observed depending of the height where the macroalgae was grown (i.e. 0.4 m height: 2.9‰ and 1.2 m height: 5.3‰ ± 1.0) (see Figure 4.4). *Fucus* δ^{15}N measurements from Staithes in 2014 had an average value of 8.0‰ (See Table 4.1) which is significantly different (p-value < 0.05) from the average value in 2015 (10.0‰ ± 1.0).

4.3.2 δ^{15}N values of *Fucus* short term *in vivo* cultures from Saithes to Tees

The results shown in Figure 4.4 indicate that all *Fucus* collections δ^{15}N measurements from Staithes (~10.0‰ ± 1) are significantly different (p-value < 0.01) from all the tips transferred to River Tees buoys (~3.5‰ ± 1.5), no matter on the week of collection. Moreover, significant differences (p-value < 0.01) are observed depending of the height in the water column (i.e. 0.4 m height: 3.4‰ ± 1.2 and 1.2 m height: 4.8‰ ± 0.9) (see Figure 4.5).

4.3.3 δ^{15}N values of *Fucus in vitro* cultures effect of nitrate concentrations

After 13 days of *Fucus* cultured under 500 μM of nitrate, *Fucus* non-fertile tips δ^{15}N values (6.52‰ ± 0.17) are significantly equal to the isotopic δ^{15}N values of the nitrate solution used (7.05‰ ± 0.35) (See Figure 4.6). After 3 days of culture we can slightly observe this trend, but the differences are not fully significant, until 13 days and 2 media changes. δ^{15}N signature of the starting tips used for the culture was ~9.0‰, which means that after 13 days a reduction of ~2.5‰ is observed.

4.3.4 δ^{15}N values of *Fucus in vitro* cultures effect because of ammonia concentrations

After 13 days of *Fucus* cultured under 500 μM of ammonia, *Fucus* non-fertile tips δ^{15}N values (6.49‰ ± 0.11) are significantly different from the initial δ^{15}N signature of the tips used for culturing

(10.5‰ ± 0.01). Thus, after 13 days a reduction of ~4.0‰ δ^{15}N is observed (See Figure 4.7). The isotopic δ^{15}N values of the ammonia solution used were 2.37‰ ± 0.04.

4.4 Discussion

4.4.1 Assessment of N pollution/eutrophication tracer using *Fucus* sp.

Many studies have been made in order to elucidate if macroalgae δ^{15}N values are useful to trace pollution of the environments (Lapointe and Bedford, 2007; Piñón-Gimate *et al.*, 2009; Savage and Elmgren, 2004). However, there has not been a final resolution to directly relate the anthropogenic inputs of N in the environment and the δ^{15}N signatures in macroalgae. In most of the cases (Lapointe and Bedford, 2007; Piñón-Gimate *et al.*, 2009; Savage and Elmgren, 2004), the δ^{15}N values of the macroalgae were directly related to the inorganic N inputs. Nevertheless, Viana and Bode (2013) analyzed δ^{15}N values of macroalgae and nitrate and ammonia in different environments and concluded that it was not possible to establish a simple relation between the N isotopic signature in macroalgae and the concentrations and N isotopic values of nitrate or ammonia in the environment. Thus, it was suggested that a great variability in the inorganic nitrogen inputs, local factors and upwelling were affecting the δ^{15}N values of the macroalgae.

Our studies show that *Fucus* cultures *in vitro* with different concentrations of nitrate with a isotopic signature of 7.05 ± 0.35‰ reach this isotopic value after 13 days (6.52 ± 0.17‰) (See Figure 4.6). And, although *Fucus* cultures *in vitro* with different concentrations of ammonia with a isotopic signature of 2.37 ± 0.04‰ do not reach this isotopic value after a 13 days (6.49 ± 0.11‰) (Figure 4.7), a greater reduction of δ^{15}N signature is observed in cultures with ammonia (~4.0‰) compared to the reduction observed in nitrate cultures (~2.5‰). This shows a clear relation between the nitrogen isotopic source and nitrogen signature in macroalgae.

However, natural environments are more complex and there are many other things that need to be considered. Thus a clear correlation is not always found (Viana and Bode, 2013). In our studies, significant changes in the N signature are observed depending on the environment where *Fucus* sp. was grown. All collections in Staithes (10.0‰ ± 1.0) are significantly different (p-value < 0.05) from all the tips transferred from Staithes to the River Tees buoys (~4.9‰ ± 1.0), although they do not reach the background levels of natural *Fucus* growing in the River (-2.9‰) (Figure 4.4 and Table 4.1). Therefore, not all the initial isotopic N value is lost, but it clearly changes. Nitrogen uptake by macroalgae is influenced by morphological factors, metabolism, tissue type, age and nutrition (Neori *et al.*, 2004; Pedersen, 1994; Rosenberg and Ramus, 1984). Nitrogen is transported from the water through the cell membrane and is assimilated into organic compounds (e.g. proteins) (McGlathery *et al.*, 1996). So, the organic compounds already synthesized in the macroalgae cell do not change their N. As such, when changing the environment of tips with a high δ^{15}N signature, we should not expect them to end up with the same δ^{15}N values of other tips naturally grown in that environment, as the N

assimilated previously is not removed completely. However, a drastic change in the δ^{15}N values of the tips is observed. Thus, it can be affirmed that the nitrogen source in Tees and Staithes is different and that *Fucus* can be used as a N tracer in this areas.

Moreover, as the background levels of δ^{15}N in *Fucus* sp. are reported to be between 4 and 6‰ (Riera, 1998; Riera *et al.*, 2000; Savage and Elmgren, 2004). The values observed in both Staithes and River Tees seem to have different anthropogenic inputs of N, which will be discussed below.

4.4.2 River Tees possible N source

Significant changes in the N signature are observed depending on the environment where *Fucus* sp. was grown. All collections in Staithes (10.0‰ ± 1.0) are significantly different (p-value < 0.05) from all the tips transferred from Staithes to River Tees buoys both in long term experiments (~4.9‰ ± 1.0) (Figure 4.4) and short term ones (~3.5‰ ± 1.5) (Figure 4.5) , although they do not reach the background levels of natural *Fucus* growing in the River (-2.9‰).

If we disregard the isotopic values of naturally Tees living *Fucus*, it seems that the obtained values in the cultures *in vivo* are normal, and, thus, it would be stated that the anthropogenic N inputs of the River are null. But, taking into account that the isotopic values of *Fucus* living naturally in the River Tees are negative and extremely different from the normal values, it cannot be affirmed that the observed values in the *in vivo* cultures are natural. It can only be stated that not all the internal N of the macroalgae tips is exchanged, a part is maintained. Thus, a prominent change in the isotopic N values from tips of Staithes to River Tees, only means that the River has lots of anthropogenic inputs of N with negative isotopic values. Normally, nitrate and ammonia δ^{15}N values are between -15 to 15‰. However, extremely low δ^{15}N values for NO_3^- can be expected near chemical plants (Hübner, 1981). The reason why this happens is because of sorption of NO_x gases, which have high δ^{15}N values in exhaust treatment plants (Hübner, 1981). Hence, it is very probable that the source of N in the River Tees is nitrate from the chemical plants of the surroundings.

The differences observed depending of the height where the macroalgae was grown both in long and short term experiments might be due to the salt wedge effect. The experiments have been performed near the mouth of the River Tees where there is a transition zone between River and maritime environments. Therefore, this part of the River Tees is influenced by tides, waves and the influx of saline water from the sea and fresh water from upstream of the River Tees. This results in the formation of a water column with fresh water at the top and marine water at the bottom. Macroalgae cultured at the bottom had an average value of δ^{15}N of 2.9‰, whereas the ones cultured at the top had an average value of 5.3‰ ± 1.0 (See Figure 4.4). This means that there is more change at the top of the River Tees, meaning that the pollution might come from the fresh water. Therefore, once again, it is very probable that the source of N in the River Tees is nitrate from the chemical plants of the surroundings which ends up in the River Tees. Thus, nitrogen treatment plants should be used to

remove the nitrogen of the chemical plants before discharge into the River Tees.

The fact that in the short term experiments (Figure 4.5) do not show the same values in different weeks but same buoys might be explained because of local and temporal factors (i.e. precipitation, upwelling).

Another remarkable observation is that after a week of *in vivo* culture of *Fucus* sp. the major change in δ^{15}N was observed and the following weeks the signature stayed constant. This fact was also reported by (Viana *et al.*, 2015) where they affirm that 15 days was the time required to reach the equilibrium between the δ^{15}N value of the tip and the seawater. Wang *et al.* (2014) stated that NO_3^- uptake by *Gracilaria tenuistipitata* macroalgae followed a rate-saturating mechanism in comparison to the linear, rate-unsaturated response of NH_4OH uptake. Thus, if that is happening to *Fucus* sp. as well, and the N source in River Tees is NO_3, we should not expect further isotopic change after a week if nitrate saturation by the tips has already occurred.

4.4.3 Staithes possible N source

δ^{15}N values of all collections in Staithes 2015 (~10.1‰ ± 1.0) are significantly different from background levels reported to be normal in *Fucus* sp. (~5.0 ± 1.0‰) (Riera, 1998; Riera *et al.*, 2000; Savage and Elmgren, 2004) and from the δ^{15}N values of collections same season in Staithes 2014 (~8.0‰ ± 1.0). Many studies have linked this fact with sewage pollution (Cohen and Fong, 2005; Gartner *et al.*, 2002; Savage, 2005) which produces discharges of nitrates and ammonia with high values of δ^{15}N (Vizzini and Mazzola, 2004). Considering that there was a sewage spillage reported by the Department of Environment Food and Rural Affairs that affected Staithes during the time that we performed our experiments, it is highly likely that the high isotopic value of N in *Fucus* sp. is because of the sewage spillage.

4.5 Conclusions

The following conclusions are drawn from the present study:

i. A clear relation between the nitrogen isotopic source and nitrogen signature in macroalgae is observed when cultures are performed *in vitro*.

ii. After a week of *in vivo* culture of *Fucus* sp. the major change in δ^{15}N was observed and the following weeks the signature stayed constant, showing that the rate of nitrogen uptake is very fast.

iii. Not all the internal N of the macroalgae tips is exchanged, a part is maintained.

iv. River Tees most probable source of N is NO_3^- from chemical plants nearby. Moreover, the pollution seems to come from the fresh water column. Therefore, it is very probable that the source of N in the River Tees is nitrate from the chemical plants of the surroundings which ends up in the

River Tees. Thus, nitrogen treatment plants should be used to remove the nitrogen of the chemical plants before discharges into the River Tees.

v. Staithes most probable source of N is sewage waste.

4.6 References

Cohen R.A. and Fong P. (2005) Experimental evidence supports the use of δ^{15}N content of the oppurtunistic green macroalga *Enteromorpha intestinalis* (Chlorophyta) to determine nitrogen sources to estuaries. J. Phycol. 41, 287-293. DOI 10.1111/j.1529-8817.2005.04022.x

de Carvalho M.C. (2008) Uso dos isotopos estaveis de carbono, nitrogeno e enxofre em estudios de ecologia costeira. Oecologia Bras 12, 694-705.

Fernandes M. Benger S. Sharma S.K. Gaylard S. Kildea T. Hoared S. Braley M. and Irving A.D. (2012) The use of δ^{15}N signatures of translocated macroalgae to map coastal plumes; improving species selection and spatial analysis of metropolitan datasets. J. Environ. Monitor. 14, 2399- 2410. DOI 10.1039/c2em10997b

Gartner A. Lavery P. and Smit A.J. (2002) Use of δ^{15}N signatures of different functional forms of macroalgae and filter-feeders to reveal temporal and spatial patterns in sewage dispersal. Mar. Ecol-Prog. Ser. 235, 63-73. DOI 10.3354/meps235063

Gustow L. Rahman M.M. Bartl K. Saborowski R. Bartsch I. and Wiencke C. (2014) Ocean acidification affects growth but not nutritional quality of the seaweed *Fucus vesiculosus* (Phaeophyceae, Fucales). J. Exp. Mar. Biol. Ecol 453, 84-90. DOI 10.1016/j.jembe.2014.01.005

Heaton T.H.E. (1986) Isotopic studies of nitrogen pollution in the hydrosphere and atmosphere: a review. Chem. Geol. 59, 87-102. DOI: 10.1016/0168-9622(86)90059-X

Hübner H. (1981) Isotope effects of nitrogen in soils and the biosphere in Fritz, P., and Fontes, J., eds., Handbook of environmental isotope geochemistry, v. 2b, The terrestrial environment: The Netherlands, Elsevier, p. 361–425.

Lapointe B.E. and Bedford B.J. (2007) Drift rhodophyte blooms emerge in Lee County, Florida, USA: Evidence of escalating coastal eutrophication. Harmful algae 6, 421-437.DOI: 10.1016/j.hal.2006.12.005

Maier G. Nimmo-Smith R.J. Glegg G.A. Tappin A.D. and Worsford P.J. (2009) Estuarine eutrophication in the UK: current incidence and future trends. Aquatic Conserv. 19, 43-56. DOI 10.1002/aqc.982

Mariotti A. Germon J.C. Hubert P. Kaiser P. Letolle R. Tardieux A. and Tardieux P. (1981) Experimental determination of nitrogen kinetic isotope fractionation: some principles; illustration for the denitrification and nitrification processes. Plant Soil 62, 413-430.DOI 10.1007/BF02374138

McGlathery K.J. Pedersen M.F. and Borum J. (1996) Changes in intracellular nitrogen pools and

feedback controls on nitrogen uptake in *Chaetomorpha linum* (chlorophyta). J. Phycol. 32, 393-401. DOI 10.1111/j.0022-3646.1996.00393.x

Minagawa M. and Wada E. (1984) Stepwise enrichment of δ^{15}N along food chains: further evidence and the relation between δ^{15}N and animal age. Geochim. Cosmochim. Acta 48, 1135-1140. DOI 10.1016/0016-7037(84)90204-7

Neori A. Chopin T. Troell M. Buschmann A.H. Kraemer G.P. Halling C. Shpigel M. and Yarish C. (2004) Integrated aquaculture: rationale, evolution and state of the art emphasizing seaweed biofiltration in modem mariculture. Aquaculture 231, 361-391. DOI 10.1016/j.aquaculture.2003.11.015

Pedersen M.F. (1994) Transient ammonium uptake in the macroalga *Ulva lactuca* (Chlorophyta) - nature, regulation, and the consequences for choice of measuring technique. J. Phycol. 30, 980-986. DOI 10.1111/j.0022-3646.1994.00980.x

Piñón-Gimate A. Soto-Jiménez M. Ochoa-Izaguirre M.J. García-Pagés E. and Páez-Osuna F. (2009) Macroalgae blooms and δ^{15}N in subtropical coastal lagoons from the Southeastern Gulf of California: discrimination among agricultural, shrimp farm and sewage effluents. Mar. Pollut. Bull. 58, 1144-1151. DOI 10.1016/j.marpolbul.2009.04.004

Riera P. (1998) δ^{15}N of organic matter sources and benthic invertebrates along an estuarine gradient in Marennes-Oleron Bay (France): implications for the study of the trophic structure. Mar. Ecol-Prog. Ser. 166, 143-150. DOI 10.3354/meps166143

Riera P. Stal L.J. and Nieuwenhuize J. (2000) Heavy δ^{15}N in Intertidal Benthic Algae and Invertebrates in the Scheldt Estuary (The Netherlands): Effect of River Nitrogen Inputs. Estuar. Coast. Shelf S. 51, 365-372. DOI 10.1006/ecss.2000.0684

Rosenberg G. and Ramus J. (1984) Uptake of inorganic nitrogen and seaweed surface-area-volume ratios. Aquat. Bot. 19, 65-72. DOI 10.1016/0304-3770(84)90008-1

Savage C. (2005) Tracing the Influence of Sewage Nitrogen in a Coastal Ecosystem Using Stable Nitrogen Isotopes. AMBIO 34, 145-150. DOI 10.1639/0044-7447(2005)034[0145:TTIOSN]2.0.CO;2

Savage C. and Elmgren R. (2004) Macroalgal (*Fucus vesiculosus*) δ^{15} values trace decrease in sewage influence. Ecol. appl. 14, 517-526. DOI 10.1890/02-5396

Viana I.G. and Bode A. (2013) Stable nitrogen isotopes in coastal macroalgae: geographic and anthropogenic variability. Sci. Total Environ. 15, 887-895. DOI 10.1016/j.scitotenv.2012.11.065

Viana I.G. Bode A. Bartholomew M. and Valiela I. (2015) Experimental assessment of the macroalgae *Ascophyllum nodosum* and *Fucus vesiculosus* for monitoring N sources at different time-scales using stable isotope composition. J. Exp. Mar. Biol. Ecol. 466, 24-33. DOI 10.1016/j.jembe.2015.01.014

Viana I.G. Fernandez J.A. Aboal J.R. and Carballeira A. (2011) Measurement of d15N in macroalgae stored in an environmental specimen bank for regional scale monitoring of eutrophication in coastal areas. Ecol. Indic. 11, 888-895.DOI 10.1016/j.ecolind.2010.12.004

Vizzini S. and Mazzola A. (2004) Stable isotope evidence for the environmental impact of a land-based fish farm in the western Mediterranean. Mar. Pollut. Bull. 49, 61-70. DOI 10.1016/j.marpolbul.2004.01.008

Wang C. Lei A. Zhou K. Hu Z. Hao W. and Yang J. (2014) Growth and Nitrogen Uptake Characteristics Reveal Outbreak Mechanism of the Opportunistic Macroalga *Gracilaria tenuistipitata*. PLoS One 9. DOI 10.1371/journal.pone.0108980

4.7 Tables and captions

Table 4.1 C, N, C/N, δ^{13}C and δ^{15}N of *Fucus* grown naturally in river Tees nearby the buoys and Staithes background levels analysed with Stable Isotope Mass spectrometer.

Sample	C	δ^{13}C	N	δ^{15}N	C/N
River Tees					
27.05.2015					
Site1	40.1 ± 1.2	-18.3 ± 0.5	-18.3 ± 0.5	3.7 ± 0.3	5.4 ± 0.1
Site2	39.0 ± 1.7	-17.4 ± 0.6	8.4 ± 0.7	3.9 ± 0.2	5.5 ± 0.3
Site3	38.9 ± 0.0	-23.3 ± 0.0	13.6 ± 0.0	-9.2 ± 0.0	3.3 ± 0.0
Site4	38.7 ± 1.6	-18.8 ± 1.0	8.4 ± 0.5	1.4 ± 0.6	5.4 ± 0.1
Site5	41.1 ± 1.0	-19.7 ± 0.4	10.0 ± 0.5	-1.1 ± 0.7	4.8 ± 0.2
site7	40.3 ± 1.9	-17.4 ± 0.4	8.6 ± 0.7	3.6 ± 0.1	5.5 ± 0.2
Site8	37.9 ± 1.8	-16.9 ± 0.1	9.0 ± 0.8	2.6 ± 0.1	5.0 ± 0.2
Site9	37.7 ± 2.2	-16.4 ± 0.2	8.8 ± 0.5	1.8 ± 0.3	5.0 ± 0.1
Site11	40.1 ± 1.6	-20.5 ± 0.4	9.5 ± 0.4	-1.5 ± 0.7	4.9 ± 0.0
Site12	43.8 ± 0.0	-24.3 ± 0.0	15.4 ± 0.0	-9.1 ± 0.0	3.3 ± 0.0
Site14	38.4 ± 1.4	-17.9 ± 0.7	8.0 ± 0.6	2.5 ± 0.5	5.7 ± 0.2
Site15	39.9 ± 2.3	-18.7 ± 0.5	9.1 ± 0.9	3.5 ± 0.2	5.2 ± 0.2
01.07.2015					
Site2	36.4 ± 1.0	-20.2 ± 0.4	9.7 ± 0.2	-6.2 ± 0.1	4.4 ± 0.0
Site3	37.3 ± 1.2	-19.1 ± 0.5	9.7 ± 0.3	-9.2 ± 0.1	4.5 ± 0.3
Site5	39.8 ± 2.2	-17.1 ± 0.4	7.3 ± 0.6	-5.2 ± 0.0	6.4 ± 0.2
Site6	36.3 ± 1.9	-20.6 ± 0.3	8.3 ± 0.4	-6.5 ± 0.1	5.1 ± 0.2
Site8	38.7 ± 1.0	-18.9 ± 0.4	9.5 ± 0.4	-8.1 ± 0.2	4.7 ± 0.2
Site9	36.3 ± 2.2	-18.0 ± 0.3	8.2 ± 0.6	-3.6 ± 0.3	5.2 ± 0.2
Site11	37.4 ± 1.4	-16.8 ± 0.3	8.4 ± 0.4	-4.8 ± 0.2	5.2 ± 0.1
Site12	36.9 ± 1.5	-20.1 ± 0.4	9.1 ± 0.5	-5.6 ± 0.2	4.7 ± 0.1
Site13	37.7 ± 2.5	-17.7 ± 0.3	8.5 ± 0.6	-1.8 ± 0.1	5.2 ± 0.1
Site14	38.7 ± 1.5	-18.7 ± 0.5	7.4 ± 0.2	-4.9 ± 0.6	6.1 ± 0.1
Average	38.2	-19.0	9.2	-2.9	5.0
Staithes 2015					
15.07.2015	38.1 ± 0.5	-15.3 ± 0.4	5.0 ± 0.2	9.9 ± 0.3	9.0 ± 0.3
22.07.2015	40.7 ± 0.3	-16.3 ± 0.0	5.7 ± 0.1	9.6 ± 0.1	8.3 ± 0.1
28.07.2015	39.2 ± 0.4	-15.8 ± 0.0	6.1 ± 0.2	10.3 ± 0.1	7.5 ± 0.1
04.08.2015	42.0 ± 1.5	-15.6 ± 0.0	2.3 ± 0.1	10.6 ± 0.1	21.4 ± 0.0
11.08.2015	35.2 ± 0.3	-15.4 ± 0.0	1.7 ± 0.1	10.2 ± 0.1	24.4 ± 1.2
17.08.2015	33.3 ± 0.3	-16.5 ± 0.0	1.8 ± 0.0	10.1 ± 0.0	21.2 ± 0.1
25.08.2015	33.3 ± 1.3	-16.8 ± 0.0	3.5 ± 0.1	10.1 ± 0.1	11.2 ± 0.0
Average	37.4	-16.0	3.7	10.1	14.7
Staithes 2014					
1 Staithes	49.1 ± 8.5	-19.0 ± 0.3	3.9 ± 0.7	6.3 ± 0.4	14.8 ± 0.2
2 Staithes	35.8 ± 0.4	-18.9 ± 0.6	2.5 ± 0.1	8.8 ± 0.2	17.0 ± 0.6
3 Staithes	35.4 ± 1.1	-19.2 ± 0.5	2.5 ± 0.0	8.8 ± 0.2	16.2 ± 0.5
4 Staithes	36.8 ± 0.4	-19.4 ± 0.1	2.4 ± 0.1	8.8 ± 0.3	18.1 ± 0.8
5 Staithes	31.6 ± 0.4	-18.8 ± 0.4	2.1 ± 0.1	8.8 ± 0.0	17.4 ± 0.8
Average	37.7	-19.1	2.7	8.0	16.7

Figure 4.1 Collection sites of *Fucus* sp. (**A**) Buoys localizations used for *in vivo* culturing macroalgae from site. (**B**) Staithes *Fucus* sp. collected for *in vivo* and *in vitro* culture experiments.

Figure 4.2 Culture representation of non-reproductive *Fucus* thallus tips. (**A**) Two meshes were put inside each jar generating three levels that each hold three non-fertile tips each (**B**). (**C**) Photo of the culture jar used.

Figure 4.3 Experimental design for *in vitro* cultures of *Fucus* thallus tips with different concentrations of nitrate or ammonia in the media solution.

Figure 4.4 δ^{15}N values for *in situ* cultures of *Fucus* sp. in River Tees over a period of 3 weeks. Graphs in the left with red markers correspond to the values of top buoy cultures, thus graphs in the right with black markers correspond to the values of bottom buoy cultures. Graphs arranged from top to bottom corresponding to buoy 1, 2, 3 and 4 respectively. All the samples had a reproducibility of <0.6 SD. In all cases, graph symbol size is greater than uncertainties.

Figure 4.5 δ^{15}N values for *in situ* cultures of *Fucus* sp. in River Tees over a period of 1 week. (**A**) From the 15^{th} to the 22^{nd} of July 2015. (**B**) From the 4^{th} to the 11^{th} of August 2015. (**C**) From the 11^{th} to the 17^{th} of August 2015. (**D**) From the 17^{th} to the 25^{th} of August 2015. All the samples had a reproducibility of <0.6 SD. In all cases, graph symbol size is greater than uncertainties.

Figure 4.6 δ^{15}N values for *in vitro* cultures of *Fucus* sp. with nitrate over a period of 3 and 13 days. Nitrate solution δ^{15}N value was of 7.05 ± 0.35‰. All the samples had a reproducibility of <0.4 SD. In all cases, graph symbol size is greater than uncertainties.

Figure 4.7 δ^{15}N values for *in vitro* cultures of *Fucus* sp. with ammonia over a period of 3 and 13 days. Ammonia solution δ^{15}N value was of 2.37 ± 0.04‰. All the samples had a reproducibility of <0.4 SD. In all cases, graph symbol size is greater than uncertainties.

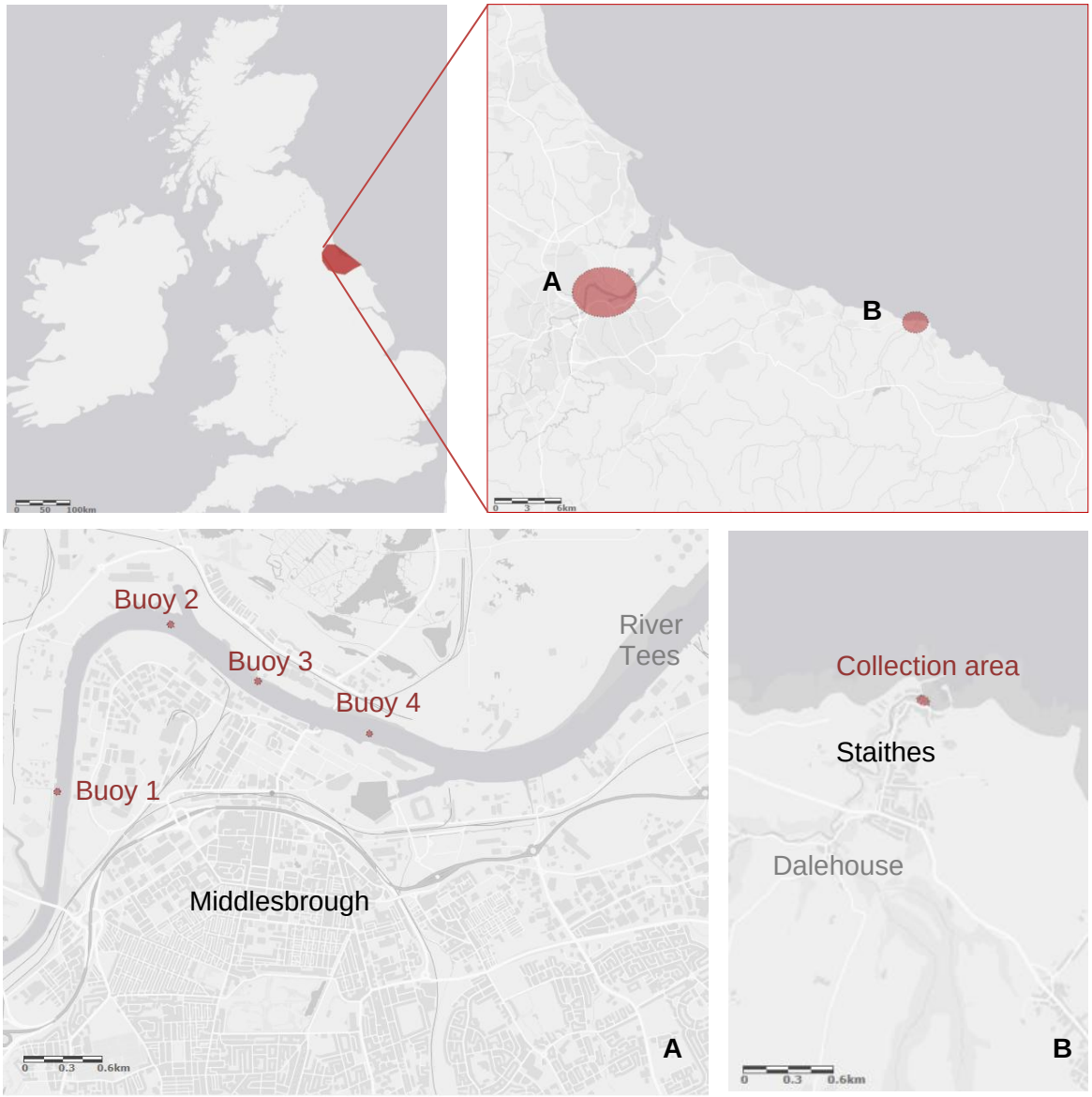

Figure 4.1 Collection sites of *Fucus* sp. (**A**) Buoys localizations used for in vivo culturing macroalgae from site **B**. (**B**) Staithes *Fucus* sp. collected for in vivo and in vitro culture experiments.

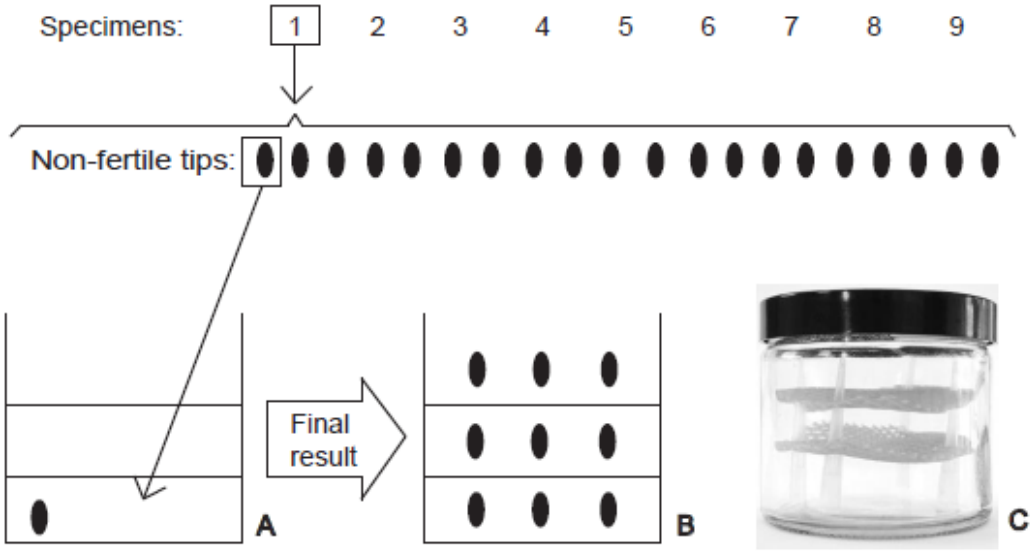

Figure 4.2 Culture representation of non-reproductive *Fucus* thallus tips. 21 tips of *Fucus* specimens from the same area were cut and a tip was displaced into one of the 21 jars (**A**). Two meshes were put inside each jar ending up with three levels that store three non-fertile tips each (**B**). (**C**) Real culture jar picture.

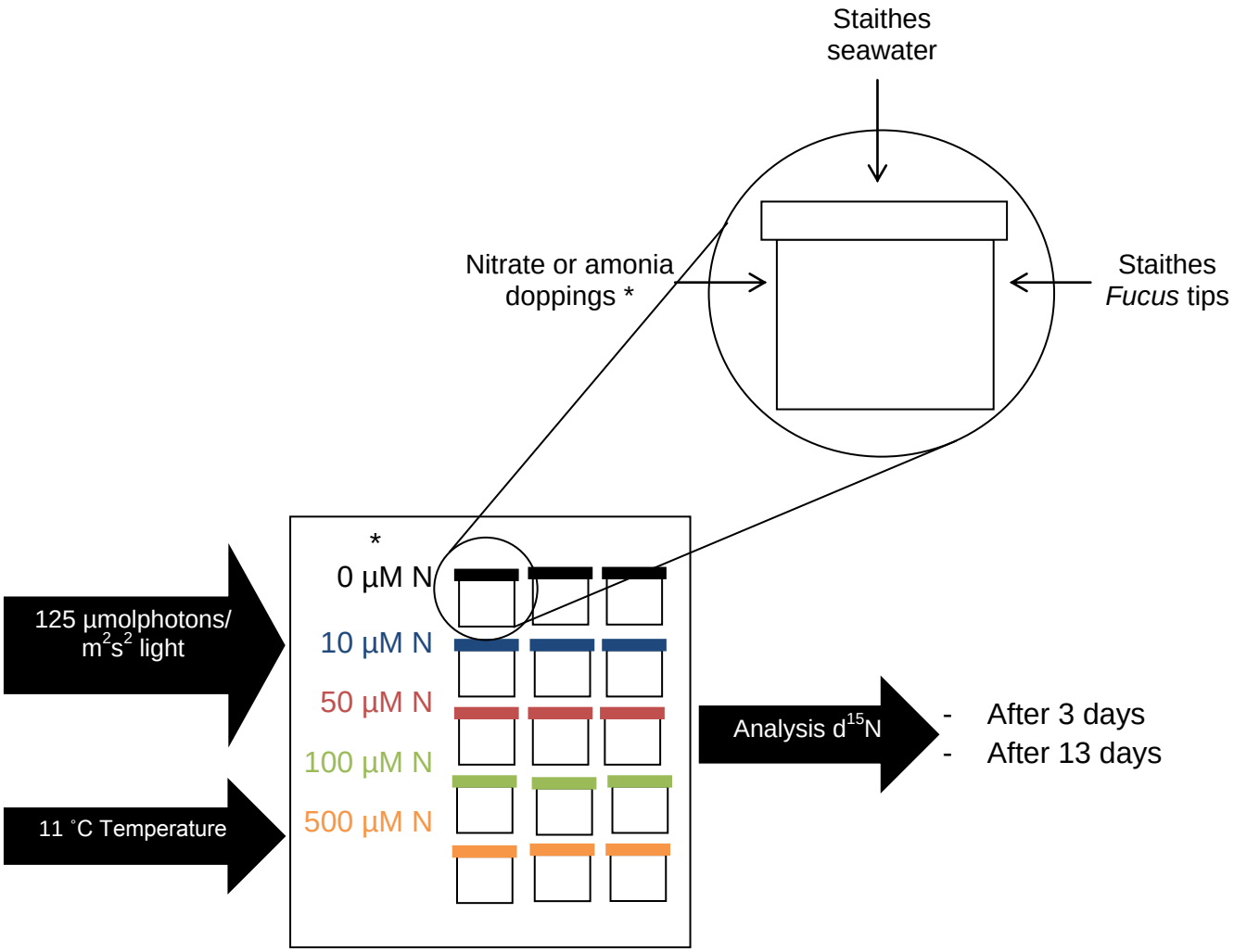

Figure 4.3 Experimental design for in vitro cultures of *Fucus* thallus tips with different concentrations of nitrate or ammonia in the media solution.

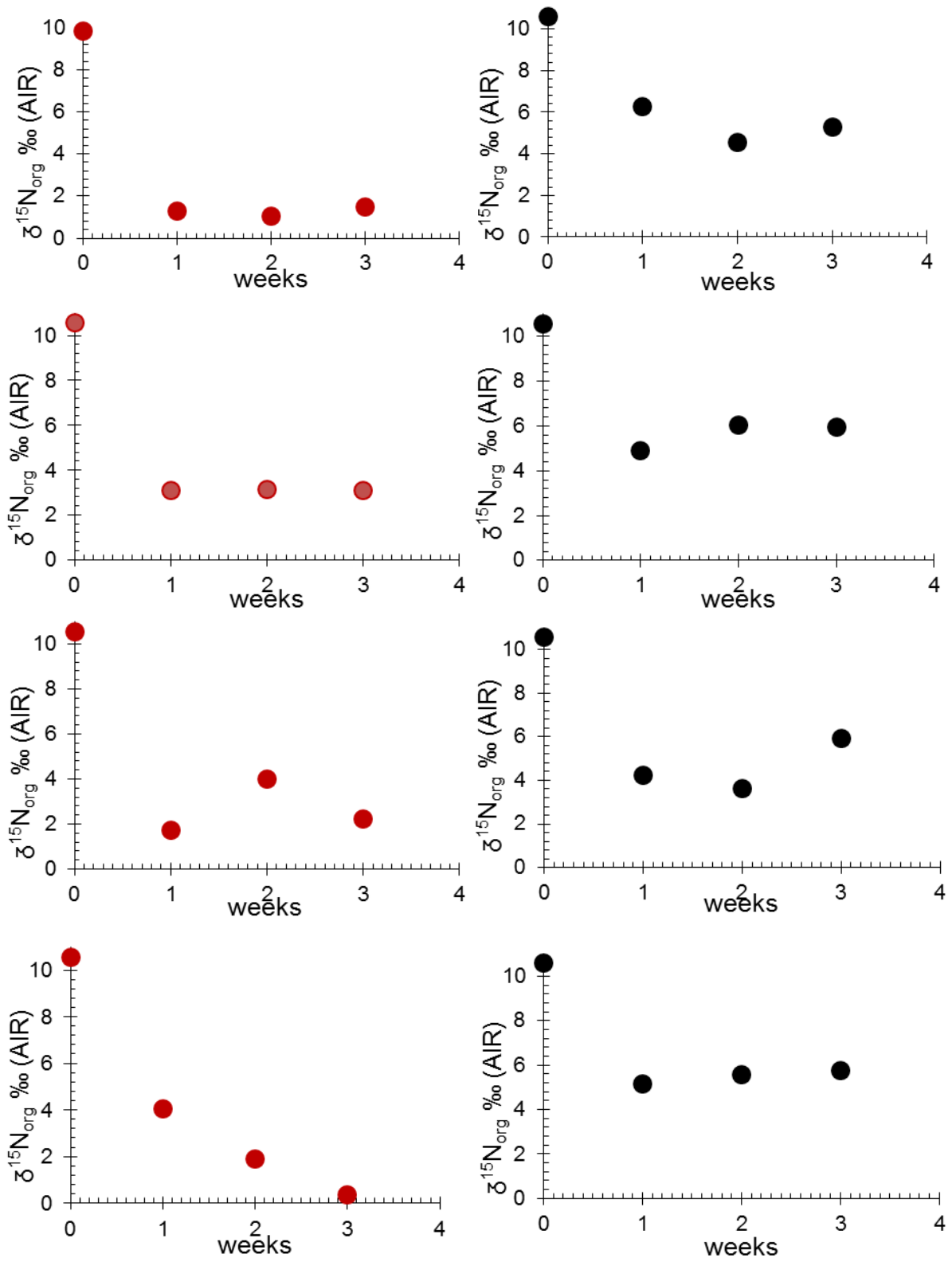

Figure 4.4 $\delta^{15}N$ values for *in situ* cultures of *Fucus* sp. in River Tees over a period of 3 weeks.Graphs in the left with red markers correspond to the values of top buoy cultures, thus graphs in the right with black markers correspond to the values of bottom buoy cultures. Graphs arranged from top to bottom corresponding to buoy 1, 2, 3 and 4 respectively. All the samples had a reproducibility of < 0.6 SD, in all cases, graph symbol size is greater than uncertainties.

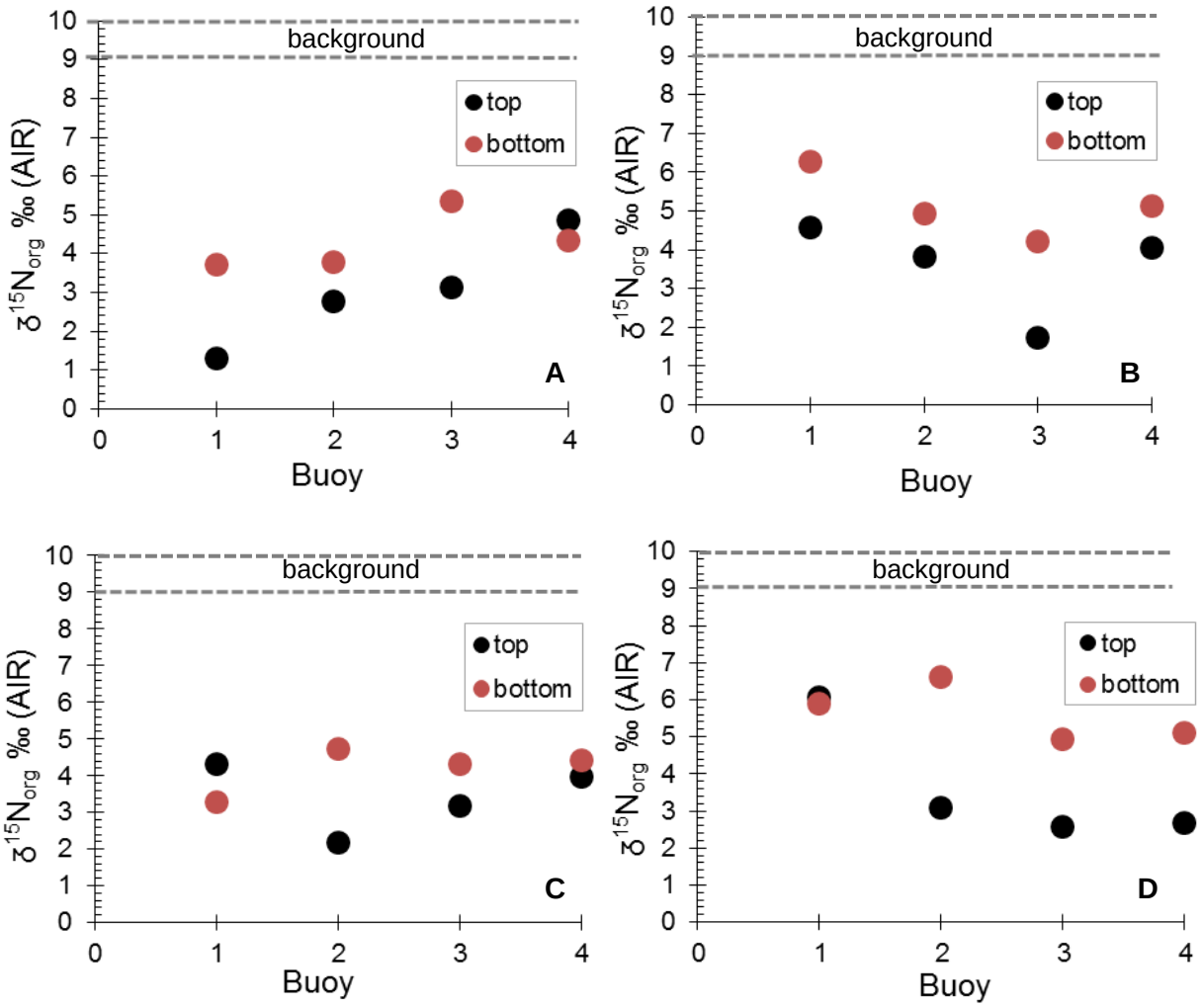

Figure 4.5 $\delta^{15}N$ values for *in situ* cultures of *Fucus* sp. in River Tees over a period of 1 week. (**A**) From the 15th to the 22nd of July 2015 (**B**) From the 4th to the 11th of August 2015 (**C**) From the 11th to the 17th of August 2015 and (**D**) From the 17th to the 25th of August 2015. All the samples had a reproducibility of < 0.6 SD, in all cases, graph symbol size is greater than uncertainties.

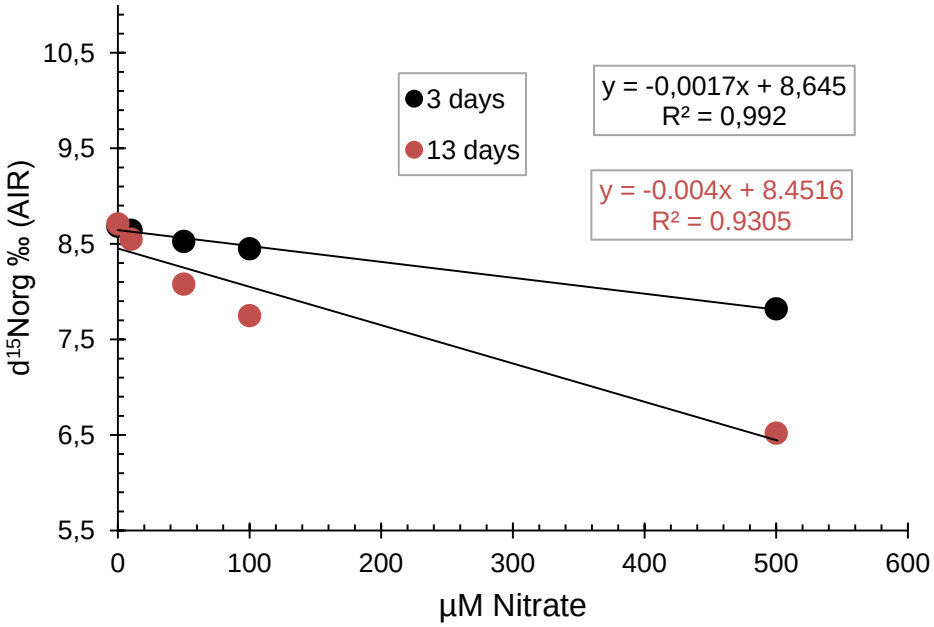

Figure 4.6 $\delta^{15}N$ values for *in vitro* cultures of *Fucus* sp. in nitrate media over a period of 3 and 13 days. Nitrate solution $\delta^{15}N$ value was of 7.05 ± 0.35‰. All the samples had a reproducibility of < 0.4 SD, in all cases, graph symbol size is greater than uncertainties.

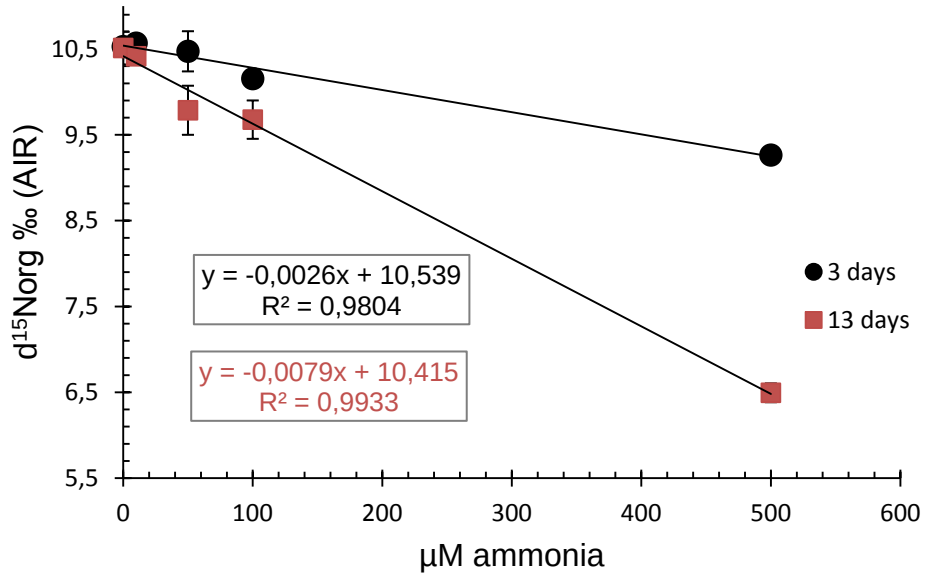

Figure 4.7 $\delta^{15}N$ values for *in vitro* cultures of *Fucus* sp. in ammonia media over a period of 3 and 13 days. Ammonia solution $\delta^{15}N$ value was of 2.37 ± 0.04‰. All the samples had a reproducibility of < 0.4 SD, in some cases, graph symbol size is greater than uncertainties.

5. General discussions and conclusions

The present research carried out during this Masters thesis has brought new insights on the uptake and distribution of Re and Os within the brown macroalgae, *F. vesiculosus*. This study has shown the importance of *F. vesiculosus* as a potential bioremediator and bioaccumulator for Re or Tc and Os, as a biomonitor of anthropogenic N inputs and as a proxy for the Os isotopic composition in seawater.

5.1 Rhenium uptake and distribution in Phaeophyceae macroalgae (*F. vesiculosus*)

The idea that macroalgae concentrates Re has previously been observed, even though it has no known biological function. This study documented the first detailed examination of the relative proportions of Re in the structures of macroalgae and gives an extensive assessment of Re uptake by *F. vesiculosus*. The following conclusions are drawn from the present study:

- **Re is not concentrated into a single macroalgae structure – all the cells contain Re.**
  The distribution of Re increases from the holdfast up to the tips. There are significant differences between the amount of Re stored in the tips (~126 ppb) *versus* Re stored in the remainder of the macroalgae (~74 ppb). Furthermore, significant concentration of Re is found in the non-fertile tips which suggests a link between Re and the meristematic and photosynthesis-specialized cells. More specifically, an average concentration of 313 ppb of Re was found in the non-fertile tips, 122 ppb in the fertile tips, 67 ppb in the blades, 66 ppb in the vesicles, 23 ppb in the stipe and 21 ppb in the holdfast. This suggests that Re is most likely stored in the photosynthetic structures and is not in the reproductive structures (receptacles).

- **Re is not accumulated in chloroplast or cytoplasm proteins.**
  In this study, the proteins were isolated whereby no disruption of the membranes was performed,

and therefore it cannot be assumed that membrane bound proteins were simultaneously extracted. Moreover, the method for protein detection used does not detect free amino acids, peptides (i.e. glutathione, metallothioneins and phytochelatins) and proteins smaller than 3 kDa. Thus, whether Re is not protein bound is inconclusive, because we cannot be certain that all the proteins were isolated. However, this study does show that Re adsorption is not related to cytoplasmic proteins bigger than 3 kDa or, if Re is very weakly bound to these larger proteins (see Figure 2.8).

- **Re is bioadsorbed (syn-life) by *F. vesiculosus*, rather than bioaccumulated, and does not follow a simple diffusion uptake mechanism.**
  If Re was taken up by simple diffusion, we would expect the same (or at least similar) uptake of Re after boiling, freezing or drying the tips, but this feature was not observed (see Figure 2.4 and 2.5). Although Re could be taken up through passive mediated transport (facilitated diffusion), it seems unlikely due to the high Re uptake observed in living *F. vesiculosus* tips relative to the concentration in seawater. Moreover, Figure 2.5 shows that the uptake mechanism is unidirectional; not a simple partition, whereby *F. vesiculosus* only uptakes and stores Re. Furthermore, the observation that little to no ReO_4^- is accumulated by metabolically inactivated *F. vesiculosus* tips indicates that if this is also the case for macroalgae organic matter that is preserved in sediments, the use of Re as a palaeo-redox may not be applicable.

- **Re recovery is observed from the seawater enriched with ReO_4^-, opening the possibility of using *F. vesiculosus* as a source of phytomining.**
  However, our experiments show that all perrhenate salts have the same linear trendline which strongly differs from perrhenate obtained from Re metal with HNO_3, highlighting the importance in choosing the Re compound for doping. Perrhenate salts ($NaReO_4$, $KReO_4$ and NH_4ReO_4) are highly soluble in water with solubilities around 1.1 g/mL. It has been observed that cations are used as a symport for perrhenate uptake in animal cells. Our results seem to show that H^+ is the best counter ion for perrhenate uptake, therefore a greater uptake is observed when $HReO_4$ is used. Moreover, H^+ could be increasing the conversion of $–NH_2$ groups of the macroalgae to $–NH_3^+$, thus allowing perrhenate to bind.

  Table 2.1 suggests that seasonal differences in perrhenate uptake are function of *F. vesiculosus* growth, thus perrhenate uptake is biologically influenced. Riget *et al.* (1995) observed that zinc had maximum concentrations in macroalgae in March and a minimum in September, and it was similarly observed, a bit less clearly, with lead and copper. Fuge and James (1973) demonstrate that macroalgae growth is the cause for seasonal variation and the results obtained by Riget *et al.* (1995) and our studies confirm this theory. A limit in the concentration of ReO_4^- for *F. vesiculosus* tips is attained, between 75 ppb and 1000 ppb of $HReO_4$ in the media, and beyond that a deleterious effect is observed (Figure 2.3). When non-fertile thallus tips

start dying they do not accumulate more Re. Thus Re is released to the media. Therefore, less accumulation of Re in those cultured macroalgae tips that started dying is expected. This happened in the macroalgae tips cultured with 2000 and 7450 ppb of $HReO_4$ in the seawater. In addition, it is worth emphasising that the more time the dying tips are left in water, the more Re is released in the seawater by macroalgae (i.e. the less accumulation of Re) (Figure 2.4)

5.2 Osmium uptake and distribution in Phaeophyceae macroalgae (*F.vesiculosus*)

This study documents the first detailed examination of the relative proportions of Os in the structures of *F.vesiculosus* and changes in Os accumulation and isotopic compositions ($^{187}Os/^{188}Os$) under changing conditions of Os in the water. The following conclusions are drawn from the present study:

- **Os is not concentrated into a single macroalgae structure, all the cells possess Os.** Moreover, there is an equivalent distribution of Os in all the structures which strongly supports the idea that Os is accumulated into a common compartment or particle present in all cells. The Os ranges from 16 to 38 ppt. The structure that contains less Os is the holdfast, with 16 ppt and the structures with the highest Os are the blades, with 38 ppt. The other structures (tips, stipe and vesicles) do have between 24 and 25 ppt Os. Although we see some differences within structures, the differences are too low to be considered significant.

- **Os is accumulated by *F. vesiculosus*.**
  At the highest concentration (i.e. 1 ppt Os in seawater), tips accumulated ~200 ppt of Os, which is around ten times higher than the background concentration of Os (Figure 3.3). Natural Os isotopic composition in *F. vesiculosus* is 0.81 which coincides with the Os isotopic composition of seawater (between 0.76 and 1.04 (Koide *et al.*, 1996; Sharma *et al.*, 1997; Woodhouse *et al.*, 1999)) (Figure 3.3). However, the Os doped in the culture experiments had an isotopic composition of 0.16. Thus, the greater Os accumulated by macroalgae, the greater the isotopic composition decrease, following an exponential correlation, as it is expected to be uptaking Os from the doping solution. The isotopic composition observed after Os doping treatments do not fit perfectly with the isotopic composition predicted, due to the Os already present in the macroalgae and the Os present in the seawater used for the dilutions, which both have around 0.85 isotopic compositions. This means that the Os already present in the macroalgae is not lost or exchanged with the media. Thus it maintains the same isotopic composition. However, a major decrease is observed, showing a clear uptake of Os by *F. vesiculosus*.

5.3 Nitrogen uptake in Phaeophyceae macroalgae, *Fucus sp.*

The present study aims to assess the usefulness of $\delta^{15}N$ measurements in macroalgae as an eutrophication or pollutant recorder and thus to understand the source of nitrogen of the River Tees

and Staithes. The following conclusions are drawn:

- ***Fucus sp.* cultures, *in vitro*, with different concentrations of nitrate reach equilibrium with the isotopic composition of that nitrate within 13 days** (see Table 4.1).
  And, although *Fucus* cultures *in vitro* with different concentrations of ammonia with a isotopic signature of 2.37 ± 0.04‰ do not reach this isotopic value after a 13 days (6.49 ± 0.11‰), a greater reduction of δ^{15}N signature is observed in cultures with ammonia (~4.0‰) compared to the reduction observed in nitrate cultures (~2.5‰), showing a clear relation between the nitrogen isotopic source and nitrogen signature in macroalgae. However, natural environments are more complex and there are many other things that need to be considered, thus a clear correlation is not always found (Viana and Bode, 2013).

- **Significant changes in the N isotopic signature are observed depending on the environment were *Fucus* sp. lived.**
  All collections in Staithes (10.0‰ ± 1.0) are significantly different (p-value < 0.05) from all the tips transferred from Staithes to the River Tees buoys both in long-term (~4.9‰ ± 1.0) and short term experiments (~3.5‰ ± 1.5); but they do not reach the same isotopic signatures of *Fucus* sp. growing in the River Tees (-2.9‰) (Table 4.1). Considering that the nitrogen isotope values of *Fucus* sp. living in the River Tees are negative and extremely different from Staithes, it cannot be affirmed that the observed values in the *in vivo* cultures are natural. It is suggested that not all the internal N of the macroalgae tips has exchanged with the surrounding environment. Typical nitrate and ammonia δ^{15}N values have been reported between -15‰ and +15‰, although extremely low δ^{15}N values for NO_3^- do occur near chemical plants (Hübner, 1981). The reason why this happens is because of sorption of NO_x gases, which have high δ^{15}N values in exhaust treatment plants (Hübner, 1981). Hence, it is very probable that the source of N in the River Tees is nitrate from the chemical plants of the surroundings.

  Moreover, the differences observed depending of the height where the macroalgae was grown confirm this statement. The mouth of the River Tees has a water column with fresh water at the top and marine water at the bottom. Macroalgae cultured at the bottom had an average value of δ^{15}N of 2.9‰ ± 1.0, whereas the ones cultured at the top had an average value of 5.3‰ ± 1.0 (See Figure 4.4). This means that that the pollution might come from the fresh water. Therefore, once again, it is very probable that the source of N in the River Tees is nitrate from the chemical plants of the surroundings which ends up in the River Tees. Thus, nitrogen treatment plants should be used to remove the nitrogen of the chemical plants before discharge into the River Tees.The fact that in the short term experiments do not show the same values in different weeks but same buoys might be explained because of local and temporal factors (i.e. precipitation, upwelling).

- **The major change in δ^{15}N was observed after a week of *in vivo* culture of *Fucus* sp. The**

following weeks the signature stayed constant.
This fact was also reported by (Viana *et al.*, 2015) where they affirm that 15 days was the time required to reach the equilibrium between the δ^{15}N value of the tip and the seawater. Wang *et al.* (2014) stated that NO_3 uptake by *Gracilaria tenuistipitata* macroalgae followed a rate-saturating mechanism in comparison to the linear, rate-unsaturated response of NH_4OH uptake. Thus, if that is happening to *Fucus* sp. as well, and the N source in river Tees is NO_3^-, we should not expect further isotopic change after a week if nitrate saturation by the tips has already occurred.

- **Confirmation of δ^{15}N measurements in macroalgae as an eutrophication or pollutant recorder in Staithes.**
δ^{15}N values of all collections in Staithes 2015 (~10.1‰ ± 1.0) are significantly different from background levels reported to be normal in *Fucus sp.* (~5.0‰ ± 1.0) (Riera, 1998; Riera *et al.*, 2000; Savage and Elmgren, 2004) and from the δ^{15}N values of collections same season in Staithes 2014 (~8.0‰ ± 1.0). Many studies have linked this fact with sewage causes (Cohen and Fong, 2005; Gartner *et al.*, 2002; Savage, 2005) which produce discharges of nitrates and ammonia with high values of δ^{15}N (Vizzini and Mazzola, 2004). And considering that there was a sewage spillage reported by the Department of Environment Food and Rural Affairs that affected Staithes during the time that we performed our experiments, it is very clear that the high isotopic value of N in *Fucus* sp. is because of the sewage spillage.

5.4 Further work

During the execution of the current project, a new window of possibilities to enlarge the studies in this field was opened. Here some suggestions of further work are outlined.

There are many chemical and physical variables affecting the uptake of chemical elements such as; pH, ionic strength, salinity, temperature, light, competition between metal ions and many others. In order to understand the uptake mechanism of Re and Os, experiments which alter these variables should be done. In the appendix section A, there is a detailed study performed about the alteration of some of these factors, and although the results are promising, more experiments need to be done to arrive to a proper conclusion.

Furthermore, to affirm that Re is not related with proteins we should re-run the column chromatography adding a detergent to disrupt the membranes and release the membranous proteins.

Finally, as reported by Park D. et al (2002) that a brown macroalgae species can reduce Cr(VI) to Cr(III), it would be interesting to see if *F. vesiculosus* can reduce Re(VII) to another Re state.

5.5 References

Bozhkov O. and Borisova L. V. (2002) Extraction and determination of trace amounts of Rhenium in plants. Intern. J. Environ. Anal. Chem. Vol. 83; 135-141. DOI 10.1080/0306731021000048627

Cohen R.A. and Fong P. (2005) Experimental evidence supports the use of δ^{15}N content of the oppurtunistic green macroalga *Enteromorpha intestinalis* (Chlorophyta) to determine nitrogen sources to estuaries. J. Phycol. 41, 287-293. DOI 10.1111/j.1529-8817.2005.04022.x

Fuge R. and James K.H. (1973) Trace metal concentrations in brown seaweeds, Cardigan Bay, Wales. Mar. Chem. 1, 281-293. DOI 10.1016/0304-4203(73)90018-2

Gartner A. Lavery P. and Smit A.J. (2002) Use of δ^{15}N signatures of different functional forms of macroalgae and filter-feeders to reveal temporal and spatial patterns in sewage dispersal. Mar. Ecol-Prog. Ser. 235, 63-73. DOI 10.3354/meps235063

Hübner H. (1981) Isotope effects of nitrogen in soils and the biosphere in Fritz, P., and Fontes, J., eds., Handbook of environmental isotope geochemistry, v. 2b, The terrestrial environment: The Netherlands, Elsevier, p. 361–425.

Koide M. Goldberg E.D. and Walker R. (1996) The analysis of seawater osmium. Deep Sea Reasources 43, 53-55. DOI 10.1016/0967-0645(95)00082-8

Riera P. (1998) δ^{15}N of organic matter sources and benthic invertebrates along an estuarine gradient in Marennes-Oleron Bay (France): implications for the study of the trophic structure. Mar. Ecol-Prog. Ser. 166, 143-150. DOI 10.3354/meps166143

Riera P. Stal L.J. and Nieuwenhuize J. (2000) Heavy δ^{15}N in Intertidal Benthic Algae and Invertebrates in the Scheldt Estuary (The Netherlands): Effect of River Nitrogen Inputs. Estuar. Coast. Shelf S. 51, 365-372. DOI 10.1006/ecss.2000.0684

Riget F. Johansen P. and Asmund G. (1995) Natural Seasonal Variation of Cadmium, Copper, Lead and Zinc in Brown Seaweed (*Fucus vesiculosus*). Mar. Pollut. Bull. 30, 409-413. DOI 10.1016/0025-326X(95)99847-W

Savage C. (2005) Tracing the Influence of Sewage Nitrogen in a Coastal Ecosystem Using Stable Nitrogen Isotopes. AMBIO 34, 145-150. DOI 10.1639/0044-7447(2005)034[0145:TTIOSN]2.0.CO;2

Savage C. and Elmgren R. (2004) Macroalgal (*Fucus vesiculosus*) δ^{15} values trace decrease in sewage influence. Ecol. appl. 14, 517-526. DOI 10.1890/02-5396

Sharma M. Papanastassiou D.A. and Wasserbug G.J. (1997) The concentration and isotopic composition of osmium in the oceans. Geochim. Cosmochim. Acta 61, 3287-3299. DOI 10.1016/S0016-7037(97)00210-X

Viana I.G. and Bode A. (2013) Stable nitrogen isotopes in coastal macroalgae: geographic and anthropogenic variability. Sci. Total Environ. 15, 887-895. DOI 10.1016/j.scitotenv.2012.11.065

Viana I.G. Bode A. Bartholomew M. and Valiela I. (2015) Experimental assessment of the

macroalgae *Ascophyllum nodosum* and *Fucus vesiculosus* for monitoring N sources at different time-scales using stable isotope composition. J. Exp. Mar. Biol. Ecol. 466, 24-33. DOI 10.1016/j.jembe.2015.01.014

Vizzini S. and Mazzola A. (2004) Stable isotope evidence for the environmental impact of a land-based fish farm in the western Mediterranean. Mar. Pollut. Bull. 49, 61-70. DOI 10.1016/j.marpolbul.2004.01.008

Wang C. Lei A. Zhou K. Hu Z. Hao W. and Yang J. (2014) Growth and Nitrogen Uptake Characteristics Reveal Outbreak Mechanism of the Opportunistic Macroalga *Gracilaria tenuistipitata*. PLoS One 9. DOI 10.1371/journal.pone.0108980

Woodhouse O.B. Ravizza G. Kenison Falker K. Statham P.J. and Peucker-Ehrenbrik B. (1999) Osmium in seawater: vertical profiles of concentration and isotopic composition in the eastern Pacific Ocean. Earth Planet. Sc. Lett. 173, 223-233.

Xiong Y. Xu J. Shan W. Lou Z. Fang D. Zang S. and Han G. (2013) A new approach for rhenium(VII) recovery by using modified brown algae *Laminaria japonica* absorbent. Bioresource Technol. 127, 464-472. DOI 10.1007/BF00008532

Appendices

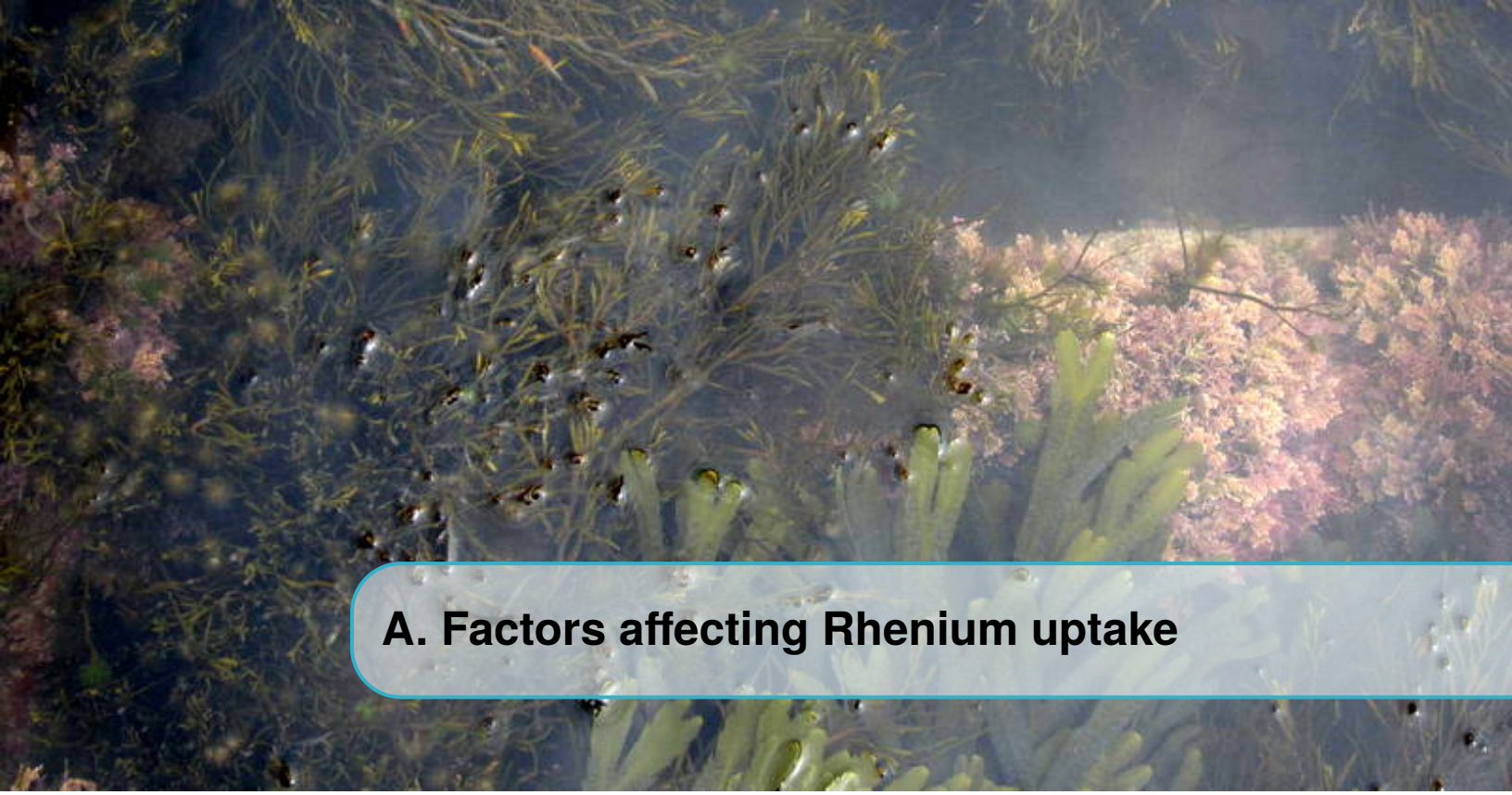

A. Factors affecting Rhenium uptake

A.1 Introduction

There are many biological, chemical and physical variables affecting the uptake of chemical elements such as; pH, ionic strength, salinity, temperature, light, competition between metal ions and many others. Most of these factors are discussed below.

- **pH**
  Dependence of metal uptake on pH is related to metal chemistry in solution and to the surface functional groups. Thus, as carboxylic and sulphonate groups are acidic, the optimum pH in solution for a maximum metal uptake is related to the pKa of these surface groups. Therefore, at low pH, both carboxylic and sulphonate groups are protonated and thereby become less available for the binding of heavy metals (Greene *et al.*, 1987; Ramelow *et al.*, 1992). Algal biomass may have an overall negative charge, which increases with increasing pH (i.e. more sites are deprotonated), therefore the binding of most metals increases with increasing pH (Schiewer and Volesky, 1995).

- **Ionic strength**
  Ionic strength or background electrolyte concentration changes influence metal binding by changing the competition of the electrolyte ion (i.e. metal of interest) and adsorbing ions for sorption sites (i.e. Na^+) and by altering the interfacial potential, thus the activity of the electrolyte ions. It has been observed an increase in metal binding with decreasing ionic strength in green (*Ulva lactuca*) and brown macroalgae (*Sargassum hemiphyllum, Petalonia fascia* and *Colpomenia sinuosa*) (Schiewer and Wong, 2000).

- **Salinity** The amount of dissolved salt content in seawater affects the photosynthesis and growth

of the organisms living in it, thus it could have an effect in metal absorption. It has been observed that in some macroalgae (i.e. *Ascophyllum nodosum*) metal uptake decreased with low salinity whereas in some other macroalgae (i.e. *F. vesiculosus* or *Ulva lactuca*) metal content increased, suggesting different uptake mechanisms between species (Connan and Stengel, 2011; Turner *et al.*, 2008).

- **Temperature** Temperature affects water chemistry and the metabolic rate of macroalgae, thus their heavy metal uptake could be affected (Lemus and Chung, 1999). However, in some cases it has been observed that enhanced temperature increased the uptake of metals like Zn and Mn in macroalgae (Munda and Hudnik, 1988), whereas in other species it has been observed that the metal uptake has little changes under temperature treatments (Zhao *et al.*, 1994).

- **Light** Light also controls the metabolic rate of macroalgae, hence their heavy metal uptake could be affected as well. Heavy metal uptake has been shown to increase in some macroalgae with increasing light (Hu *et al.*, 1996).

- **Competition between metal ions** Some metal binding decreases in the presence of multi-metallic systems while some other metals are totally unaffected (Kuyucak and Volesky, 1989). Hence, biosorption of metals in a multi-metallic solution depends on two things, a) the physicochemical nature of the solution and b) the interaction between metals.

- **Growth rate** Is has been observed that metal accumulation in macroalgae increase or decrease as the specific growth rate increases, which might indicate the metals metabolic regulation (Rice, 1984) or an increase in the metal-to-biomass ratio (Göthberg *et al.*, 2004; Greger *et al.*, 1991; Wang and Dei, 1999).

- **Humic substances** The presence of humic substances in the aquatic environment has been observed to reduce the bioavailability and toxicity of heavy metals by complexation of the metals and other elements with the dissolved organic matter, hence, reducing the concentration of free ionic metals in the aquatic environment (Guo *et al.*, 2001; Kim *et al.*, 1999; Tubbing *et al.*, 1994).

- **Nutrient concentrations** Nutrient concentration is another factor reported to affect metal bioavailability. In rich nutrient environments, metal uptake can be inhibited as a result of complex formation between the ion metal and the nutrient (Göthberg *et al.*, 2004; Haglund *et al.*, 1996).

- **Seasonal variation** Changes in macroalgae physiology and metabolism are observed throughout the year (Kang *et al.*, 2011). Seasonal variation in growth could be affecting macroalgae element binding; it has been observed that seasonal variation in temperature does not affect

heavy metal accumulation (Zumdahl, 1992).

- **Heights and tidal levels** Changes in height and tide levels affect many of the factors mentioned above, such as nutrient concentrations, humic substances, light and temperature. As such, the metal or element uptake might be influenced by the height were the macroalgae grow.

There are no studies made on how any of these factors affect Re uptake by macroalgae. Thus, this work aims to take a deeper look into Re uptake by *F. vesiculosus* when some of these factors are present.

A.2 Material and methods

A.2.1 Macroalgae used in the study: *F. vesiculosus*

F. vesiculosus is a common brown macroalgae found along sheltered shores of the North Sea, Baltic Sea, Atlantic Ocean and Pacific Ocean. *F. vesiculosus* is a tethered macroalgae with air bladders that are produced annually allowing the individual fronds to float. The specie comprises a holdfast, a frond made up of a stipe, blades, tips and vesicles (Figure A.1). The growth rate ranges between 0.05–0.80 cm/day (Carlson, 1991; Strömgren, 1977), with the species having a life span between 3 to 5 years (White, 2008). The species is annually episodic, gonochoristic and highly fecund (i.e. prolific; White, 2008). Gametes are released into the seawater and the eggs are fertilized externally to form a zygote that starts to develop as soon as it settles into a substrate (Graham and Wilcox, 2000). The gametes are released from receptacles, which are found in the fertile tips of the macroalgae. However, *F. vesiculosus* also has non-fertile tips without these structures. Non-fertile tips are composed of a parenchymatous thallus (i.e. tissue like structure) (Graham and Wilcox, 2000; Hiscock, 1991; White, 2008).

A.2.2 Macroalgae collection sites

All specimens of *F. vesiculosus* were collected from Boulmer Beach, Northumberland, UK (55º25'N 1º34'W) in October and November in 2014 and from January to June in 2015.

A.2.3 Macroalgae cultures under different conditions and Re

To investigate Re uptake by macroalgae, non-reproductive apical thallus tips of nine *F. vesiculosus* specimens (length > 1.5 cm; wet weight (WW) = 0.12–0.15 g), without visible microalgae (i.e. epiphytes), from Boulmer beach, were cultured in seawater (modified after; Gustow *et al.* (2014)) with a known concentration of Re. In brief, tips were placed into separate 250 mL glass jars containing two mesh shelves. Some tips were placed in the bottom of the jar and some tips to each mesh, having in total from 9 to 15 tips depending on the experiment in each jar.

To reduce evaporation all the jars were loosely covered with lids, while allowing gaseous exchange with the atmosphere. No nutrients were added into the seawater or artificial seawater. The algae

tips inside the bottles were transferred into an incubator with a set light/dark rhythm of 16:8, light intensity of 125 μmol photons/m^2s^2 and a temperature of 11ºC. The WW of the algal tips, per jar, was measured every 2–3 days during culturing period. At the same time, the medium was changed to avoid accumulation of metabolites. The pH and salinity of each jar was measured once a week.

In order to study the light affection in Re uptake, a set of 9 tips collected on November 2014 was placed in each jar. Almost all jars were filled with sterile filtered (0.7 μm) seawater from Boulmer beach. Each set of nine jars replicates were treated with known light intensities: 0 μmol/m^2s, 70 μmol/m2s and 170 μmol/m2s, produced by covering with foil (0 μmol/m2s) and meshes (70 μmol/m2s) the jars. Moreover, each set of nine jars was subdivided in groups of 3 filled with seawater, artificial seawater or doped 1000× with $HReO_4$ (i.e. 7.45 ppb), respectively. Thus, having as a result 27 jars, and 3 replicates with same conditions.

To investigate phosphate competition with $NaReO_4$, a set of 9 tips collected during April 2015 was placed in each jar. All jars were filled with sterile filtered (0.7 μm) seawater from Boulmer beach. Each set of nine jars replicates were treated with known phosphate concentrations: 1 μM, 100 μM, 1000 μM and 4000 μM. Moreover, each set of twelve jars was subdivided in groups of 3 filled with seawater, doped 100× with Re (0.75 ppb), 1000× with Re (i.e. 7.45 ppb) and 10000× with Re (i.e. 74.50 ppb), respectively. Having as a result 36 jars, and 3 replicates with same conditions.

pH affect in Re upakte was studied by placing 9 tips collected in June 2015 in each jar and filling them with with sterile filtered (0.7 μm) seawater from Boulmer beach. Each set of four jars were treated with pHs of 7, 8 and 9. And each set of 4 jars was divided by two, thus a half of the jars was doped 1000× (i.e. 7.45 ppb) with $HReO_4$ and the other half with $NaReO_4$ salt. Resulting in 12 jars and 2 replicates per treatment.

Same procedure and tips collected in the same month as described above was used to study the salinity affect, but instead of treating them with different pHs, each groups of 4 jars were treated with 25%, 50%, 75% and 100% salinity. 100% salinity is the normal salinity of seawater and other lower salinities were obtained by adding different amounts of DI water.

Moreover, some more cultures were performed in order to gain more knowledge in the uptake rate. 15 tips from June 2015 were placed in each jar and samples (3 tips) were analyzed each day during 4 days. Two groups with 3 jars each were made and each set was filled with sterile filtered seawater from Boulmer and doped 1000× (i.e. 7.45 ppb) with $HReO_4$ or $NaReO_4$.

A.2.4 Alginate bead formation

For the formation of alginate beads drops of 2% sodium alginate were added to a solution of 0.3M Calcium Chloride dihydrate. A total of 120 beads were formed and divided in 6 groups. Each group, with 20 beads was treated with same concentration of 18 ppb but different Re types (i.e. $HReO_4$,

$NaReO_4$, $KReO_4$ and NH_4ReO_4. Moreover, 20 beads were analyzed directly without any treatment done.

A.2.5 Re abundance determinations and data treatment

Rhenium abundance determinations for all samples were obtained at the Durham Geochemistry Centre in the Laboratory for Sulphide and Source Rock Geochronology and Geochemistry. Each sample was oven-dried at 60 ºC for 24 h and ground into a powder with an agate mortar and pestle. Approximately 100 mg of the sample powder were used for analysis. Abundances were obtained by both direct calibration and isotope-dilution methodologies. For the latter samples were doped with a known amount of ^{185}Re tracer solution (isotope dilution methodology). The sample and if used, the tracer solution, were digested in a mix of 3 ml of 12 N HCl and 6 ml of 16 N HNO_3 at 120ºC overnight in a PFA sallivex 22mL vial. The dissolved sample solution was evaporated to dryness at 80 ºC. Rhenium was isolated from the dried sample using 5 mL 5 N NaOH 5 mL acetone solvent extraction procedure (Cumming *et al.*, 2013; Prouty *et al.*, 2014). The Re-bearing acetone was evaporated to dryness at 60 ºC. For ICP-MS the dried Re fraction was dissolved in 1.2 mL of 0.8 N HNO_3. For samples analysed by isotope dilution to determine absolute Re abundance, all sources of uncertainty (e.g., standard measurement, isotope measurement, calibration of the tracer solution, fractionation correction and blank values) are propagated to yield a final uncertainty. For direct calibration, prior to each analysis, an instrument performance check was done to confirm satisfactory execution of the ICP-MS. Five freshly prepared standards were made each time and formed calibration lines with $R > 0.999$ and error < 2% RSD. Moreover, all the samples had a reproducibility of < 5% RSD.

T-tests statistical analyses, using a significance level of 0.05, were performed using R Studio software (Pruim, 2011). For testing the statistical hypothesis, p-values are used. The p-value is defined as the probability of obtaining a result more extreme or equal to what was actually observed, thus, if p-value is smaller or equal to the significance level, it suggests that the observed data are consistent.

A.3 Results

A.3.1 Light intensity and Re uptake by *F. vesiculosus*

Figure A.1 shows that under same concentrations of $HReO_4$ in solution, tips grown with no light have the highest Re rate of accumulation (~16000 ppb) followed by tips grown with mid light intensity (~11000 ppb) and finally with tips grown with very high light intensity (~9000 ppb). Although 3 repeats in each condition were performed, only one repeat was analyzed, thus differences are observed between treatments, but it cannot be said that they are significant, because we do not have enough repeats analyzed in order to test if they are truly significant. However, we can say that it seems to be a tendency of greater Re accumulation when there is less light.

A.3.2 Phosphate and Re uptake by *F. vesiculosus*

The results shown in Figure A.2 indicate that there seems to be phosphate (PO_4^-) uptake competition against $NaReO_4$. However, only one repeat out of three per treatment was analyzed so the results cannot be statistically proofed. Competition is observed mainly after 72 h, not much competition is observed after 3, except cultures grown with 4000 μM of phosphate and 7.5 ppb of Re (Figure A.2 B). Concentrations of 1 μM of phosphate seem not to affect Re uptake, 100 μM of phosphate do affect the uptake under 0.75 and 7.5 ppb of Re, but not with 75 ppb Re. 1000 and 4000 μM phosphate concentrations inhibit Re uptake when 0.75 and 7.5 ppb Re and reduce the uptake when 75 ppb Re.

A.3.3 pH, salinity and Re uptake by *F. vesiculosus*

F. vesiculosus tips were treated under different pHs and salinities. Initial pH ranges were 7, 8 and 9; however at the end of the culture the macroalgae had stabilized a bit the pHs, having a closer range of between 7.5 and 8.5 (Figure A.3). No significant differences in Re uptake rate between pHs are observed (p-value > 0.05) when $NaReO_4$ or $HReO_4$ used, although at a simple sight it seems that there is a tendency when the higher the pH the lower Re uptake. Moreover, no significant differences (p-value> 0.05) between salinities are observed when $NaReO_4$ (Figure A.4).

A.3.4 Re uptake rate analysis by *F. vesiculosus*

F. vesiculosus samples were analysed every 24 h in order to study Re uptake rate. Both $HReO_4$ and $NaReO_4$ show the greatest uptake the first day. Knowing the amount of Re doped in the media (7.5 ppb), the maximum amount of Re accumulation by *F. vesiculosus* should be 2189 ppb. Thus, we are seeing that after 24 h, *F. vesiculosus* tips accumulate up to 55% (uptake rate = 1.1 µg/g d^{-1}) of Re(III) and 7.5% (uptake rate = 0.16 μg/g d^{-1}) of Re(VII), after 3 more days, there is accumulation but it much slower, 21% Re(III) and 3.2% Re(VIII) (Figure A.5).

A.3.5 Alginate Re uptake

Alginate beads were prepared in order to decipher differences in binding mechanisms between $HReO_4$ and $NaReO_4$. All alginate beads seem to uptake $NaReO_4$ but not $HReO_4$ (Figure A.6).

A.4 Discussion

A.4.1 Light intensity and Re uptake by *F. vesiculosus*

Our experiments show that $HReO_4$ uptake increases when less light is present (Figure A. 1). Although the differences observed cannot be statistically proved for the reasons mentioned previously, it seems that light has an important role in Re uptake, thus the results obtained in this study will be discussed here, but further analysis needs to be done for reliability.

Currently, Re is being used in artificial light harvesting, mimicking photosynthesis using man-made leaves, for a better photon absorption (Yamamoto *et al.*, 2014). Our previous results shown in

chapter 2 concluded that chloroplast had no Re, or if they had the bound was not strong, thus Re was released during the isolation. However, if this second case was the true, we could hypothesize that as *F. vesiculosus* gets less light, it uptakes more Re to absorb more efficiently the very few photons that receives.

Another hypothetic explanation might be that the channel where Re is entering to the cell is light regulated. It has been shown that sodium arsenate ($NaH_2AsO_4 \cdot 7H_2O$) and sodium arsenite ($NaAsO_2$) have greater uptake by *Fucus sp.* when dark, concluding that energy is required to pump arsenic and it is derived from respiration rather than photosynthesis (Klumpp, 1980).

Moreover, a third hypothesis can be extracted looking at the result factors obtained with changes in light intensities such as pH. When there is light, *F. vesiculosus* tips are able to do the photosynthesis, thus they grow more which leads to an increase of pH in the water solution. pHs were; 8.3 when 0 μmol/m^{2}s, 9 when 70 μmol/m^{2}s and 9.2 when 170 μmol/m^{2}s. As this range of pHs is out of the range used in our studies we cannot say that there might not be an effect on Re uptake due to the pH. As high pHs lead to a lower percentage of protonated amino groups, if Re binding involves amino groups then, under high pH less Re uptake should be observed. That is exactly what our results show.

However, much more work should be done in this field in order to confirm any of these hypotheses.

A.4.2 Phosphate and Re uptake by *F. vesiculosus*

Figure A.2 seems to shows a competition between ReO_4^- and PO_4^- uptake. As said above the results obtained cannot be statistically tested, thus the results obtained are not reliable, but they will be discussed below.

Competition is observed mainly after 72 h, not much competition is observed after 3, except cultures grown with 4000 μM of phosphate and 7.5 ppb of Re (Figure A.2). No competition with 4000 μM after 3 days is observed when 7.5 ppb and 75 ppb of Re in the media and it could be because the concentration of Re accumulated is too low and too high, respectively to compete with the phosphate up-taken after 3 days. If this is the case, it could be explained because Re and phosphate are up-taken through different pumps. Tagami *et al.* 2005, showed that there was a positive correlation between the K^+ and the Re accumulated in seaweed and explained this as a result of ReO_4^- being uptaken by mistake of Cl^- as a counter ion for K^+ uptake. And if the uptake of Re is faster than phosphate uptake, then after 3 h we should observe high levels of Re in *F. vesiculosus*.

We do observe that there is a decrease in Re uptake after 72 h, when high levels of phosphate are present (1000 μM and 4000 μM). If we believe that phosphate and Re have different mechanisms for entering the cell, then competition should come from another source. Kim *et al.* 2003 showed that ReO_4^- had a high binding interaction with chitosan which is basically a polymer of glucosamine.

Chitosan is only reported in nature in some fungi and termite queen's abdominal wall. However, Nishino *et al.* 1994 isolate and characterized a novel polysaccharide containing an appreciable amount of glucosamine in *F. vesiculosus*. If this is true, ReO_4^- could be entering to the cells through the K^+ uptake mechanism and staying in the cell bind to this novel polysaccharide of glucosamine Nishino found. Besides, other studies have shown that phosphate can be highly bound to the amino groups of chitosan which are the same groups where ReO_4^- binds to (Liu and Zhang, 2015). Thus, we should expect a competition of phosphate with rhenium after 72 h for this reason, the binding of Re in the amino group is not very strong, thus removed under high concentrations of phosphate.

A.4.3 pH, salinity and Re uptake by *F. vesiculosus*

Algal biomass may have an overall negative charge, which increases with increasing pH (i.e. more sites are deprotonated), therefore the binding of most metals increases with increasing pH (Schiewer and Volesky, 1995). However, as Re studied here is an anion we should expect more uptake when more sites are protonated, thus with less pH, more Re should be accumulated. No significant differences in Re uptake rate between pHs are observed when $NaReO_4$ or $HReO_4$ used. However, the pH range was too narrow in order to really say if there is an effect or not. Further experiments with a wider range of pHs should be done and considering the natural buffering conditions of macroalgae. Carbonates are also important to have in mind, once pH change, carbonates also change, and they can alter Re uptake. Between pHs of 6 and 9 the same carbonate species is found, so the results shown here are not affected by carbonates, but if further studies with a wider pH range are done, carbonates should be considered.

Our results show that there are no significant differences between salinities are observed when $NaReO_4$ (Figure A.4). The amount of dissolved salt content in seawater affects the photosynthesis and growth of the organisms living in it, thus it could have an effect in metal absorption. It has been observed that in some macroalgae (i.e. *Ascophyllum nodosum*) metal uptake decreased with low salinity whereas in some other macroalgae (i.e. *F. vesiculosus* or *Ulva lactuca*) metal content increased, suggesting different uptake mechanisms between species (Connan and Stengel, 2011; Turner *et al.*, 2008). Our cultures would fit in this latter case, salinity does not affect Re uptake.

A.4.4 Re uptake rate analysis by *F. vesiculosus*

Our results show that both $HReO_4$ and $NaReO_4$ show the greatest uptake by *F. vesiculosus* the first day (55% of $HReO_4$ uptake and 7.5% $NaReO_4$ uptake), after that the concentration increases but more slowly (21% of $HReO_4$) uptake and 3.2% $NaReO_4$ uptake) (Figure A.5). The uptake rates after 24 h for $HReO_4$ and $NaReO_4$ are 1.1 μg/g d^{-1} and 0.16 μg/g d^{-1}, respectively. Wang and Dei (1999) have shown that in *Ulva lactuca* and *Gracilaria blodgettii* the uptake rate of the anionic metals Cr and Se was considerably slower than the cationic Cd and Zn. Moreover, Cr and Se show similar uptake rates to $NaReO_4$ and Cd and Zn to $HReO_4$, reassuring the differences in $HReO_4$ and $NaReO_4$

uptake mechanisms observed in this study and in previous studies explained in chapter 2.

A.4.5 Alginate Re uptake

To decipher any differences in Re storage or binding between $HReO_4$ and $NaReO_4$, alginate beads were prepared and put in contact with different solutions of $HReO_4$ and $NaReO_4$. Interestingly, Re accumulation is only observed when alginate beads were in contact with $NaReO_4$, but not with $HReO_4$. Alginate is famous for binding lots of cation metals as it has lots of negative charged binding sites (Banerjee *et al.*, 2007; Jeon *et al.*, 2002; Lagoa and Rodrigues, 2009; Vijaya *et al.*, 2008), for this reason we should expect $HReO_4$ to be bind by the alginate. However, as what we generated is beads of alginate by mixing $CaCl_2$, what could have hypothetically happen is that the alginate beads became positively charged, if some Calcium is bound just with one ligand to the alginate leaving a ligand free to bind $NaReO_4$. This would explain why we are observing $NaReO_4$ uptake by the beads but not $HReO_4$, however, such reasoning is very unlikely because calcium alginate beads have been shown to bind positive charged metals (Lagoa and Rodrigues, 2009; Vijaya *et al.*, 2008), so it should bind $HReO_4$, if we do not observe it, might really mean that $HReO_4$ does not interact with alginate. But, further analysis should be done in order to arrive to a conclusion; these experiments are not reliable and should be repeated several times with solutions made with DI water instead of seawater, as salt can be affecting the results and use dry beads instead of gel beads, because they have been shown to be better for metal binding (Lagoa and Rodrigues, 2009).

A.5 Conclusions

The following conclusions are extracted from the work described above. These initial data is promising, but further research in this area is needed to make proper conclusions and gain more knowledge about the uptake mechanism of Re by *F. vesiculosus*

- Light seems to have an effect in Re uptake, the less light, the more Re accumulation. However, no final conclusion can be extracted on why the light affects, but three hypotheses are postulated: Re being used for photon absorption, entrance of Re through a light regulated channel or as a result of protonations/deprotonations of amino groups which bind Re.
- Re and Phosphate seem to have different mechanisms of entering the cell, it is hypothesised that Re uptake is faster than phosphate uptake, but phosphate binding is more specific than Re binding.
- $HReO_4$ uptake seems to be influenced by pH, but not $NaReO_4$. The lower the pH the major uptake and might be due to the increase in protonated sites. No significant affect in Re uptake is observed due to salinity.
- Major $HReO_4$ and $NaReO_4$ uptake occurs within 24 h.

- Comparison between Re uptake rates made in different culture sets should be avoided due to different conditions, such as; media changes, days of culture and pH and seasonal variations.

A.6 References

Banerjee A. Nayak D. and Lahiri S. (2007) A new method of synthesis of iron doped calcium alginate beads and determination of iron content by radiometric method. Biochem. Eng. J. 33, 260-262.

Carlson L. (1991) Seasonal variation in growth, reproduction and nitrogen content of *Fucus vesiculosus* in the Öresund, Southern Sweden. Bot. Mar. 34, 447-453.

Connan S. and Stengel D.B. (2011) Impacts of ambient salinity and copper on brown algae: 1. Interactive effects on photosynthesis, growth, and copper accumulation. Aquat. Toxicol. 104, 94-107.

Cumming V.M. Poulton S.W. Rooney A.D. and Selby D. (2013) Anoxia in the terrestrial environment during the late Mesoproterozoic. Geology 41, 583-586.

Göthberg A. Greger M. Holm K. Bengtsson B. (2004) Influence of nutrients on uptake and effects of Hg, Cd and Pb in Ipomoea aquatica. J. Environ. Qual. 33, 1247-1255.

Graham L.E. and Wilcox L.W. (2000) Algae. , United States of America.

Greene B. McPherson R. and Darnall D. (1987) Algal sorbents for selective metal ion recovery.Lewis, Chelsea, MI.

Greger M. Brammer E. Lindberg S. Larsson G. and Idestam-Almquist J. (1991) Uptake and physiological effects of cadmium in sugar beet (Beta vulgaris) related to mineral provision. J. Exp. Bot. 42, 729-737.

Guo L. Hunt B.J. Santschi P.H. and Ray S.M. (2001) Effect of Dissolved Organic Matter on the Uptake of Trace Metals by American Oysters. Environ. Sci. Technol. 35, 885-893.

Gustow L. Rahman M.M. Bartl K. Saborowski R. Bartsch I. and Wiencke C. (2014) Ocean acidification affects growth but not nutritional quality of the seaweed *Fucus vesiculosus* (Phaeophyceae, Fucales). J. Exp. Mar. Biol. Ecol. 453, 84-90.

Haglund K. Björklund M. Gunnare S. Sandberg A. Olander U. and Pedersén M. (1996) New method for toxicity assessment in marine and brackish environments using the macroalga Gracilaria tenuistipitata (Gracilariales, Rhodophyta). Hydrobiologia 326-327, 317-325.

Hiscock S. (1991) Brown seaweeds. A field key to the british., Shrewsbury, Montford Bridge.

Hu S. Tang C.H. and Wu M. (1996) Cadmium accumulation by several seaweeds. Sci. Total Environ. 187, 65-71.

Jeon C. Park J.Y. and Yoo Y.J. (2002) Novel immobilization of alginic acid for heavy metal

removal. Biochem. Engi. J. 11, 159-166.

Kang J.C. Choi H.G. and Kim M.S. (2011) Macroalgal species composition and seasonal variation in biomass on Udo, Jeju Island, Korea. Algae 26, 333-342.

Kim S.D. Ma H. Allen H.E. and Cha D.K. (1999) Influence of dissolved organic matter on the toxicity of copper to Ceriodaphnia dubia: effect of complexation kinetics. Environ. Toxicol. Chem. 18, 2433-2437.

Klumpp D.W. (1980) Characteristics of Arsenic accumulation by the seaweeds *Fucus spiralis* and *Ascophyllum nodosum*. Mar. Biol. 58, 257-264.

Kuyucak N. and Volesky B. (1989) Accumulation of gold on algal biosorbent. Biorecovery 1.

Lagoa R. and Rodrigues J.R. (2009) Kinetic analysis of metal uptake by dry and gel alginate particles. Biochem. Eng. J. 46, 320-326.

Lemus M.J. and Chung K.S. (1999) Effect of temperature on copper toxicity, accumulation and purification in tropical fish juveniles Petenia Kraussii (Pisces: Cichlidae). J. Caribbean 35, 64-69.

Liu X. and Zhang L. (2015) Removal of phosphate anions using the modified chitosan beads: adsorption kinetic, isotherm and mechanism studies. Powder Technol. 277, 112-119.

Mas J.L. Tagami K. and Uchida S. (2004) Rhenium measurements on North Atlantic seaweed samples by ID-ICP-MS: An observation on the Re concentration factors. J. Radioanal. Nucl. Chem. 265 361-365.

Munda I.M. and Hudnik V. (1988) The effects of Zn, Mn and Co accumulation on growth and chemical composition of Fucus vesiculosus L. under different temperature and salinity conditions. Mar. Ecol. 9, 213-225.

Prouty N.G. Roark E.B. Koenig A.E. Demopoulos A.W.J. Batista F.C. Kocar B.D. Selby D. McCarty M.D. Mienis F. and Ross S.W. (2014) Deep-sea coral record of human impact on watershed quality in the Mississippi River Basin. Global Biogeochem. Cy. 28, 29-43.

Ramelow G.J. Fralick D. and Zhao Y. (1992) Factors affecting the uptake of aqueous metal ions by dried seaweed biomass. Microbios 72, 81-93.

Rice D.L. (1984) A simple mass transport model for metal uptake by marine macroalgae growing at different rates. J. Exp. Mar. Biol. Ecol. 821, 175-182.

Schiewer S. and Volesky B. (1995) Modeling of the proton-metal ion exchange in biosorption. Environ. Sci.Technol. 29, 3049-3058.

Schiewer S. and Wong M.H. (2000) Ionic strenth effects in biosorption of metals by marine algae. Chemosphere 41, 271-282.

Strömgren T. (1977) Short-term effect of temperature upon the growth of intertidal Fucales. J. Exp. Mar. Biol. Ecol. 29.

Tubbing D.M.J. Admiraal W. Cleven R.F.M.J. Iqbal M. van de Meent D. and Verweij W. (1994)

The contribution of complexed copper to the metabolic inhibition of algae and bacteria in synthetic media and river water. Water Res. 28, 37-44.

Turner A. Pedroso S.S. and Brown M.T. (2008) Influence of salinity and humic substances on the uptake of trace metals by marine macroalga, Ulva lactuca: experimental observations and modelling using WHAM. Mar. Chem. 110, 176-184.

Vijaya Y. Popuri S.R. Boddu V.M. and Krishnaiah A. (2008) Modified chitosan and calcium alginate biopolymer sorbents for removal of nickel (II) through adsorption. Carbohyd. Pol. 72, 261-271.

Wang W.X. and Dei R.C.H. (1999) Kinetic measurements of metal accumulation in two marine macroalgae. Mar. Biol. 135, 11-23.

White N. (2008) *Fucus vesiculosus*. Bladder wrack., in: [on-line]., M.L.I.N.B.a.S.K.I.S.-p. (Ed.), Plymouth: Marine Biological Association of the United Kingdom. Accessed January 2015

Yamamoto Y. Takeda H. Yui T. Ueda Y. Koike K. Inagaki S. and Ishitani O. (2014) Efficient light harvesting via sequential two-step energy accumulation using a Ru-Re5 multinuclear complex incorporated into periodic mesoporous organosilica. Chem. Sci. 5, 639-648.

Zhao Y. Hao Y. and Ramelow G.J. (1994) Evaluation of treatment techniques for increasing the uptake of metal ions from solution by nonliving seaweed algal biomass. Environ. Monit. Assess 33, 61-70.

Zumdahl S.S. (1992) Chemical Principles D.C., Canada.

A.7 Figures

Figure A.1 Re accumulation by *F. vesiculosus* under different light intensity treatments. Black markers treated with no light, blue ones with 70 μmol/m^{2}s and red ones with 170 μmol/m^{2}s).

Figure A.2 $NaReO_4$ uptake rates after 3 and 72 h of culture and under different phosphate concentrations; 1 μM (black marker), 100 μM (blue marker), 1000 μM (green marker) and 4000 μM (red marker). Using **A**) Re concentration of 100x (0.75 ppb) **B**) Re concentration of 1000x (7.5 ppb) and **B**) Re concentration of 10000x (75 ppb).

Figure A.3 $NaReO_4$ and $HReO_4$ accumulation by *F. vesiculosus* under different pH treatments (7.5, 8 and 8.5).

Figure A.4 $NaReO_4$ accumulation by *F. vesiculosus* under different salinity treatments (25‰, 50‰ and 75‰) and constant Re treatment (0.75 ppb).

Figure A.5 $NaReO_4$ (black marker) and $HReO_4$ (red marker) accumulation by *F. vesiculosus* after 1, 2, 3 and 4 days.

Figure A.6 $NaReO_4$, NH_4ReO_4, $KReO_4$ and $HReO_4$ uptake by alginate beads.

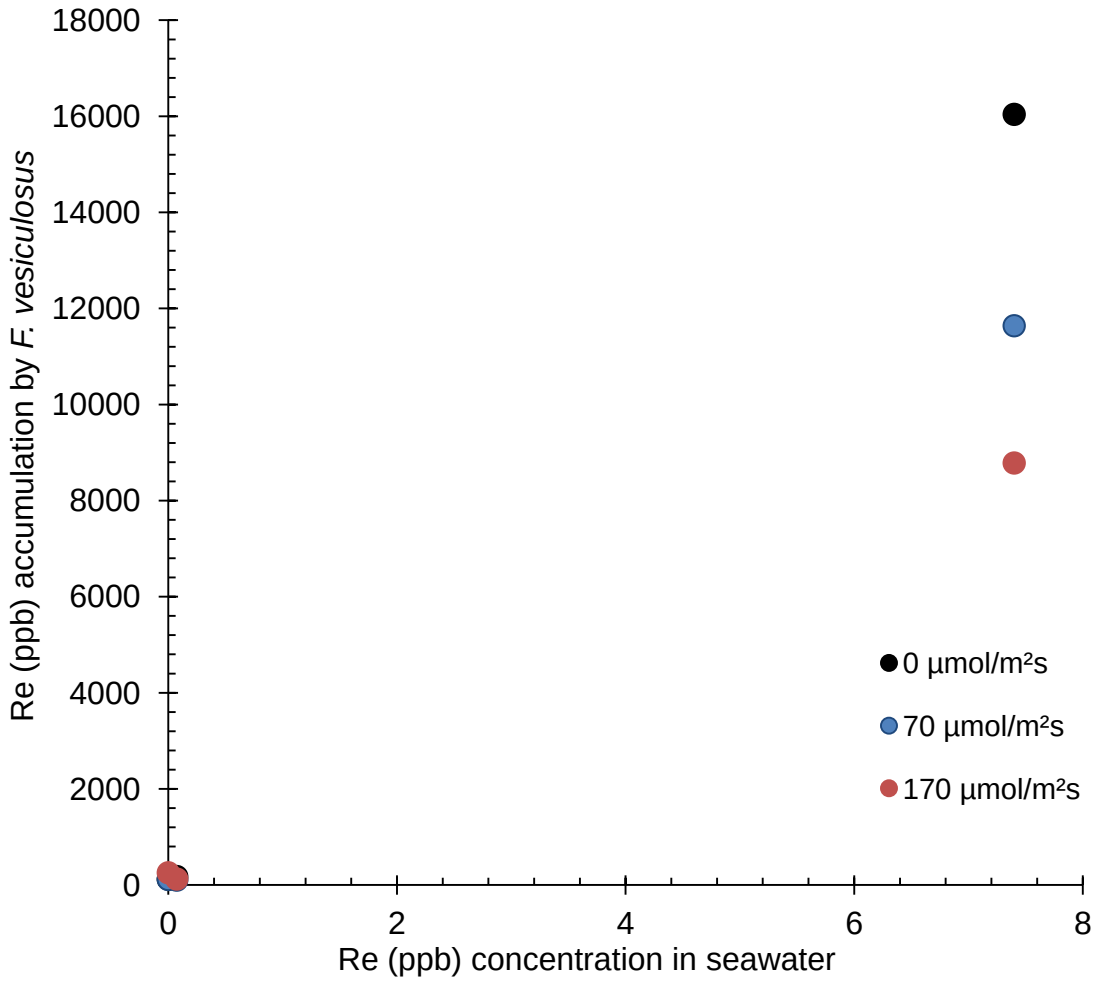
18000
16000
14000
12000
10000
8000
6000
4000
2000
0
Re (ppb) accumulation by F. vesiculosus
0
2
4
6
8
Re (ppb) concentration in seawater
0 µmol/m²s
70 µmol/m²s
170 µmol/m²s

Figure A.1

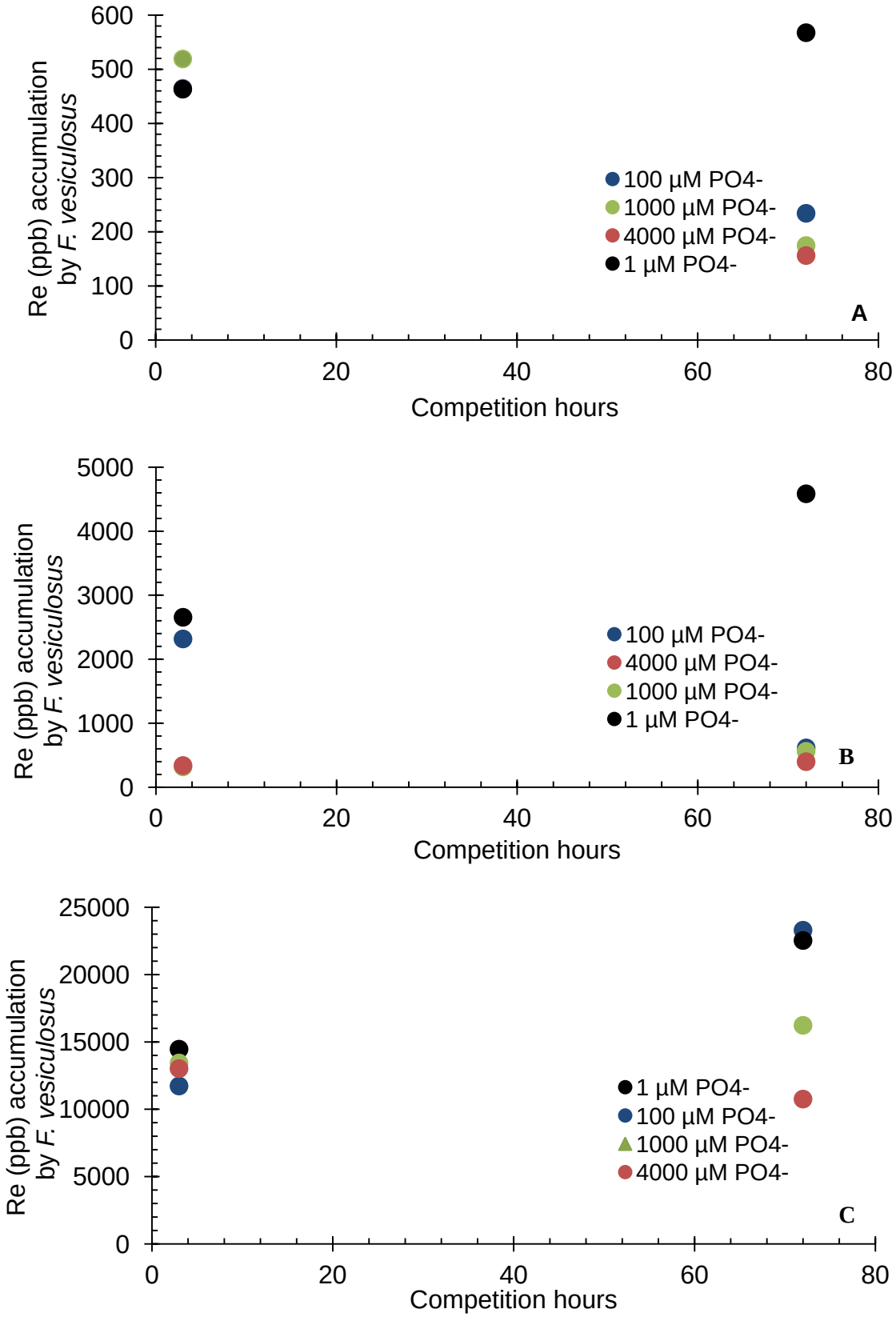
Re (ppb) accumulation by F. vesiculosus
Competition hours
100 µM PO4-
1000 µM PO4-
4000 µM PO4-
1 µM PO4-
A
B
C

Figure A.2

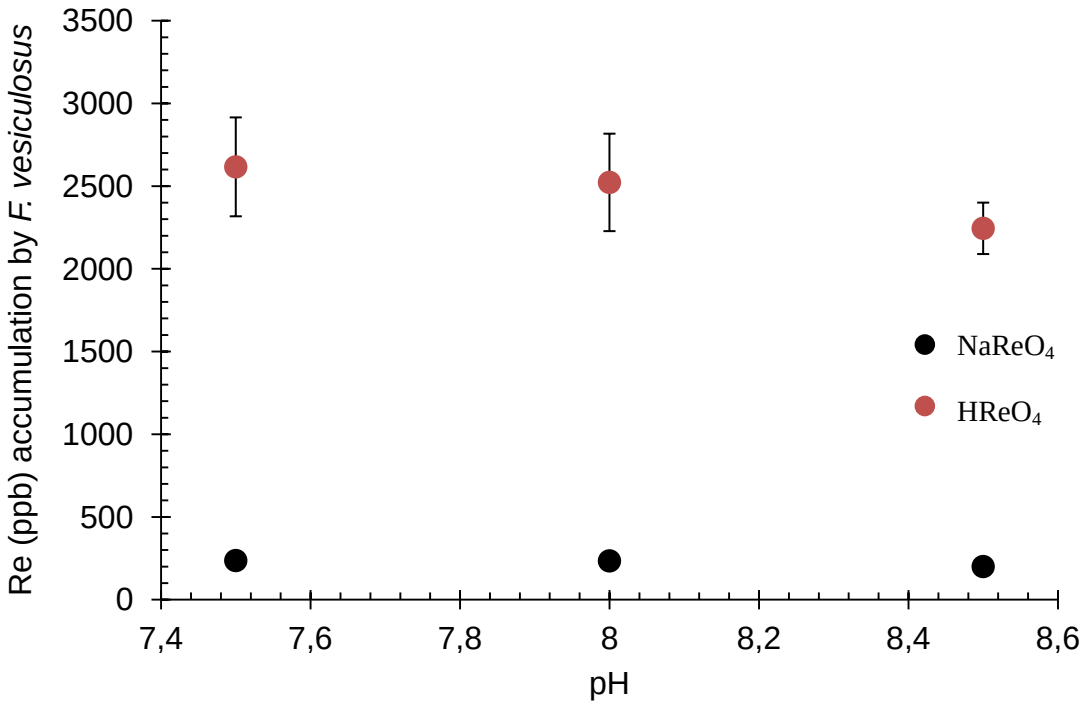

Figure A.3

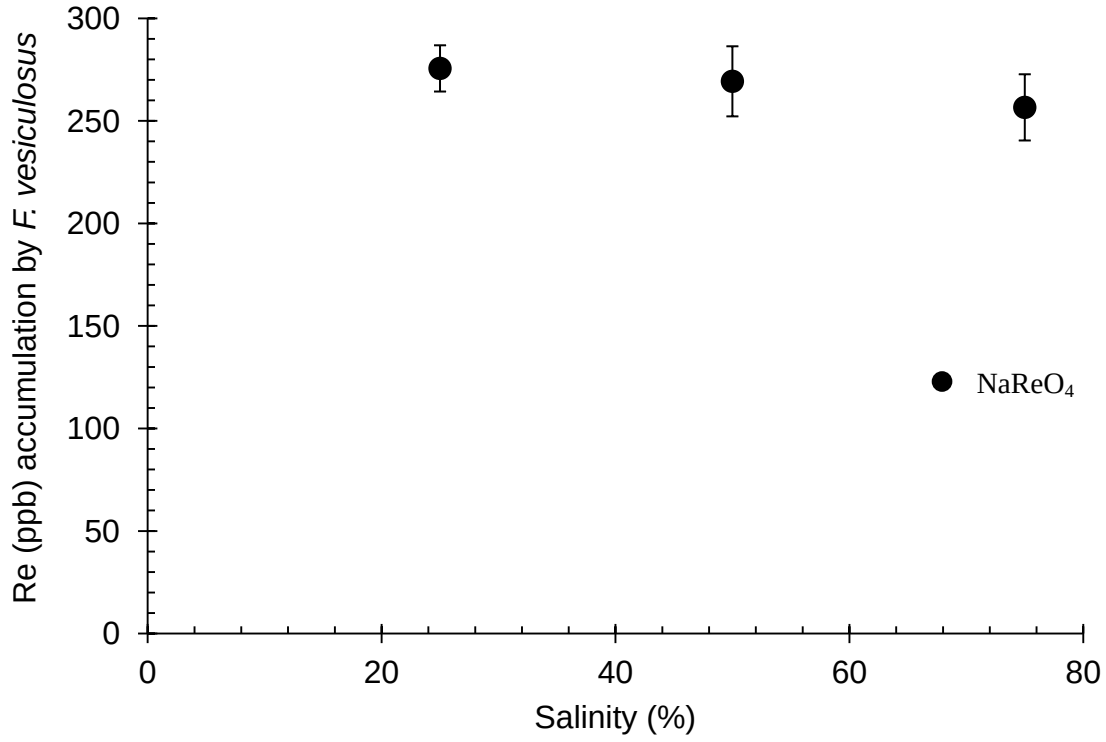

Figure A.4

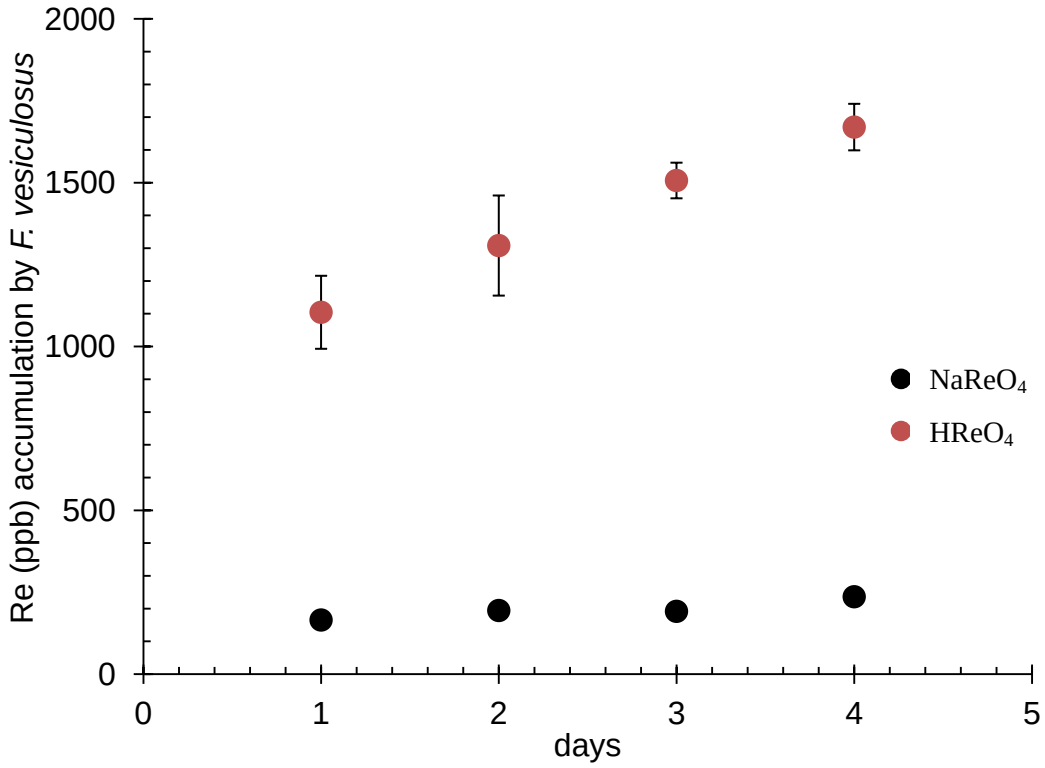

Figure A.5

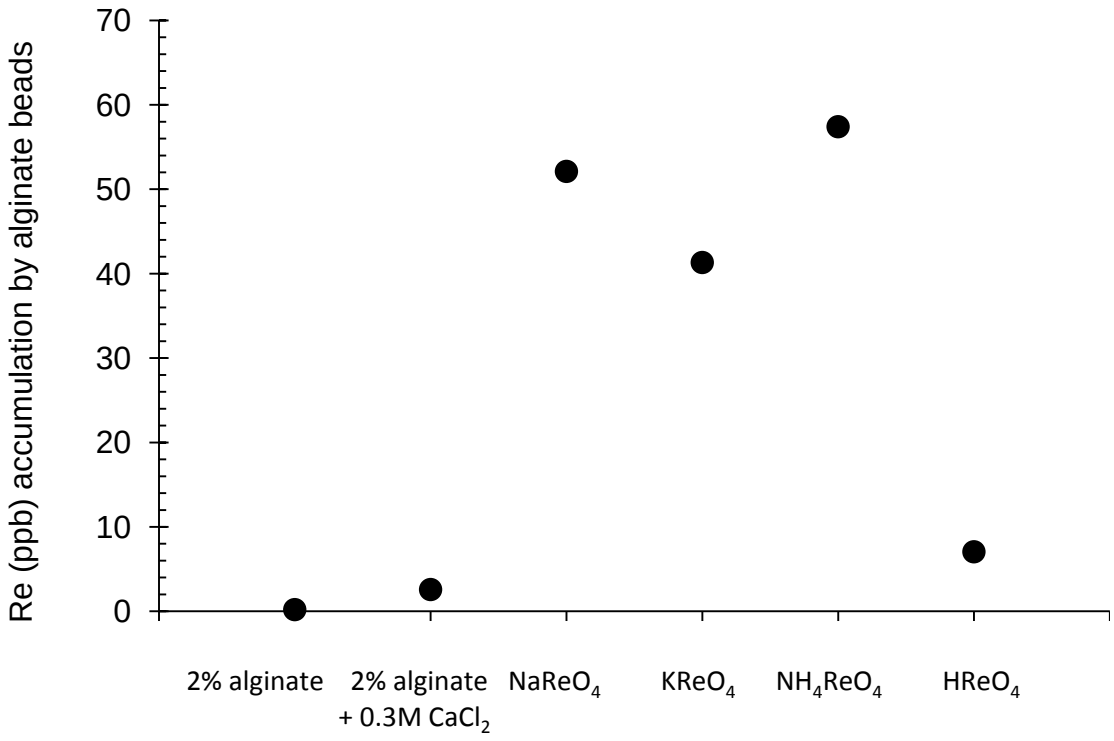

Figure A.6

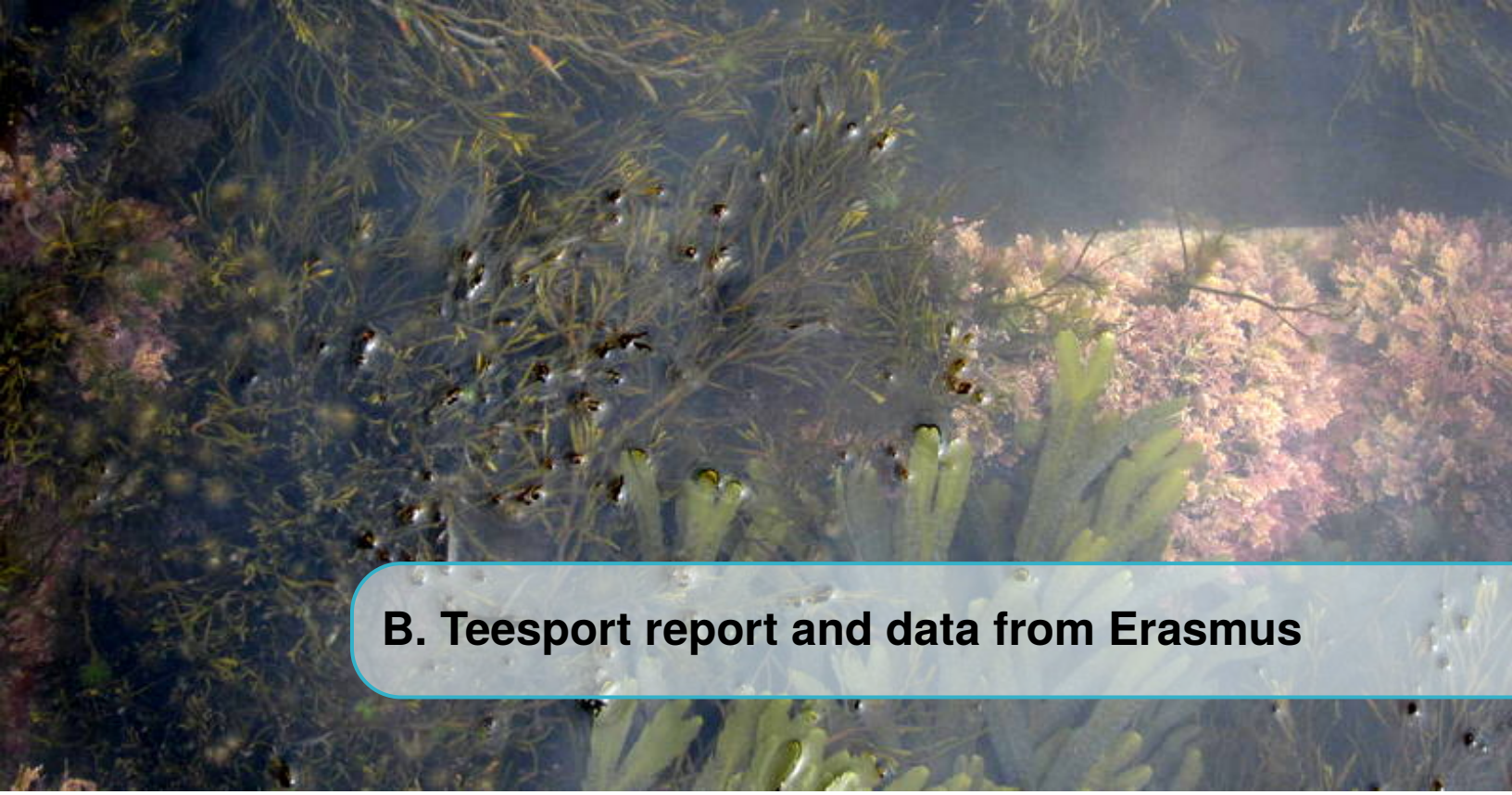

B. Teesport report and data from Erasmus

The current section consists on a report made with the data collected during the Erasmus period (February to June 2014) and older collections

B.1 Introduction

This work is a continuation of Flint's report (Flint, 2013), which used nitrogen isotopes of macroalgae to detect relative changes in the concentration of nitrates and phosphates (eutrophication) of the River Tees, Middlesborough, UK. Eutrophication is commonly caused by water pollution (industrial or fertilizers) in modern water masses. As a consequence of the nutrient enrichment excessive floral growth is produced (i.e., macroalgae – seaweed), which subsequently makes it difficult for other plants and/or animals to survive and take up nutrients. In addition, the death of these macroalgal blooms promotes oxygen depletion in the water column causing anoxia, again restricting the environment in which other flora and/or animals can live. To monitor such changes in water mass eutrophication nitrogen isotopes of organic matter have been used (de Carvalho, 2008; Fernandes *et al.*, 2012; Maier *et al.*, 2009).

Nitrogen (N) is a chemical element in Group 15 of the periodic table with the atomic number 7. N is the most abundant element on Earth (~78% of Earth atmosphere), therefore it was formally discovered before Re and Os, in 1772 by Daniel Rutherford (Elvira, 1932). N shows a large variety of oxidation states, ranging from -3 to +5, and has two stable naturally occurring isotopes; ^{14}N and ^{15}N, being ^{14}N, by far, the most abundant (i.e. 99.6%). However, N concentration and composition can change depending on the metabolic routes that the molecule follows. To express the isotopic

ratios of natural substances, a delta notation is used:

$$\delta\ ^{15}\text{N}\ ‰ = (\text{R}_{sample}:\text{R}_{standard} - 1) \times 1000$$

R is the relation between the light and heavy isotopes (i.e. ^{14}N: ^{15}N) of a substance. The standard is atmospheric dinitrogen (N_2).

Changes in the concentration and/or composition of nitrogen within the environment can affect the organisms living within it. Previous studies by Mariotti *et al.* (1981) have shown that in biological reactions the substrates are enriched in ^{15}N (i.e., a more positive δ^{15}N signature), whereas the products are subsequently depleted in ^{15}N (i.e., δ^{15}N signatures that are near zero or negative).

The nitrogen cycle has been heavily influenced by human activity. Industrialization, sewage, groundwater and other wastes are normally more enriched in ^{15}N than seawater (Vizzini and Mazzola, 2004), although agricultural waste products are normally more depleted in ^{15}N (Heaton, 1986).

The utilization of nitrogen isotope analysis of macroalgae has been used to trace eutrophication on this premise. The levels of δ^{15}N in macroalgae are significantly altered due to the enrichment of nitrates in a river. These variations in macroalgae were initially documented by Minagawa and Wada (1984), and more recently there have been further studies (Savage and Elmgren, 2004; Viana *et al.*, 2011). Viana *et al.* (2011) measured δ^{15}N signatures in macroalgal tissues in coastal areas between 1990 and 2007 and found a decrease in δ^{15}N over the successive analyses, which the authors related to eutrophication. Savage and Elmgren (2004) reported the same conclusion, i.e. decreases of $\delta\ ^{15}$N values in *F. vesiculosus* are found under sewage influence.

The objectives of this project are to:

- Assess the usefulness of δ^{15}N measurements in macroalgae as an eutrophication recorder (i.e., pollution).
- Detect changes in δ^{15}N, δ^{13}C and C/N within the different structures of macroalgae (e.g., tips, holdfast, veins, vesicles, blades and stipe).
- Determine differences in δ^{15}N of macroalgae growing at different tidal levels (e.g., high tide versus low tide).

B.2 Material and methods

B.2.1 Macroalgae collection sites

The River Tees estuary is a highly industrialised region near the town of Stockton-on-Tees and the city of Middlesbrough in the county of Cleverland, UK. The mouth of the River Tees also has an area dominated by intertidal mudflats and tidal channels (called Seal Sands) and another region; Bran

Sands (Figure B.1). The presence of macroalgae in Seal Sands has been increasing over the last couple of decades, due to the nutrient enrichment (i.e., eutrophication) (Elliot *et al.*, 2008), and has been causing accumulation of sediments resulting in the deterioration of a site of special scientific interest, one of N W Europe's largest wading bird feeding grounds. Despite the nutrient enrichment in the River Tees channel, where the current is much stronger, macroalgal blooms do not occur. This shows that physical conditions are potentially the primarily controllers of macroalgal blooms.

B.2.2 Samples collection

Macroalgae samples were collected by boat on May 2014 from 49 sites (see Figure B.1). Several sampling sites taken in 2012 and 2013 were also sampled in this study. Almost all the samples were of the genus *Fucus* (Phaephyceae), mostly *Fucus ceranoides*, though a couple of samples were of *Laminaria digitata* and some others were green macroalgae: *Ulva lactuca* and *Cladophora rupestris*, and the red macroalgae, *Mastocarpus stellatus*. All macroalgae samples taken were approximately the same size and four samples were taken from different water depths.

The macroalgae samples were stored in individual freezer bags and transported to the freezer and kept at –10 ºC until processing.

B.2.3 Sample processing

The macroalgae material that was collected in December 2013 was processed with the material collected for this study in May 2014. The samples were defrosted gradually in a refrigerator before being processed for isotopic analysis. All the samples were washed and soaked in deionised (Milli-Q^{TM}) water to remove any attached sediment, organisms and salts. The samples were then dried in an oven at 60 ºC for 24 h, after which the samples were ground to a powder with a mortar and pestle. The powders were then stored in glass vials and covered with tin foil.

Aliquots of the powder, weighing between 1.3 and 1.5 mg, were placed into tin capsules and stored in a desiccator until analysis. δ^{15}N, δ^{13}C, %C, %N and C/N ratio were analysed using a Costech Elemental Analyser (ECS 4010) connected to a ThermoFinnigan Delta V Advantage Isotope Ratio Mass Spectrometer, in the Stable Isotope Biogeochemistry Laboratory (SIBL) at Durham University. Carbon-isotope ratios are corrected for 17O contribution. Carbon and nitrogen isotope ratios are reported in standard delta (δ) notation in per mil (‰) relative to the VPDB and AIR scale respectively. Data accuracy is monitored through routine analyses of in-house standards, which are stringently calibrated against international standards (e.g., USGS 40, USGS 24, IAEA 600, IAEA N1, IAEA N2). Analytical uncertainty for δ^{13}C and δ^{15}N measurements is typically ±0.1‰for replicate analyses of the international standards and typically <0.2‰on replicate sample analysis. Total organic carbon and total nitrogen data was obtained as part of the isotopic analysis using an internal standard (i.e., Glutamic Acid, 40.82 % C and 9.52 % N). The statistical analyses were performed with R-Studio software. δ^{15}N, δ^{13}C, %C, %N and C/N ratio of the samples were tested

using a HSD Tukey Test and T-Student.

Results and discussion

B.2.4 δ^{15}N variation in macroalgae (River Tees, May 2014 collection)

Red macroalgae and *Laminaria digitata* samples seem to have stable nitrogen isotope ratios (δ^{15}N) more negative than green macroalgae and Fucus samples. See Figure B.2. There were no open ocean samples collected from the ocean in this study, although these were collected in June 2013. All samples reported in this study were collected from the River Tees and Seal Sands. It is observed that 63% of the samples have negative δ^{15}N values (ranging from 0‰to –14 ‰). 16% of the samples have values of δ^{15}N close to zero and just 21% of the samples gave positive measurements. This observation of more depleted estuarine δ^{15}N values is contrary to that reported in Spain by Viana *et al.* (2011). And Raimonet *et al.* (2013) reported positive nitrogen isotope ratios within the estuaries in Galicia (Spain) and Charente (France) in comparison to Atlantic Ocean nearby the estuaries, and inferred this elevation as a result of eutrophication. The range of River Tees δ^{15}N values does not correspond to treated human waste (i.e., sewage), that typically have δ^{15}N values around +10‰(Ahad *et al.*, 2006). It does not correspond either to agricultural wastes, which have δ^{15}N values ranging between –5‰to +5‰(Maier *et al.*, 2009).

However, a recent study by Swart *et al.* (2014), who grew *Ulva* sp. and Agardhiella sp. in different concentrations of NO_3^-, showed that δ^{15}N in macroalgal tissues decreased with increasing concentrations of nitrate. It was inferred by Swart *et al.* (2014) that the macroalgae performed denitrification processes leaving the residual nitrates, to become progressively ^{15}N-enriched. If this can be translated to the natural environment, then could indicate that the River Tees is elevated in nitrate, the macroalgae is subsequently incorporating ^{14}N and the remaining water is becoming ^{15}N-enriched. An alternative hypothesis could be that some industrial N is ^{15}N-depleted.

Nitrification and denitrification processes are shown in the Figure 3. Basically, the nitrification processes are biological oxidations of ammonia with oxygen and denitrification processes are a set of reactions of nitrate reduction that ultimately produce nitrogen gas (N_2).

B.2.5 δ^{15}N variation in *Fucus* samples collection from the River Tees

Fucus sp. δ^{15}N values are presented in Figure B.4. Positive δ^{15}N values are observed in open ocean samples, the Tees Channel (Seal Sands) and in the Tees Barrage: with the exception of a few positive δ^{15}N values recorded in the River Tees (see Figure B.4). This means that less NO_3^- (nitrate) is found in those waters. Tees Barrage is found up river, far from the industry. The region affected by industry is in the lower River Tees, where the levels of δ^{15}N become negative. Figure B.5 shows the River Tees and Tees Barrage nitrogen isotope values, which show a significant trend from the mouth of the

river to the Tees Barrage (more riverine).

A possible explanation could be a simple trend of increasing nitrates discharges of the industries down the river towards Tees Channel. Nitrates discharges follow the flux of the river and arrive to Tees Barrage. As algal blooms occur in the Seal Sands of Tees Channel, more denitrification processes can be done, reducing and dispersing the nitrate of the water. This explanation coincides with the one stated by Swart *et al.* (2014) that δ^{15}N values increase when the nitrate reservoir has been depleted. Even though there is a correlation between industry polluted areas with negative values, lot of variation between samples is observed, it can be seen to follow a zig-zag.

B.2.6 δ^{15}N in *Fucus* sp from different depths

Macroalgae samples collected from different depths in the same region were studied to determine if this was a source for the δ^{15}N variations recorded between samples. There are significant differences between samples collected from different depths. Samples collected deeper in the water have δ^{15}N values that are more negative than samples near to the surface (see Figure B.6). When the level of the tide is high, both upper level and sea surface samples are in contact with water-air interface, but when the level of the tide falls just the sea surface samples are in contact with the water-air interface.

Knowing this fact, the results obtained are more comprehensible. Sea level samples are depleted in δ^{15}N values, because they are more time in contact with the water, which have nitrates and, consequently, macro-algae do denitrification processes and become more ^{15}N-enriched. As upper level samples are less time in contact with the nitrates of the water their δ^{15}N are increased compared to the sea level samples.

B.2.7 δ^{15}N in *Fucus* sp based on river location

Data in Elliot *et al.* (2008), show that the wind in the area generally comes from the South-West which would help to push nutrients out of the estuary. This type of wind could also be leading the nitrates from the West side of the river to the East side of the river making the macroalgae of the East side more depleted in δ^{15}N values. However, plotting the different sides of the river (see Figure B.7) and making the pertinent statistical test; no significant differences are observed.

B.2.8 δ^{15}N in *Fucus* sp based on collection

Fucus samples, as well as most other macroalgae, have lots of seasonal variability (Villares *et al.*, 2013). Samples of *Fucus* were clustered between collections, Figure B.8. No differences can be significantly observed. Samples with a similar location have similar values. This does not mean that there are not seasonal variations; it probably means that there are lots of other variables in this model and they hide the detection of the variability produced by seasonality.

B.2.9 Isotopic and elemental variation in *Fucus* structures

Fucus macroalgae samples were separated into different structures: holdfast, leaves, vesicles (blades), stipe and tips. No significant differences are observed in δ^{15}N measurements of each structure. Interestingly a trend ranging from the tips to the holdfast is found for δ^{13}C values and C/N ratio (see Figure B.9). More negative values of δ^{13}C are found in the tips, the values increase significantly in the leaves and there is even more increase in the stipe and the holdfast, though no significant differences are found between the holdfast and stipe. The different letters in each plot shown in Figure 8 are from the HSD Test, different letters mean significant differences, and same letters mean non-significant differences.

B.3 Conclusions

With the current study we can extract the following conclusions:

- Industrial contaminated waters discharge nitrates contents to the river, which is reflected by the negative δ^{15}N values found in *Fucus* species.
- There is lot of variability between δ^{15}N values of different macroalgae species (brown, green and red macroalgae).
- River macroalgae close to the water surface are more depleted in ^{15}N. More time in contact with water with high amounts of nitrates leads to more amount of ^{15}N in the macroalgae observed (δ^{15}N more negative).
- No significant differences between river sides were observed (East versus West).
- No significant differences observed between seasons.
- No significant differences in δ^{15}N between different structures of macroalgae, but significant differences in δ^{15}N and C/N ratios.

B.4 References

Ahad, J.M.E., Ganeshram, R.S., Spencer, R.G.M., Uher, G., Upstill-goddard, R.C., Cowie, G.L., 2006. Evaluating the sources and fate of anthropogenic dissolved inorganic nitrogen (DIN) in two contrasting North Sea estuaries. Science of the Environment 372, 317-333.

de Carvalho, M.C., 2008. Uso dos isotopos estaveis de carbono, nitrogeno e enxofre em estudios de ecologia costeira. Oecologia Bras 12, 694-705.

Elliot, M., Boyes, S.J., Burdon, D., 2008. A Scientific understanding of the Tees Estuary to determine the cause of Macroalgal mats at seal sands, in: Institute of Estuarine and Coastal studies (IECS) (Ed.). University of Hull, prepared for the Environmental agency and Northumbrian water

Ltd.

Fernandes, M., Benger, S., Sharma, S.K., Gaylard, S., Kildea, T., Hoared, S., Braley, M., Irving, A.D., 2012. The use of d15N signatures of translocated macroalgae to map coastal plumes; improving species selection and spatial analysis of metropolitan datasets. Journal of Environmental Monitoring 14, 2399- 2410.

Flint, B., 2013. Determining the cause of macroalgal blooms on Seal Sands using stable isotope mass spectrometry, Durham University.

Heaton, T.H.E., 1986. Isotopic studies of nitrogen pollution in the hydrosphere and atmosphere: a review. Chemical Geology 59, 87-102.

Maier, G., Nimmo-Smith, R.J., Glegg, G.A., Tappin, A.D., Worsford, P.J., 2009. Estuarine eutrophication in the UK: current incidence and future trends. Aquatic Conservation: Marine Freshwater Ecosystem 19, 43-56.

Mariotti, A., Germon, J.C., Hubert, P., Kaiser, P., Letolle, R., Tardieux, A., Tardieux, P., 1981. Experimental determination of nitrogen kinetic isotope fractionation: some principles; illustration for the denitrification and nitrification processes. Plant Soil 62, 413-430.

Minagawa, M., Wada, E., 1984. Stepwise enrichment of 15Nalong food chains: further evidence and the relation between d15N and animal age. Geochimica Cosmochimica Acta 48, 1135-1140.

Raimonet, M., Guillou, G., Mornet, F., Richard, P., 2013. Macroalgae d15N values in well-mixed estuaries: indicator of anthropogenic nitrogen input or macroalgae metabolism? Estuarine, Coastal and Shelf Science 119, 126-138.

Savage, C., Elmgren, R., 2004. Macroalgal (Fucus vesiculosus) d15N values trace decrease in sewage influence. Ecological applications 14 517-526.

Swart, K., Evans, S., Capo, T., Altabet, M.A., 2014. The fractionation of nitrogen and oxygen isotopes in macroalgae during the assimilation of nitrate. Geosciences Discussions 11, 6909-6943.

Viana, I.G., Fernandez, J.A., Aboal, J.R., Carballeira, A., 2011. Measurement of d15N in macroalgae stored in an environmental specimen bank for regional scale monitoring of eutrophication in coastal areas. Ecological Indicators 11, 888-895.

Villares, R., Fernandez-Lema, E., Lopez-Mosquera, E., 2013. Seasonal variations in concentrations of macro and micronutrients in three species of brown seaweed. Botanica Marina 56, 49-61.

Vizzini, S., Mazzola, A., 2004. Stable isotope evidence for the environmental impact of a land-based fish farm in the western Mediterranean. Marine Pollution 49, 61-70.

B.5 Figures

Figure B.1 Study area of the sample collections along the river Tees and its mouth. Collections of December 2012, December 2013, June 2013 and May 2014.

Figure B.2 δ^{15}N measurements of macroalgae collected on May 2014. Values of red macroalgae, green macroalgae, *Fucus* species and *Laminaria* species are represented in crosses, squares, rounds and triangles respectively.

Figure B.3 Representation of nitrification and denitrification processes.

Figure B.4 δ^{15}N values of *Fucus* macroalgae samples of all the four collection periods from open oceanic to the Tees Barrage.

Figure B.5 δ^{15}N values of *Fucus* macroalgae samples of all the four collection periods within the River Tees and Tees Barrage.

Figure B.6 δ^{15}N values of *Fucus* macroalgae samples collected from the same region but at different depth levels. Significant differences observed (p-value: 0.03).

Figure B.7 δ^{15}N values of *Fucus* macroalgae samples from all collections grouped by the side of the river. No significant differences (p-value: 0.4)

Figure B.8 δ^{15}N values of *Fucus* macroalgae samples from all collections (December 2012 in blue, June 2013 in red, December 2013 in green and May 2014 in purple).

Figure B.9 C/N ratio, δ^{13}C and δ^{15}N values of *Fucus* structures: holdfast, stipe, tips, leaves, blades (vesicles) plotted. C/N in the top left graph, δ^{15}N in the top right graph and δ^{13}C in the ground left graph. Statistical differences between samples represented by letters, HSD Tukey Test.

Figure B.1

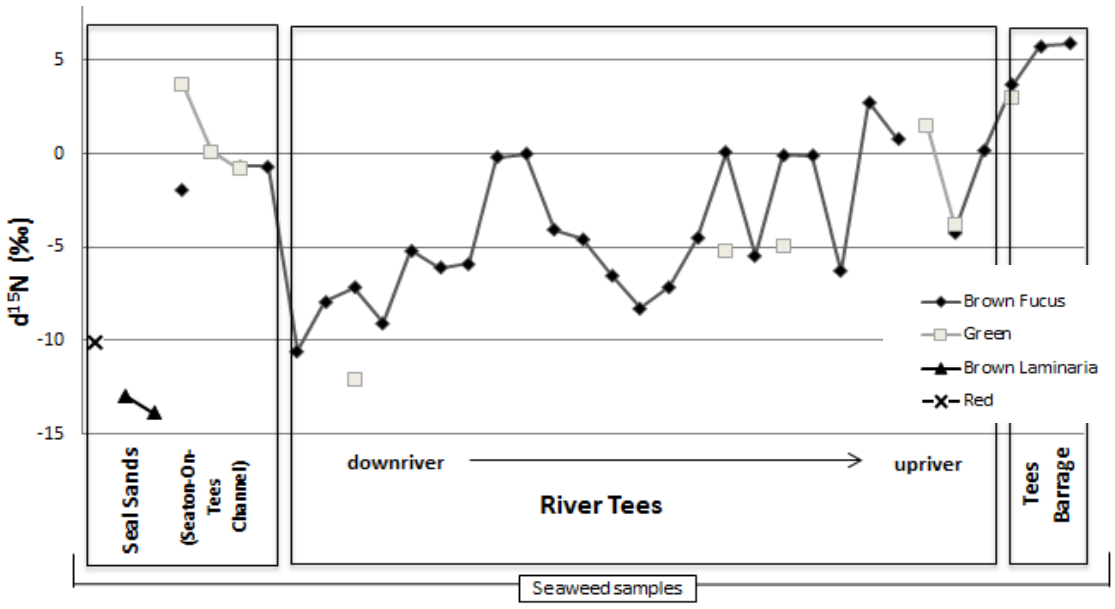

Figure B.2

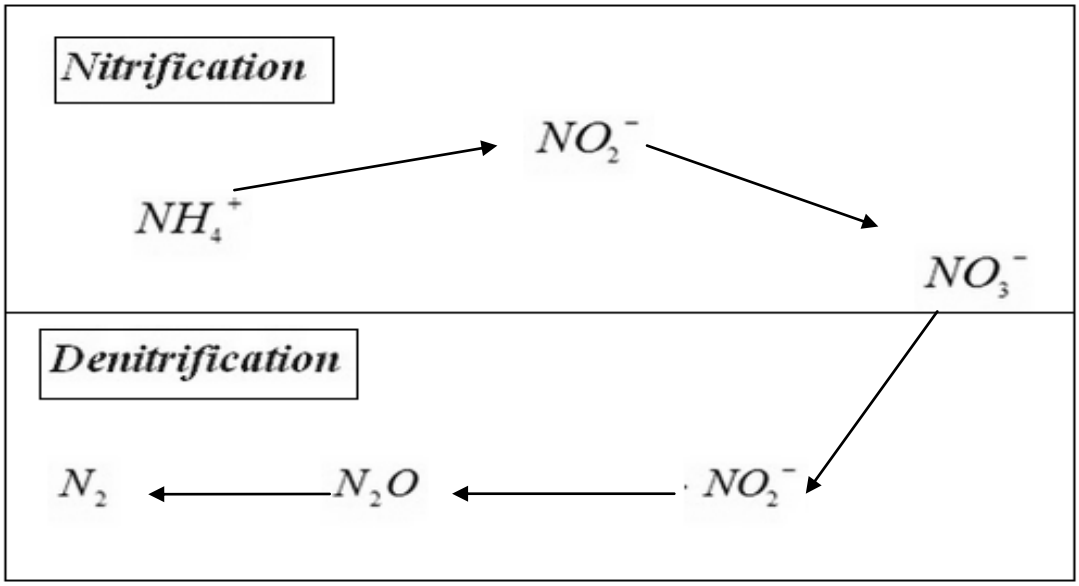

Figure B.3

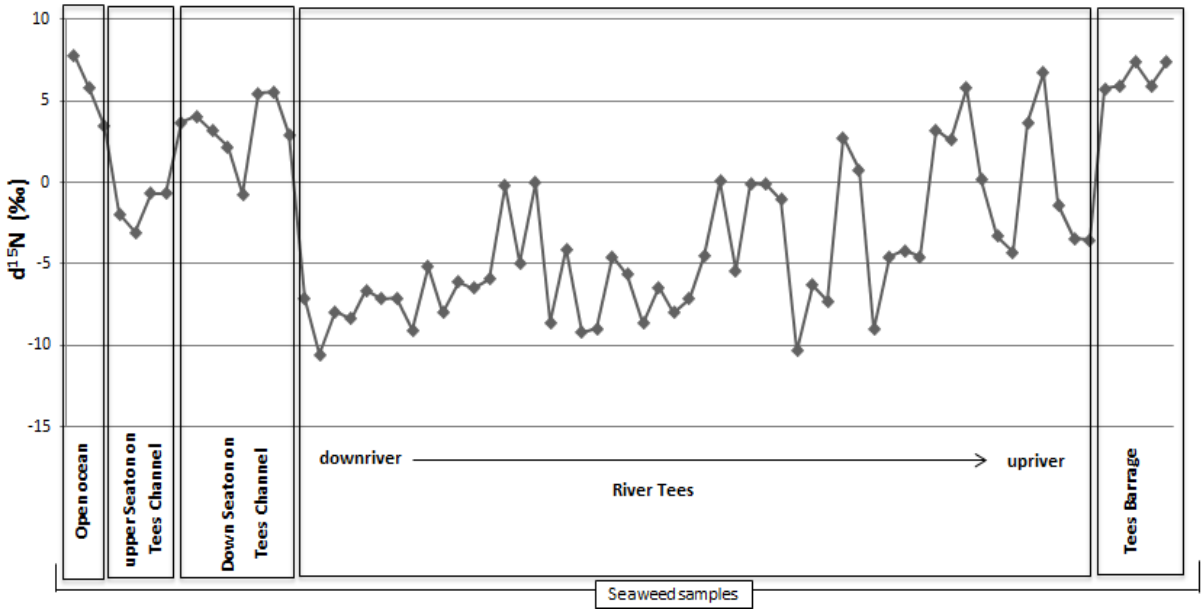

Figure B.4

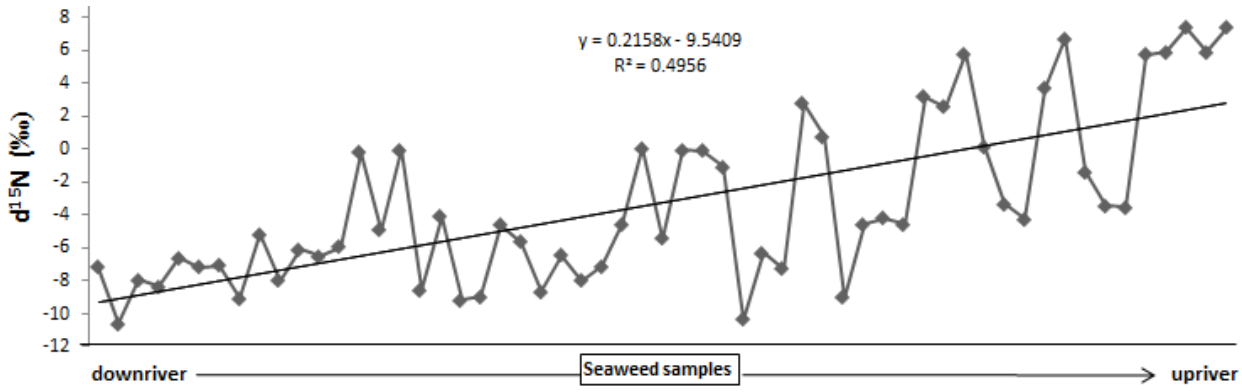

Figure B.5

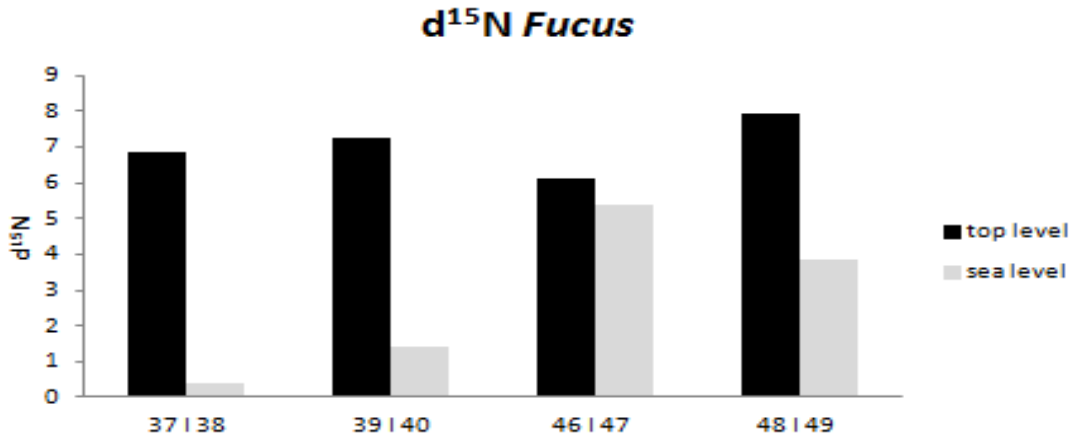

Figure B.6

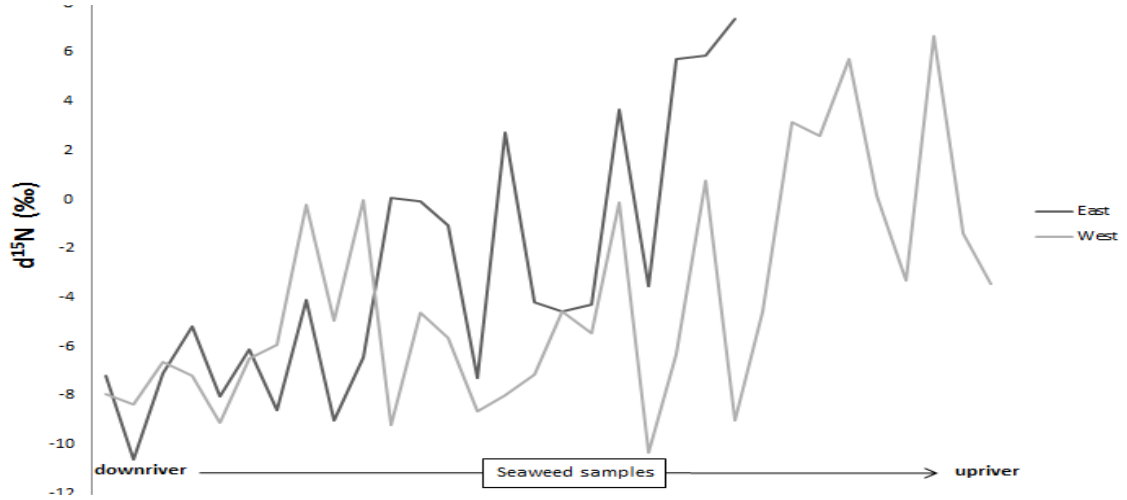

Figure B.7

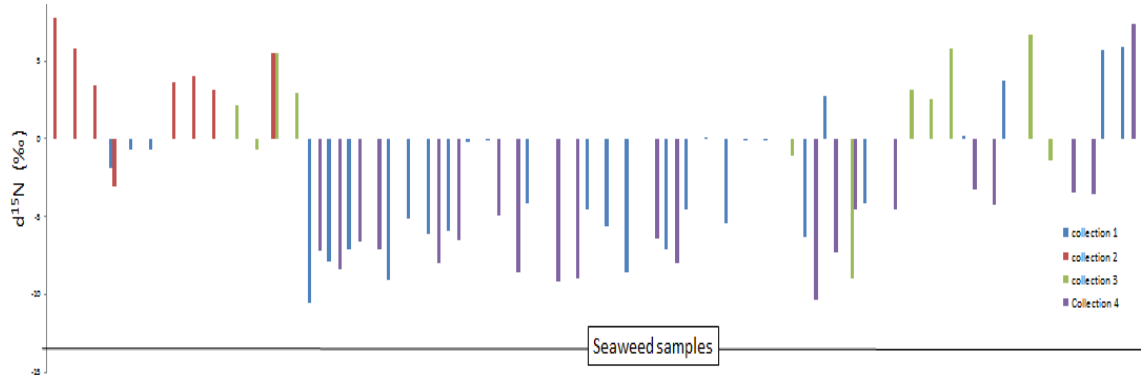

Figure B.8

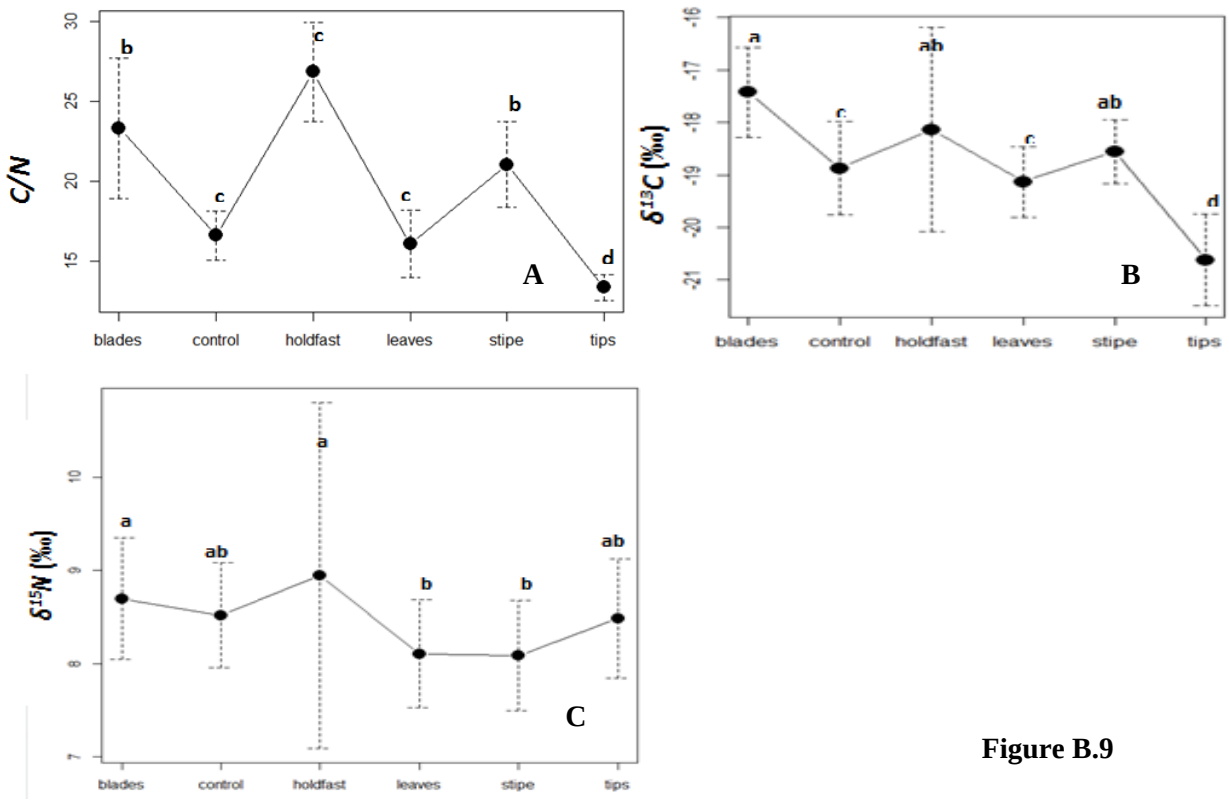

Figure B.9

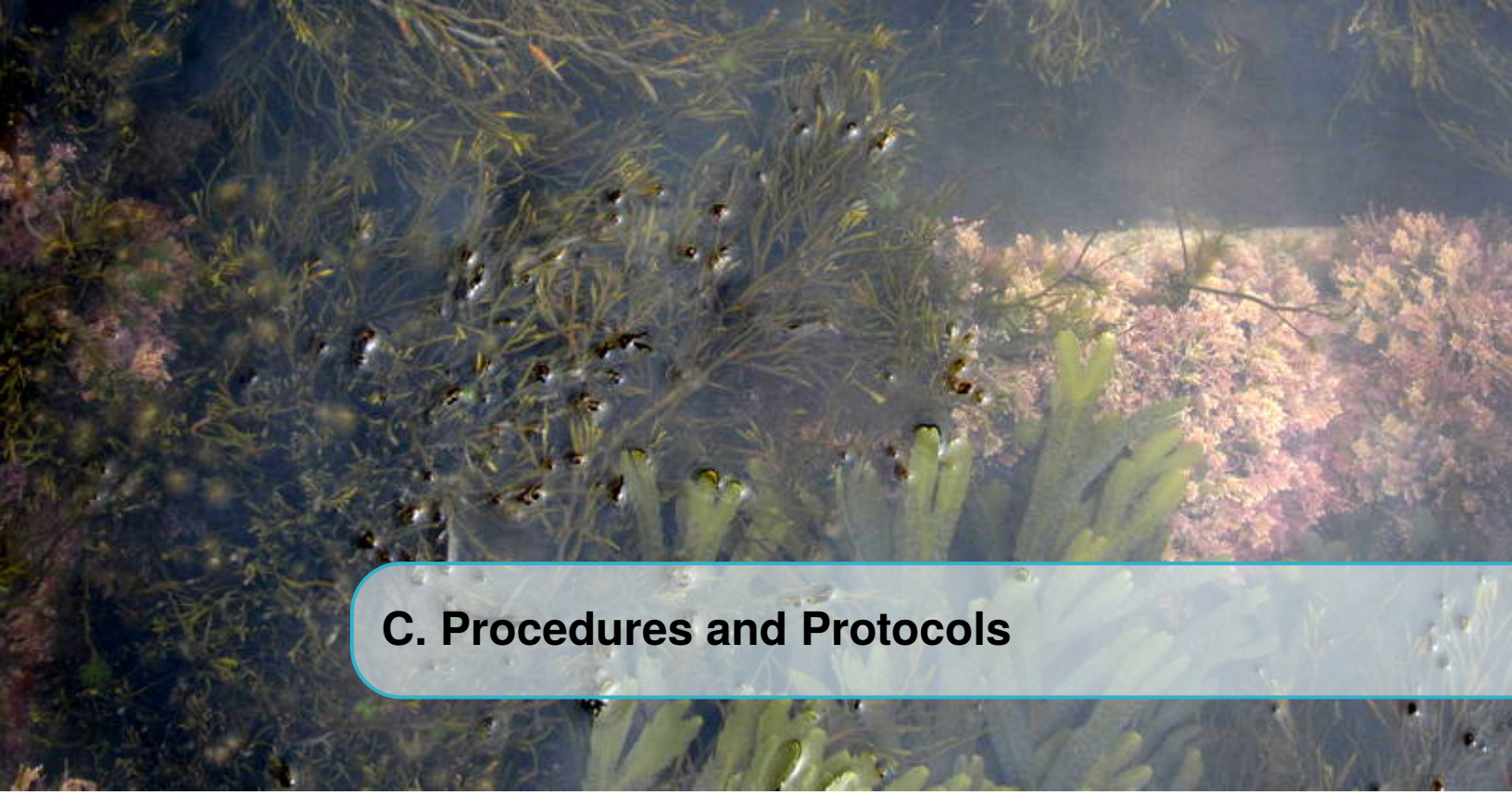

C. Procedures and Protocols

This section gathers all the protocols used in this thesis. The following list specifies all the procedures enclosed.

C.1. Macroalgae culture procedures

C.2. Macroalgae sample processing for Re analysis in ICP Mass Spectrometer.

C.3. Macroalgae sample processing for Re/Os analysis in TRITON Mass Spectrometer.

C.4. Macroalgae sample processing for N analysis in TFD-V Advantage Isotope Ratio MS.

C.5. Chloroplast isolation procedure.

C.6. Cytoplasm proteins isolation protocol.

C.7. Alginate beats formation procedure.

C.1 Macroalgae culture procedures

C.1.1 Previous preparation

- Filter seawater (from Newcastle, Boulmer or Staithes) with a 0.45 micron pore size filter.
- Autoclave seawater.
- Put two meshes subjected by pipette tips into each 250 mL screw top bottle.

C.1.2 Culture preparation

- Collect *F. vesiculosus*
- Keep *F. vesiculosus* in a tank to transport and overnight before cutting and storing them into the bottles.
- Cut off from *F. vesiculosus* non-reproductive apical thallus tips (length: > 2cm; wet weight (WW): 0.15-0.18 g) without visible epiphytes.
- Fill 36 screw top bottles with 250 mL of the sterile filtered (0.45 micron) seawater each bottle.
- Blot the tips on paper roll, and weigh the tips (= FW = fresh weight).
- Transfer 3 algal tips onto each mesh and 3 to the bottom of the bottle, giving a total of 9 algal tips per each screw top bottle.
- Transfer the bottles opened into the incubator
- Set Temperature of the incubator at 11 ºC.
- Set 16:8 light/dark cycle Illuminated with the incubator white tubes (125 μmol/m^{2}s).
- Change the medium every 2-3 days to avoid accumulation of metabolites and nutrient depletion. Control contamination of the incubator by cleaning once a week.
- Measure pH (pH meter) and the salinity (refractometer) once a week.
- Duration of the culture: Between 1 day and 4 weeks, depending on the experiment, but mostly a month.
- Measurement of the total biomass (FW) of all algal pieces in each bottle and divide by the number of algal tips per compartment to calculate the average biomass of the algal tips.
- Ready for analysis.

C.1.3 List of cultures and element concentrations performed

03/06/2014 $HReO_4$ culture

Number of culture jar replicates					
Name type	**Control +**	**Control -**	**10x Re**	**50x Re**	**100x Re**
Explanation	Natural Seawater without Re spiked	Artificial Seawater without Re spiked	Seawater with 400 pM Re spiked	Seawater with 2000 pM Re spiked	Seawater with 4000 pM Re spiked
Number of culture jar replicates					
Name type	**500x Re**	**1000x Re**			
Explanation	Seawater with 20000 pM Re spiked	Seawater with 40000 pM Re spiked			

24/10/2014 $HReO_4$ culture in different conditions

	Seawater (control +)	Artifitial seawater (control -)	1000x Re spiked
0 µmol/m^2s of light intensity			
70 µmol/m^2s of light intensity			
170 µmol/m^2s of light intensity			
Boiled			
Freeze			

26/11/2014 Os cultures

Number of culture jar replicates					
Name type	**Control +**	**Control -**	**10x Os**	**100x Os**	**1000x Os**
Explanation	Natural Seawater without Re spiked	Artificial Seawater without Re spiked	Seawater with 0.01 ppt Os spiked	Seawater with 0.1 ppt Os spiked	Seawater with 1 ppt Os spiked

26/11/2014 $HReO_4$ Cultures

Number of culture jar replicates					
Name type	**Control +**	**Control -**	**20 ppb Re**	**75 ppb Re**	**1000 ppb Re**
Explanation	Natural Seawater without Re spiked	Artificial Seawater without Re spiked	Seawater with 107 nM Re spiked	Seawater with 403 nM Re spiked	Seawater with 5.3 mM Re spiked

Number of culture jar replicates	
Name type	**2000 ppb Re**
Explanation	Seawater with 10.7 mM Re spiked

22/01/2015 $NaReO_4$ Cultures

Number of culture jar replicates				
Name type	**Control +**	**10x Re**	**100x Re**	**1000x Re**
Explanation	Natural Seawater without Re spiked	Seawater with 400 pM Re spiked	Seawater with 4000 pM Re spiked	Seawater with 40000 pM Re spiked

25/02/2015 Re vs phosphate Cultures

Re / Phosphate	10x	100x	1000x
1 µM			
100 µM			
1000 µM			
4000 µM			

26/02/2015 $NaReO_4$ Cultures

Number of culture jar replicates					
Name type	**Control +**	**10x Re**	**50x Re**	**100x Re**	**1000x Re**
Explanation	Natural Seawater without Re spiked	Seawater with 400 pM Re spiked	Seawater with 2000 pM Re spiked	Seawater with 4000 pM Re spiked	Seawater with 40000 pM Re spiked

20/04/2015 $NaReO_4$ Cultures

Number of culture jar replicates					
Name type	**Control +**	**10x Re**	**50x Re**	**100x Re**	**1000x Re**
Explanation	Natural Seawater without Re spiked	Seawater with 400 pM Re spiked	Seawater with 2000 pM Re spiked	Seawater with 4000 pM Re spiked	Seawater with 40000 pM Re spiked

20/04/2015 $KReO_4$ Cultures

Number of culture jar replicates					
Name type	**Control +**	**10x Re**	**50x Re**	**100x Re**	**1000x Re**
Explanation	Natural Seawater without Re spiked	Seawater with 400 pM Re spiked	Seawater with 2000 pM Re spiked	Seawater with 4000 pM Re spiked	Seawater with 40000 pM Re spiked

20/04/2015 NH_4ReO_4 Cultures

Number of culture jar replicates				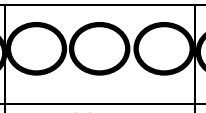	
Name type	**Control +**	**10x Re**	**50x Re**	**100x Re**	**1000x Re**
Explanation	Natural Seawater without Re spiked	Seawater with 400 pM Re spiked	Seawater with 2000 pM Re spiked	Seawater with 4000 pM Re spiked	Seawater with 40000 pM Re spiked

20/04/2015 Re recovery Cultures

Day 1: Spike the 3 jars with **1000x Re**

Day 3: Take 3 tips of each pot to analyze and change media spiking the jars with **10X [Re]**

Day 6; Take 3 tips of each pot to analyze and culture the tips with **normal SW** and no Re spiked

Day 9: Take 3 tips of each pot to analyze.

11/06/2015 Re uptake vs. pH Cultures

[Re] / pH	100x $NaReO_4$	100x $HReO_4$
~ 7		
~ 8		
~ 9		

11/06/2015 Re uptake vs. salinity Cultures

[Re] / Salinity	100x ReO_4	100x $HReO_4$
25 %		
50 %		
75 %		
100 %	Control	Control

09/06/2015 Re uptake rate Cultures

Spike 3 jars with 1000x Re of 40000 pM and take tip samples every day during a week.

09/06/2015 $HReO_4$ vs. ReO_4 salts Cultures

[Re] / Re source	10x	100x	1000x
$NaReO_4$			
$KReO_4$			
NH_4ReO_4			
Re(III)			

23/07/2015 NO_3 Cultures

Number of culture jar replicates					
$[NO_3]$	0 µM	10 µM	50 µM	100 µM	500 µM

29/07/2015 tips from Staithes cultured in jars filled with river Tees seawater

Fill 3 jars with tips from Staithes with seawater from river Tees.

17/08/2015 NH_3 Cultures

Number of culture jar replicates					
[NH_3]	0 µM	0.01 M	0.05 M	0.1 M	0.5 M

19/08/2015 NH_4OH Cultures

Number of culture jar replicates					
[NH_4OH]	0 µM	10 µM	50 µM	100 µM	500 µM

26/08/2015 Os cultures

Number of culture jar replicates				
Name type	**Control +**	**10x Os**	**100x Os**	**1000x Os**
Explanation	Natural Seawater without Re spiked	Seawater with 0.01 ppt Os spiked	Seawater with 0.1 ppt Os spiked	Seawater with 1 ppt Os spiked

02/09/2015 NH_4OH Cultures

Number of culture jar replicates					
[NH_4OH]	0 µM	10 µM	50 µM	100 µM	500 µM

C.2 Macroalgae sample processing for Re analysis in ICP Mass Spectrometer

Day 1

- Wash the samples with MQ water, put the samples in brown paper and to the oven O/N.

Day 2

- With mortar and pestle chop the dried sample; grind into powder and displace it into a vial.
- Label savilex beakers and lids with a permanent ink pen.
- On weighing paper weigh 100 mg of each sample and record sample weight.
- Add sample to savillex beaker (20 ml vial).
- Spike sample of Re test spike, making sure to record type and amount of spike (we used 10 µl of spike 4 in some experiments, but mostly we did not spike for analysis with the calibration curve method). Remember a clean pipette tip for each sample!!!
- Move samples to hood and take out Re test acid box found under the left-hand hood.
- To each sample add a mix of 3 ml of 12N HCl and 6 ml of 16N HNO_3 using the measuring cylinder found in the box. Make sure to rinse the cylinder with MQ between each sample.
- Place lid tightly on beaker and invert in order to mix sample and place on hot plate at 120ºC O/N.

Day 3

- If next day any sediment is undissolved, then empty samples into centrifuge tubes (15 m) and centrifuge for 2 min.
- Use a blue pipette to remove the liquid and place it back into the vial.
- Remove samples from hot plate and leave in hood to cool.
- Take lid off beaker and place both on hot plate to dry down overnight at 90ºC

Day 4

- If not dry next day, increase to 120ºC

Re Acetone Solvent Extraction

- To the dried sample add 5 mL 5N sodium hydroxide solution. With a clean pipette per sample, crush the dried stuff to dissolve. Leave for 30 minutes. Add the sodium hydroxide to a 15ml centrifuge tube.
- Add 5mL acetone to the centrifuge tube.

- Agitate the sodium hydroxide / acetone mix for five minutes.
- Centrifuge for 10 min. Acetone is less dense than sodium hydroxide.
- While waiting, clean Teflon vial, rinse with MQ and reflux with 1.5N HCl at 80 ºC (Put a little HCl to cover the bottom of the vial and leave it for aprox. 1 h at 90 ºC) with the lids closed.
- Pipette off the acetone (now Re bearing) to the cleaned Teflon vial. Evaporate acetone at 60ºC overnight. (Leave the lids opened).
- Place lid tightly on beaker and invert in order to mix sample and place on hot plate at O/N.

Day 5

- To the dried cake add 1.2 mL 0.8N HNO_3 for 30 min.
- Transfer into small vials 1.5 mL (ready for ICP analysis)
- Clean the Teflon vials: erase the marker with acetone. Rinse the beaker with MQ water and throw it into the acid waste. Then add 1 ml approx. of HCl and 2 ml approx. of HNO_3. Close the vials with the lids. Then put in the hotplate at 100 ºC for approx. 2 h. Turn off the hotplate and leave the vials in the hood to cool down for 1 h. Then rinse them with MQ and then drop them in the box next to the sink.

C.3 Macroalgae sample processing for Re/Os analysis in TRITON Mass Spectrometer

Day 1

- Wash the samples with MQ water, put the samples in brown paper and to the oven at 60ºC O/N.

Day 2

- With a mortar and a pestle chop the dried sample, grind into powder and displace the dried sample in a vial.

Day 3

Sample weighing and digestion

- Cut a pipette from the tip and from the top part and displace it in the neck of the carius tube. Mark each the carious tube with the number that follows the batch of the lab (e.g. R0554) and the samples with a marker ink
- Weigh 0,2 g of the dried sample (less than 0,2 g not more (This is the standard procedure but the weight and spike can change depending on the sample)
- Put the 0.2 g of sample inside the carius tube through the top part of the cut pipette.
- Write down the exact weigh (number, sample sale and mass)

- Clean the balance with MQ water
- Put 1 μL of spike 3 (again the type and amount of spike depends, this is the standard protocol) at the neck of the cut pipette, where we can see the drop (Each spike contains known specific isotopes of Re and Os, which makes possible for the MS to generate isotopes ratios that can be used to know the amount and isotopic composition of Re and Os in each sample
- Place the carious tubes in dry ice with ethanol
- Put 3 mL of HCl and 6 mL of HNO_3 in each tube (always through the pipette).
- See if the drop of spike has gone down

Carius tube sealing

- Put the fancy glasses on and open the circuit red and blue. Previously the gas cylinders from the outside must be opened.
- Open the flame and the hood (with a lighter and open the red button, then the blue one and when the flame is not red means that is ready to be used).
- Put the carious tube in the hood
- Flame a glass stick and stick it into the carious tube. Then cut the carious tube with the flame rounding a little bit the glass stick, place the carius tube in the ice again.
- Close the circuits and the hood
- Brush the leftover glass. Clean
- Put the carious tubes into the metal jackets
- Then put the metal jackets into the oven (leave for 2 h before for the tubes to cool up to room temperature, then): 1 h at 50 degrees, 1 h at 130 degrees and 24 h at 220 degrees

Day 4

Carius tube unsealing

- Turn off the oven and leave the door open to cool down for 1 h.
- Remove the samples from the oven and put them into dry ice with ethanol until they are frozen.
- Then with a scrower (or a thick knife), scratch the carious tubes
- Open the flame and the hood (also open with the vessels in the vessels room).
- Put the carious tube in the hold hood.

- Flame a little bit the neck of the carious tube
- Flame a stick and stick it into the scratch, then the carious tube should break, remove the top part with a hammer
- Put the carious tubes in the dry ice
- Switch off everything (vessels etc etc)

HBr/Chlroform stage

- Put the carious tubes in the sample rack
- Put 3 mL of chloroform to each carious tube and wait until defrost
- Rinse beakers (beaker per sample) with MQ water and put 1,5N HCl into the bottom of the beakers and to a hotplate at 80 degrees for at least 1 h.
- When defrost, put the samples of the carious tubes to the 50 mL centrifuge tubes of the sample rack.
- Vortex 2 min between 6-7.
- Put them into the water bath for 15 min.
- Clean and store everything.
- Centrifuge 1 min
- Put 3 mL of chloroform to each carious tube.
- Then with a Pasteur pipette just pipe the bottom liquid (chloroform) of the centrifuge tubes and put it into the 22 mL vials.
- Put the other 3 mL of chloroform of the carious tubes into the centrifuge tubes.
- Vortex 2 min between 6-7.
- Centrifuge for 1 min.
- Put 3 mL of chloroform to each carious tube
- With a Pasteur pipette just pipe the bottom liquid of the centrifuge tubes and put it into the 22 mL vials.
- Put the chloroform of the carious tubes into the centrifuge tubes.
- Vortex 2 min between 6-7.

- Centrifuge for 1 min.
- With a Pasteur pipette just pipe the bottom liquid and put it into the 22 mL vials. (All in all we end up having 9 mL of chloroform)
- Put the small flat tubes into the agitator O/N (for Os analysis).
- Put the excess of chloroform into the waste solvent beaker
- Remove the HCl from the beakers of the hotplate and put it in acid waste beaker. Then rinse the beakers of HCl with MQ water and put the residue of the chloroform (so the sample itself) of the centrifuge tubes into the beakers and to the hotplate 80 degrees O/N.
- Rinse with water the carious tubes and centrifuge tubes. And then throw into the glass bean the carious tubes and into the waste bean the centrifuge tubes.
- Switch off the hood and clean!

Day 5

Sample preparation for Re analysis

- Add 5 mL NaOH 5N into the beakers and rest for at least 20 min.
- With a pipette tip break the solid.
- Put the samples of the beakers to centrifuge tubes.
- Add 5 mL NaOH 5N into the beakers
- With a pipette tip break the solid.
- Put the samples of the beakers to centrifuge tubes.
- Add 5 mL NaOH 5N into the beakers
- With a pipette tip break the solid.
- Put the samples of the beakers to centrifuge tubes.
- Add 15 mL of acetone for Re to each big tube.
- Put the big tubes to the vortex for 2 min.
- Put to the centrifuge for 10 min.
- With the beakers already used but with no solution inside: rinse with MQ water and throw the excess to the acid waste. Then put HCl just to cover the bottom of the beaker and put it into

the hotplate of 80 degrees for 1 h (while waiting prepare Os).

- Remove the beakers from the hotplate.
- Put the acid into the acid waste
- Rinse with MQ water and throw to the acid waste
- Take the new big tubes of the centrifuge
- With a Pasteur pipette, pipe the top liquid of the centrifuge tubes and put it into the beakers
- Put the beakers into a hotplate of 60 degrees O/N.

Sample preparation for Os analysis

- Remove the 22 mL vials of the agitator
- Remove the excess of chloroform (part del mig!) and throw it into the waste solvent with a Pasteur pipette (so we keep the HBr).
- Put the part that rests there into smaller vials. Don't throw the caps (for next day!)
- Put the smaller vials without the caps into a hotplate at 80 degrees O/N.

Day 6

For Re separation (anion chromatography)

- Cut the top of the large pipette and the bottom slightly diagonal.
- Put a little piece of silicone wool into the tip of the large pipettes, with the help of a plastic stick.
- Put the large pipettes into the pipette rack
- Put waste beakers down the large pipettes
- Take the MARCH (del calaix d'analisi de Re) and pour it into a beaker. Then put MQ water into the beaker and with a Pasteur pipette pipe up and down to homogenate the solution.
- Put MQ water into the large pipettes and cover the top of the pipette with the finger and press with the others to get rid of the bubbles. Keep on doing it until there are no bubbles in the large pipettes. And keep the water level high.
- Put 10-20 drops of the new liquid solution of MARCH with a Pasteur pipette. And then put MQ water. Keep on repeating this process until the level of the liquid solution is in the neck of the large pipette.

- Take a paper form of "Re separation using anion chromatography"
- Fill the spaces and start with the column preparation
- Put all the ml in two turns.
- Add 1 ml of 8N HNO_3 (leave aprox 15 min)
- Add 3 ml of 8N HNO_3 (leave aprox 45 min)
- Put 2 mL of 0.2N HNO_3 (wait aprox. 30 min)
- Put 2 mL of 0.2N HNO_3 (wait aprox. 30 min)
- Put 3 mL 0.2N HNO_3 to the beakers with the dissolved dried Re samples (leave for 30-60 min and centrifuge if necessary)
- Load the samples into the columns (wait 45 min)
- Mark 2 new beakers and put them with 1,5N HCl and to the hotplate 80 degrees for then using them.
- Rinse 4 times with 0.25 mL 0.2N HNO_3 (wait 5 min each rinse)
- Rinse 2 times with 1 mL 0.2N HNO_3 (wait 15 min each rinse)
- Wash 2 times with 1 mL 0.2N HCl (wait 15 min each rinse)
- Wash with 2 mL 6N HNO_3 (wait 30 min)
- Change the waste beakers down the column for the ones of the hotplate or new ones?? without the HCl they had!!!
- Collect the Re adding 2 mL 6N HNO_3 (wait 30 min) and again 2 mL 6N HNO_3 (wait 30 min)
- Put the beakers into a hotplate 80 degrees O/N During the rinsing and washing, make sure there are no bubbles in the column and that all the bubbles of the solution are in the liquid, not spread around.

For Os separation

- Take the smaller vials and the caps of the other day.
- Add 3 drops of HBr 9N (be careful!!) into the middle of the tubes
- Leave for 30 min
- With a yellow pipette, mix good the sample and the HBr

- Pipe 60 μL (all the sample + HBr)
- Put it into the cap as a big drop and be careful not to have bubbles inside
- Put the cap into a hotplate at 80 degrees O/N

Day 7

Os separation

- Remove from the hotplate the cap and store it.

Re separation

- Remove from the hotplate the beaker and store it.

Day 8

Os micro-distillation

- Place 20 µl of 9N HBr directly to the base of the Tristar vial and turn the Tristar vial up side down and place on to a kim wipe. Because of the surface tension between the Tristar vial and the HBr, the HBr is held in the tip of the up side down Tristar vial.
- To the dried HBr on the cap (now $OsBr_2^-$) of the Tristar vial using a clean pipette tip for each sample add 30 µl of CrO_3 – 12N H_2SO_4 solution. Make sure of NO air bubbles!
- Carefully seal the Tristar vial so not to disturb the HBr.
- Carefully place the up side down sealed Tristar vial on to the hot digital plate (80 degrees). Leave for approximately 3-4 hours.
- The Os is volatized by the CrO_3 and reduced by the HBr.
- Remove cap and dry down Os-bearing HBr sample at 60degrees in the Tristar vial. Dry until ~1µl of the HBr remains
- Discard cap.
- Place parafilm over tristar vial and take to mass spec for loading.
- Repeat for multiple samples.

Day 12

Load samples to the mass spectrometer. To load the samples we should put a the drop we have in the tristar vial into the Ni filament. And then add 5 μl to cover the drop with Os spike. The Os does crystallizations, so we should see a thin layer of it turning more whitish. Store them into a box before putting them into the TRITON Mass Spectrometer.

C.4 Macroalgae sample processing for N analysis in ThermoFinnigan Delta V Advantage Isotope Ratio Mass Spectrometer

Day 1

- Wash the samples with MQ water, put the samples in brown paper and to the oven at 60ºC O/N.

Day 2

- With a mortar and a pestle chop the dried sample, grind into powder and displace the dried sample in a vial.
- Displace between 1.0. and 1.5 mg sample into a tin capsule
- Leave on the desiccator until analysis

C.5 Chloroplast isolation procedure

- Cut the tips (20 g) into 2 mm squares using a chopping knife on a plastic block.
- Wash them by stirring in 200 mL of Millipore filtered seawater at 8 degrees and collect them from the viscous extract with a stainless steel strainer.
- Repeat this washing procedure 10 times to remove the greater part of the mucilage
- Wash the tips 3 times in 75 mL in grinding medium at 2 degrees.
- Store in the freezer
- Maintain the same T for all subsequent preparative steps
- Remove the cut tips from the grinding medium
- Divide the tissue into four portions
- Each ground separately with a mortar and pestle, gradually increasing the medium volume to 50 mL. Grinding caused the release of additional mucilage.
- The combined slurries were diluted to 200 mL of medium
- Pass them through a 0.5 mm nylon grid and then 4 layers of cheese cloth.
- Centrifuge at 5500 g for 7 min.
- Re-suspend the pellet using a glass Teflon mixer and washed in 80 mL of the reaction medium.
- Centrifuge at 5500 g for 7 min

- Re-suspend the pellet using 8 mL of HEPES.
- Analyze the content of Chloroplasts by microscopy and with a spectrophotometer
- Store in the freezer until analysis.
- Analyze Re and Mn and Mg.

Grinding medium: 1M sorbitol, 1 mM $MnCl_2$, 1 mM $MgCl_2$, o.5 mM K_2HPO_4, 5mM EDTA, 2mM $NaNO_3$, 2mM Na-isoascorbate, 2 mM cysteine, 0.2% (w/v) BSA and 40 mM Mes buffer (pH: 6.1).

Reaction medium: 1 M sorbitol, 1 mM $MnCl_2$, 2 mM EDTA, 0.5 mM K_2HPO_4, and 50 mM HEPES (pH 7.6)

C.6 Cytoplasm proteins isolation protocol

Solvent preparation

- Homogenize seaweed tips (dry and grind)
- Weight 2 g of seaweed tips put into a beaker
- Add 4 mL buffer (10 mM HEPES (pH 7.8))
- Vortex few seconds
- Add 5 more mL of buffer
- Centrifuge 1000 rpm for 1 min twice
- Sonication for 30 seconds 10 times
- Centrifuge 4500 rpm 5 min
- Resuspend the supernatant (SN) into 2 Eppendorf (800 µL)
- Centrifuge 14000 rpm 10 min
- Add 48 μL of Calcium
- Vortex 1900 rpm 15 min
- Centrifuge 14000 rpm 5 min
- Add 48 more μL of Calcium
- Vortex 1900 rpm 5 min

- Centrifuge 14000 rpm 5 min
- Take the SN and put them into a new Eppendorf (both SN fit in one)
- If not load to the column directly put the Eppendorf in ice just to avoid damage in the proteins

Column Chromatography

- Hold the column with a stand and displace a beaker below it
- Cut the tip of the column and take the lid off.
- Let the liquid inside run throw. Once all run, put 1 mL of 1mM EDTA and let them all run throw.
- Put 1 mL of buffer
- Displace the buffer reservoir in the top of the column and pour buffer all throw the reservoir twice.
- Look at the seaweed solvent Eppendorf stored in ice, if not clarified give it another spin (14000 for 10 min).
- Put a lid on the tip of the column and carefully run 1 mL of the solvent
- Label 15 new Eppendorf (1-15) and make a mark of the 1 mL (easy to see afterwards) and put them opened into a ruck. Change the beaker below the column for the ruck with the first Eppendorf right below the tip.
- Take off the lid of the Eppendorf and collect the first mL
- Put 1 mL of buffer and displace the ruck so that the next collection is in the Eppendorf 2. Keep on repeating this until the 15 samples are collected.
- Make a protein assay of the samples collected. Take 100 μL of each Eppendorf and put them into a plate with 100 μL of blue Coomassie (it dye the aminoacids).
- Wait for some minutes for the stain to react and then read the measures with a photometer in a wavelength of 595 nm.

C.7 Alginate beats formation procedure

Prepare a solution of 2% Sodium alginate, for this: Mix 20 mL of DI water with 0.4 g of sodium alginate (Manugel DMB low viscosity sodium alginate). For a better mixing tend to pour the water first into the 50mL centrifuge tube. Then leave the centrifuge tube into a shaker for about 30 min

until you see that the alginate gel is formed.

Prepare a solution of 0.3M Calcium Chloride dihydrate ($CaCl_2x2H_2O$), for this: Mix 100 mL of DI water with 4.41g of $CaCl_2$ into a flask, do not pour all the water first, use the water to put the residual $CaCl_2$ of the weighing container into the flask.

Pour some $CaCl_2$ (about 30 mL) into a 50 mL centrifuge tube, for this: And add drops with a pipette or with a syringe of the sodium alginate formed to the $CaCl_2$. We should see the transparent beats floating if there are bubbles in the alginate or submerged at the end of the tube if there are no bubbles. Leave for 1 h to lie up. After this time the beads are ready to use.

D. Datasets

D.1 Introduction

This section gathers all the data and standard deviations used in the current work.

D.1. Chapter 2 dataset

D.2. Chapter 4 dataset

D.3. Appendix A) dataset.

D.4. Appendix B) dataset.

D.2 Chapter 2 dataset

Table D1.1. pH and salinity measures of the cultures performed with diferent concentrations of Re spiked in the seawater and different treatments.

$HReO_4$ (ppb) doped in the seawater	week 1		week 2		week 3	
	pH	Salinity (ppm)	pH	Salinity (ppm)	pH	Salinity (ppm)
0.008	8.7	35	8.6	35	8.8	35
0.000	8.9	30	8.5	30	8.8	29
0.075	9.0	35	8.7	35	8.8	35
0.373	8.8	35	8.8	35	8.8	35
0.745	8.9	35	8.9	35	8.9	35
3.745	8.7	35	8.7	35	8.7	35
7.450	9.0	35	8.7	35	8.7	36
20.000	8.6	35	8.6	34	8.6	35
75.000	8.7	35	8.7	33	8.8	35
1000.000	8.6	34	8.6	34	8.5	34
2000.000	8.5	34	8.4	34	3.3	34
7450.000	NA	NA	NA	NA	3.5	36
$NaReO_4$ doped in seawater (March)	Week 1		Week 2		Week 3	
	pH	Salinity (ppm)	pH	Salinity (ppm)	pH	Salinity (ppm)
0.075	8.9	35	9.0	30	8.9	34
0.373	8.9	35	8.9	32	9.0	29
0.745	9.0	35	9.1	34	9.0	31
7.450	8.9	34	9.0	35	8.9	35
$NaReO_4$ doped in seawater (May)	Week 1		Week 2		Week 3	
	pH	Salinity (ppm)	pH	Salinity (ppm)	pH	Salinity (ppm)
0.075	9.0	30	9.1	35	8.9	36
0.373	9.0	30	9.0	31	8.9	35
0.745	9.1	30	9.1	35	9.0	36
7.450	9.0	30	9.4	35	8.1	35
NH_4ReO_4 doped in seawater (May)	Week 1		Week 2		Week 3	
	pH	Salinity (ppm)	pH	Salinity (ppm)	pH	Salinity (ppm)
0.075	9.0	29	9.0	35	8.9	36
0.373	9.0	30	9.1	35	8.8	36
0.745	9.0	31	9.2	35	8.8	36
7.450	9.2	29	9.2	35	8.9	35
$KReO_4$ doped in seawater (May)	Week 1		Week 2		Week 3	
	pH	Salinity (ppm)	pH	Salinity (ppm)	pH	Salinity (ppm)
0.075	9.0	30	9.0	35	9.1	35
0.373	9.0	25	9.2	35	8.8	35
0.745	9.0	30	9.3	35	8.9	36
7.450	9.1	30	9.1	35	8.0	35
$HReO_4$ doped in seawater (June)	Week 1		Week 2			
	pH	Salinity (ppm)	pH	Salinity (ppm)		
0.075	8.7	33	9.2	35		

0.745	8.8	32	9.0	36		
7.450	8.7	31	9.1	35		
$NaReO_4$ doped in seawater (June)	Week 1		Week 2			
	pH	Salinity (ppm)	pH	Salinity (ppm)		
0.075	8.8	35	9.0	35		
0.745	8.8	34	9.1	35		
7.450	8.8	32	9.1	35		
NH_4ReO_4 doped in seawater (June)	Week 1		Week 2			
	pH	Salinity (ppm)	pH	Salinity (ppm)		
0.075	8.8	34	9.1	35		
0.745	8.7	33	9.1	35		
7.450	8.7	31	9.2	35		
$KReO_4$ doped in seawater (June)	Week 1		Week 2			
	pH	Salinity (ppm)	pH	Salinity (ppm)		
0.075	8.9	33	9.2	35		
0.745	8.8	33	9.1	35		
7.450	8.8	31	9.1	35		
Sample treatment	week 1		Week 2		Week 3	
	pH	Salinity (ppm)	pH	Salinity (ppm)	pH	Salinity (ppm)
Boiled 5 min	6.5	35	7.5	35	7.4	30
Dryed 72 h	6.8	35	7.8	35	7.7	33
Freezed with liquid Nitrogen	6.1	32	7.6	35	7.9	30
Boiled 2 h	7.7	31	7.3	35	7.6	35

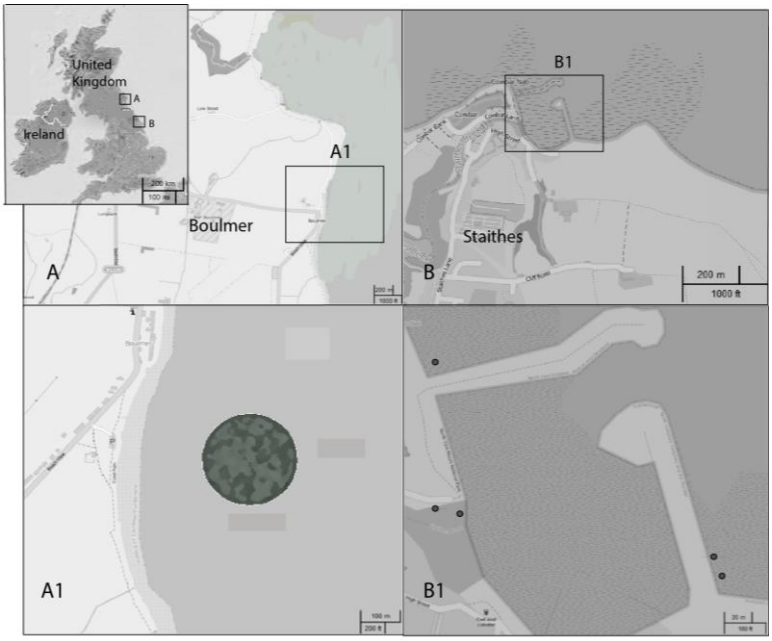

Figure D1.1 A) Location sites of the seventeen specimens of *F. vesiculosus* collected in Boulmer Beach, North East England from North Sea (55º25'N 01º34'W) in May and October, 2014. **A1**) Collection area of the samples coloured. **B**) Location sites of the five specimens of *F. vesiculosus* collected in Staithes, North Yorkshire UK (54°33'N 00°47'W) in May, 2014. **B1**)Specific location of each specimen.

D.3 Chapter 4 dataset

Table D2.1 C, N, C/N, $\delta^{13}C$ and $\delta^{15}N$ of short term experiment *Fucus* grown in vivo in river Tees and analysed with Stable Isotope Mass spectrometer.

Sample (*Sample IDs*)	C	$\delta^{13}C$	N	$\delta^{15}N$	C/N
week 15.07.15 to 22.07.15					
Buoy 1 Top					
22-07-1Tc	35,3	-17,5	3,4	1,3	12,1
22-07-1Tb	34,1	-17,2	3,3	1,3	11,9
22-07-1Ta	35,1	-17,5	3,6	1,3	11,3
Average Buoy 1 Top	34,8 ± 0,6	-17,4 ± 0,2	3,4 ± 0,2	1,3 ± 0,0	11,8 ± 0,4
Buoy 1 Bottom					
22-07-1Bc	34,3	-15,9	3,4	3,7	11,7
22-07-1Bb	34,0	-15,9	3,1	3,8	12,9
22-07-1Ba	33,8	-15,9	3,3	3,7	11,9
Average Buoy 1 Top	34,0 ± 0,3	-15,9 ± 0,0	3,3 ± 0,2	3,7 ± 0,1	12,1 ± 0,6
Buoy 2 Top					
22-07-2Tc	32,6	-17,7	3,2	2,7	11,9
22-07-2Tb	32,0	-17,8	3,0	2,8	12,3
22-07-2Ta	32,8	-17,9	3,3	2,8	11,5
Average Buoy 2 Top	32,5 ± 0,4	-17,8 ± 0,1	3,2 ± 0,2	2,8 ± 0,1	11,9 ± 0,4
Buoy 2 Bottom					
22-07-2Bc	34,4	-17,0	3,0	4,1	13,2
22-07-2Bb	34,7	-16,9	3,2	3,7	12,6
22-07-2Ba	34,1	-17,0	3,4	3,5	11,8
Average Buoy 2 Bottom	34,4 ± 0,3	-17,0 ± 0,1	3,2 ± 0,2	3,8 ± 0,3	12,5 ± 0,7
Buoy 3 Top					
22-07-3Tc	32,9	-17,4	3,3	2,9	11,5
22-07-3Tb	34,0	-17,2	3,5	3,1	11,2
22-07-3Ta	32,5	-17,4	3,6	3,4	10,4
Average Buoy 3 Top	33,1 ± 0,8	-17,3 ± 0,1	3,5 ± 0,2	3,1 ± 0,3	11,0 ± 0,6
Buoy 3 Bottom					
22-07-3Bc	33,0	-16,3	3,0	5,3	13,0
22-07-3Bb	33,2	-16,8	3,0	5,5	12,7
22-07-3Ba	33,8	-16,6	3,1	5,3	12,8
Average Buoy 3 Bottom	33,3 ± 0,4	-16,6 ± 0,3	3,0 ± 0,1	5,4 ± 0,1	12,8 ± 0,2
Buoy 4 Top					
22-07-4Tc	32,8	-18,1	3,2	5,2	12,1
22-07-4Tb	33,5	-18,2	3,1	4,9	12,5
22-07-4Ta	33,2	-18,1	3,2	4,5	12,1
Average Buoy 4 Top	33,2 ± 0,4	-18,1 ± 0,1	3,2 ± 0,1	4,8 ± 0,4	12,2 ± 0,2
Buoy 4 Bottom					
22-07-4Bc	34,6	-16,8	3,0	4,3	13,3
22-07-4Bb	35,2	-16,8	3,2	4,1	12,8
22-07-4Ba	35,3	-16,8	3,1	4,6	13,4

Average Buoy 4 Bottom	35,0 ± 0,5	-16,8 ± 0,0	3,1 ± 0,1	4,3 ± 0,3	13,2 ± 0,3
week 22.07.15 to 28.07.15					
Buoy 1 Top					
28-07-BUOY-TOP-FROM-22-07 C	33,5	-18,2	3,0	3,6	13,2
28-07-BUOY-TOP-FROM-22-07 B	33,7	-18,4	2,9	4,2	13,5
28-07-BUOY-TOP-FROM-22-07 A	33,3	-18,1	2,8	3,9	13,7
Average Buoy 1 Top	33,5 ± 0,2	-18,3 ± 0,2	2,9 ± 0,1	3,9 ± 0,3	13,5 ± 0,3
week 28.07.15 to 04.08.15					
Buoy 1 Top					
04.08A B1T1W	33,2	-16,3	2,6	5,1	14,7
04.08B B1T1W	33,4	-16,3	2,7	5,1	14,5
04.08C B1T1W	33,0	-16,3	2,7	5,3	14,4
Average Buoy 1 Top	33,2 ± 0,2	-16,3 ± 0,0	2,7 ± 0,0	5,2 ± 0,1	14,5 ± 0,2
week 04.08.15 to 11.08.15					
Buoy 1 Top					
11.08A B1T1W	35,4	-16,0	3,1	4,1	13,3
11.08B B1T1W	35,5	-16,2	2,9	5,0	14,4
11.08C B1T1W	35,6	-16,2	3,0	4,8	14,1
Average Buoy 1 Top	35,5 ± 0,1	-16,1 ± 0,1	3,0 ± 0,1	4,6 ± 0,5	13,9 ± 0,6
Buoy 1 Bottom					
11.08A B1B1W	34,8	-15,7	2,8	6,4	14,3
11.08B B1B1W	34,7	-15,7	2,8	6,6	14,5
11.08C B1B1W	34,7	-15,9	3,0	5,9	13,3
Average Buoy 1 Top	34,7 ± 0,0	-15,8 ± 0,1	2,9 ± 0,1	6,3 ± 0,3	14,0 ± 0,6
Buoy 2 Top					
11.08A B2T1W	36,0	-16,7	3,1	3,9	13,6
11.08B B2T1W	35,6	-16,6	3,1	3,5	13,2
11.08C B2T1W	35,4	-16,5	3,0	4,2	13,6
Average Buoy 2 Top	35,7 ± 0,3	-16,6 ± 0,1	3,1 ± 0,1	3,8 ± 0,3	13,5 ± 0,2
Buoy 2 Bottom					
11.08A B2B1W	33,0	-16,3	2,8	4,9	13,9
11.08B B2B1W	33,5	-16,5	2,9	4,6	13,5
11.08C B2B1W	33,0	-15,8	3,0	5,4	12,9
Average Buoy 2 Bottom	33,2 ± 0,3	-16,6 ± 0,4	2,9 ± 0,1	4,9 ± 0,4	13,4 ± 0,5
Buoy 3 Top					
11.08A B3T1W	34,6	-16,5	3,3	2,3	12,1
11.08B B3T1W	34,8	-16,8	3,2	1,3	12,5
11.08C B3T1W	34,7	-16,7	3,3	1,9	12,3
Average Buoy 3 Top	34,7 ± 0,1	-16,7 ± 0,22	3,3 ± 0,0	1,7 ± 0,5	12,3 ± 0,2
Buoy 3 Bottom					
11.08A B3B1W	33,7	-17,0	2,9	4,5	13,4
11.08B B3B1W	34,0	-16,8	2,7	4,3	14,9
11.08C B3B1W	34,0	-16,7	3,0	3,8	13,1

Average Buoy 3 Bottom	33,9 ± 0,2	-16,8 ± 0,1	2,9 ± 0,2	4,2 ± 0,4	13,7 ± 1,0
Buoy 4 Top					
11.08A B4T1W	35,4	-16,8	2,8	4,2	14,7
11.08B B4T1W	35,3	-16,7	2,6	4,0	15,8
11.08C B4T1W	35,2	-16,8	2,7	4,0	15,2
Average Buoy 4 Top	35,3 ± 0,1	-16,8 ± 0,0	2,7 ± 0,1	4,1 ± 0,1	15,2 ± 0,6
Buoy 4 Bottom					
11.08A B4B1W	33,5	-16,2	2,5	5,7	15,5
11.08B B4B1W	33,7	-16,4	2,9	5,2	13,6
11.08c B4B1W	32,6	-16,4	2,7	4,6	14,3
Average Buoy 4 Bottom	33,3 ± 0,6	-16,3 ± 0,1	2,7 ± 0,2	5,1 ± 0,6	14,4 ± 1,0

week 11.08.15 to 17.08.15

Buoy 1 Top					
17-08A B1B1 WEEK	33,7	-16,6	3,0	3,7	13,1
17-08B B1B1 WEEK	33,5	-16,6	3,1	3,5	12,7
17-08C B1B1 WEEK	33,9	-16,5	3,2	2,7	12,2
Average Buoy 1 Top	33,7 ± 0,2	-16,6 ± 0,1	3,1 ± 0,1	3,2 ± 0,5	12,6 ± 0,4
Buoy 1 Bottom					
17-08A B1T1 WEEK	32,4	-15,2	3,0	4,1	12,5
17-08B B1T1 WEEK	33,1	-15,0	3,1	4,4	12,3
17-08C B1T1 WEEK	33,7	-15,2	3,2	4,5	12,3
Average Buoy 1 Bottom	33,1 ± 0,6	-15,1 ± 0,1	3,1 ± 0,1	4,3 ± 0,2	12,4 ± 0,1
Buoy 2 Top					
17-08A B2T1W	34,2	-17,2	3,2	2,3	12,5
17-08B B2T1W	34,9	-17,0	3,2	2,1	12,7
Average Buoy 2 Top	34,6 ± 0,5	-17,1 ± 0,2	3,2 ± 0,0	2,2 ± 0,2	12,6 ± 0,1
Buoy 2 Bottom					
17-08A B2B1W	33,9	-16,4	3,0	4,8	13,1
17-08B B2B1W	34,5	-16,2	2,8	4,7	14,3
Average Buoy 2 Bottom	34,2 ± 0,4	-16,3 ± 0,1	2,9 ± 0,1	4,7 ± 0,1	13,6 ± 0,9
Buoy 3 Top					
17-08A B3T1W	34,1	-16,6	3,0	3,2	13,3
17-08B B3T1W	34,1	-16,8	3,1	3,1	12,7
Average Buoy 3 Top	34,1 ± 0,0	-16,7 ± 0,1	3,1 ± 0,1	3,2 ± 0,1	13,0 ± 0,4
Buoy 3 Bottom					
17-08A B3B1W	34,5	-15,5	3,0	4,3	13,6
17-08B B3B1W	34,0	-15,5	3,0	4,3	13,4
Average Buoy 3 Bottom	34,3 ± 0,4	-15,5 ± 0,0	3,0 ± 0,0	4,3 ± 0,0	13,5 ± 0,2
Buoy 4 Top					
17-08A B4T1W	35,4	-15,9	3,2	3,8	13,0
17-08B B4T1W	34,9	-16,0	3,0	4,1	13,7
Average Buoy 4 Top	35,1 ± 0,3	-16,0 ± 0,1	3,1 ± 0,1	4,0 ± 0,2	13,4 ± 0,5
Buoy 4 Bottom					
17-08A B4B1W	34,0	-16,4	2,9	4,2	13,8
17-08B B4B1W	34,2	-16,5	2,7	4,7	14,6
Average Buoy 4 Bottom	34,1 ± 0,1	-16,4 ± 0,1	2,8 ± 0,1	4,4 ± 0,4	14,2 ± 0,6

week 17.08.15 to 25.08.15					
Buoy 1 Top					
25-08B-B1T1W	34,6	-18,1	2,9	5,8	13,7
25-08A-B1T1W	34,9	-18,4	2,8	6,3	14,5
Average Buoy 1 Top	34,8 ± 0,3	-18,3 ± 0,2	2,8 ± 0,1	6,0 ± 0,3	14,1 ± 0,6
Buoy 1 Bottom					
25-08B-B1B1W	35,7	-18,6	3,1	5,9	13,6
25-08A-B1B1W	33,5	-18,6	2,9	5,9	13,6
Average Buoy 1 Bottom	34,6 ± 1,5	-18,6 ± 0,0	3,0 ± 0,1	5,9 ± 0,0	13,6 ± 0,0
Buoy 2 Top					
25-08B-B2T1W	36,3	-17,3	3,2	3,2	13,2
25-08A-B2T1W	36,6	-17,4	3,3	3,0	13,0
Average Buoy 2 Top	36,5 ± 0,2	-17,4 ± 0,0	3,2 ± 0,1	3,1 ± 0,1	13,1 ± 0,2
Buoy 2 Bottom					
25-08B-B2B1W	36,4	-17,5	3,1	6,6	13,8
25-08A-B2B1W	31,4	-17,6	2,7	6,6	13,5
Average Buoy 2 Bottom	33,7 ± 3,5	-17,5 ± 0,1	2,9 ± 0,3	6,6 ± 0,0	13,6 ± 0,2
Buoy 3 Top					
25-08B-B3T1W	36,6	-17,5	3,1	2,6	13,8
25-08A-B3T1W	33,7	-17,7	2,9	2,6	13,6
Average Buoy 3 Top	35,1 ± 2,1	-17,6 ± 0,1	3,0 ± 0,1	2,6 ± 0,0	13,7 ± 0,1
Buoy 3 Bottom					
25-08B-B3B1W	35,5	-17,5	3,1	5,2	13,5
25-08A-B3B1W	35,5	-18,1	3,1	4,7	13,4
Average Buoy 3 Bottom	35,5 ± 0,0	-17,8 ± 0,4	3,1 ± 0,0	4,9 ± 0,4	13,4 ± 0,1
Buoy 4 Top					
25-08B-B4T1W	35,3	-18,6	3,2	2,7	13,0
25-08A-B4T1W	35,1	-18,3	3,2	2,7	12,9
Average Buoy 4 Top	35,2 ± 0,1	-18,5 ± 0,2	3,2 ± 0,0	2,7 ± 0,0	12,9 ± 0,1
Buoy 4 Bottom					
25-08B-B4B1W	35,2	-17,8	2,9	5,0	14,1
25-08A-B4B1W	34,8	-17,9	2,9	5,2	14,1
Average Buoy 4 Bottom	35,0 ± 0,3	-17,9 ± 0,1	2,9 ± 0,0	5,1 ± 0,1	14,1 ± 0,0

Table D2.2 C, N, C/N, $\bar{\delta}^{13}C$ and $\bar{\delta}^{15}N$ of long term experiment *Fucus* grown in vivo in river Tees and analysed with Stable Isotope Mass spectrometer.

Sample (*Sample IDs*)	C	$\bar{\delta}^{13}C$	N	$\bar{\delta}^{15}N$	C/N
Buoy 1 Top					
After 1 week					
22-07-1Tc	35,3	-17,5	3,4	1,3	12,1
22-07-1Tb	34,1	-17,2	3,3	1,3	11,9
22-07-1Ta	35,1	-17,5	3,6	1,3	11,3
Average after 1 week	24,8 ± 0,6	-17,4 ± 0,2	3,4 ± 0,2	1,3 ± 0,0	11,8 ± 0,4
After 2 weeks					
28-07-BUOY-TOP-WEEK-2C	34,0	-18,7	3,7	0,8	10,6
28-07-BUOY-TOP-WEEK-2B	34,3	-18,0	3,7	1,3	10,9
28-07-BUOY-TOP-WEEK-2A	33,9	-18,5	3,7	1,1	10,7

Average after 2 weeks	34,1 ± 0,2	-18,3 ± 0,4	3,7 ± 0,0	1,0 ± 0,3	10,7 ± 0,2
After 3 weeks					
04.08A B1T4W	33,1	-18,8	3,6	1,6	10,6
04.08B B1T4W	33,2	-18,4	3,7	1,7	10,3
04.08C B1T4W	32,8	-18,6	3,5	1,7	10,9
Average after 3 weeks	33,0 ± 0,2	-18,5 ± 0,2	3,6 ± 0,1	1,7 ± 0,1	10,6 ± 0,3
After 4 weeks					
11.08A B1T4W	35,6	-18,8	4,2	1,3	9,8
11.08B B1T4W	33,7	-18,7	3,9	1,6	10,1
11.08C B1T4W	35,8	-18,8	4,2	1,7	10,0
Average after 4 weeks	35,0 ± 1,1	-18,8 ± 0,0	4,1 ± 0,2	1,5 ± 0,2	10,0 ± 0,2
After 5 weeks					
17-08A B1T5 WEEK	32,5	-18,5	3,8	0,8	9,8
17-08B B1T5 WEEK	33,0	-18,0	4,0	1,4	9,7
17-08C B1T5 WEEK	32,9	-18,4	4,4	1,3	8,8
Average after 5 weeks	32,8 ± 0,2	-18,2 ± 0,2	4,0 ± 0,3	1,1 ± 0,3	9,4 ± 0,6
Buoy 1 Bottom					
After 1 week					
11.08A B1B1W	34,8	-15,7	2,8	6,4	14,3
11.08B B1B1W	34,7	-15,7	2,8	6,6	14,5
11.08C B1B1W	34,7	-15,9	3,0	5,9	13,3
Average after 1 week	34,7 ± 0,0	-15,8 ± 0,1	2,9 ± 0,1	6,3 ± 0,3	14,0 ± 0,6
After 2 weeks					
17-08A B1B2 WEEK	33,7	-16,6	2,9	4,8	13,6
17-08B B1B2 WEEK	33,5	-16,4	2,8	4,4	14,1
17-08C B1B2 WEEK	33,8	-16,6	2,8	4,5	14,2
Average after 2 weeks	33,7 ± 0,2	-16,5 ± 0,1	2,8 ± 0,1	4,5 ± 0,2	14,0 ± 0,3
After 3 weeks					
25-08B-B1B3W	37,0	-16,4	3,4	5,0	12,5
25-08A-B1B3W	37,1	-16,1	3,2	5,6	13,6
Average after 3 weeks	37,0 ± 0,1	-16,2 ± 0,2	3,3 ± 0,2	5,3 ± 0,5	13,1 ± 0,8
Buoy 2 Top					
After 1 week					
11.08A B2T1W	36,0	-16,7	3,1	3,9	13,6
11.08B B2T1W	35,6	-16,6	3,1	3,5	13,2
11.08C B2T1W	35,4	-16,5	3,0	4,2	13,6
Average after 1 week	35,7 ± 0,3	-16,6 ±0,1	3,1 ± 0,1	3,8 ± 0,3	13,5 ± 0,2
After 2 weeks					
17-08A B2T2W	33,2	-16,0	3,1	5,6	12,5
17-08B B2T2W	32,0	-17,0	2,9	4,4	12,8
Average after 2 weeks	32,6 ± 0,9	-16,5 ± 0,7	3,0 ± 0,1	4,9 ± 0,8	12,6 ± 0,2
After 3 weeks					
25-08B-B2T3W	37,1	-16,4	2,8	3,9	15,3
25-08A-B2T3W	36,5	-17,1	2,6	4,3	16,3
Average after 3 weeks	36,8 ± 0,4	-16,8 ± 0,5	2,7 ± 0,2	4,1 ± 0,3	15,8 ± 0,7
Buoy 2 Bottom					
After 1 week					

11.08A B2B1W	33,0	-16,3	2,8	4,9	13,9
11.08B B2B1W	33,5	-16,5	2,9	4,6	13,5
11.08C B2B1W	33,0	-15,8	3,0	5,4	12,9
Average after 1 week	33,2 ± 0,3	-16,5 ± 0,4	2,9 ± 0,1	4,9 ± 0,4	13,4 ± 0,5
After 2 weeks					
17-08A B2B2W	32,4	-15,6	2,6	5,9	14,7
17-08B B2B2W	32,8	-15,3	2,7	6,2	14,2
Average after 2 weeks	32,6 ± 0,3	-15,4 ± 0,2	2,6 ± 0,1	6,1 ± 0,2	14,5 ± 0,3
After 3 weeks					
25-08B-B2B3W	36,1	-16,0	2,7	6,3	15,4
25-08A-B2B3W	36,5	-16,3	3,3	5,7	13,1
Average after 3 weeks	36,3 ± 0,3	-16,2 ± 0,2	3,0 ± 0,4	5,9 ± 0,4	14,1 ± 1,6
Buoy 3 Top					
After 1 week					
11.08A B3T1W	34,6	-16,5	3,3	2,3	12,1
11.08B B3T1W	34,8	-16,8	3,2	1,3	12,5
11.08C B3T1W	34,7	-16,7	3,3	1,9	12,3
Average after 1 week	34,7 ± 0,1	-16,7 ± 0,2	3,3 ± 0,0	1,7 ± 0,5	12,3 ± 0,2
After 2 weeks					
17-08A B3T2W	34,0	-16,6	3,2	4,3	12,4
17-08B B3T2W	33,9	-16,4	3,1	3,7	12,7
Average after 2 weeks	34,0 ± 0,0	-16,5 ± 0,1	3,2 ± 0,1	4,0 ± 0,5	12,5 ± 0,2
After 3 weeks					
25-08B-B3T3W	37,2	-16,9	2,9	1,8	15,1
25-08A-B3T3W	36,6	-16,7	3,4	2,7	12,4
Average after 3 weeks	36,9 ± 0,4	-16,8 ± 0,1	3,1 ± 0,4	2,2 ± 0,6	13,6 ± 1,9
Buoy 3 Bottom					
After 1 week					
11.08A B3B1W	33,7	-17,0	2,9	4,5	13,4
11.08B B3B1W	34,0	-16,8	2,7	4,3	14,9
11.08C B3B1W	34,0	-16,7	3,0	3,8	13,1
Average after 1 week	33,9 ± 0,2	-16,9 ± 0,1	2,9 ± 0,2	4,2 ± 0,4	13,7 ± 1,0
After 2 weeks					
17-08A B3B2W	32,8	-16,3	3,1	3,7	12,2
17-08B B3B2W	32,7	-16,5	3,1	3,6	12,2
Average after 2 weeks	32,8 ± 0,1	-16,4 ± 0,1	3,1 ± 0,0	3,6 ± 0,0	12,2 ± 0,0
After 3 weeks					
25-08B-B3B3W	37,6	-15,9	3,0	5,9	14,6
25-08A-B3B3W	37,6	-16,2	3,0	5,6	14,7
Average after 3 weeks	37,6 ± 0,0	-16,1 ± 0,2	3,0 ± 0,0	5,8 ± 0,2	14,6 ± 0,0
Buoy 4 Top					
After 1 week					
11.08A B4T1W	35,4	-16,8	2,8	4,2	14,7
11.08B B4T1W	35,3	-16,7	2,6	4,0	15,8
11.08C B4T1W	35,2	-16,8	2,7	4,0	15,2
Average after 1 week	35,3 ± 0,1	-16,8 ± 0,0	2,7 ± 0,1	4,1 ± 0,1	15,2 ± 0,6
After 2 weeks					

17-08A B4T2W	34,3	-16,3	3,7	1,3	10,9
17-08B B4T2W	34,1	-16,7	3,2	2,5	12,3
Average after 2 weeks	34,2 ± 0,1	-16,5 ± 0,3	3,4 ± 0,3	1,7 ± 0,8	11,6 ± 0,9
After 3 weeks					
25-08B-B4T3W	38,7	-16,6	2,4	0,4	18,6
25-08A-B4T3W	38,2	-16,9	2,8	0,3	15,8
Average after 3 weeks	38,5 ± 0,4	-16,8 ± 0,2	2,6 ± 0,3	0,4 ± 0,0	17,1 ± 2,0
Buoy 4 Bottom					
After 1 week					
11.08A B4B1W	33,5	-16,2	2,5	5,7	15,5
11.08B B4B1W	33,7	-16,4	2,9	5,2	13,6
11.08c B4B1W	32,6	-16,4	2,7	4,6	14,3
Average after 1 week	33,3 ± 0,6	-16,3 ± 0,1	2,7 ± 0,2	5,1 ± 0,6	14,4 ± 1,0
After 2 weeks					
17-08A B4B2W	32,8	-17,5	2,7	5,7	14,1
17-08B B4B2W	31,3	-17,3	2,3	5,5	15,8
Average after 2 weeks	32,0 ± 1,0	-17,4 ± 0,1	2,5 ± 0,3	5,6 ± 0,1	14,9 ± 1,2
After 3 weeks					
25-08B-B4B3W	37,0	-16,9	2,6	6,0	16,6
25-08A-B4B3W	36,8	-16,5	3,2	5,5	13,4
Average after 3 weeks	36,9 ± 0,2	-16,7 ± 0,3	2,9 ± 0,4	5,7 ± 0,4	14,8 ± 2,3

Table D2.3 C, N, C/N, $\delta^{13}C$ and $\delta^{15}N$ of Staithes *Fucus* background levels and analysed with Stable Isotope Mass spectrometer.

Date (*Sample IDs*)	C	$\delta^{13}C$	N	$\delta^{15}N$	C/N
Staithes 2015					
15.07.2015					
STAITHES-18-WHOLE	31,7	-15,7	1,7	11,1	21,6
STAITHES-17-WHOLE	30,3	-16,2	1,5	9,3	22,9
STAITHES-16-WHOLE	31,7	-15,2	1,7	10,3	22,2
STAITHES-15-WHOLE	30,7	-15,1	1,7	9,9	21,5
STAITHES-14-WHOLE	32,2	-15,7	1,7	9,6	22,2
STAITHES-13-WHOLE	31,5	-16,8	1,6	9,6	22,8
STAITHES-12-WHOLE	30,0	-14,7	1,7	9,6	20,2
STAITHES-11-WHOLE	32,6	-14,6	1,5	9,1	25,4
STAITHES-10-WHOLE	32,0	-15,2	1,9	10,1	19,9
STAITHES-9-WHOLE	31,8	-14,2	1,5	9,9	25,1
Average 15.07.15	31,4 ± 0,8	-15.3 ± 0.8	1,6 ± 0.1	9.9 ± 0.6	22,3 ± 1,8
22.07.2015					
22-07-staithes-N-Fc	33,1	-16,4	1,8	9,5	21,3
22-07-staithes-N-Fb	34,3	-16,2	2,0	9,6	20,4
22-07-staithes-N-Fa	33,2	-16,3	1,9	9,7	20,7
Average 22.07.2015	33,5 ± 0.7	-16.3 ± 0.1	1,9 ± 0.1	9.6 ± 0.1	20,8 ± 0.5

28.07.2015					
28-07-STAITHES	32,8	-15,8	2,1	10,2	18,3
28-07-STAITHES	32,8	-15,8	2,1	10,6	18,2
28-07-STAITHES	31,5	-15,9	1,9	10,1	19,6
Average 28.07.2015	32,4 ± 0.8	-15.8 ± 0.1	2,0 ± 0.1	10.3 ± 0.3	18,7 ± 0.8
04.08.2015					
03.08A BACKST	39,7	-15,6	2,2	10,5	21,3
03.08B BACKST	40,0	-15,6	2,2	10,7	21,4
03.08C BACKST	46,3	-15,5	2,5	10,5	21,5
Average 04.08.2015	42.0 ± 3,0	-15.6 ± 0.0	2.3 ± 0.2	10.6 ± 0.2	21.4 ± 0.0
11.08.2015					
11.08A BACKST	34,8	-15,4	1,7	10,2	24,0
11.08B BACKST	34,4	-15,3	1,4	10,1	28,5
11.08C BACKST	35,8	-15,5	1,8	10,1	22,7
11.08D BACKST	35,6	-15,5	1,9	10,6	22,4
Average 11.08.2015	35.2 ± 0.6	-15.4 ± 0.0	1.7 ± 0.2	10.2 ± 0.2	24.4 ± 2,4
17.08.2015					
17-08C STAITH BACK	34,0	-16,6	1,9	10,0	21,4
17-08A STAITH BACK	32,7	-16,4	1,8	10,1	20,9
17-08A B1T1 WEEK	32,4	-15,2	3,0	4,1	12,5
Average 17.08.2015	33.3 ± 0.6	-16.5 ± 0.0	1.8 ± 0.0	10.1 ± 0.0	21.2 ± 0.2
25.08.2015					
25-08-BACK-ST-B	30,7	-16,8	1,8	9,8	20,4
25-08-BACK-ST-A	35,8	-16,8	2,1	10,4	20
Average 25.08.2015	33.1 ± 3,6	-16.8 ± 0.0	1,9 ± 0.2	10.1 ± 0.2	20,2 ± 0.3
Average Staithes ‘15	37.4	-16.0	3.7	10.1	14.7

Staithes 2014

1 Staihes					
1.1 ST	66,1	-19,6	5,4	5,6	14,4
1.2 ST	32,0	-18,4	2,5	7,1	15,2
Average 1 Staihes	49.1 ± 17,0	-19.0 ± 0.6	3.9 ± 1,4	6.3 ± 0.8	14.8 ± 0.4
2 Staithes					
2.1 ST	35,0	-20,0	2,2	8,4	18,3
2.2 ST	36,6	-17,8	2,7	9,2	15,8
Average 2 Staithes	35.8 ± 0.8	-18.9 ± 1,2	2.5 ± 0.2	8.8 ± 0.4	17.0 ± 1,2
3 Staithes					
3.1 ST	37,7	-18,2	2,6	9,2	17,1
3.2 ST	33,2	-20,2	2,5	8,3	15,3
Average 3 Staithes	35.4 ± 2,2	-19.2 ± 1,0	2.5 ± 0.0	8.8 ± 0.4	16.2 ± 1,0
4 Staithes					

4.1 ST	36,0	-19,2	2,1	8,5	19,7
4.2 ST	37,7	-19,6	2,7	7,5	16,6
Average 4 Staithes	36.8 ± 0.8	-19.4 ± 0.2	2.4 ± 0.2	8.0 ± 0.6	18.1 ± 1,6
5 Staithes					
5.1 ST	32,3	-18,0	2,0	8,0	19,1
5.2 ST	30,9	-19,7	2,3	7,9	15,8
Average 5 Staithes	31.6 ± 0.8	-18.8 ± 0.4	2.1 ± 0.2	8.0 ± 0.0	17.4 ± 1,6
Average Staithes '14	37.7	-19.1	2.7	8.0	16.7

Table D2.4 $\delta^{15}N$ of *Fucus* grown in different concentrations of nitrate and analysed with Stable Isotope Mass spectrometer.

Sample (*Sample IDs*)	C	$\delta^{13}C$	N	$\delta^{15}N$	C/N
3 days					
0 µM					
27-07-CONTROL-3-0MN	32,6	-17,7	1,7	8,6	22,7
27-07-CONTROL-2-0MN	32,9	-18,7	1,6	8,7	24,2
27-07-CONTROL-1-0MN	33,3	-16,5	1,7	8,7	22,6
Average 0 µM	33,0 ± 0,3	-17,7 ± 1,1	1,7 ± 0,1	8,7 ± 0,0	23,1 ± 0,9
10 µM					
27-07-3-10MN	33,2	-16,2	1,7	8,7	22,8
27-07-2-10MN	32,7	-18,1	1,6	8,5	23,8
27-07-1-10MN	32,2	-17,5	1,6	8,7	23,5
Average 10 µM	32,7 ± 0,5	-17,5 ± 1,0	1,6 ± 0,1	8,6 ± 0,1	23,4 ± 0,5
50 µM					
27-07-3-50MN	32,2	-16,1	1,7	8,5	21,8
27-07-2-50MN	31,8	-16,7	1,8	8,2	21,1
27-07-1-50MN	32,7	-16,0	1,7	8,9	21,9
Average 50 µM	32,2 ± 0,5	-16,1 ± 1,0	1,7 ± 0,1	8,5 ± 0,1	21,6 ± 0,5
100 µM					
27-07-3-100MN	32,6	-15,0	1,8	8,5	20,7
27-07-2-100MN	33,3	-17,5	1,8	8,4	21,7
27-07-1-100MN	33,2	-18,5	1,9	8,5	20,4
Average 100 µM	33,0 ± 0,4	-17,5 ± 1,8	1,8 ± 0,1	8,4 ± 0,1	20,9 ± 0,7
500 µM					
27-07-3-500MN	33,6	-17,1	1,9	8,0	20,6
27-07-2-500MN	33,9	-16,9	2,3	7,6	17,6
27-07-1-500MN	32,9	-17,1	2,0	7,9	19,1
Average 500 µM	33,5 ± 0,5	-17,1 ± 0,1	2,0 ± 0,2	7,8 ± 0,2	19,0 ± 1,5
1 week					
0 µM					
2-1 WEEK 0 MMN	33,5	-15,0	1,3	8,4	27,0
3-1 WEEK 0 MMN	33,6	-14,9	1,5	8,8	29,1
1-1 WEEK 0 MMN	33,6	-15,1	1,5	8,9	26,3
Average 0 µM	33,6 ± 0,0	-15,0 ± 0,1	1,4 ± 0,1	8,7 ± 0,3	27,4 ± 1,5
10 µM					

1-1 WEEK 10 MMN	33,6	-15,3	1,4	8,6	27,9
2-1 WEEK 10 MMN	34,0	-14,2	1,6	8,5	24,3
3-1 WEEK 10 MMN	31,7	-16,0	1,5	8,5	25,4
Average 10 µM	33,1 ± 1,2	-15,3 ± 0,9	1,5 ± 0,1	8,6 ± 0,1	25,8 ± 1,8
50 µM					
1-1 WEEK 50 MMN	31,4	-14,9	1,6	8,1	23,6
2-1 WEEK 50 MMN	33,0	-13,5	1,7	8,2	22,2
3-1 WEEK 50 MMN	33,3	-14,3	1,8	8,0	21,5
Average 50 µM	32,6 ± 1,0	-14,3 ± 0,7	1,7 ± 0,1	8,1 ± 0,1	22,4 ± 1,1
100 µM					
1-1 WEEK 100 MMN	33,4	-15,0	1,9	8,1	20,9
2-1 WEEK 100 MMN	32,8	-14,8	1,9	7,5	20,5
3-1 WEEK 100 MMN	33,2	-14,9	1,9	7,6	20,4
Average 100 µM	33,1 ± 0,3	-14,9 ± 0,1	1,9 ± 0,0	7,7 ± 0,3	20,6 ± 0,3
500 µM					
1-1 WEEK 500 MMN	32,8	-15,4	2,2	6,3	17,5
2-1 WEEK 500 MMN	33,0	-14,7	2,2	6,7	17,6
3-1 WEEK 500 MMN	33,7	-15,2	2,4	6,5	16,5
Average 500 µM	33,2 ± 0,5	-15,2 ± 0,4	2,2 ± 0,1	6,5 ± 0,2	17,2 ± 0,6

Table D2.5 $\delta^{15}N$ of *Fucus* grown in different concentrations of amonia and analysed with Stable Isotope Mass spectrometer.

Sample (*Sample IDs*)	C	$\delta^{13}C$	N	$\delta^{15}N$	C/N
3 days					
0 µM					
3-0C3D	35,4	-14,9	1,8	10,5	22,4
2-0C3D	35,8	-15,9	1,8	10,5	23,6
1-0C3D	36,0	-15,4	1,9	10,5	22,0
Average 0 µM	35,7 ± 0,3	-15,4 ± 0,5	1,8 ± 0,1	10,5 ± 0,0	22,7 ± 0,8
10 µM					
3-10C3D	42,5	-15,1	2,0	10,8	25,2
2-10C3D	34,3	-15,5	2,6	10,3	15,6
1-10C3D	35,9	-15,1	2,2	10,6	18,8
Average 10 µM	37,2 ± 4,4	-15,3 ± 0,3	2,2 ± 0,3	10,6 ± 0,3	19,1 ± 4,9
50 µM					
3-50C3D	37,4	-16,5	1,9	10,6	22,4
2-50C3D	35,5	-15,0	2,2	11,0	18,8
1-50C3D	36,1	-16,0	1,7	9,8	24,1
Average 50 µM	36,3 ± 0,4	-16,0 ± 0,8	1,9 ± 0,3	10,5 ± 0,8	21,5 ± 3,8
110 µM					
3-100C3D	36,0	-16,2	2,1	10,2	20,3
2-100C3D	33,0	-15,9	2,0	10,2	19,1
1-100C3D	37,1	-15,5	2,0	10,1	21,9
Average 100 µM	35,3 ± 2,1	-15,8 ± 0,3	2,0 ± 0,0	10,2 ± 0,0	20,4 ± 1,4
500 µM					
3-500C3D	35,3	-16,2	2,1	9,3	19,5
2-500C3D	37,0	-15,2	2,1	9,2	20,8

1-500C3D	36,5	-16,3	2,4	9,3	17,6
Average 500 µM	36,2 ± 0,9	-15,6 ± 0,6	2,2 ± 0,2	9,3 ± 0,1	19,2 ± 1,6
1 week					
0 µM					
1-0B13D	36,3	-18,7	1,8	10,3	24,2
2-0B13D	38,5	-14,5	1,8	10,5	25,5
3-0B13D	39,4	-13,4	1,8	11,4	25,4
Average 0 µM	38,0 ± 16	-15,9 ± 2,8	1,8 ± 0,0	10,7 ± 0,6	25,0 ± 0,7
10 µM					
1-10B13D	40,1	-14,2	2,1	10,5	22,5
2-10B13D	39,6	-13,2	1,8	10,0	25,6
3-10B13D	40,2	-15,4	2,0	10,9	23,8
Average 10 µM	40,0 ± 0,3	-14,3 ± 1,1	1,9 ± 0,1	10,5 ± 0,4	23,9 ± 1,6
50 µM					
1-50B13D	37,9	-15,0	1,6	9,6	27,3
2-50B13D	36,8	-13,6	2,2	10,9	19,2
3-50B13D	36,1	-15,7	1,9	9,9	22,1
Average 50 µM	36,9 ± 0,9	-14,9 ± 1,1	1,9 ± 0,3	10,1 ± 0,7	22,4 ± 4,1
110 µM					
1-100B13D	36,8	-14,0	2,0	9,7	21,9
2-100B13D	37,3	-14,7	2,0	9,3	21,4
3-100B13D	35,6	-13,6	2,1	10,1	19,4
Average 100 µM	36,5 ± 0,9	-14,1 ± 0,5	2,0 ± 0,1	9,7 ± 0,4	20,8 ± 1,3
500 µM					
1-500B13D	36,3	-14,8	3,0	7,3	14,2
2-500B13D	37,5	-13,3	3,4	7,0	13,0
3-500B13D	36,5	-14,5	2,9	6,1	14,9
Average 500 µM	36,7 ± 0,6	-14,4 ± 0,8	3,1 ± 0,3	6,8 ± 0,6	14,0 ± 0,9

Table D2.6 C, N, C/N, $\bar{\delta}^{13}C$ and $\bar{\delta}^{15}N$ of *Fucus* grown naturally in river Tees buoys used for the experiments and nearby and analysed with Stable Isotope Mass spectrometer.

Sample (*Sample IDs*)	C	$\bar{\delta}^{13}C$	N	$\bar{\delta}^{15}N$	C/N
River Tees 27.05.2015					
Site 1					
27-05-S1-FERTILE-OLD	30,6	-19,5	2,6	3,0	13,9
27-05-S1-BLADES	35,3	-19,9	3,3	2,5	12,5
27-05-S1-NON-FERTILE	32,9	-16,8	3,0	4,3	12,7
27-05-S1-FERTILE-YOUNG	32,1	-18,3	2,7	4,8	14,1
Average Site 1	32,6 ± 2,0	-18.3 ± 1,4	2,9 ± 0.3	3.4 ± 1,1	13,3 ± 0.8
Site 2					
27-05-S2-FERTILE-OLD	27,1	-17,4	2,2	4,2	14,5
27-05-S2-BLADES	35,1	-19,7	3,5	3,8	11,5
27-05-S2-FERTILE-YOUNG	29,8	-16,8	2,3	4,1	15,3
27-05-S2-NONFERTILE	35,6	-16,2	3,2	4,5	12,8
Average Site2	31,5 ± 4,1	-17.4 ± 1,5	2,7 ± 0,6	4,1 ± 0.3	13,4 ± 1,7

Site 4					
27-05-S4-BLADES	35,5	-20,7	3,3	0,6	12,4
27-05-S4-FERTILE-OLD	28,0	-17,6	2,3	2,3	14,3
Average Site4	31,3 ± 5,3	-18.8 ± 2,2	2,7 ± 0.7	1.0 ± 1,2	13,3 ± 1,3
Site 5					
27-05-S5-FERTILE-YOUNG	31,0	-19,0	2,9	-0,6	12,4
27-05-S5-NONFERTILE	34,4	-19,6	3,9	0,4	10,2
27-05-S5-FERTILE-OLD	32,4	-18,9	3,0	-0,5	12,4
27-05-S5-BLADES	36,8	-21,2	3,5	-2,8	12,4
Average Site5	33,5 ± 2,5	-19.7 ± 1,1	3,3 ± 0,5	-1,1 ± 1,4	11,8 ± 1,1
Site 7					
27-05-S7-NONFERTILE	34,9	-17,4	3,4	4,0	12,1
27-05-S7-BLADES	23,2	-16,8	1,8	1,8	15,2
27-05-S7-FERTILE-OLD	29,1	-16,9	2,3	3,7	14,7
27-05-S7-FERTILE-YOUNG	32,3	-16,8	2,5	3,8	15,1
Average Site7	29,2 ± 0,3	-17.4 ± 0.3	2,4 ± 0,7	3.0 ± 1,0	14,1 ± 1,5
Site 8					
27-05-S8-NONFERTILE	34	-17,2	3,6	2,9	11,1
27-05-S8-FERTILE-YOUNG	34,4	-18,9	3,1	3,1	12,8
Average Site8	34,2 ± 0,3	-16.9 ± 1.2	3,3 ± 0,4	3,0 ± 0,1	11,9 ± 1,2
Site 9					
27-05-S9-NONFERTILE	35,6	-16,3	3,4	2,3	12,1
27-05-S9-FERTILE-OLD	30,4	-19	3,5	1,3	10,1
27-05-S9-FERTILE-YOUNG	28	-17	2,8	1,7	11,7
Average Site9	31,0 ± 3,9	-16.4 ± 1,4	3,2 ± 0,4	1.7 ± 0.5	11,2 ± 1,1
Site 10					
27-05-S10-FERTILE-OLD	30,2	-15,9	2,6	2,4	13,3
27-05-S10-BLADES	30,2	-19,7	2,9	-0,8	12,2
27-05-S10-NONFERTILE	34,0	-19,9	3,4	0,6	11,6
27-05-S10-FERTILE-YOUNG	35,4	-21,6	3,4	-2,3	12,1
Average Site10	32,3 ± 2,7	-20.5 ± 2,4	3,0 ± 0.4	-1.5 ± 2,0	12,3 ± 0,7
Site 13					
27-05-S13-BLADES	33,1	-20,4	3,1	-1,6	12,4
27-05-S13-FERTILE	33,6	-19,5	3,1	1,5	12,8
27-05-S13-FERTILE-OLD	31,8	-16,5	2,5	3,8	14,6
27-05-S13-NONFERTILE	34,8	-16,7	3,0	3,4	13,6
Average Site13	33,3 ± 1,2	-17.9 ± 2,0	2,9 ± 0,3	2.5 ± 2,5	13,3 ± 1,0
Site 14					
27-05-S14-NONFERTILE	35,3	-17,4	3,5	3,9	11,9
27-05-S14-FERTILE	26,7	-16,7	2,1	2,4	14,8
27-05-S14-BLADES	27,1	-17,3	2,2	3,5	14,5
Average Site14	29,2 ± 4,9	-17,0 ± 0,4	2,5 ± 0,8	3.1 ± 0.8	13,6 ± 1,6

River Tees 04.06.2015

Site2					
04-06-S2-FERTILE	29,6	-19,4	3,4	-6,1	10,1
04-06-S2-BLADES	35,2	-20,7	3,7	-4,5	11,2
04-06-S2-NONFERTILE	32,9	-20,2	3,7	-8,4	10,4

Average Site2	32,4 ± 2,8	-20.1 ± 0,7	3,6 ± 0.2	-6.4 ± 2,0	10,5 ± 0.6
Site 3					
04-06-S3-NONFERTILE	33,6	-18,8	3,5	-7,5	11,1
04-06-S3-BLADES	36,3	-20,5	3,3	-7,5	12,8
04-06-S3-FERTILE	31,4	-18,4	2,9	-4,8	12,5
Average Site2	32,4 ± 2,8	-19.2 ± 0,7	3,6 ± 0.2	-6.6 ± 2,0	10,5 ± 0,6
Site 5					
04-06-S5-FERTILE	29,3	-17,4	2,8	-2,6	12
04-06-S5-NONFERTILE	32,9	-17,3	3,5	-2,7	11
04-06-S5-BLADES	32,3	-18,7	3,4	-3	11
Average Site 5	31,4 ± 1,9	-17.8 ± 0,8	3,2 ± 0.4	-2.8 ± 0.2	11,3 ± 0.6
Site 6					
04-06-S6-BLADES	34,4	-21	2,9	-6,4	13,7
04-06-S6-NONFERTILE	34	-19,4	3,5	-4,4	11,3
04-06-S6-FERTILE	32,1	-19,7	3,4	-5,3	11,1
Average Site 6	32,2 ± 2,1	-20.0 ± 1,3	3,2 ± 0.2	-5.4 ± 1,1	11,6 ± 0,3
Site 8					
04-06-S8-BLADES	34,3	-19,3	3,4	-4,3	11,8
04-06-S8-FERTILE	30,2	-16,8	3,0	-2,1	11,8
04-06-S8-NONFERTILE	32,3	-18,4	3,3	-2,8	11,3
Average Site 8	39.1 ± 2,0	-18.2 ± 1,0	9.8 ± 0.6	-3.1 ± 1,0	4.6 ± 0.2
Site 9					
04-06-S9-FERTILE	31,3	-19,6	2,8	-5,9	12,9
04-06-S9-NONFERTILE	32,1	-19,3	3,1	-3,9	11,9
04-06-S9-BLADES	34,7	-20,5	2,9	-5,8	14
Average Site 9	32.6 ± 1,8	-19.8 ± 0.6	2,9 ± 0,2	-5.2 ± 1,1	12,9 ± 1,1
Site 11					
04-06-S11-FERTILE	24,4	-16,6	2,0	-2,8	14,1
04-06-S11-BLADES	15,6	-17,9	1,2	-3,6	14,7
04-06-S11-NONFERTILE	29,5	-17,9	2,7	-2,4	12,9
Average Site 11	21,6 ± 7,0	-17.5 ± 0.8	1,8 ± 0,8	-2.9 ± 0.6	13,9 ± 0.9
Site 12					
04-06-S12-NONFERTILE	35,3	-21,1	3,5	-5,5	11,9
04-06-S12-BLADES	34,3	-22,8	3,3	-8,1	12,1
04-06-S12-FERTILE	27,5	-20,7	2,6	-5,9	12,6
Average Site 12	32,0 ± 4,2	-21.5 ± 1,1	3,1 ± 0,5	-6.5 ± 1,4	12,2 ± 0.4
Site 14					
04-06-S14-FERTILE	29,6	-17,8	2,7	-3,3	12,5
04-06-S14-BLADES	29,8	-19,7	3,0	-4,6	11,5
04-06-S14-NONFERTILE	34,6	-17,2	3,3	-1,9	12,2
Average Site 14	31,2 ± 2,8	-18.2 ± 1,3	3,0 ± 0,3	-3.3 ± 1,4	12,1 ± 0.5
Site 15					
04-06-S15-FERTILE-OLD	15,3	-17,4	1,4	3,1	12,4
04-06-S15-NONFERTILE	31,4	-17,0	3,2	3,2	11,4
04-06-S15-BLADES	18,3	-20,3	1,9	-1,1	11,2
Average Site 15	19,8 ± 8,6	-18.2 ± 1,8	1,9 ± 0,9	1.7 ± 2,5	11,6 ± 0,6

River Tees 01.07.2015

Site2					
01-07-S2-NONFERTILE	30,6	-19,7	3,2	-6,3	11,2
01-07-S2-BLADES	16,3	-17,6	1,5	3,8	12,4
01-07-S2-FERTILE	32,1	-19,9	3,3	-5,8	11,5
Average Site2	24,0 ± 8,7	-19,0 ± 1,3	2,3 ± 1,0	-3,1 ± 5,7	11,7 ± 0,6
Site 3					
01-07-S3-BLADES	28,7	-17,9	3,5	-8,5	9,6
01-07-S3-NONFERTILE	32,4	-18,9	3,2	-9,1	11,8
01-07-S3-FERTILE	30,9	-21,3	3,3	-6,5	11,1
Average Site 3	30,6 ± 1,9	-19.1 ± 1,7	3,3 ± 0,2	-7,9 ± 1,4	10,8 ± 1,1
Site 5					
01-07-S5-FERTILE	40,5	-17,8	2,8	-4,4	17,1
01-07-S5-BLADES	35,3	-19,7	2,5	-5,0	16,6
01-07-S5-NON-FERTILE	35,1	-16,3	2,9	-5,0	14,3
Average Site 5	36,8 ± 3,1	-17.6 ± 1,7	2,7 ± 0,2	-4,8 ± 0,3	15,9 ± 1,5
Site 6					
01-07-S6-NONFERTILE	32,3	-20,6	3,3	-5,4	11,5
01-07-S6-BLADES	28,0	-20,1	2,5	-6,2	12,9
01-07-S6-FERTILE	26,9	-17,5	1,9	-4,9	16,9
Average Site 6	28,9 ± 2,9	-19,0 ± 1,7	2,4 ± 0,7	-5,6 ± 0,7	13,4 ± 2,8
Site 8					
01-07-S8-BLADES	30,1	-18,5	3,0	-8,1	11,6
01-07-S8-NONFERTILE	33,1	-18,2	3,5	-7,8	11,1
01-07-S8-FERTILE	34,6	-21,7	2,8	-6,7	14,2
Average Site 8	32,5 ± 2,3	-18.9 ± 1,9	3,1 ± 0,4	-7,6 ± 0,7	12,2 ± 1,7
Site 9					
01-07-S9-BLADES	22,7	-17,6	1,9	-2,7	13,9
01-07-S9-NONFERTILE	32,9	-17,3	3,3	-2,6	11,6
01-07-S9-FERTILE	34,6	-20,1	3,1	-7,4	13,2
Average Site 9	29,0 ± 6,4	-18.0 ± 1,5	2,6 ± 0,8	-4.6 ± 2,7	12,8 ± 1,2
Site 11					
01-07-S11-BLADES	25,7	-16,4	2,2	-3,8	13,6
01-07-S11-FERTILE	35,5	-19,0	2,8	-3,9	14,8
01-07-S11-NONFERTILE	32,5	-16,8	3,0	-5,2	12,7
Average Site 11	30,7 ± 5,0	-17,5 ± 1,4	2,6 ± 0,4	-4.8 ± 0,8	13,6 ± 1,1
Site12					
01-07-S12-BLADES	32,5	-21,6	3,1	-5,3	12,2
01-07-S12-NONFERTILE	32,8	-19,8	3,3	-4,2	11,5
01-07-S12-FERTILE	39,6	-21,1	3,4	-4,7	13,4
Average Site 12	34,7 ± 4,0	-20.1 ± 0,9	3,3 ± 0,2	-4,9 ± 0,6	12,3 ± 1,0
Site13					
01-07-S13-BLADES	34,7	-18,7	2,9	-1,7	13,9
01-07-S13-FERTILE	28	-17,1	2,4	-1,3	13,4
01-07-S13-NONFERTILE	33,4	-17,6	3,1	-1,1	12,4
Average Site 13	31,8 ± 3,6	-17.8 ± 0,8	2,8 ± 0,4	-1,5 ± 0,3	13,2 ± 0,8
Site14					
01-07-S15-NONFERTILE	31,8	-20,0	1,5	10,8	24,6
01-07-S15-BLADES	34,1	-20,3	1,4	8,6	27,5

01-07-S15-FERTILE	30,5	-17,2	2,3	-3,2	15,3
Average Site 14	32,1 ± 1,8	-18.7 ± 1,7	1,7 ± 0,5	2,5 ± 7,5	21,1 ± 6,4
Average river Tees 2015	38.2	-19.0	9.2	-2.9	5.0
River Tees 19.05.2014					
Average (n = 3)	C	$\delta^{13}C$	N	$\delta^{15}N$	C/N
1 Tees	35.6 ± 0.3	-18.6 ± 0.1	3.2 ± 0.0	-0.7 ± 0.1	12.9 ± 0.1
2 Tees	36.2 ± 0.3	-17.6 ± 0.1	4.7 ± 0.1	-0.8 ± 0.0	9.0 ± 0.2
3 Tees	36.4 ± 0.8	-17.3 ± 0.0	2.7 ± 0.1	-0.7 ± 0.2	15.7 ± 0.2
4 Tees	30.2 ± 0.0	-18.0 ± 0.0	3.8 ± 0.0	0.1 ± 0.0	9.4 ± 0.0
5 Tees	36.2 ± 0.7	-18.0 ± 0.1	3.5 ± 0.0	-1.9 ± 0.4	12.1 ± 0.2
6 Tees	34.8 ± 0.1	-14.9 ± 0.0	5.4 ± 0.0	3.7 ± 0.0	7.5 ± 0.0
7 Tees	27.8 ± 0.5	-14.9 ± 0.0	2.6 ± 0.0	-13.9 ± 0.3	12.7 ± 0.3
8 Tees	33.9 ± 0.1	-15.8 ± 0.0	2.8 ± 0.0	-12.9 ± 0.0	14.0 ± 0.1
9 Tees	33.7 ± 0.2	-16.3 ± 0.0	4.4 ± 0.1	-10.2 ± 0.1	9.0 ± 0.2
10 Tees	35.8 ± 0.2	-20.5 ± 0.1	3.2 ± 0.0	-7.9 ± 0.3	12.9 ± 0.0
11 Tees	33.9 ± 0.1	-21.8 ± 0.1	3.6 ± 0.1	-10.6 ± 0.0	10.9 ± 0.2
12 Tees	38.8 ± 0.0	-21.3 ± 0.0	5.6 ± 0.0	-12.1 ± 0.1	8.1 ± 0.0
13 Tees	35.0 ± 0.2	-19.8 ± 0.1	3.4 ± 0.0	-7.2 ± 0.1	12.0 ± 0.1
14 Tees	34.0 ± 0.1	-21.7 ± 0.0	3.1 ± 0.1	-5.2 ± 0.1	12.8 ± 0.2
15 Tees	34.1 ± 0.1	-23.0 ± 0.2	3.3 ± 0.0	-6.1 ± 0.3	12.0 ± 0.1
16 Tees	32.7 ± 0.5	-21.9 ± 0.1	3.1 ± 0.1	-5.9 ± 0.2	12.3 ± 0.3
17 Tees	36.2 ± 0.0	-20.3 ± 0.6	3.1 ± 0.0	-0.2 ± 0.0	13.6 ± 0.2
18 Tees	34.5 ± 0.3	-20.6 ± 0.1	3.4 ± 0.1	0.0 ± 0.1	11.9 ± 0.2
19 Tees	34.5 ± 0.3	-21.4 ± 0.0	3.7 ± 0.0	-4.1 ± 0.3	10.9 ± 0.2
20 Tees	35.0 ± 0.3	-20.5 ± 0.1	3.6 ± 0.0	-4.6 ± 0.1	11.3 ± 0.0
21 Tees	36.4 ± 0.3	-21.6 ± 0.2	3.7 ± 0.1	-8.0 ± 0.7	11.4 ± 0.2
22 Tees	33.3 ± 0.2	-23.1 ± 0.0	3.7 ± 0.0	-5.6 ± 0.0	10.5 ± 0.2
23 Tees	35.5 ± 0.1	-22.3 ± 0.1	4.7 ± 0.1	-8.3 ± 0.0	8.8 ± 0.1
24 Tees	35.4 ± 0.2	-19.8 ± 0.0	5.2 ± 0.0	-5.2 ± 0.0	8.0 ± 0.0
25 Tees	35.1 ± 0.1	-21.1 ± 0.1	3.3 ± 0.0	0.1 ± 0.0	12.3 ± 0.2
26 Tees	35.5 ± 0.1	-22.0 ± 0.0	4.0 ± 0.0	-9.1 ± 0.0	10.4 ± 0.0
27 Tees	65.5 ± 0.0	-21.5 ± 0.0	8.0 ± 1.0	-7.4 ± 0.1	9.6 ± 0.0
28 Tees	35.7 ± 0.2	-21.3 ± 0.1	3.6 ± 0.0	-4.5 ± 0.1	11.5 ± 0.0
29 Tees	33.0 ± 0.5	-21.6 ± 0.2	3.2 ± 0.1	-5.4 ± 0.1	12.2 ± 0.1
30 Tees	38.7 ± 0.1	-18.9 ± 0.0	5.7 ± 0.0	-5.0 ± 0.1	7.9 ± 0.0
31 Tees	34.7 ± 0.3	-21.6 ± 0.1	3.3 ± 0.0	-0.1 ± 0.3	12.2 ± 0.2
32 Tees	34.0 ± 0.1	-21.9 ± 0.0	4.0 ± 0.1	-6.3 ± 0.2	9.9 ± 0.1
33 Tees	36.8 ± 0.1	-22.4 ± 0.3	3.6 ± 0.0	2.8 ± 0.3	12.0 ± 0.0
34 Tees	35.2 ± 0.1	-22.9 ± 0.0	3.3 ± 0.1	-4.2 ± 0.2	12.3 ± 0.2
35 Tees	74.0 ± 0.0	-18.9 ± 0.0	10.4 ± 1.3	-3.9 ± 0.1	8.3 ± 0.0
36 Tees	31.9 ± 0.0	-21.6 ± 0.0	3.0 ± 0.1	0.2 ± 0.2	12.4 ± 0.2
37 Tees	34.8 ± 0.1	-17.6 ± 0.0	4.5 ± 0.0	0.4 ± 0.0	9.0 ± 0.0
38 Tees	29.1 ± 0.4	-19.8 ± 0.2	2.7 ± 0.1	6.9 ± 0.0	12.4 ± 0.2
39 Tees	33.5 ± 0.1	-20.4 ± 0.0	2.9 ± 0.0	7.3 ± 0.1	13.3 ± 0.2
40 Tees	34.1 ± 0.2	-21.6 ± 0.0	3.4 ± 0.0	1.4 ± 0.2	11.7 ± 0.0
41 Tees	35.0 ± 0.0	-18.5 ± 0.0	3.7 ± 0.0	4.8 ± 0.0	11.2 ± 0.1
42 Tees	33.6 ± 0.2	-16.6 ± 0.1	4.1 ± 0.0	-1.4 ± 0.0	9.5 ± 0.0

43 Tees	37.3 ± 0.1	-20.6 ± 0.0	4.5 ± 0.0	-3.3 ± 0.1	9.6 ± 0.0
44 Tees	35.2 ± 0.2	-15.4 ± 0.1	4.0 ± 0.0	4.5 ± 0.0	10.2 ± 0.1
45 Tees	33.1 ± 0.1	-20.7 ± 0.1	3.5 ± 0.0	-0.1 ± 0.3	11.0 ± 0.1
46 Tees	35.5 ± 0.1	-19.7 ± 0.1	2.9 ± 0.0	6.1 ± 0.0	14.3 ± 0.0
47 Tees	35.1 ± 0.0	-21.5 ± 0.1	3.3 ± 0.0	5.4 ± 0.0	12.5 ± 0.1
48 Tees	32.0 ± 1.3	-19.9 ± 0.0	2.7 ± 0.1	7.9 ± 0.0	13.9 ± 0.2
49 Tees	33.6 ± 0.0	-20.8 ± 0.0	3.3 ± 0.0	3.9 ± 0.0	11.9 ± 0.0

Table D2.7. pH and salinity measures of the cultures performed with diferent concentrations of nitrate and ammonia

Sample	Salinity (ppm)	pH
Nitrate		
0 µM	27	8.8
10 µM	29	8.7
50 µM	28	8.7
100 µM	26	8.8
500 µM	25	8.8
Amonia		
0 µM	25	8.8
10 µM	25	8.8
50 µM	25	8.8
100 µM	25	8.9
500 µM	25	8.8

D.4 Appendix A) dataset

Table D3.1. Re abundance for *F. vesiculosus* under different light treatments analysed with Thermo Scientific X-Series ICP-MS isotope dilution methodology.

Sample		Re (ppb)	2σ (±)
0 µmol/m^2s			
	1000x $HReO_4$	16040.0	0.0
	Seawater	175.3	0.0
	Artificial seawater	121.6	0.0
70 µmol/m^2s			
	1000x $HReO_4$	11640.0	0.1
	Seawater	100.8	0.0
	Artificial seawater	113.9	0.0
170 µmol/m^2s			
	1000x $HReO_4$	8783.0	0.0
	Seawater	122.7	0.0
	Artificial seawater	254.0	0.0

Table D3.2. Re abundance for *F. vesiculosus* under different phosphate and Re(VII) treatments analysed with Thermo Scientific X-Series ICP-MS isotope dilution methodology.

Sample		Re (ppb)	2σ (±)
After 3 hours			
1 µM PO_{4^-}			
	100x Re	463.3	2.1
	1000x Re	2654.3	1.2
	10000x Re	14460.5	0.0
100 µM PO_{4^-}			
	100x Re	464.8	0.0
	1000x Re	2315.4	0.0
	10000x Re	11726.6	0.0
1000 µM PO_{4^-}			
	100x Re	519.1	0.1
	1000x Re	317.3	0.0
	10000x Re	13441.0	0.0
1000 µM PO_{4^-}			
	100x Re	463.7	0.0
	1000x Re	337.8	0.0
	10000x Re	13021.9	0.0
After 72 hours			
1 µM PO_{4^-}			
	100x Re	567.6	0.0
	1000x Re	4583.5	0.0
	10000x Re	22531.5	0.0
100 µM PO_{4^-}			

	100x Re	234.1	0.1
	1000x Re	613.5	0.0
	10000x Re	23295.6	0.0
1000 µM PO_4-			
	100x Re	174.6	0.0
	1000x Re	559.8	0.0
	10000x Re	16231.4	0.0
1000 µM PO_4-			
	100x Re	156.2	0.0
	1000x Re	397.8	0.0
	10000x Re	10754.7	0.0

Table D3.3. Re abundance for *F. vesiculosus* under different Salinity, pH and Re treatments analysed with Thermo Scientific X-Series ICP-MS isotope dilution methodology.

Replicate number	Initial pH	Re (ppb)	2σ (±)	Replicates average	SD (±)
1000x $HReO_4$					
1	7.0	2171.3	0.0		
2	7.0	2216.4	0.0	2616.4	298.9
3	7.0	3461.5	0.0		
1	8.0	1657.3	0.0		
2	8.0	2274.8	0.0	2522.4	294.6
3	8.0	3335.2	0.0		
1	9.0	1978.3	0.2		
2	9.0	2075.3	0.0	2244.8	155.4
3	9.0	2680.8	0.0		
1000x $NaReO_4$					
1	7.0	239.9	0.0		
2	7.0	176.8	0.1	236.5	23.7
3	7.0	292.7	0.0		
1	8.0	235.3	0.0		
2	8.0	165.8	0.1	234.4	27.8
3	8.0	302.0	0.0		
1	9.0	180.1	0.0		
2	9.0	209.1	0.1	200.2	7.1
3	9.0	211.3	0.0		
Replicate number	Salinity	Re (ppb)	2σ (±)	Replicates average	SD (±)
1000x $NaReO_4$					
1	25%	253.1	0.0		
2	25%	267.2	0.0	275.6	11.3
3	25%	306.4	0.0		
1	50%	264.0	0.0		
2	50%	230.3	0.0	269.3	11.1
3	50%	313.5	0.1		
1	75%	235.5	0.0		
2	75%	232.0	0.1	256.6	16.1
3	75%	302.2	0.0		

Table D3.4. Re abundance for *F. vesiculosus* every 24 h under 1000x Re analysed with Thermo Scientific X-Series ICP-MS isotope dilution methodology.

Replicate number	Day	Re (ppb)	2σ (±)	Replicates average	SD (±)
1000x $NaReO_4$					
1	1	192.9	0.0		
2	1	181.3	0.0	165.4	15.5
3	1	122.0	0.0		
1	2	212.5	0.2		
2	2	226.4	0.0	194.4	18.0
3	2	144.2	0.7		
1	3	244.3	0.0		
2	3	183.6	0.0	191.9	19.9
3	3	147.7	0.5		
1	4	242.3	0.0	236.4	3.0
2	4	230.5	0.0		
1000x $HReO_4$					
1	1	1229.8	0.0		
2	1	1292.3	0.0	1104.5	111.4
3	1	791.5	0.0		
1	2	1469.4	0.0		
2	2	1574.8	0.0	1308.2	152.8
3	2	880.3	0.0		
1	3	1615.5	0.0	1506.8	54.4
2	3	1398.0	0.0		
1	4	1527.8	0.0	1669.8	71.0
2	4	1811.8	0.0		

Table D3.5. Re abundance for *F. vesiculosus* under different Re treatments and alginate beads analysed with Thermo Scientific X-Series ICP-MS isotope dilution methodology.

Sample	Re (ppb)	2σ (±)
Alginate beads with		
18 µM $NaReO_4$	52.1	0.1
18 µM $KReO_4$	41.3	0.1
18 µM NH_4ReO_4	57.4	0.1
18 µM $HReO_4$	7.1	0.0
2% Alginate	0.2	0.0
2% Alginate + 0.3M $CaCl_2$	2.6	0.0

Table D3.6. pH and salinity measures of the cultures performed with diferent light intensities, pH and salinity.

Light intensities	week 1		week 2		week 3	
	pH	Salinity (ppm)	pH	Salinity (ppm)	pH	Salinity (ppm)
0 µmol/m^2s						
1000x $HReO_4$	8.4	30	8.2	35	8.1	35

Seawater	7.9	30	8.0	24	8.0	36
Artificial seawater	8.1	21	7.9	25	8.1	29
70 µmol/m^2s						
1000x $HReO_4$	9.0	30	8.7	35	9.0	35
Seawater	8.6	34	8.8	32	8.8	35
Artificial seawater	9.1	21	8.9	25	8.8	26
170 µmol/m^2s						
1000x $HReO_4$	9.2	30	8.9	35	8.8	35
Seawater	9.1	30	9.0	34	9.0	34
Artificial seawater	9.1	21	8.9	25	8.7	28

Initial pH	pH	Salinity (ppm)
$HReO_4$		
7.0	8.5	33
8.0	8.6	35
9.0	8.7	35
$NaReO_4$		
7.0	8.5	35
8.0	8.6	35
9.0	8.7	35

Salinity	pH	Salinity (ppm)
25%	8.7	20
50%	8.7	26
75%	8.7	30

D.5 Appendix B) dataset

Table D4.1 C, N, C/N, $\delta^{13}C$ and $\delta^{15}N$ of macroalgae collections during 19.05.2014.

Sample number	C%	d13C	N%	d15N	C/N
1 Staihes	49.1 ± 8.5	-19.0 ± 0.3	3.9 ± 0.7	6.3 ± 0.4	14.8 ± 0.2
2 Staithes	35.8 ± 0.4	-18.9 ± 0.6	2.5 ± 0.1	8.8 ± 0.2	17.0 ± 0.6
3 Staithes	35.4 ± 1.1	-19.2 ± 0.5	2.5 ± 0.0	8.8 ± 0.2	16.2 ± 0.5
4 Staithes	36.8 ± 0.4	-19.4 ± 0.1	2.4 ± 0.1	8.0 ± 0.3	18.1 ± 0.8
5 Staithes	31.6 ± 0.4	-18.8 ± 0.4	2.1 ± 0.1	8.0 ± 0.0	17.4 ± 0.8
1 Tees	35.6 ± 0.3	-18.6 ± 0.1	3.2 ± 0.0	-0.7 ± 0.1	12.9 ± 0.1
2 Tees	36.2 ± 0.3	-17.6 ± 0.1	4.7 ± 0.1	-0.8 ± 0.0	9.0 ± 0.2
3 Tees	36.4 ± 0.8	-17.3 ± 0.0	2.7 ± 0.1	-0.7 ± 0.2	15.7 ± 0.2
4 Tees	30.2 ± 0.0	-18.0 ± 0.0	3.8 ± 0.0	0.1 ± 0.0	9.4 ± 0.0
5 Tees	36.2 ± 0.7	-18.0 ± 0.1	3.5 ± 0.0	-1.9 ± 0.4	12.1 ± 0.2
6 Tees	34.8 ± 0.1	-14.9 ± 0.0	5.4 ± 0.0	3.7 ± 0.0	7.5 ± 0.0
7 Tees	27.8 ± 0.5	-14.9 ± 0.0	2.6 ± 0.0	-13.9 ± 0.3	12.7 ± 0.3
8 Tees	33.9 ± 0.1	-15.8 ± 0.0	2.8 ± 0.0	-12.9 ± 0.0	14.0 ± 0.1
9 Tees	33.7 ± 0.2	-16.3 ± 0.0	4.4 ± 0.1	-10.2 ± 0.1	9.0 ± 0.2
10 Tees	35.8 ± 0.2	-20.5 ± 0.1	3.2 ± 0.0	-7.9 ± 0.3	12.9 ± 0.0
11 Tees	33.9 ± 0.1	-21.8 ± 0.1	3.6 ± 0.1	-10.6 ± 0.0	10.9 ± 0.2
12 Tees	38.8 ± 0.0	-21.3 ± 0.0	5.6 ± 0.0	-12.1 ± 0.1	8.1 ± 0.0
13 Tees	35.0 ± 0.2	-19.8 ± 0.1	3.4 ± 0.0	-7.2 ± 0.1	12.0 ± 0.1
14 Tees	34.0 ± 0.1	-21.7 ± 0.0	3.1 ± 0.1	-5.2 ± 0.1	12.8 ± 0.2
15 Tees	34.1 ± 0.1	-23.0 ± 0.2	3.3 ± 0.0	-6.1 ± 0.3	12.0 ± 0.1
16 Tees	32.7 ± 0.5	-21.9 ± 0.1	3.1 ± 0.1	-5.9 ± 0.2	12.3 ± 0.3
17 Tees	36.2 ± 0.0	-20.3 ± 0.6	3.1 ± 0.0	-0.2 ± 0.0	13.6 ± 0.2
18 Tees	34.5 ± 0.3	-20.6 ± 0.1	3.4 ± 0.1	0.0 ± 0.1	11.9 ± 0.2
19 Tees	34.5 ± 0.3	-21.4 ± 0.0	3.7 ± 0.0	-4.1 ± 0.3	10.9 ± 0.2
20 Tees	35.0 ± 0.3	-20.5 ± 0.1	3.6 ± 0.0	-4.6 ± 0.1	11.3 ± 0.0
21 Tees	36.4 ± 0.3	-21.6 ± 0.2	3.7 ± 0.1	-8.0 ± 0.7	11.4 ± 0.2
22 Tees	33.3 ± 0.2	-23.1 ± 0.0	3.7 ± 0.0	-5.6 ± 0.0	10.5 ± 0.2
23 Tees	35.5 ± 0.1	-22.3 ± 0.1	4.7 ± 0.1	-8.3 ± 0.0	8.8 ± 0.1
24 Tees	35.4 ± 0.2	-19.8 ± 0.0	5.2 ± 0.0	-5.2 ± 0.0	8.0 ± 0.0
25 Tees	35.1 ± 0.1	-21.1 ± 0.1	3.3 ± 0.0	0.1 ± 0.0	12.3 ± 0.2
26 Tees	35.5 ± 0.1	-22.0 ± 0.0	4.0 ± 0.0	-9.1 ± 0.0	10.4 ± 0.0
27 Tees	65.5 ± 0.0	-21.5 ± 0.0	8.0 ± 1.0	-7.4 ± 0.1	9.6 ± 0.0
28 Tees	35.7 ± 0.2	-21.3 ± 0.1	3.6 ± 0.0	-4.5 ± 0.1	11.5 ± 0.0
29 Tees	33.0 ± 0.5	-21.6 ± 0.2	3.2 ± 0.1	-5.4 ± 0.1	12.2 ± 0.1
30 Tees	38.7 ± 0.1	-18.9 ± 0.0	5.7 ± 0.0	-5.0 ± 0.1	7.9 ± 0.0
31 Tees	34.7 ± 0.3	-21.6 ± 0.1	3.3 ± 0.0	-0.1 ± 0.3	12.2 ± 0.2
32 Tees	34.0 ± 0.1	-21.9 ± 0.0	4.0 ± 0.1	-6.3 ± 0.2	9.9 ± 0.1
33 Tees	36.8 ± 0.1	-22.4 ± 0.3	3.6 ± 0.0	2.8 ± 0.3	12.0 ± 0.0
34 Tees	35.2 ± 0.1	-22.9 ± 0.0	3.3 ± 0.1	-4.2 ± 0.2	12.3 ± 0.2
35 Tees	74.0 ± 0.0	-18.9 ± 0.0	10.4 ± 1.3	-3.9 ± 0.1	8.3 ± 0.0
36 Tees	31.9 ± 0.0	-21.6 ± 0.0	3.0 ± 0.1	0.2 ± 0.2	12.4 ± 0.2

37 Tees	34.8 ± 0.1	-17.6 ± 0.0	4.5 ± 0.0	0.4 ± 0.0	9.0 ± 0.0
38 Tees	29.1 ± 0.4	-19.8 ± 0.2	2.7 ± 0.1	6.9 ± 0.0	12.4 ± 0.2
39 Tees	33.5 ± 0.1	-20.4 ± 0.0	2.9 ± 0.0	7.3 ± 0.1	13.3 ± 0.2
40 Tees	34.1 ± 0.2	-21.6 ± 0.0	3.4 ± 0.0	1.4 ± 0.2	11.7 ± 0.0
41 Tees	35.0 ± 0.0	-18.5 ± 0.0	3.7 ± 0.0	4.8 ± 0.0	11.2 ± 0.1
42 Tees	33.6 ± 0.2	-16.6 ± 0.1	4.1 ± 0.0	-1.4 ± 0.0	9.5 ± 0.0
43 Tees	37.3 ± 0.1	-20.6 ± 0.0	4.5 ± 0.0	-3.3 ± 0.1	9.6 ± 0.0
44 Tees	35.2 ± 0.2	-15.4 ± 0.1	4.0 ± 0.0	4.5 ± 0.0	10.2 ± 0.1
45 Tees	33.1 ± 0.1	-20.7 ± 0.1	3.5 ± 0.0	-0.1 ± 0.3	11.0 ± 0.1
46 Tees	35.5 ± 0.1	-19.7 ± 0.1	2.9 ± 0.0	6.1 ± 0.0	14.3 ± 0.0
47 Tees	35.1 ± 0.0	-21.5 ± 0.1	3.3 ± 0.0	5.4 ± 0.0	12.5 ± 0.1
48 Tees	32.0 ± 1.3	-19.9 ± 0.0	2.7 ± 0.1	7.9 ± 0.0	13.9 ± 0.2
49 Tees	33.6 ± 0.0	-20.8 ± 0.0	3.3 ± 0.0	3.9 ± 0.0	11.9 ± 0.0

Table D4.2 C, N, C/N, $\delta^{13}C$ and $\delta^{15}N$ of macroalgae collections during December 2013.

Sample number	C%	d13C	N%	d15N	
BSW-1	37.2 ± 0.1	-20.1 ± 0.0	2.8 ± 0.1	-8.4 ± 0.3	15.9 ± 0.7
BSW-2	35.7 ± 0.0	-21.9 ± 0.0	3.1 ± 0.0	-7.2 ± 0.0	13.6 ± 0.0
BSW-3	38.3 ± 0.1	-19.7 ± 0.1	3.0 ± 0.1	-6.6 ± 0.3	14.9 ± 0.2
BSW-4	39.2 ± 0.5	-21.0 ± 0.0	3.0 ± 0.1	-7.1 ± 0.2	15.4 ± 0.2
BSW-5	37.8 ± 0.4	-22.8 ± 0.0	2.9 ± 0.0	-8.0 ± 0.0	15.3 ± 0.2
BSW-6	35.7 ± 0.1	-20.8 ± 0.2	2.5 ± 0.0	-6.5 ± 0.1	16.5 ± 0.2
BSW-7	36.3 ± 0.1	-21.0 ± 0.1	2.8 ± 0.1	-4.9 ± 0.6	14.9 ± 0.4
BSW-8	35.7 ± 0.0	-21.3 ± 0.1	2.9 ± 0.0	-8.6 ± 0.1	14.5 ± 0.2
BSW-9	37.1 ± 0.0	-21.7 ± 0.1	3.5 ± 0.2	-9.2 ± 0.1	14.2 ± 0.0
BSW-10	36.6 ± 0.0	-21.8 ± 0.3	2.9 ± 0.1	-9.0 ± 0.2	14.7 ± 0.7
BSW-11	35.6 ± 0.5	-23.0 ± 0.2	2.9 ± 0.2	-6.4 ± 0.7	14.2 ± 0.6
BSW-12	37.0 ± 0.0	-21.4 ± 0.0	3.0 ± 0.0	-8.0 ± 0.0	14.5 ± 0.0
BSW-13	35.0 ± 0.1	-21.9 ± 0.0	3.1 ± 0.0	-10.3 ± 0.0	12.9 ± 0.0
BSW-14	36.2 ± 0.0	-21.7 ± 0.0	2.9 ± 0.0	-7.3 ± 0.0	14.4 ± 0.0
BSW-15	35.3 ± 0.0	-20.6 ± 0.3	3.0 ± 0.0	-4.6 ± 0.1	13.3 ± 0.0
BSW-16	34.4 ± 0.0	-22.9 ± 0.0	2.8 ± 0.0	-4.6 ± 0.0	14.3 ± 0.0
BSW-17	35.5 ± 0.3	-22.6 ± 0.2	2.8 ± 0.0	-3.3 ± 0.3	14.9 ± 0.0
BSW-18	34.6 ± 0.1	-21.8 ± 0.1	2.8 ± 0.0	-4.3 ± 0.1	14.3 ± 0.0
BSW-19	35.5 ± 0.1	-22.3 ± 0.0	2.9 ± 0.0	-3.5 ± 0.0	14.4 ± 0.2
BSW-20	36.4 ± 0.0	-21.4 ± 0.1	2.5 ± 0.1	-3.4 ± 0.0	17.0 ± 0.6

Table D4.3 C, N, C/N, $\delta^{13}C$ and $\delta^{15}N$ of macroalgae collections during June 2013.

Sample number	C%	$d^{13}C$	N%	$d^{15}N$	C/N
SITE 1 TP	37.8	-23.0	3.3	-9.0	13.3
SITE 10 TP	38.5	-20.9	2.9	-0.7	15.2
SITE 11 TP	37.6	-20.8	2.9	2.2	15.2
SITE 2 TP	38.9	-21.7	3.9	3.2	11.7
SITE 3 TP	38.1	-21.7	3.3	2.6	13.4
SITE 4 TP	38.1	-22.4	3.3	5.8	13.4

SITE 5 TP	37.4	-21.8	3.1	6.7	14.3
SITE 6 TP	36.2	-22.4	3.4	-1.4	12.6
SITE 7 TP	36.3	-22.3	3.2	-1.1	13.4
SITE 8 TP	36.9	-20.9	4.0	2.9	10.9
SITE 9 TP	38.3	-21.1	3.1	5.5	14.5
STAITHES OUTER	33.7	-20.0	3.4	6.4	11.5
STAITHES SOUTH	34.2	-19.4	3.1	6.9	13.1
STRAITHES HARBOUR	33.8	-19.3	3.0	9.1	13.2

Table D4.5 Coordinates of macroalgae collections during 19.05.2014.

19/05/2014 Site 1 River Tees 54°37'93.9"N 01°11'33.4"W	19/05/2014 Site 2 River Tees 54°37'82.6"N 01°11'65.5"W	19/05/2014 Site 3 River Tees 54°37'82.6"N 01°11'65.5"W	19/05/2014 Site 4 River Tees 54°37'82.6"N 01°11'65.5"W	19/05/2014 Site 5 River Tees 54°37'93.6"N 01°10'60.3"W
19/05/2014 Site 6 River Tees 54°37'93.6"N 01°10'60.3"W	19/05/2014 Site 7 River Tees 54°37'91.5"N 01°10'31.6"W	19/05/2014 Site 8 River Tees 54°37'82.3"N 01°10'13.7"W	19/05/2014 Site 9 River Tees 54°37'91.2"N 01°09'24.3"W	19/05/2014 Site 10 River Tees 54°37'32.1"N 01°09'14.8"W
19/05/2014 Site 11 River Tees 54°37'19.2"N 01°09'53.6"W	19/05/2014 Site 12 River Tees 54°35'73.6"N 01°10'86.4"W	19/05/2014 Site 13 River Tees 54°35'73.6"N 01°10'86.4"W	19/05/2014 Site 14 River Tees 54°35'27.6"N 01°11'24.8"W	19/05/2014 Site 15 River Tees 54°34'93.4"N 01°11'83.5"W
19/05/2014 Site 16 River Tees 54°34'94.4"N 01°12'28.2"W	19/05/2014 Site 17 River Tees 54°34'92.3"N 01°12'54.5"W	19/05/2014 Site 18 River Tees 54°34'94.6"N 01°12'86.1"W	19/05/2014 Site 19 River Tees 54°35'03.2"N 01°13'75.7"W	19/05/2014 Site 20 River Tees 54°35'40.1"N 01°14'45.2"W
19/05/2014 Site 21 River Tees 54°35'48.5"N 01°15'28.0"W	19/05/2014 Site 22 River Tees 54°35'48.0"N 01°15'30.1"W	19/05/2014 Site 23 River Tees 54°35'42.5"N 01°15'41.5"W	19/05/2014 Site 24 River Tees 54°35'28.6"N 01°15'40.8"W	19/05/2014 Site 25 River Tees 54°35'28.6"N 01°15'40.8"W
19/05/2014 Site 26 River Tees 54°35'33.6"N 01°15'49.6"W	19/05/2014 Site 27 River Tees 54°35'35.7"N 01°15'48.2"W	19/05/2014 Site 28 River Tees 54°35'30.1"N 01°15'515"W	19/05/2014 Site 29 River Tees 54°35'23.0"N 01°15'54.9"W	19/05/2014 Site 30 River Tees 54°35'21.1"N 01°15'43.7"W
19/05/2014 Site 31 River Tees 54°35'21.1"N 01°15'43.7"W	19/05/2014 Site 32 River Tees 54°34'82.0"N 01°15'606"W	19/05/2014 Site 33 River Tees 54°34'72.5"N 01°15'540"W	19/05/2014 Site 34 River Tees 54°34'29.7"N 01°15'64.7"W	19/05/2014 Site 35 River Tees 54°34'29.7"N 01°15'64.7"W
19/05/2014 Site 36 River Tees 54°34'04.6"N 01°16'32.6"W	19/05/2014 Site 37 River Tees 54°34'01.4"N 01°16'37.2"W	19/05/2014 Site 38 River Tees 54°34'01.4"N 01°16'37.2"W	19/05/2014 Site 39 River Tees 54°34'01.4"N 01°16'37.2"W	19/05/2014 Site 40 River Tees 54°34'01.4"N 01°16'37.2"W
19/05/2014 Site 41 River Tees 54°34'30.3"N 01°15'41.2"W	19/05/2014 Site 42 River Tees 54°34'22.8"N 01°15'452"W	19/05/2014 Site 43 River Tees 54°34'22.8"N 01°15'452"W	19/05/2014 Site 44 River Tees 54°34'30.3"N 01°15'41.2"W	19/05/2014 Site 45 River Tees 54°35'05.6"N 01°11'58.2"W
19/05/2014 Site 46 River Tees 54°35'05.6"N 01°15'58.2"W	19/05/2014 Site 47 River Tees 54°33'52.6"N 01°17'01.2"W	19/05/2014 Site 48 River Tees 54°33'53.1"N 01°16'56.6"W	19/05/2014 Site 49 River Tees 54°33'53.2"N 01°16'56.4"W	

Table D4.6 Coordinates of macroalgae collections during December 2013.

Sample	Latitude/Longitude (deg/min/sec)	Comment
1	54-37-13 / 01-09-52	N Bank; Jetty
2	54-37-31 / 01-09-12	S Bank; Wharf
3	54-35-75 / 01-10-83	N Bank; Mooring Point
4	54-35-44 / 01-10-98	Jetty
5	54-34-95 / 01-11-74	S Bank; Ruined Jetty
6	54-34-93 / 01-12-27	N Bank; Jetty
7	54-34-95 / 01-12-88	N Bank; Old wall (wood)
8	54-34-98 / 01-13-38	S Bank; Old Wharf
9	54-35-14 / 01-13-81	N bank; Wilton Grp
10	54-35-32 / 01-14-53	S Bank; AV Dawson
11	54-35-35 / 01-15-36	S Bank; Jetty
12	54-35-34 / 01-15-49	N Bank
13	54-34-83 / 01-15-60	N Bank; Simron Riverside
14	54-34-72 / 01-15-55	Riverside Park
15	54-34-39 / 01-15-78	Creek; E Bank
16	54-34-27 / 01-15-67	S Bank;
17	54-34-04 / 01-16-31	Jetty
18	54-34-02 / 01-16-29	Opposite Site 17
19	54-33-92 / 01-16-92	Creek; East Bank
20	54-33-93 / 01-16-97	Creek; Opposite to above

Figure D4.1 Coordinates of *Fucus* sp. and their $\delta^{15}N$ measurements of 19.05.2015.

Figure D4.2 Coordinates of *Fucus* sp. and their $\delta^{15}N$ measurements of December 2012.

Figure D4.3 Coordinates of *Fucus* sp. and their $\delta^{15}N$ measurements of June 2013.

Figure D4.4 Coordinates of *Fucus* sp. and their $\delta^{15}N$ measurements of December 2013.

E. Manuscripts

This section gathers all the papers published or sent for publishing.

ROYAL SOCIETY OPEN SCIENCE

rsos.royalsocietypublishing.org

Research

Cite this article: Racionero-Gómez B, Sproson AD, Selby D, Gröcke DR, Redden H, Greenwell HC. 2016 Rhenium uptake and distribution in phaeophyceae macroalgae, *Fucus vesiculosus*. *R. Soc. open sci.* **3**: 160161. http://dx.doi.org/10.1098/rsos.160161

Received: 5 March 2016
Accepted: 12 April 2016

Subject Category:
Biology (whole organism)

Subject Areas:
biochemistry/biogeochemistry/chemical biology

Keywords:
rhenium, macroalgae, uptake, distribution, phytomining, bioremediation

Authors for correspondence:
B. Racionero-Gómez
e-mail: blancaraci@gmail.com
H. C. Greenwell
e-mail: chris.greenwell@durham.ac.uk

THE ROYAL SOCIETY PUBLISHING

Rhenium uptake and distribution in phaeophyceae macroalgae, *Fucus vesiculosus*

B. Racionero-Gómez[1], A. D. Sproson[1], D. Selby[1], D. R. Gröcke[1], H. Redden[1,2] and H. C. Greenwell[1,2]

[1]Department of Earth Sciences, and [2]Department of Chemistry, Durham University, Durham DH1 3LE, UK

Owing to Rhenium (Re) having no known biological role, it is not fully understood how Re is concentrated in oil kerogens. A commonly held assumption is that Re is incorporated into decomposing biomass under reducing conditions. However, living macroalgae also concentrate Re to several orders of magnitude greater than that of seawater. This study uses *Fucus vesiculosus* to assess Re uptake and its subsequent localization in the biomass. It is demonstrated that the Re abundance varies within the macroalgae and that Re is not located in one specific structure. In *F. vesiculosus*, the uptake and tolerance of Re was evaluated via tip cultures grown in seawater of different Re(VII) compound concentrations (0–7450 ng g^{-1}). A positive correlation is shown between the concentration of Re-doped seawater and the abundance of Re accumulated in the tips. However, significant differences between Re(VII) compounds are observed. Although the specific cell structures where the Re is localized is not known, our findings suggest that Re is not held within chloroplasts or cytoplasmic proteins. In addition, metabolically inactivated *F. vesiculosus* does not accumulate Re, which indicates that Re uptake is via syn-life bioadsorption/bioaccumulation and that macroalgae may provide a source for Re phytomining and/or bioremediation.

1. Introduction

The behaviour of rhenium (Re) in seawater is defined by the low reactivity of the perrhenate ion (ReO_4^-; Re(VII)), which is the only significant Re species found in ocean waters [1]. The concentration of Re in the open ocean (0.0074–0.009 ng g^{-1}; [2,3]) is a factor of three higher than average river water (approx. 0.005 pg g^{-1}; [4]) and much lower compared with terrestrial environments (continental crust values of 0.2–2 ng g^{-1}; organic-rich sedimentary rocks values 0.2–100 ng g^{-1}; [5] and references therein) and sulfide minerals (low ng g^{-1} to hundreds of mg g^{-1}; [6]).

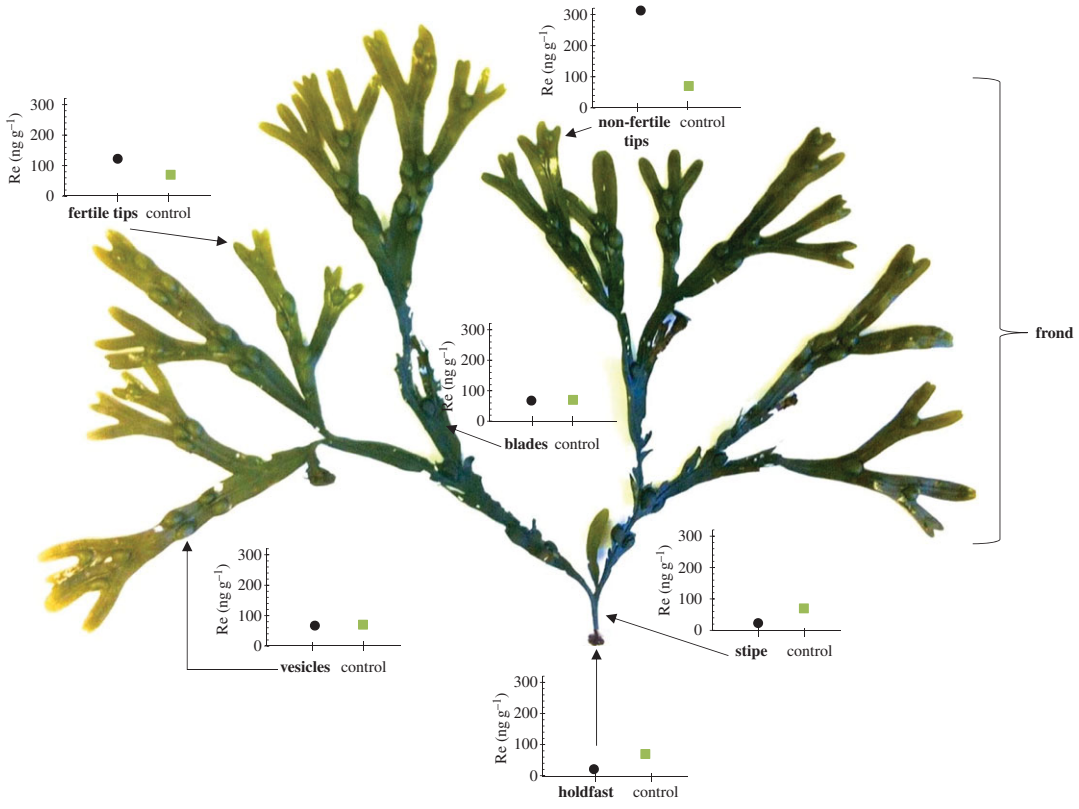

Figure 1. Average (two to five samples) concentration of rhenium (ng g^{-1}) in the different structures of *F. vesiculosus*. Round marker symbolizes Re abundance in each particular structure and square marker symbolizes Re abundance of a mixture of all the structures (control). All the samples had a reproducibility of less than 5% RSD; in some cases, graph symbol size is greater than uncertainties. The concentrations shown are in dry mass, and although the concentration of each structure might change when wet mass, the differences of Re concentration are greater than the differences in water loss.

Although the Re concentration in seawater is low in comparison with the terrestrial realm, and despite there being no known biological use of Re, marine macroalgae (i.e. seaweed), especially brown macroalgae, are known to concentrate Re up to several hundreds of ng g^{-1} [7–9], in addition to many metal cations and oxoanions through forming a variety of metal complexes with, for example, alginate, proteins, polysaccharides of the cell wall, fucans, etc. [10]. To date, positively charged metals associated with macroalgae have been extensively studied [11–14]; however, relatively little is known about the mechanisms by which macroalgae take up negatively charged metal oxoanions such as the perrhenate ion. Experiments have shown that Re is most likely stored within algal cells, rather than on the algal cell surface or within the intercellular matrix [9,15]. Specifically, it has been proposed that protonated amino groups could be involved, forming an ion pair with perrhenate [15,16]. Moreover, Kim *et al.* [17] showed that ReO_4^- interacted strongly with chitosan, a cationic polymer of glucosamine. Chitosan is only reported in nature in some fungi, crustacea and the termite queen's abdominal wall. However, Nishino *et al.* [18] isolated and characterized a novel polysaccharide containing an appreciable amount of glucosamine in *F. vesiculosus*, which suggests a further route to possible Re uptake.

Assuming that Re is being stored inside the macroalgae cells, a mechanism for Re uptake into the cells should be identifiable. Macroalgae could inadvertently take up ReO_4^- (ionic radius of 2.60 Å) by confusing it for phosphate (PO_4^{3-}; ionic radius of 2.38 Å). A similar mechanism is proposed for arsenate (AsO_4^{3-}) [19]. Sulfate (SO_4^{2-}), nitrate (NO_3^-) and chloride (Cl^-) also have similar ionic radii to ReO_4^- (i.e. 2.58, 1.96 and 1.81 Å, respectively). Thus, these ions could be also competing with ReO_4^-. For instance, Tagami & Uchida [20] showed that there is a positive correlation between K^+ and technetium (Tc) accumulated in three plant species (*Cucumis sativus L.*, *Raphanus sativus L.* and *Brassica chinensis L.*) and explained this as a result of TcO_4^- being taken up by mistaken identity for Cl^-, as a counter ion for K^+ uptake. As Re is a Tc analogue [9,17,21], ReO_4^- might be taken up in a similar manner. In addition, competitive incorporation between ReO_4^- and NO_3^- in sodalites has also been found [22]; however, as

sodalite is a mineral, ReO_4^- incorporation cannot be compared with ReO_4^- concentration in biologically active organisms.

Importantly, understanding the uptake of Re will help to elucidate the uptake of Tc, which is produced in nuclear power stations. Moreover, a better knowledge on the uptake mechanism could open the possibility to use macroalgae as bioconcentrators of Re and Tc, thus bioremediation of Tc-contaminated waters and phytomining of Re could be achieved using *F. vesiculosus*, as well as potentially providing an alternative hypothesis for the high concentration of Re within oil-forming kerogens.

This study uses a brown macroalgae (Phaeophyceae) to establish: (i) where Re is stored; (ii) the limit of Re uptake; and (iii) the uptake mechanism of Re (i.e. active concentration in which the transport requires energy to oppose the concentration gradient, or passive concentration, with transport requiring no energy and entirely correlated with the concentration). The Re abundance data for the different structures of *F. vesiculosus*: holdfast, stipe, fertile tips, non-fertile tips, vesicles and blades (figure 1), and isolated cytoplasmic proteins and chloroplasts are investigated. The uptake limit of Re in macroalgae is determined via cultures of *F. vesiculosus* under different ReO_4^- concentrations and using different ReO_4^- chemical compounds (i.e. $HReO_4$ (Re metal dissolved in HNO_3), $KReO_4$, $NaReO_4$ and NH_4ReO_4). Cultured versus dead macroalgae were used to provide insights into the uptake mechanism of ReO_4^- in macroalgae.

2. Material and methods

2.1. Macroalgae used in the study: *Fucus vesiculosus*

The available Re data for brown macroalgae (Phaeophyceae) indicate it has the highest Re accumulation of all macroalgae, with *Fucus vesiculosus* possessing the highest Re concentrations measured to date for a macroalgae [7]. *F. vesiculosus* is a common macroalgae found along sheltered shores of the North Sea, Baltic Sea, Atlantic Ocean and Pacific Ocean. *F. vesiculosus* is a tethered macroalgae with air bladders that are produced annually allowing the individual fronds to float. The growth rate ranges between 0.05 and 0.14 cm d^{-1} [23,24] and they have a lifespan in the order of 3–5 years [25]. The species is annually episodic, gonochoristic and highly fecund (i.e. prolific) [25]. Gametes are released into the seawater, and the eggs are fertilized externally to form a zygote that starts to develop as soon as it settles into a substrate [26]. The gametes are released from receptacles, which are found in the fertile tips of the macroalgae. However, *F. vesiculosus* also has non-fertile tips without these structures. Non-fertile tips are composed by a parenchymatous thallus (i.e. tissue-like structure) [25–27]. The structures of *F. vesiculosus* are shown in figure 1.

2.2. Macroalgae collection sites

Five specimens of *F. vesiculosus* were collected from Staithes, North Yorkshire, UK (54°33′ N 00°47′ W) in May 2014. These samples were used to determine the Re abundance of specific structures of the macroalgae. An additional six samples were collected each month at Boulmer Beach, Northumberland, UK (55°25′ N 1°34′ W) in May, June, October and November in 2014, and January to June in 2015, for fertile and non-fertile tip separation, all the culture experiments, chloroplast isolation and protein purification.

2.3. Rhenium abundance and distribution in macroalgae structures

Prior to analysis, all specimens were kept individually in plastic sample bags for transport, and stored in a freezer (−10°C) for 48 h. Each specimen was washed and soaked in deionized (Milli-Q™) water to remove any attached sediment and salt. To establish the abundance and distribution of Re in the macroalgae, the sample was divided into different structural components; fertile tips, non-fertile tips, vesicles, stipe, holdfast, blades (figure 1). In addition, all the algae components were mixed to assess an average Re abundance. Each structure was dried in an oven at 60°C for 12 h.

2.4. Rhenium uptake of macroalgae

To investigate the uptake of Re by macroalgae, non-reproductive apical thallus tips of nine *F. vesiculosus* specimens (length = greater than 1.5 cm; wet weight (WW) = 0.12–0.15 g), without visible microalgae (i.e. epiphytes), from Boulmer Beach were cultured in seawater (modified after Gustow *et al*. [28]) with

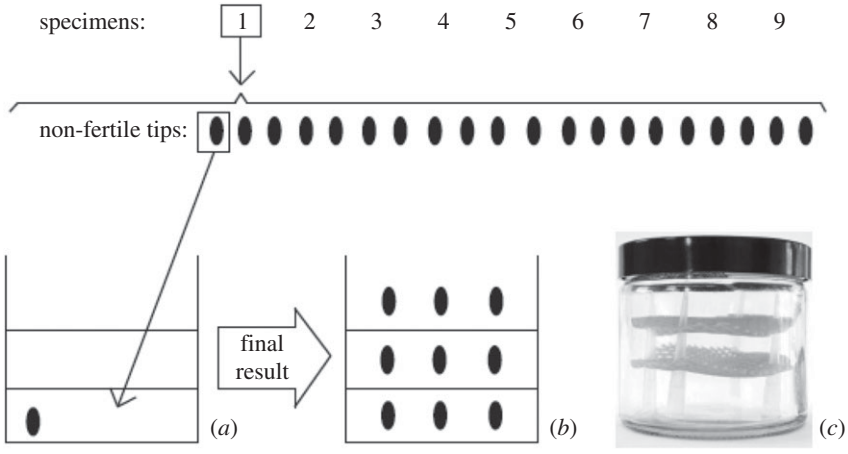

Figure 2. Culture representation of non-reproductive *F. vesiculosus* thallus tips. Twenty-one tips of each *F. vesiculosus* specimen were cut and a tip from each specimen was displaced into one of the 21 jars (*a*). Two meshes were put inside each jar ending up with three levels that store three non-fertile tips each (*b*). (*c*) Real culture jar picture.

a known concentration of Re. In brief, the culture experiments were performed using a 250 ml glass jar containing two mesh shelves. Three tips were placed in the bottom of the jar and three tips to each mesh, having in total nine tips, with each set of tips taken from a different specimen (figure 2). All jars were filled with sterile filtered (0.7 µm) seawater from Boulmer Beach. A huge diversity of macroalgae grow naturally at Boulmer Beach, thus water obtained at Boulmer water is expected to be nutrient replete as it permits the growth of a wide variety of species. Each set of three jar replicates were doped using a known volume of ReO_4^- from different Re compounds: an already prepared solution of Re metal with nitric acid ($HReO_4$; i.e. 83787 Sigma Aldrich) or commercially obtained Re(VII) salts ($KReO_4$, NH_4ReO_4 and $NaReO_4$).

[!p]

HNO_3 dissolves Re metal forming $HReO_4$ [29]. For the cultures using $HReO_4$, Boulmer seawater ReO_4^- concentration was analysed. The Re abundance in the seawater was determined by isotope dilution inductively coupled plasma mass spectrometry (ICP–MS) (details below). The seawater possesses a Re abundance of approximately $0.007\,ng\,g^{-1}$ ($6.95 \pm 0.19\,pg\,g^{-1}$) coinciding with the concentrations reported by Anbar *et al.* [2]. The seawater culture experiments were conducted in Re concentrations equal to that of seawater, and 10×, 50×, 100×, 500×, 1000×, 2667×, 10 000×, 133 333× and 266 667× that of the concentration of seawater (i.e. 0.007, 0.075, 0.373, 0.745, 3.725, 7.450, 20, 75, 1000 and $2000\,ng\,g^{-1}$, respectively). In addition, three jars were filled with artificial seawater that was not doped with Re, and one jar was doped with a concentration a million times that of the Re seawater concentration in order to reach an extreme concentration of $7450\,ng\,g^{-1}$.

For the cultures using Re(VII) (perrhenate) salts, the same approach was used, where the doped Re concentrations of seawater in the cultures were 10×, 50×, 100× and 1000× that of seawater (i.e. 0.075, 0.373, 0.745 and $7.45\,ng\,g^{-1}$, respectively).

To reduce evaporation, while allowing gaseous exchange with the atmosphere, all the jars were loosely covered with lids. No additional nutrients were added into the seawater or artificial seawater. The algae tips inside the bottles were transferred into an incubator with a set light/dark rhythm of 16 : 8, light intensity of 125 µmol photons $m^{-2}\,s^{-2}$ and a temperature of 11°C. The WW of the algal tips, per jar, was measured every 2–3 days during 25 days of the culturing period for all cultures except the cultures of June 2015, which only lasted 15 days. At the same time, the media were changed (between four and seven times for all cultures) to avoid accumulation of metabolites and replenish nutrients. The salinity (approx. 35 ppt) of the Re-doped seawater did not appreciably change from that of natural seawater collected from Boulmer and remained constant throughout the culture experiments. The pH (approx. 9.0), however, changed from that of the natural seawater collected from Boulmer (approx. 8.2) owing to the metabolic activity of the macroalgae (photosynthesis) and remained constant throughout the culture experiments.

Two additional sets of culture experiments were conducted to establish if ReO_4^- is taken up by syn-life bioabsorption/bioaccumulation or passive processes. Understanding syn-life bioaccumulation and bioabsorption as the biological sequestration of substances or chemicals through any route at a higher concentration than that at which it occurs in the surrounding environment/medium when macroalgae

Table 1. Re abundance for *F. vesiculosus* structures analysed with Thermo Scientific X-series ICP–MS isotope dilution methodology.

sample	Re (ng g^{-1})	2σ (±)
macroalgae 1		
control	69.8	0.1
tips 1	163.4	0.1
leaves	28.4	0.1
stipe	23.0	0.2
holdfast	21.0	0.2
blades	67.3	0.1
veins	33.8	0.1
blades without veins	65.8	0.1
macroalgae 2		
fertile tips	117.4	<0.1
non-fertile tips	383.2	<0.1
tips	76.0	0.1
control	51.0	0.1
macroalgae 3		
fertile tips	145.0	<0.1
non-fertile tips	363.2	<0.1
tips	144.1	<0.1
control	103.4	0.1
macroalgae 4		
fertile tips	106.4	0.1
non-fertile tips	273.5	<0.1
tips	158.5	0.1
control	61.0	0.1
macroalgae 5		
fertile tips	120.7	0.1
non-fertile tips	229.1	<0.1
tips	147.2	0.1
control	84.3	0.1
macroalgae 6		
non-fertile tips	382.5	<0.1
fertile tips	129.5	0.1
tips	105.1	0.1
macroalgae 7		
control[a]	64.0	0.7
tips[a]	138.0	0.7
blades[a]	56.8	0.3
stipe[a]	22.5	0.2
holdfast[a]	21.6	0.2
blades2[a]	58.9	0.4

[a]Samples analysed with Thermo Scientific Triton Mass Spectrometer.

Table 2. Re concentrations of the media used for Re uptake experiments for boiled (2 h and 5 min), dried, and frozen with liquid nitrogen *F. vesiculosus* tips. Re abundances determined with Thermo Scientific X-series ICP–MS isotope calibration methodology.

non-reproductive thallus tips treatment	Re (ng g^{-1}) doped in seawater media previously	Re (ng g^{-1}) in seawater media afterwards	2σ ($\pm$)
boiled			
2 h	7.5	7.1	0.0
5 min	7.5	7.1	0.1
dried 72 h	7.5	2.6	0.0
frozen with N_2 liquid	7.5	6.6	0.0
non-treated macroalgae (control)	7.5	0.3	0.0

Table 3. Re concentrations of the boiled (2 h and 5 min), dried, and frozen with liquid nitrogen *F. vesiculosus* tips following Re uptake experiments. Re abundances determined with Thermo Scientific X-series ICP–MS isotope calibration methodology.

non-reproductive thallus tips treatment	Re (ng g^{-1}) doped in seawater media	Re (ng g^{-1}) uptaken by *F. vesiculosus*	2σ ($\pm$)
boiled			
2 h	7.5	36.2	0.1
2 h	0.0075	1.1	1.0
2 h	0.0	0.5	1.0
5 min	7.5	20.9	$<$0.1
dried 72 h	7.5	24.1	$<$0.1
frozen with N_2 liquid	7.5	20.0	$<$0.1

is metabolically active (i.e. alive) [30]. Therefore, in order to assess bioaccumulation, non-reproductive thallus tips were killed through either boiling, drying or freezing. Specifically, non-reproductive thallus tips ($n = 81$) from Boulmer Beach were heated for 2 h at 100°C, and a further 21 tips were heated at 100°C for only 5 min. Additionally, 21 non-reproductive thallus tips were air dried for 72 h, and another 21 tips were frozen with liquid nitrogen. In total, 18 jars were filled with sterile (i.e. autoclaved at 121°C for 30 min) and filtered (0.7 µm) seawater from Boulmer Beach. The jars containing boiled tips were divided into three subgroups composed of three replicates of each with the following treatments: seawater and seawater doped with 7.45 ng g^{-1} of $HReO_4$. The other set of three replicates containing dried, boiled (5 min) or frozen non-reproductive thallus tips, respectively, were only treated with seawater spiked with 7.45 ng g^{-1} $HReO_4$.

In order to reconfirm the uptake mechanism, four tips were placed in the bottom of the jar and four tips to each mesh, having in total 12 tips of different specimens in each jar. All jars were filled with sterile filtered (0.7 µm) seawater from Boulmer Beach and doped with 7.45 ng g^{-1} $NaReO_4$. After 3 days, the media solution was changed and set to 0.075 ng g^{-1} of $NaReO_4$ and, finally, after another 3 days, the media solution was changed and not doped. Prior to each change of the media four sample tips were taken for Re analysis.

2.5. Chloroplast isolation

A procedure modified from Popovic *et al.* [31] was used for the isolation of chloroplasts. Approximately 10 g of non-reproductive thallus tips were cut into 2 mm^2 pieces using scissors. These were washed by stirring with 2 l of filtered seawater with 75 ml of grinding medium added. The grinding medium consisted of 1 M sorbitol, 2 mM $MnCl_2$, 1 mM $MgCl_2$, 0.5 mM K_2HPO_4, 5 mM EDTA, 2 mM $NaNO_3$, 2 mM ascorbate, 2 mM cysteine, 0.2% (w/v) BSA and 50 mM of MES buffer (pH 6.1). All the subsequent steps were undertaken in ice water. The washed tissue was divided into two portions, each ground with a mortar and pestle, increasing gradually the volume to 50 ml. Then, each portion was diluted into 100 ml of medium and passed through a stainless steel strainer and four layers of cheese cloth. Chloroplasts were

Table 4. Re concentration of macroalgae tips cultured under the different concentrations of $HReO_4$ in the media. Re abundances determined with Thermo Scientific X-series ICP–MS with isotope calibration methodology.

replicate number	$HReO_4$ (ng g^{-1}) seawater	Re (ng g^{-1}) uptake by *F. vesiculosus*	2σ (±)	replicates average	SD (±)
1	0.0075	187.0	0.4	168.2	9.5
2	0.0075	149.4	0.2		
1	0.07	549.6	0.2		
2	0.07	391.0	0.1	415.4	50.6
3	0.07	305.7	1.0		
1	0.4	995.2	16.0		
2	0.4	1190.0	1.3	1275.6	135.2
3	0.4	1641.7	52.0		
1	0.8	1668.1	0.3		
2	0.8	2007.3	3.0	1769.6	84.4
3	0.8	1633.3	2.4		
1	3.7	8575.0	18.1		
2	3.7	10 505.9	2.9	9218.6	455.1
3	3.7	8575.0	12.8		
1	7.5	15 961.8	37.9		
2	7.5	16 387.0	5.0	16 208.7	90.1
3	7.5	16 277.3	50.2		
1	20.0	48 738.7	69.0		
2	20.0	52 521.9	74.0	48 007.2	2009.2
3	20.0	42 760.9	68.0		
1	75.0	51 477.0	72.0		
2	75.0	59 611.8	16.5	63 283.4	5718.7
3	75.0	78 761.5	99.0		
1	1000.0	53 009.5	45.0		
2	1000.0	61 752.1	85.5	55 588.2	2188.9
3	1000.0	52 003.1	99.5		
1	2000.0	23 488.8	4.0		
2	2000.0	21 070.8	26.5	22 472.5	512.0
3	2000.0	22 857.8	16.0		
1	7450.0	33 061.0	50.0	33 061	

isolated by centrifugation for 7 min at 5500*g*. The pellet was resuspended with 10 ml of a reaction medium containing 1 M sorbitol, 1 mM $MnCl_2$, 1 mM $MgCl_2$, 2 mM EDTA, 0.5 mM K_2HPO_4 and 50 mM HEPES (pH 8.1). Another centrifugation at 5500*g* for 7 min was performed, and chloroplasts were re-suspended with 2 ml of HEPES buffer. To test the isolation, the absorbance spectrum of the last solution obtained was observed under a light microscope. The extracted chloroplasts were preserved using HEPES (as it does not contain Re) and stored in a fridge for 3 days. In order to remove HEPES from the chloroplasts, the HEPES–chloroplast mixture was centrifuged. The chloroplast pellet was white–brown, and the HEPES solution was green–brown. The observation showed that the pigments had released and were free in the solution.

2.6. Cytoplasmic proteins isolation

A procedure modified from Boer *et al.* [32] was employed for the isolation of cytoplasmic proteins. Approximately 2 g of freshly ground non-reproductive thallus tips were used for protein extraction. The tips were mixed with 9 ml of 10 mM HEPES (pH 7.8) buffer, vortexed and centrifuged twice at 1000*g* for 1 min. The homogenate was sonicated for 1 min, 10 times and centrifuged at 4500*g* for 5 min. The supernatant was centrifuged at 14 000*g* for 10 min. A 60 mM saturated $CaCl_2$ solution was used to re-suspend the pellet, which was agitated and then centrifuged at 14 000*g* for 5 min. The supernatant was then separated via gel filtration (i.e. size exclusion column chromatography). A PD-10 desalting column

Table 5. Re concentration of macroalgae tips cultured under the different concentrations of Re(VII) salts and $HReO_4$ in the media. Re abundances determined with Thermo Scientific X-series ICP–MS with isotope calibration methodology.

replicate number	$NaReO_4$ (ng g^{-1}) seawater (March)	Re (ng g^{-1}) uptake by *F. vesiculosus*	2σ (±)	replicates average	SD (±)
2	0.074	206.3	0.2	219.6	6.6
3	0.074	232.9	0.5		
2	0.373	624.5	0.8	629.5	2.5
3	0.373	634.5	1.0		
2	0.745	986.7	2.3	1033.6	23.4
3	0.745	1080.4	2.1		
2	7.450	8421.4	6.3	8064.2	178.6
3	7.450	7706.9	11.5		

replicate number	$NaReO_4$ (ng g^{-1}) seawater (May)	Re (ng g^{-1}) uptake by *F. vesiculosus*	2σ (±)	replicates average	SD (±)
2	0.0074	95.3	<0.1	86.1	4.6
3	0.0074	76.9	<0.1		
2	0.074	175.0	<0.1	132.9	21.0
3	0.074	90.9	<0.1		
2	0.373	214.3	0.1	200.3	7.0
3	0.373	186.4	0.1		
2	0.745	227.9	0.3	225.7	1.1
3	0.745	223.5	0.2		
2	7.450	1268.0	1.1	1203.9	32.0
3	7.450	1139.9	1.7		

replicate number	NH_4ReO_4 (ng g^{-1}) seawater (May)	Re (ng g^{-1}) uptake by *F. vesiculosus*	2σ (±)	replicates average	SD (±)
2	0.074	230.6	<0.1	226.1	2.2
3	0.074	221.6	<0.1		
2	0.373	128.6	<0.1	129.4	9.4
3	0.373	130.1	<0.1		
2	0.745	283.6	<0.1	268.9	7.3
3	0.745	254.3	0.1		
2	7.450	1244.6	0.3	1208.1	18.2
3	7.450	1171.6	2.1		

replicate number	$KReO_4$ (ng g^{-1}) seawater (May)	Re (ng g^{-1}) uptake by *F. vesiculosus*	2σ (±)	replicates average	SD (±)
2	0.074	88.0	0.1	91.9	7.0
3	0.074	95.9	0.1		
2	0.373	143.6	<0.1	138.4	2.6
3	0.373	133.2	0.1		
2	0.745	166.5	<0.1	176.1	4.8
3	0.745	185.8	0.3		
2	7.450	1260.3	0.5	1251.1	4.4
3	7.450	1242.2	0.6		

replicate number	NH_4ReO_4 (ppb) seawater (May)	Re (ppb) uptake by *F. vesiculosus*	2σ (±)	replicates average	SD (±)
2	0.074	81.0	0.2	82.3	0.7
1	0.074	83.7	<0.1		
2	0.745	125.4	0.2	129.2	1.9
1	0.745	133.0	<0.1		
2	7.450	689.2	3.3	732.8	21.8
1	7.450	776.4	0.2		

(*Continued*.)

Table 5. (*Continued*.)

replicate number	$KReO_4$ (ng g^{-1}) seawater (June)	Re (ng g^{-1}) uptake by *F. vesiculosus*	2σ (±)	replicates average	SD (±)
2	0.074	51.9	0.1	58.3	3.2
1	0.074	64.6	<0.1		
2	0.745	233.8	0.6	272.4	2.2
1	0.745	242.6	1.0		
2	7.450	587.0	0.4	564.9	10.7
1	7.450	544.4	<0.1		

replicate number	$HReO_4$ (ng g^{-1}) seawater (June)	Re (ng g^{-1}) uptake by *F. vesiculosus*	2σ (±)	replicates average	SD (±)
2	0.074	125.6	<0.1	128.6	1.5
1	0.074	131.8	<0.1		
2	0.745	733.79	0.2	722.5	5.6
1	0.745	711.3	41.0		
2	7.450	5924.3	33.5	6741.4	408.6
1	7.450	7558.6	56.5		

containing *Sephadex G-25 medium* as matrix was used to separate molecules from the supernatant by their molecular size. Larger molecules than the *Sephadex* matrix pores are eluted first and smaller molecules than the matrix pores are eluted later, depending on the molecular size, the molecules will penetrate the matrix pores to varying extent. The separation was carried out following the gravity protocol detailed in PD-10 Desalting Columns Instructions [33] using the same buffer described above. Of 1 ml elution fractions obtained were analysed by ICP–MS after being diluted 10 times with 0.8 N HNO_3. Protein content of the fractions was analysed based on the absorbance shift of the dye Coomassie brilliant blue G-250.

2.7. Re abundance determinations and data treatment

Rhenium abundance determinations for all samples were obtained at the Durham Geochemistry Centre in the Laboratory for Sulfide and Source Rock Geochronology and Geochemistry. Each sample of *F. vesiculosus* was oven-dried at 60°C for 24 h and ground into a powder with an agate mortar and pestle. Approximately 100 mg of the sample powder was spiked. Abundances were obtained by both direct calibration and isotope dilution methodologies (tables 1–5). For the latter, samples were doped with a known amount of ^{185}Re tracer solution (isotope dilution methodology). The sample and, if used, the tracer solution were digested in a mix of 3 ml of 12 N HCl and 6 ml of 16 N HNO_3 at 120°C overnight in a PFA Savillex 22 ml vial. The dissolved sample solution was evaporated to dryness at 80°C. The rhenium abundance of seawater from Boulmer Beach was determined by isotope dilution ICP–MS. Approximately 30 ml of seawater was doped with a known amount of ^{185}Re tracer solution and evaporated. The rhenium fraction was further purified using standard anion chromatography methodology. Rhenium for all macroalgae samples was isolated from the dried sample using 5 ml 5 N NaOH 5 ml acetone solvent extraction procedure [8,34]. The Re-bearing acetone was evaporated to dryness at 60°C. For ICP–MS, the dried Re fraction was dissolved in 1.2 ml of 0.8 N HNO_3. For thermal ionization mass spectrometry in negative ion mode analysis, the purified Re fraction was loaded onto a Ni wire filament, with the Re isotope compositions determined using Faraday cup measurements on a Thermo Scientific TRITON mass spectrometer. Total procedural blanks are 1 ± 0.1 pg ($n = 6$). For samples analysed by isotope dilution to determine absolute Re abundance, all sources of uncertainty (e.g. standard measurement, isotope measurement, calibration of the tracer solution, fractionation correction and blank values) are propagated to yield a final uncertainty. For direct calibration, prior to each analysis, instrument performance checks confirm satisfactory performance of the ICP–MS. Five freshly prepared standards were made each time and formed calibration lines with an *R*-value more than 0.999 and less than 2% RSD uncertainty. Moreover, all the samples had a reproducibility of less than 5% RSD.

Statistical analysis, *t*-test and Tukey's HSD tests, using a significance level of 0.05, were performed using R STUDIO software. For testing the statistical hypothesis, *p*-values are used. The *p*-value is defined as the probability of obtaining a result more extreme or equal to what was actually observed, thus, if *p*-value is smaller or equal to the significance level, it suggests that the observed data are consistent with the hypotheses.

3. Results

3.1. Location of Re within *Fucus vesiculosus* structures

All analysed structures of *F. vesiculosus* are naturally enriched in Re by approximately 1000 times that found in seawater (figure 1). The contents of Re range from 23 to 313 ng g^{-1} (figure 1). Significant differences were observed (*p*-value: 0.02) between the five samples of macroalgae tips (approx. 126 ng g^{-1}) and the sample representing a mix of the plant components (approx. 74 ng g^{-1}). Further, significant differences were also observed (*p*-value: 0.003) between fertile (approx. 123 ng g^{-1}) and non-fertile tips (approx. 313 ng g^{-1}; figure 1).

3.2. Uptake of Re by *Fucus vesiculosus* culture tips

The natural Re abundance of the seawater collected from Boulmer Beach and used for the culture experiments is 6.95 ± 0.19 pg g^{-1} (approx. 0.007 ng g^{-1}), which is in agreement with previous studies of coastal waters [2]. The results shown in figures 3–5 indicate that in 25 days the Re content of the macroalgae increased proportionally to the amount of Re species doped in the seawater. However, variation in the uptake capacity by *F. vesiculosus* of the different ReO_4^- compounds doped in seawater is observed. Moreover, a significant variation (*p*-value less than 0.05) in uptake capacity between months of collection (i.e. February, March, May and June cultures with Re(VII) salts) was observed only after 0.37 ng g^{-1} of doped Re(VII) in the media. March cultures accumulated approximately 7000 ng g^{-1} more Re than February, May and June culture tips (table 6). Moreover, cultures doped with $HReO_4$ and Re(VII) salts also show different amounts of accumulation. The accumulation of Re in *F. vesiculosus* grown with all Re(VII) salts is significantly lower (*p*-value less than 0.05) than the accumulation obtained with cultures made with $HReO_4$, also only after 0.37 ng g^{-1} of doped Re to the media (figure 3). It is observed that cultures in Re-doped solution made from $HReO_4$ take up 50% of the amount of Re in seawater, in contrast to only 0.03–15% for solution doped with Re from Re(VII) salts (table 6). Because of this, cultures with high concentrations of ReO_4 in the media were made only with $HReO_4$. A linear correlation is observed between the amount of Re doped in the cultures and the accumulation of Re in the alive cultured macroalgae until an accumulation of 63 284 ng g^{-1} of Re was reached, after which Re uptake ceased as the macroalgae died (figure 4). We also observed there is a limit on the uptake of Re in the cultured macroalgae between 75 and 1000 ng g^{-1} of $HReO_4$ in the seawater media. Furthermore, visually, the macroalgae tips grown in high concentrations (2000 and 7450 ng g^{-1}) did not seem as metabolically active as those in lower concentrations. In total, macroalgae tips extracted up to approximately 60 000 ng g^{-1} of Re in 25 days (figures 4 and 5).

Fucus vesiculosus non-fertile tips under 7.45 ng g^{-1} of $NaReO_4$ in the media, after 3 days were capable of accumulating approximately 150 ng g^{-1} more than the background Re concentration in them (figure 6). These tips were then transferred to subsequent lower concentrations of $NaReO_4$ (0.075 and 0.007 ng g^{-1}) and exhibited accumulations of approximately 100 ng g^{-1} more than the background concentration of Re. Therefore, a release of 50 ng g^{-1} was found after transference (figure 6).

In comparison with living organism samples, *F. vesiculosus* non-fertile thallus tips metabolically deactivated by boiling, freezing with liquid nitrogen or drying showed appreciably little to no accumulation of Re (between 36 and 19 ng g^{-1}) compared with the concentration reached in fresh tips (i.e. alive; approx. 16 000 ng g^{-1}) with the same $HReO_4$ concentrations in the media of 7.45 ng g^{-1} (figure 7). Also, the majority of the Re content in the macroalgae was released in the media within the first 2–3 days of the experiment, and the media turned brown.

3.3. Chloroplast isolation

Chloroplasts were isolated from *F. vesiculosus* non-fertile tips. The non-fertile tips as a whole contain between 100 and 200 ng g^{-1} of Re. Chloroplasts are found throughout the whole macroalgae organism, although they exist in greater abundance in the non-fertile tips. Both the HEPES solution and the

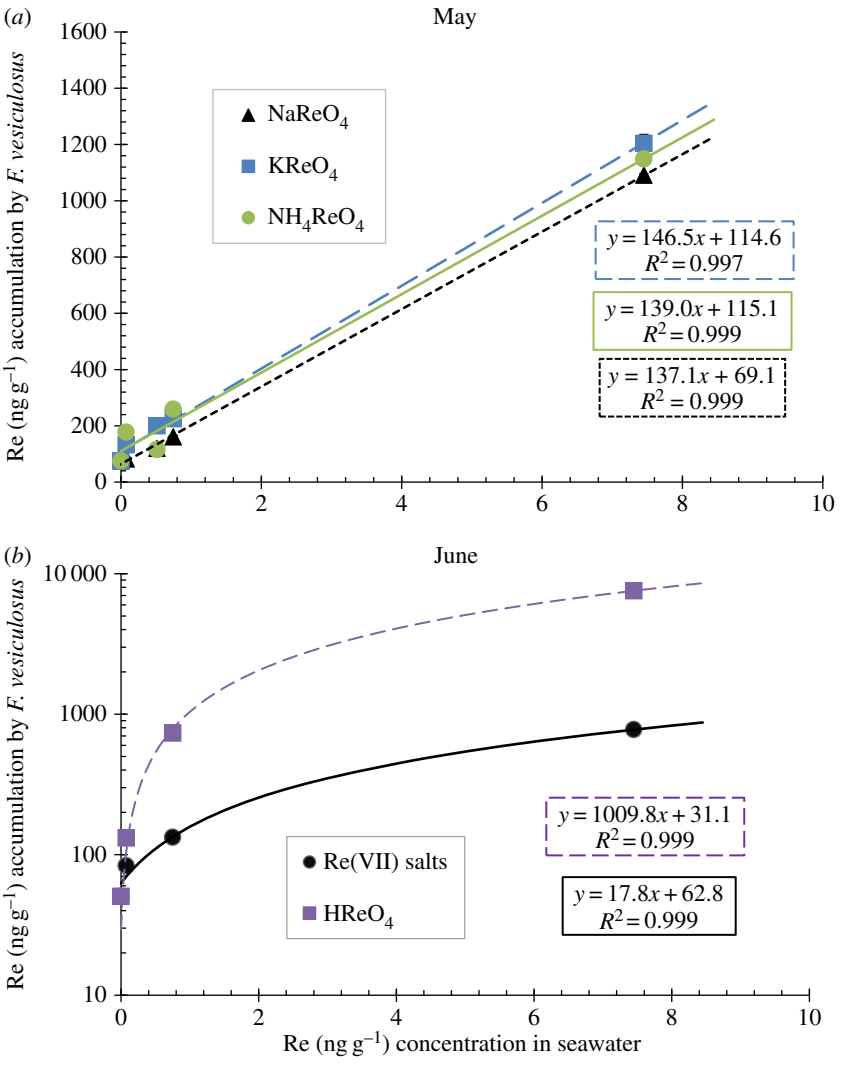

Figure 3. (*a*) Rhenium (ng g^{-1}) accumulation in *F. vesiculosus* under different Re(VII) salts concentrations. Cultures made with NH_4ReO_4 represented with a round marker, $KReO_4$ with a square marker and $NaReO_4$ with a triangle marker. (*b*) Rhenium (ng g^{-1}) accumulation in *F. vesiculosus* under different Re(VII) salts (round marker) and $HReO_4$ (square marker) plotted in logarithmic scale. All the samples had a reproducibility of less than 5% RSD; in some cases, graph symbol size is greater than uncertainties.

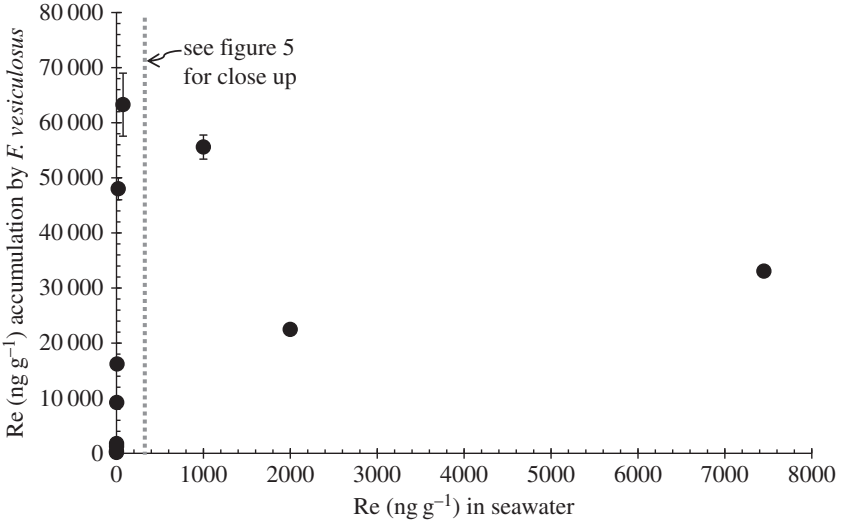

Figure 4. Rhenium (ng g^{-1}) accumulation in *F. vesiculosus* under different $HReO_4$-doped seawater concentrations. It follows a logarithmic trend line. All the samples had a reproducibility of <5% RSD; in some cases, graph symbol size is greater than uncertainties.

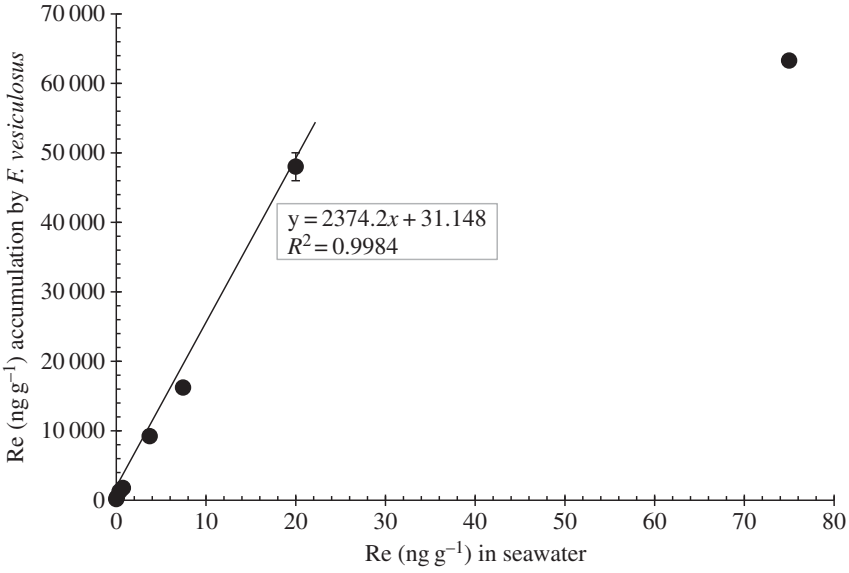

Figure 5. Rhenium (ng g^{-1}) accumulation in *F. vesiculosus* under different $HReO_4$-doped seawater concentrations. All the samples had a reproducibility of <5% RSD; in some cases, graph symbol size is greater than uncertainties.

Table 6. Seasonal uptake percentage variation of Re(VII) salts (i.e. NH_4ReO_4, $KReO_4$ and $NaReO_4$) cultures done in 2015 versus uptake rate of $HReO_4$ cultures performed in June 2014 and 2015.

	Re(VII) salts				$HReO_4$	
	February 2015	March 2015	May 2015	June 2015	June 2014	June 2015
number of media changes	5	5	7	4	5	4
total ReO_4 (ng) in seawater [doped ng × number of media changes]	12 500	12 500	17 500	10 000	9300	7440
possible Re (ng g^{-1}) accumulation by *F. v.*[a]	~25 000	~25 000	~35 000	~20 000	~18 600	~14 880
real Re (ng g^{-1}) accumulation by *F.v.*	~1700	~8000	~1200	~800	~9300	~7400
% uptake [real/possible accumulation]	6.80	32.00	3.40	4.00	50.00	49.70

[a]Total Re in seawater/average dry weight of macroalgae tips (0.5 g).

Table 7. Concentration of Re (ng g^{-1}) in chloroplasts and in HEPES solution where chloroplasts were stored.

sample	Re concentration (ng g^{-1})
chloroplast pellet	~1
HEPES solution	~3

chloroplast pellet were analysed. In the chloroplast extract, 1 ng g^{-1} of Re was detected, and 3 ng g^{-1} of Re was detected in the HEPES solution in which the chloroplasts were stored (table 7). Regardless of the difficulty in isolating the chloroplast, less than 1% of the Re is present in the chloroplast relative to the host structure (non-fertile tips) which possesses approximately 150 ng g^{-1}.

3.4. Cytoplasmic proteins purification

Cytoplasmic proteins (approx. 48 µg) were purified from 2 g of wet (i.e. 0.6 g dry) *F. vesiculosus* non-fertile tips. Proteins possess sizes in excess of 5 kDa, and were only found in fractions 4–6 eluting (1 ml fractions were collected with a G25 column). No Re was observed in the elutions containing the

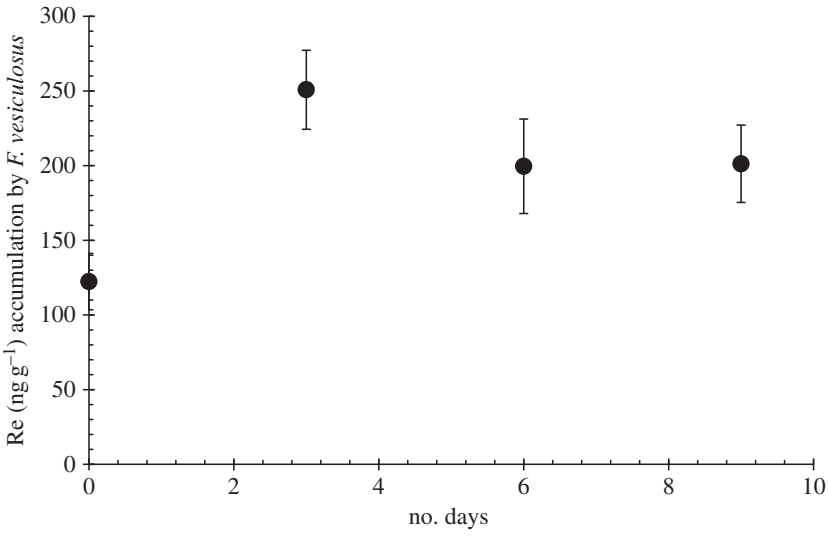

Figure 6. Re (ng g^{-1}) accumulation in *F. vesiculosus* under changing concentrations of Re(VII) salts in the media. From day 1 to 3, Re concentration of 7.45 ng g^{-1}; from day 3 to 6, 0.075 ng g^{-1}; and from day 6 to 9, 0.0075 ng g^{-1}. Day 0 measure is the background concentration of Re found in the seaweed cultured. All the samples had a reproducibility of <5% RSD.

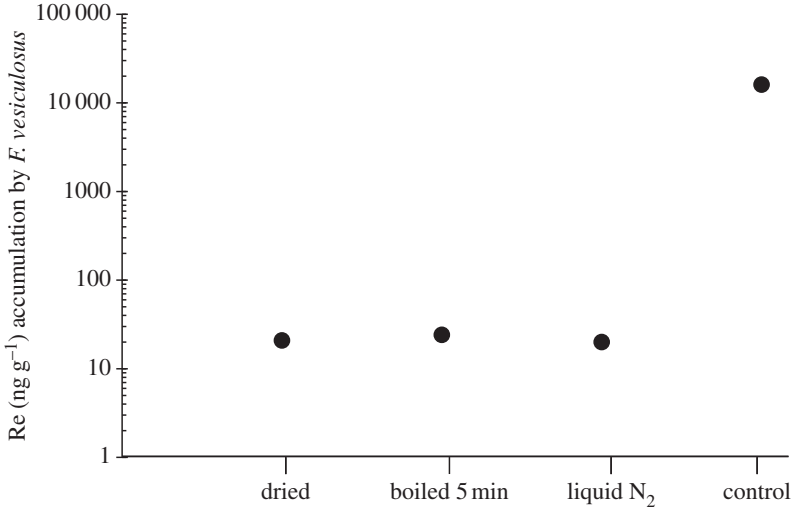

Figure 7. Accumulation of ReO_4^- in *F. vesiculosus* under different treatments (previously heated at 100°C for 5 min, liquid nitrogen frozen, and 30°C dried) and 7.45 ng g^{-1} $HReO_4$ media concentration. All the samples had a reproducibility of <5% RSD.

proteins (figure 8). However, a total amount of approximately 200 ng of Re was removed from the chromatography from elutions 10–14 with other unknown particles smaller than 5 kDa. Given the total volume of macroalgae used for the isolation of the protein (i.e. 0.6 g of dry weight), this equates to a concentration of approximately 300 ng g^{-1} Re, as it is between the range of Re expected to be in the non-fertile tips, it can be stated that all Re from the tips structures was eluted.

4. Discussion

4.1. Localization of Re within *Fucus vesiculosus* structures

The apical growth in the Phaeophyceae family is thought to occur by division of cells in cylindrical directions, with daughter cells generating a parenchymatous tissue construction [26]. Parenchyma tissue cells are capable of cell division if stimulated and can differentiate into specialized cells for photosynthesis, reproduction, growth and nutrient uptake. In Phaeophyceae, it is possible to distinguish

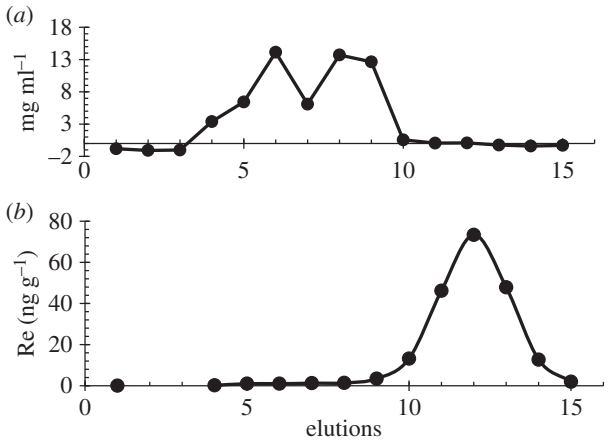

Figure 8. (*a*) Concentration of proteins (µg ml) in each elution (i.e. fraction eluted, corresponding to 1 ml). There are two protein peaks in elutions 6 and 8–9. (*b*) Concentration of rhenium (ng g^{-1}) in each elution. The peak is in elution 12.

five types of cells: epidermal cells, primary cortical cells, secondary cortical cells, medullary cells and hyphae [35]. The non-fertile tips are the apical meristems of *F. vesiculosus*, therefore, they are composed of cells that can divide and differentiate, including photosynthetic cells. Although there is variability between the different macroalgae specimens collected, the relative levels of Re vary significantly within the macroalgae structures. There are significant differences (*p*-value less than 0.05) between the amount of Re stored in the tips (approx. 126 ng g^{-1}) versus Re stored in the remainder of the macroalgae (approx. 74 ng g^{-1}; figure 1). Furthermore, significant concentration of Re is found in the non-fertile tips, which suggests a link between Re and the meristematic and photosynthetic specialized cells. More specifically, an average concentration of 313 ng g^{-1} of Re was found in the non-fertile tips, 122 ng g^{-1} Re in the fertile tips, 67 ng g^{-1} Re in the blades, 66 ng g^{-1} Re in the vesicles, 23 ng g^{-1} Re in the stipe and 21 ng g^{-1} Re in the holdfast. This suggests that Re is most likely stored in the photosynthetic structures, and it is not involved in the reproductive structures (receptacles). In herbaceous plants, the distribution of Re is also higher in photosynthetic structures, with 86% of the plant Re reported to be at the leaves [36]. Bozhkov & Borisova [37] stated that, in plants, Re is accumulated in chlorophylls forming $Mg(ReO_4)_2$. However, no Re was found in the chloroplasts of *F. vesiculosus*, thus our study suggests that Re is not strongly bound by/to chlorophylls. The concentrations of Re in the chloroplast extraction and the HEPES solution where the chloroplasts were stored are 1 and 3 ng g^{-1} of Re, respectively (table 7). These concentrations are very low, much lower than the concentrations expected given the observed concentration on the tip structures (approx. 100 ng g^{-1}).

It should be emphasized that the data in table 1 show that there is Re in all parts of *F. vesiculosus*, i.e. Re is not locally concentrated into a single structure, or a small number of structures, which means that Re is present in all cell types. In previous studies, it was demonstrated that the cell surface is not the main accumulation site of Re in the brown macroalgae *Pelvetia fastigiata* [9]. As a result, it would be expected that Re enters into the cell and remains in the cytoplasmic or a cell compartment. Moreover, Xiong *et al.* [15] made a macroalgae cell gel by chemically modifying brown macroalgae with sulfuric acid, obtaining a gel of the macroalgae alginate and fucoidan matrix. The resulting gel had a high Re affinity, and it was stated that amino acids were taking part in Re absorption, as it was observed in the IR (i.e. infrared) spectra that the intensity of the peaks corresponding to amino $-NH_2$ groups decreased after adsorption. Moreover, this fact was supported by removal of the amino acids of the gel (i.e. previously boiling the brown algae) which showed no adsorption of Re. Thus, this could mean that Re is not found in the cell wall in macroalgae, but interacts with cell membrane proteins or other molecules that contain $-NH_2$ groups in the cell, while not interacting with cytoplasmic proteins (figure 8). As in this study, no disruption of the membranes was carried out, it cannot be assumed that membrane bound proteins were simultaneously extracted. Moreover, the method for protein detection used does not detect free amino acids, peptides (i.e. glutathione, metallothioneins and phytochelatins) and proteins smaller than 3 kDa. Thus, it cannot be stated absolutely that Re is not protein bound, because we cannot be sure to have isolated all the proteins, but it can be stated that it is not related to cytoplasmic proteins larger than 3 kDa or, if it is, the Re binding of the protein is sufficiently weak that the analytical protocol for protein isolation is capable of breaking any Re protein associated bond.

4.2. Comparison of perrhenate compounds ($HReO_4$, $NaReO_4$, $KReO_4$ and NH_4ReO_4) uptake by cultured *Fucus vesiculosus* tips

A sorption study of Re onto organic polymers was undertaken by Kim *et al.* [17], who concluded that negatively charged perrhenate ions interacted with protonated amine groups in chitosan. The authors explain the sorption by a combination of a Langmuir–Freundlich-type mechanism and the electric diffuse double layer model. Our experiments show that all perrhenate salts have the same linear trendline (figure 3*a*) which strongly differs from perrhenate obtained from $HReO_4$ (figure 3*b*). This unexpected result highlights the importance of the chemical species of Re compound used for doping, which we further discuss below.

Perrhenate salts ($NaReO_4$, $KReO_4$ and NH_4ReO_4) are highly soluble in water with solubilities around 1.1 g ml^{-1}. It has been observed that cations are used as a symport for perrhenate uptake in animal cells [20]. Our results seem to show that H^+ is the best counter ion for perrhenate uptake; therefore, a greater uptake is observed when $HReO_4$ is used. Moreover, H^+ could be increasing the conversion of $-NH_2$ groups of the macroalgae to $-NH_3^+$, thus allowing perrhenate to bind. Therefore, more polymers of glucosamine and amino groups in *F. vesiculosus* [15,18] could be positively charged allowing more perrhenate binding, as it has been observed that perrhenate interacts strongly with polymers of glucosamine [17] and amino groups [15]. Although the difference of such discrepancy cannot be resolved here, uptake of ReO_4^- is observed no matter what form of perrhenate compound is used. The mechanisms that control Re entry into the cells of macroalgae have not been identified. There are many reports studying cation metal transporters, [38–40], but little is known about anion transporters (pumps) of macroalgae. Phosphate, chloride, sulfate, nitrate and molybdate transporters are all anion transporters reported in cells. Macroalgae could take up Re as perrhenate instead of other substrates of these transporters. Other trace metals in seawater exist, rather than as the free metal ion, as oxoanions (e.g. perrhenate, chromate, vanadate, molybdate, arsenate). The existing active transport pumps (e.g. sulfate, nitrate, phosphate) could be taking up such metal oxoanions, or there could be metal-specific pumps [41]. It has been observed that arsenate and phosphate have a common mechanism of uptake in bacteria and yeast [42], but not in phytoplankton [43] and brown macroalgae [19], although high concentrations of phosphate inhibit the uptake of arsenate. Nitrate could be also competing with perrhenate; however, this has been observed only for the mineral sodalite, and not in living organisms [22].

The seasonal Re(VII) salt uptake variation of cultures (table 6) suggest that perrhenate uptake is biologically influenced. Riget *et al.* [44] observed that zinc obtained maximum concentrations in macroalgae in March and a minimum in September, and it was similarly observed, albeit less clearly, with lead and copper. Macroalgae growth is the most likely cause for seasonal variations in metal uptake [44,45]. Although our studies seem to support this theory, a monthly perrhenate uptake research should be done in order to confirm it more strongly and decipher if it is simply a dilution effect or if perrhenate has a real metabolic role in the macroalgae. Here, we did not perform any seasonal experiments using $HReO_4$.

Our study also shows that when non-fertile thallus tips start dying they do not accumulate more Re and start to degrade, thus Re is released to the media (table 6 and figure 4). Therefore, less accumulation of Re in those cultured macroalgae tips that started dying is expected. This happened in the macroalgae tips cultured with 2000 and 7450 ng g^{-1} of $HReO_4$ in the seawater. In addition, it is worth emphasizing that the more time the dying tips are left in the water, the more Re is released in the seawater by macroalgae (i.e. the less accumulation of Re). Thus, this explains the results obtained in figure 4, where non-fertile thallus tips grown with a concentration of 2000 ng g^{-1} of $HReO_4$ accumulate less Re than those cultured with 7450 ng g^{-1}, because the first sets were cultured for 15 more days than the tips grown with 7450 ng g^{-1} of $HReO_4$.

Therefore, a good linear correlation fit between $HReO_4$ doped in seawater and Re taken up by *F. vesiculosus* is observed up to 75 ng g^{-1} Re in seawater, but with higher concentrations (i.e. 1000, 2000 and 7450 ng g^{-1}), there is no linear correlation (figures 4 and 5) owing to the probable metabolic inactivation of the tips. This indicates that the limit of uptake by the tips occurs when the tips are grown in a media of between 75 and 1000 ng g^{-1} of Re.

Phytoaccumulation (or phytoextraction) of metals by plants and algae is widely known [46], and refers to the concentration of metals from the environment into plant tissues. Plants absorb substances through the root, and then they transport and store these substances into the stems or leaves. There are two types of phytoextraction species: accumulator species and hyperaccumulator species. The main

difference between those two types is stated in Rascio & Navarri-Izzo [47]. Hyperaccumulator species are able to extract higher concentrations of metals and have a faster root-to-shoot transport system compared with non-hyperaccumulator species without showing phytotoxic effects. However, from the data obtained in this study, it cannot be stated that *F. vesiculosus* is a hyperaccumulator species, because the thallus tips grown with the highest concentrations of ReO_4^- started to decrease in growth and die; although they were at concentrations not typical of any environmental setting.

4.3. An understanding of Re uptake: active or passive

Figures 6 and 7 show that Re uptake is not by simple diffusion, as it is observed that only living *F. vesiculosus* tips concentrate Re. Re levels in tips with high Re media concentration ($7.45\,ng\,g^{-1}$) do not decrease when subsequently placed in media with lower Re concentrations: this suggests that the adsorption is not driven by simple equilibria. If Re was taken up by simple diffusion, then we would expect the same uptake of Re after boiling, freezing or drying the tips, as the membranes are not affected, and a direct correlation between the concentration of Re in the solution and in the macroalgae tips would be expected. Although Re could be taken up through passive mediated transport (facilitated diffusion), because after metabolically inactivating the macroalgae tips the transport proteins of the membranes are expected to be denatured (as happens when tips are boiled), thus no uptake is observed. However, this seems unlikely, owing to the high Re uptake observed in living *F. vesiculosus* tips relative to the Re concentration in seawater. In addition, our results show that the uptake mechanism is syn-life, therefore Re is bioabsorbed. It can also be concluded that Re is not taken up by simple diffusion, at least for the perrhenate compounds used here. Finally, figure 6 shows that the uptake mechanism of the macroalgae is unidirectional, not a simple partition, as we observe that once living *F. vesiculosus* has accumulated Re, it does not release it back to the media.

4.4. Implications of bioaccumulation of Re

Our results show little to no Re accumulation by metabolically inactivated *F. vesiculosus*, thus, if this is the case of macroalgae preserved in sediments as organic matter, using Re as a palaeoredox may not strictly apply. However, we do suggest that once *F. vesiculosus* has died we may see release back to the water column as the macroalgae breaks down. Thus, anoxia may be how the Re is stabilized, through prevention of macroalgae degradation.

Despite *F. vesiculosus* being a non-hyperaccumulator macroalgae, it is seen that until a limit, *F. vesiculosus* can accumulate up to $50\,000\,ng\,g^{-1}$ when $HReO_4$ was present in the media, recovering the metal from the media. Thus, *F. vesiculosus* could be used as a source of phytomining of Re. Although differences in Re uptake are associated with the form of the perrhenate compounds, all ReO_4^- compounds used here permit the uptake of Re by *F. vesiculosus*. Moreover, as Re is also a Tc analogue [17], *F. vesiculosus* could be used for bioremediation of contaminated waters with Tc residues, as it has been found in ocean waters near to the Fukushima nuclear accident [48]. Tc is a radioactive metal, mainly artificially produced within nuclear reactors as a fission product of uranium and plutonium.

5. Conclusion

The observation that macroalgae concentrates Re, an element with no known biological use, raises interesting questions. This study documents the first detailed examination of the relative proportions of Re in the structures of the macroalgae. The following conclusions are drawn from this study.

1. Re is not solely concentrated into a single macroalgae structure, all the cells possess Re. There is a distribution of Re that increases from the holdfast to the tips. Non-reproductive thallus tips exhibit the most Re accumulation, even more than reproductive thallus tips. As the only difference between them is the reproductive structures (receptacles), we can say that Re is not bound in the reproductive structures.
2. Our data show that Re is bioadsorbed by *F. vesiculosus*, rather than bioaccumulated, and does not follow a simple diffusion uptake mechanism. The uptake is unidirectional, not a simple partition; however, the data show conclusively that *F. vesiculosus* takes up and stores Re.
3. Re recovery is observed from seawater enriched with ReO_4^-, opening the possibility of using *F. vesiculosus* as a source of phytomining.

4. A difference in the uptake of Re between pherrenate salts and $HReO_4$ is observed; however, the cause has yet to be established.
5. The seasonal differences in Re uptake associated with pherrenate salts are a function of *F. vesiculosus* growth.
6. There is a limit on the uptake of Re in the cultured macroalgae between 75 and 1000 ng g^{-1} of $HReO_4$ in the seawater media, and beyond that a deleterious effect is observed.
7. Re is not accumulated in the cytoplasmic proteins or chloroplasts.

Data accessibility. All the data that support the results in the article are included in tables 1–5 of this article.

Authors' contributions. H.R. and B.R-G. identified and collected macroalgae specimens from Boulmer Beach. B.R-G. performed the culture experiments, chloroplast isolation and protein purification. D.R.G., H.C.G., H.R. and D.S. oversaw the whole experimentation procedure. D.S., A.D.S. and B.R-G. performed TRITON and ICP–MS analyses. B.R-G. wrote the manuscript; H.C.G., D.R.G., D.S. and A.D.S. critically read it and contributed to it. All the authors gave final approval for publication.

Competing interests. We declare we have no competing interests.

Funding. We are very grateful to OEA Labs Ltd for funding the project and scholarship (B.R-G.).

Acknowledgements. We express special thanks to Dr Carl Patterson, Dr Deenah Osman and Professor Nigel Robinson for their help with the protein column preparation, protein analysis and discussions, and to Dr Chris Ottley, Dr Joanna Hesselink and Dr Emily Unsworth for their help with the ICP–MS. We are very grateful to the School of Biological and Biomedical Sciences of Durham University for the culture experiment facilities. Finally, we acknowledge the constructive remarks by Bernhard Peucker-Ehrenbrink and an anonymous reviewer, which have improved this manuscript.

References

1. Koide M, Hodge VF, Yang JS, Stallard M, Goldberg EG, Calhoun J, Bertine KK. 1986 Some comparative marine chemistries of rhenium, gold, silver and molybdenum. *Appl. Geochem.* **1**, 705–714. (doi:10.1016/0883-2927(86)90092-2)
2. Anbar AD, Creaser RA, Papanastassiou DA, Wasserburg GJ. 1992 Rhenium in seawater: confirmation of generally conservative behavior. *Geochim. Cosmochim. Acta* **56**, 4099–4103. (doi:10.1016/0016-7037(92)90021-A)
3. Helz GR, Dolor MK. 2012 What regulates rhenium deposition in euxinic basins? *Chem. Geol.* **304–305**, 131–141. (doi:10.1016/j.chemgeo.2012.02.011)
4. Miller CA, Peucker-Ehrebrink B, Walker BD, Marcantonio F. 2011 Re-assessing the surface cycling of molybdenum and rhenium. *Geochim. Cosmochim. Acta* **75**, 7146–7179. (doi:10.1016/j.gca.2011.09.005)
5. Selby D, Creaser RA. 2003 Re-Os geochronology of organic rich sediments: an evaluation of organic matter analysis methods. *Chem. Geol.* **200**, 225–240. (doi:10.1016/S0009-2541(03)00199-2)
6. Stein HJ. 2013 Dating and tracing the history of ore formation. *Treatise Geochem.* **13**, 87–118. (doi:10.1016/B978-0-08-095975-7.01104-9)
7. Mas JL, Tagami K, Uchida S. 2005 Rhenium measurements on North Atlantic seaweed samples by ID-ICP-MS: an observation on the Re concentration factors. *J. Radioanal. Nucl. Chem.* **265**, 361–365. (doi:10.1007/s10967-005-0833-3)
8. Prouty NG *et al.* 2014 Deep-sea coral record of human impact on watershed quality in the Mississippi River Basin. *Glob. Biogeochem. Cycle* **28**, 29–43. (doi:10.1002/2013GB004754)
9. Yang JS. 1991 High rhenium enrichment in brown algae: a biological sink of rhenium in the sea? *Hydrobiologia* **211**, 165–170. (doi:10.1007/BF00008532)
10. Davis TA, Volesky B, Mucci A. 2003 A review of the biochemistry of heavy metal biosorption by brown algae. *Water Res.* **37**, 4311–4330. (doi:10.1016/S0043-1354(03)00293-8)
11. Chapman V, Chapman D. 1980 *Seaweeds and their uses*, 3rd edn. New York, NY: Chapman and Hall.
12. Lobban CS, Harrison PJ. 1994 *Seaweed ecology and physiology*. Cambridge, UK: Cambridge University.
13. Ragan MA, Smidsrod O, Larsen B. 1979 Chelation of divalent metal ions by brown algal polyphenols. *Mar. Chem.* **7**, 265–271. (doi:10.1016/0304-4203(79)90043-4)
14. Raize O, Argaman Y, Yannai S. 2004 Mechanisms of biosorption of different heavy metals by brown marine macroalgae. *Biotechnol. Bioeng.* **87**, 451–458. (doi:10.1002/bit.20136)
15. Xiong Y, Xu J, Shan W, Lou Z, Fang D, Zang S, Han G. 2013 A new approach for rhenium(VII) recovery by using modified brown algae *Laminaria japonica* absorbent. *Bioresour. Technol.* **127**, 464–472. (doi:10.1016/j.biortech.2012.09.099)
16. Meilián C, Kremer C, Suescun L, Mombrú A, Mariezcurrena R, Kremer E. 2000 Re(V) complexes with amino acids based on the '3 + 2' approach. *Inorg. Chim. Acta* **306**, 70–77. (doi:10.1016/S0020-1693(00)00151-1)
17. Kim E, Benedetti MF, Boulègue J. 2004 Removal of dissolved rhenium by sorption onto organic polymers: study of rhenium as an analogue of radioactive technetium. *Water Res.* **38**, 448–454. (doi:10.1016/j.watres.2003.09.033)
18. Nishino T, Nishioka C, Ura H, Nagumo T. 1994 Isolation and partial characterisation of a novel amino sugar-containing fucan sulfate from commercial *Fucus vesiculosus fucoidan*. *Carbohyd. Res.* **255**, 213–224. (doi:10.1016/S0008-6215(00)90980-7)
19. Klumpp DW. 1980 Characteristics of arsenic accumulation by the seaweeds *Fucus spiralis* and *Ascophyllum nodosum*. *Mar. Biol.* **58**, 257–264. (doi:10.1007/BF00390774)
20. Tagami K, Uchida S. 2005 A comparison of concentration ratios for technetium and nutrient uptake by three plant species. *Chemosphere* **60**, 714–717. (doi:10.1016/j.chemosphere.2005.03.087)
21. Harvey BR, Williams KJ, Lovett MB, Ibbett RD. 1991 Determination of technetium-99 in environmental material with rhenium as a yield monitor. *J. Radioanal. Nucl. Chem.* **158**, 417–436. (doi:10.1007/BF02047127)
22. Dickson JO, Harsh JB, Flury M, Lukens WW, Pierce EM. 2014 Competitive incorporation of perrhenate and nitrate into a soladite. *Environ. Sci. Technol.* **48**, 12 851–12 857. (doi:10.1021/es503156v)
23. Carlson L. 1991 Seasonal variation in growth, reproduction and nitrogen content of *Fucus vesiculosus* in the Öresund, Southern Sweden. *Bot. Mar.* **34**, 447–453. (doi:10.1515/botm.1991.34.5.447)
24. Strömgren T. 1977 Short-term effect of temperature upon the growth of intertidal Fucales. *J. Exp. Mar. Biol. Ecol.* **29**, 181–195. (doi:10.1016/0022-0981(77)90047-8)
25. White N. 2008 *Fucus vesiculosus. Bladder wrack. Marine life information network: biology and sensitivity key information sub-programme* [*on-line*]. Plymouth, UK: Marine Biological Association of the United Kingdom. http://www.marlin.ac.uk/speciesinformation.php?speciesID=3348 (accessed 9 September 2015).
26. Graham LE, Wilcox LW. 2000 *Algae*. NJ: Prentice Hall.
27. Hiscock S. 1991 *A field key to the British Brown Seaweeds* (*Phaeophyta*). Preston: Field Studies Council.
28. Gustow L, Rahman MM, Bartl K, Saborowski R, Bartsch I, Wiencke C. 2014 Ocean acidification

affects growth but not nutritional quality of the seaweed *Fucus vesiculosus* (Phaeophyceae, Fucales). *J. Exp. Mar. Biol. Ecol.* **453**, 84–90. (doi:10.1016/j.jembe.2014.01.005)

29. Gaines P. 1985–2014 *Sample preparation guide*. Christiansburg, VA: Inorganic Ventures. http://www.inorganicventures.com/samples-containing-rhenium (accessed 16 December 2015).
30. U.S. Geological Survey. 2007 *Water Basics Glossary–Bioaccumulation*. http://water.usgs.gov/water-basics_glossary.html (accessed 24 February 2016).
31. Popovic R, Colbow K, Vidaver W, Bruce D. 1983 Evolution of O_2 in brown algal chloroplasts. *Plant Physiol.* **73**, 889–892. (doi:10.1104/pp.73.4.889)
32. de Boer E, Tromp MGM, Plat H, Krenn GE, Wever R. 1986 Vanadium(V) as an essential element for haloperoxidase activity in marine brown algae: purification and characterization of a vanadium(V)-containing bromoperoxidase from *Laminaria saccharina*. *Biochem. Biophys. Acta* **872**, 104–115. (doi:10.1016/0167-4838(86)90153-6)
33. GE Healthcare. 2007 *PD-10 desalting columns. Instructions 52-1308-00-88*. Uppsala, Sweden. See https://www.gelifesciences.com/gehcls_images/GELS/Related%20Content/Files/13147231166 57/litdoc52130800BB_20110830191706.pdf.
34. Cumming VM, Poulton SW, Rooney AD, Selby D. 2013 Anoxia in the terrestrial environment during the late Mesoproterozoic. *Geology* **41**, 583–586. (doi:10.1130/G34299.1)
35. Davy de Virville A, Feldmann J. 1961 *IV International symposium on seaweed*. Biarritz: Pergamon Press.
36. Bozhkov O, Christina T, Borisova L, Ernakov V, Ryabukhin V. 2006 Study of rhenium accumulation in plants. *Trends Inorg. Chem.* **9**, 1–9.
37. Bozhkov O, Borisova L. 2002 Extraction and determination of trace amounts of Rhenium in plants. *Int. J. Environ. Anal. Chem.* **83**, 135–141. (doi:10.1080/03067310210000486 27)
38. Cobbett CS, Hussain D, Haydon MJ. 2003 Structural and functional relationships between type 1_B heavy metal-transporting P-type ATPases in *Arabidopsis*. *New Phytol.* **159**, 315–321. (doi:10.1046/j.1469-8137.2003.00785.x)
39. Mäser P *et al.* 2001 Phylogenetic relationships within cation transporter families of *Arabidopsis*. *Plant Physiol.* **126**, 16 461–16 667. (doi:10.1104/pp.126.4.1646)
40. Williams LE, Pittman JK, Hall JL. 2000 Emerging mechanisms for heavy metal transport in plants. *Biochim. Biophys. Acta* **1465**, 104–126. (doi:10.1016/S0005-2736(00)00133-4)
41. Dallinger R, Rainbow PS. 1993 *Ecotoxicology of metals in invertebrates*. Boca Raton, FL: CRC Press.
42. Rothstein A, Donovan K. 1963 Interactions of arsenate with the phosphate-transporting system of yeast. *J. Gen. Physiol.* **46**, 1075–1085. (doi:10.1085/jgp.46.5.1075)
43. Andrae MO, Klumpp DW. 1979 Biosynthesis and release of organoarsenic compounds by marine algae. *Environ. Sci. Technol.* **13**, 738–741. (doi:10.1021/es60154a001)
44. Riget F, Johansen P, Asmund G. 1995 Natural seasonal variation of cadmium, copper, lead and zinc in brown seaweed (*Fucus vesiculosus*). *Mar. Pollut. Bull.* **30**, 409–413. (doi:10.1016/0025-326X(95)99847-W)
45. Fuge R, James KH. 1973 Trace metal concentrations in brown seaweeds, Cardigan Bay, Wales. *Mar. Chem.* **1**, 281–293. (doi:10.1016/0304-4203(73)90018-2)
46. Lasat MM. 2002 Phytoextraction of toxic metals: a review of biological mechanisms. *J. Environ. Qual.* **31**, 109–120. (doi:10.2134/jeq2002.1090)
47. Rascio N, Navarri-Izzo F. 2011 Heavy metal hyperaccumulating plants: how and why do they do it? And what makes them so interesting? *Plant Sci.* **180**, 169–181. (doi:10.1016/j.plantsci.2010.08.016)
48. Steinhauser G. 2014 Fukushima's forgotten radionuclides: a review of the understudied radioactive emissions. *Environ. Sci. Technol.* **48**, 4649–4663. (doi:10.1021/es405654c)

Available online at www.sciencedirect.com

ScienceDirect

Geochimica et Cosmochimica Acta 199 (2017) 48–57

Geochimica et Cosmochimica Acta

www.elsevier.com/locate/gca

Osmium uptake, distribution, and $^{187}Os/^{188}Os$ and $^{187}Re/^{188}Os$ compositions in Phaeophyceae macroalgae, *Fucus vesiculosus*: Implications for determining the $^{187}Os/^{188}Os$ composition of seawater

B. Racionero-Gómez [a,*], A.D. Sproson [a], D. Selby [a,*], A. Gannoun [b], D.R. Gröcke [a], H.C. Greenwell [a], K.W. Burton [a]

[a] *Department of Earth Sciences, Durham University, Durham DH1 3LE, UK*
[b] *Campus Universitaire des Cézeaux, 6 Avenue Blaise Pascal TSA 60026 – CS 60026, 63178 Aubiere Cedex, France*

Received 6 April 2016; accepted in revised form 20 November 2016; available online 30 November 2016

Abstract

The osmium isotopic composition ($^{187}Os/^{188}Os$) of seawater reflects the balance of input from mantle-, continental- and anthropogenic-derived sources. This study utilizes the Phaeophyceae, *Fucus vesiculosus*, to analyse its Os abundance and uptake, as well as to assess if macroalgae records the Os isotope composition of the seawater in which it lives. The data demonstrates that Os is not located in one specific biological structure within macroalgae, but is found throughout the organism. Osmium uptake was measured by culturing *F. vesiculosus* non-fertile tips with different concentrations of Os with a known $^{187}Os/^{188}Os$ composition (~0.16), which is significantly different from the background isotopic composition of local seawater (~0.94). The Os abundance of cultured non-fertile tips show a positive correlation to the concentration of the Os doped seawater. Moreover, the $^{187}Os/^{188}Os$ composition of the seaweed equalled that of the culture medium, strongly confirming the possible use of macroalgae as a biological proxy for the Os isotopic composition of the seawater.

Keywords: Osmium; Macroalgae; Rhenium; Isotope composition; Seawater; *Fucus vesiculosus*

1. INTRODUCTION

Osmium (Os) is one of the least abundant elements in seawater, with a concentration in the open ocean of ~0.01 ppt (Sharma et al., 1997; Levasseur et al., 1998; Chen and Sharma, 2009; Gannoun and Burton, 2014), which is significantly lower than the average crustal abundance (30–50 ppt; Wedepohl, 1995; Peucker-Ehrenbrink and Jahn, 2001). Thermodynamic data predict that Os in seawater likely exists as the species OsO_4^0, $HOsO_5^-$ and $H_3OsO_6^-$ (Palmer et al., 1988; Yamashita et al., 2007), with all speciated forms present in the highest oxidation state available to Os. However, chloride complexing is also possible ($OsCl_6^-$, Cotton and Wilkinson, 1988), and it has also been suggested that Os exists as an organo-complex (Levasseur et al., 1998). Osmium in seawater has been shown to exhibit both conservative and non-conservative behaviour (Chen and Sharma, 2009; Gannoun and Burton, 2014), with the present day seawater Os isotope ($^{187}Os/^{188}Os$) composition inferred to reflect Earth surface processes, i.e. the balance of inputs from radiogenic continental-derived and unradiogenic mantle-derived sources (Peucker-Ehrenbrink and Ravizza, 2000; Cohen et al., 2003; Banner, 2004).

* Corresponding authors. Fax: +44 0191 3342301 (D. Selby).
E-mail addresses: blancaraci@gmail.com (B. Racionero-Gómez), david.selby@durham.ac.uk (D. Selby).

http://dx.doi.org/10.1016/j.gca.2016.11.033
0016-7037/

Brown macroalgae (i.e. seaweed) are known to concentrate many metal cations and metal oxoanions in a variety of complexes with biopolymers, e.g. alginate, proteins, polysaccharides of the cell wall, fucans, etc. (Davis et al., 2003). To date, positively charged metals associated with macroalgae have been extensively studied (e.g., Ragan et al., 1979; Chapman and Chapman, 1980; Karez et al., 1994; Lobban and Harrison, 1994; Raize et al., 2004). However, relatively little is known about the mechanisms by which macroalgae uptake negatively charged metal oxoanions. To our knowledge, there have been no studies discussing the uptake amount and accumulation of Os by any macroalgae species, although it is known that Os, in addition to Re can accumulate in seaweed (Scadden, 1969; Yang, 1991; Mas et al., 2005; Prouty et al., 2014; Racionero-Gómez et al., 2016; Rooney et al., 2016). The brown macroalgae (Phaeophyceae) *Fucus vesiculosus* is observed to be one of the greatest accumulators of metals (Scadden et al., 1969; Morries and Bale, 1975; Bryan, 1983; Yang, 1991; Rainbow and Phillips, 1993; Karez et al., 1994; Mas et al., 2005; Racionero-Gómez et al., 2016).

As such, this study investigates *F. vesiculosus* to establish both the specific sites and the mechanisms of Os accumulation. We also evaluate the importance of macroalgae in recording the direct Os isotope composition of seawater. Here we present the Os abundance for different structures of *F. vesiculosus*: holdfast, stipe, tips, vesicles and blades (Fig. 1) and we determine the uptake rate of Os in macroalgae via cultures of *F. vesiculosus* under different Os concentrations. We also demonstrate experimentally that macroalgae records the Os isotope composition of the local environment in which it lives (i.e. seawater), indicating that seaweed has the ability to record the interaction between the ocean and the Earth's surface, a mechanism proposed for brown algae based on samples collected from the west coast of Greenland and the Gulf of Mexico (Rooney et al., 2016). In addition, we present the rhenium (Re) abundance, and the $^{187}Re/^{188}Os$ composition of the macroalgae studied.

2. MATERIAL AND METHODS

2.1. Macroalgae used in this study: *F. vesiculosus*

F. vesiculosus is a common brown macroalgae found along sheltered shores of the North Sea, Baltic Sea, Atlantic Ocean and Pacific Ocean. *F. vesiculosus* produces air bladders annually allowing the individual fronds to float in the upper portion of the water column to permit photosynthesis. The species comprises an anchoring holdfast and a frond made up of a stipe, blades, tips and vesicles (Fig. 1). The growth rate of *F. vesiculosus* ranges between 0.05 and 0.14 cm/day (Strömgren, 1977; Carlson, 1991), with the species having a life span between 3 and 5 years (White, 2008). The species is annually episodic, gonochoristic and highly fecund (i.e. prolific; White, 2008). *F. vesiculosus* has both fertile tips and non-fertile tips. Fertile tips contain receptacles from which the gametes are released to the seawater and the eggs are fertilized externally. The zygote then starts to develop as soon as it settles into a substrate (Graham and Wilcox, 2000). Non-fertile tips are composed of a parenchymatous thallus i.e. tissue like structure (Hiscock, 1991; Graham and Wilcox, 2000; White, 2008).

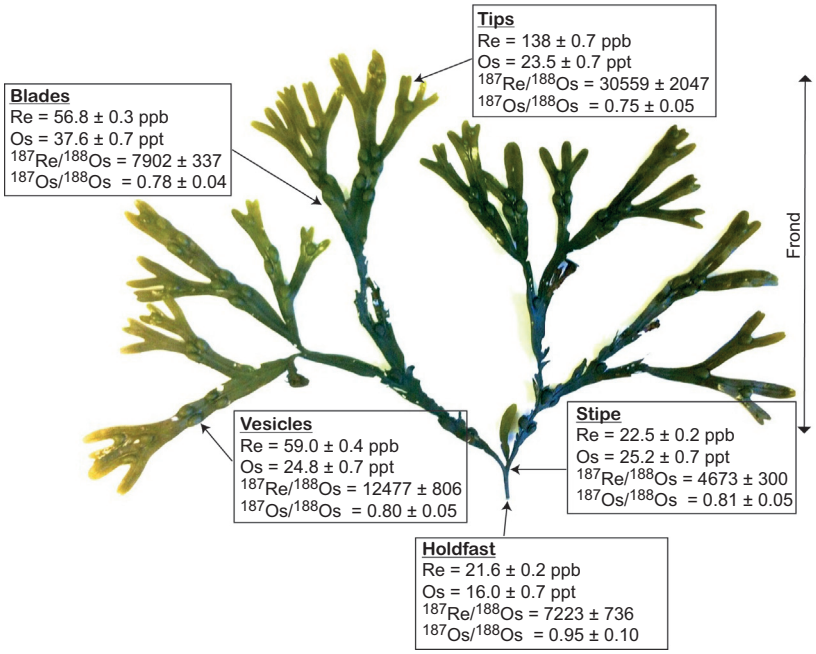

Fig. 1. Photo exhibiting the key structures of *F. vesiculosus*. Also shown are the Re and Os abundances, and Re–Os isotope compositions (data including uncertainties are given in Table 1).

The *F. vesiculosus* samples were collected from within the harbour at Staithes and adjacent to the eastern (seaward) side of the east harbour wall, North Yorkshire, UK (Fig. 2) in May, 2014 and June, 2015 (Fig. 2). The Lower Pliensbachian Staithes Sandstone Formation (a 30 m thick argillaceous silty sandstone interbedded with 2–4 m thick sequences of fine-grained laminated sandstone) comprises the geology of the harbour, beach and village of Staithes, with the cliffs to the east of the harbour consisting of the Upper Pliensbachian Cleveland Ironstone Formation (dark argillaceous siltstone and silty sandstone with ooidal ironstone; Rawson and Wright, 2000). The May 2014 *F. vesiculosus* collection (Five *F. vesiculosus* specimens held on the same rock) were taken from the eastern side of the east harbour wall (54°33′32.5″N 00°47′15.5″W; Fig. 2). These *F. vesiculosus* samples were utilised to determine the Os abundance of specific structures of the macroalgae. Additional *F. vesiculosus* samples collected in June 2015 were taken from a single location to avoid genetic variation from the mouth of Staithes Beck within the harbour of Staithes (54°33′32.8″N 00°47′25.5″W; Fig. 2). The non-fertile tips (~100) of the June 2015 sample collection were utilised for culture experiments. Seawater used in the culture experiments was taken from the same location as the June 2015 *F. vesiculosus* sample set. An aliquot of the collected seawater was utilised for Re-Os abundance and isotope composition determination.

2.2. Sample preparation and culturing

Prior to analysis all collected specimens were kept individually in plastic sample bags for transport, and stored in a freezer (−10 °C) for 48 h. Each specimen was washed and rinsed in deionised (Milli-Q™) water to remove any attached sediment and salt. To establish the abundance and distribution of Os in the macroalgae the sample was divided into different structural components: fertile tips, non-fertile tips, vesicles, stipe, holdfast, and blades (Fig. 1). In addition, a mixture of the above components was created to determine an average Os abundance of the whole macroalgae structure. Each structure was dried in an oven at 60 °C for 12 h, prior to powdering to a powder in an agate pestle and a mortar.

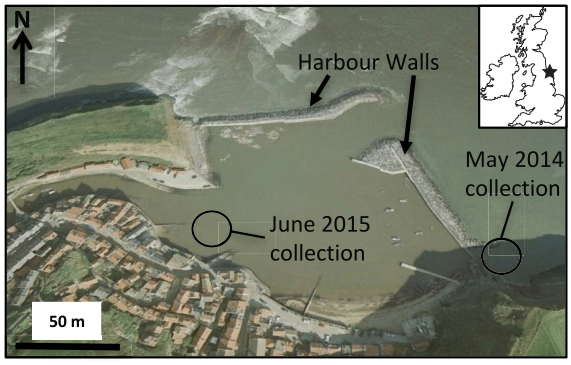

Fig. 2. *F. vesiculosus* sample locations for May 2014 and June 2015.

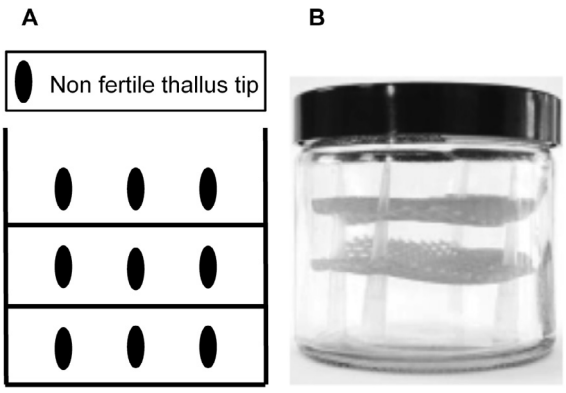

Fig. 3. Representation of culture growth set-up of non-reproductive *F. vesiculosus* thallus tips. (A) Two meshes were put inside each jar generating three levels that each hold three non-fertile tips each. (B) Photo of the culture jar used.

In addition, to investigate the uptake of Os by macroalgae, culture experiments were conducted in seawater (modified after Gustow et al. (2014)) in the School of Biological and Biomedical Sciences at Durham University. In total, three separate culture experiments were conducted, with each experiment replicated a total of three times. For each experiment, non-reproductive apical thallus tips were taken from separate *F. vesiculosus* June 2015 specimens of the geographical area (length $\geqslant$1.5 cm; wet weight (WW) = 0.12–0.15 g) without visible microalgae (i.e. epiphytes). The apical thallus tips were placed into a 250 mL glass jars containing two plastic mesh shelves. Three tips were placed in the bottom of the jar and three tips were placed in each mesh, having in total nine tips of different specimens in each jar (see Fig. 3). All culture experiments were carried out using filtered (0.7 μm) seawater from Staithes, North Yorkshire, UK (54°33′32.8″N 00°47′25.5″W; Fig. 2) collected in June 2015. The seawater was collected and stored in cleaned PFA Teflon bottles (following the method of Sharma et al., 2012). The source of Os used to dope the natural seawater for the culture experiments is DROsS (Durham Romil Osmium Standard; Nowell et al., 2008). DROsS is an in-house Os solution reference material that possesses a $^{187}Os/^{188}Os$ composition of 0.160924 ± 04 (2SD; Nowell et al., 2008). The DROsS solution utilized in this study is in chloride form. The Re and Os abundance and isotope composition of the collected seawater at Staithes was also determined as part of this study (see methodology below).

To reduce evaporation while to allowing gaseous exchange with the atmosphere all the jars were loosely sealed. No nutrients were added to the Os doped seawater culture solution. The jars, plus tips, were placed into an incubator with a set light/dark rhythm of 16:8, light intensity of 125 μmol photons/$m^2 \cdot s^2$ and a temperature of 11 °C. The wet weight (WW) of the algal tips in each jar was measured every 2–3 days during the 14 day culturing period. At the same time, the seawater Os-doped culture medium was changed (5 times in total) to avoid accumulation of metabolites. The pH (~9) and salinity (~16 psu) of the Os doped seawater culture medium did not appreciably change from that of the natural seawater collected from Staithes, which

is also ~9, and remained constant throughout the culture experiments. The recorded pH is higher than the normal pH range of seawater. This is probably due to the higher levels of photosynthesis relative to respiration during the day or, dissolution of carbonates from the surrounding bedrock. Following the culture experiment, each sample was oven-dried at 60 °C for 24 h and ground into a powder with an agate mortar and pestle.

2.3. Re–Os analysis

2.3.1. Macroalgae

The Re–Os abundance and isotope composition determinations for all *F. vesiculosus* samples were obtained by isotope-dilution negative ion mass spectrometry (ID-NTIMS) at the Durham Geochemistry Centre in the Laboratory for Sulphide and Source Rock Geochronology and Geochemistry. Approximately 80–100 mg of sample powder was utilised for the Re–Os analysis. The powdered sample was added to a Carius tube with a known amount of a mixed $^{185}Re + ^{190}Os$ tracer solution. To prevent any sample reaction prior to sealing, the Carius tubes were placed into an ethanol/dry ice bath and 3 mL of 11 N HCl and 6 mL of 15.5 N HNO_3 were added. After sealing, the Carius tubes were placed into an oven and heated to 220 °C for 24 h. The Os was isolated from the acid medium using $CHCl_3$ solvent extraction, with the Os back extracted into HBr. The Os was further purified using a CrO_3–H_2SO_4–HBr micro-distillation methodology (Cohen and Waters, 1996; Birck et al., 1997). The resultant Re-bearing acid medium was evaporated to dryness at 80 °C, with the Re isolated and purified using both NaOH–acetone solvent extraction and HNO_3–HCl anion chromatography (Cumming et al., 2013).

2.3.2. Seawater

The Os abundance and isotope composition of the seawater at Staithes was determined using the liquid bromine (Br_2) methodology (Gannoun and Burton, 2014) at the Laboratoire Magmas et Volcans at the Campus Universitaire des Cézeaux. In brief, ~60 g of water sample, plus a known amount of mixed ($^{190}Os + ^{185}Re$) tracer solution, together with 2 mL of Br_2, 2 mL of CrO_3–H_2SO_4 solution and 1.5 mL of 98% H_2SO_4 were sealed into a 120 mL Savillex vial and heated to 100 °C in an oven for 72 h. Following the spike-sample equilibrium stage, to test that excess Cr^{6+} still exists in the CrO_3–H_2SO_4 solution, a drop (~30 µl) of the aqueous phase was pipetted and added to 3% v/v H_2O_2 solution. This resulted in the CrO_3 reacting with the H_2O_2 by producing intense bubbling with a transient dense blue colour formed, thus confirming the presence of excess Cr^{6+}. Osmium was extracted from the sample into liquid Br_2. To increase the extraction yield of Os, a second extraction of Os was conducted using 1 mL of Br_2. The 1 mL of liquid Br_2 was added to the sample solution reacted for 1 h and then removed. The extracted Br_2 was mixed with 1 mL of 9 N HBr and evaporated to dryness. The Os was further purified using a CrO_3–H_2SO_4–HBr micro-distillation. The Os extracted, Re-bearing solution was evaporated to dryness. The Re was purified as described for the macroalgae samples (NaOH–acetone solvent extraction and HNO_3–HCl anion chromatography, Cumming et al., 2013) at the laboratories at the Durham Geochemistry Centre.

2.4. Mass spectrometry

The purified Re and Os fractions were loaded onto Ni and Pt filaments, respectively and measured using NTIMS (Creaser et al., 1991; Völkening et al., 1991) on a Thermo Scientific TRITON mass spectrometer using Faraday collectors in static mode, and an electron multiplier in dynamic mode, respectively. The Re and Os abundances and isotope compositions are presented with 2 sigma absolute uncertainties which include full error propagation of uncertainties in the mass spectrometer measurements, blank, spike and sample and spike weights. Full analytical blank values for the macroalgae analysis are 2.4 ± 0.04 pg for Re, 0.05 ± 0.02 pg for Os, with a $^{187}Os/^{188}Os$ composition of 0.25 ± 0.15 (1 SD, $n = 3$). For the seawater analysis the full analytical blank values are 10.0 ± 1.3 pg for Re, 0.043 ± 0.002 pg for Os, with a $^{187}Os/^{188}Os$ composition of 0.72 ± 0.02 (1 SD, $n = 4$).

To monitor the long-term reproducibility of mass spectrometer measurements Re and Os (DROsS, DTM) reference solutions were analysed. The 125 pg Re solution yields an average $^{185}Re/^{187}Re$ ratio of 0.5983 ± 0.0024 (2 SD, $n = 5$), which is in agreement with the published values (e.g., Cumming et al., 2013). A 50 pg DROsS solution gave an $^{187}Os/^{188}Os$ ratio of 0.16088 ± 0.0008 (2 SD, $n = 5$), which is in agreement with the reported value for the DROsS reference solution (Nowell et al., 2008). For the seawater Os analysis at the Laboratoire Magmas et Volcans instrument reproducibility is monitored using a 1 pg DTM Os solution, which yields an $^{187}Os/^{188}Os$ value of 0.1740 ± 0.0002 (2 SD, $n = 4$), which is in agreement with published values (Chen and Sharma, 2009; Gannoun and Burton, 2014).

3. RESULTS

3.1. Re and Os abundances and isotope compositions of Staithes seawater

The Staithes seawater possesses a Re and Os abundance of 8.2 and 0.0156 ppt, respectively, with a $^{187}Re/^{188}Os$ value of 2790.6 ± 49.7 and a $^{187}Os/^{188}Os$ composition of 0.94 ± 0.04 (Table 1). The filtered seawater was doped with DROsS to create a seawater culture solution with an Os concentration 3× (~0.05 ppt), 6× (~0.1 ppt) and 200× (~3 ppt) that of seawater, which respectively have $^{187}Os/^{188}Os$ compositions of 0.38 ± 0.02, 0.29 ± 0.01, and 0.18 ± 0.01 (Table 2).

3.2. Re and Os abundances and isotope compositions within *F. vesiculosus* structures

The natural total Os abundance within all structures of *F. vesiculosus* collected during May 2014 directly from the seaward side of the Staithes harbour wall and not cultured,

Table 1
Rhenium (ppb), osmium (ppt) and Re–Os isotope compositions in *F. vesiculosus* structures and culture experiment.

Sample	Weight (g)	Re (ppb)	Os (ppt)	$^{187}Re/^{188}Os$	$^{187}Os/^{188}Os$
May 2014 collection					
Tips	0.201	138.0 ± 0.7	23.5 ± 0.7	30558.8 ± 2046.6	0.75 ± 0.05
Blades	0.200	56.8 ± 0.3	37.6 ± 0.7	7902.1 ± 336.9	0.78 ± 0.04
Stipe	0.200	22.5 ± 0.2	25.2 ± 0.7	4672.6 ± 299.8	0.81 ± 0.05
Holdfast	0.200	21.6 ± 0.2	16.0 ± 0.7	7223.4 ± 736.2	0.95 ± 0.10
Vesicles	0.200	59.0 ± 0.4	24.8 ± 0.7	12476.6 ± 805.9	0.80 ± 0.05
Mix of structures	0.204	64.0 ± 0.7	33.8 ± 0.7	9930.3 ± 469.9	0.81 ± 0.04
June 2015 collection					
Tips	0.101	47.4 ± 0.1	7.8 ± 0.4	34794.1 ± 2074.4	0.91 ± 0.07
Culture experiment					
1 – 3x seawater[1]	0.102	79.3 ± 0.2	21.2 ± 0.4	18585.9 ± 866.6	0.35 ± 0.02
2 – 3x seawater[1]	0.101	77.7 ± 0.2	20.5 ± 0.1	18819.6 ± 757.5	0.34 ± 0.01
1 – 6x seawater[1]	0.102	71.3 ± 0.2	28.6 ± 0.5	12235.8 ± 421.2	0.28 ± 0.01
2 – 6x seawater[1]	0.102	71.1 ± 0.2	32.7 ± 0.5	10696.6 ± 323.4	0.28 ± 0.01
1 – 200x seawater[1]	0.081	67.1 ± 0.2	201.6 ± 0.8	1615.0 ± 12.7	0.18 ± 0.00
2 – 200x seawater[1]	0.081	66.8 ± 0.2	194.3 ± 0.8	1668.6 ± 13.4	0.18 ± 0.00
Staithes seawater					
Seawater[2]	64.5	8.20 ± 0.08	15.7 ± 0.2	2790.6 ± 49.7	0.94 ± 0.04

All uncertainties are quoted at the 2s level.
The Re–Os abundances are based on the dry mass of the seaweed.
[1] Culture experiment uses tips from specimens collected in June 2015.
[2] Seawater Re concentrations in ppt; Os concentrations given in ppq.

is between 1600 and 3700 times greater than the concentration found in seawater (Fig. 1). The Os abundance in the *F. vesiculosus* structures ranges from 16 to 38 ppt (Fig. 1; Table 1). The structure that contains the least amount of Os is the holdfast (16 ppt), with the blades possessing the highest Os abundance (38 ppt). The remaining structures (tips, stipe and vesicles) possess similar concentrations (24 and 25 ppt Os). A mixture of all the *F. vesiculosus* structures possesses ~34 ppt Os, which is reasonable if we take the value as a reference as the approximate relative proportions of each structure of *F. vesiculosus*. For example, *F. vesiculosus* is comprised of 67% tips and blades, 30% stipe and vesicles and 3% holdfast (Fig. 1).

A previous study showed that the natural Re abundance within *F. vesiculosus* varies (23–313 ppb) and that Re is not located in one specific structure (Racionero-Gómez et al., 2016). In agreement with this previous study, we show that the Re abundance is highly variable throughout *F. vesiculosus*, with Re abundances ranging from ~22 to 138 ppb, being between 3100 and 19,700 times greater than that found in seawater (Table 1). Similar to Os, the holdfast (and stipe) possess the least amount of Re (~22 ppb). However, in contrast to Os, the tips possess the greatest enrichment of Re (~138 ppb).

The variability in Re and Os abundance means that the $^{187}Re/^{188}Os$ values for *F. vesiculosus* structures is highly variable (Table 1). The $^{187}Re/^{188}Os$ values range between ~4672 (stipe) and 30,558 (tips), with the holdfast and blades possessing similar values to those of the stipe. The $^{187}Os/^{188}Os$ values for the *F. vesiculosus* structures, with the exception of the holdfast, possesses an average composition of 0.80 ± 0.03 (1 SD) that reflects a moderately radiogenic composition; this is identical, within uncertainty, to the mixture of all the structures (0.81 ± 0.04).

3.3. Uptake of Osmium by *F. vesiculosus* culture tips

The natural Os abundance of the tips of a specimen of *F. vesiculosus* collected in June 2015 possesses significantly less Os (7.8 ppt; Table 1) than that of the same structure from a specimen collected in May 2014 (23.5 ppt; Table 1). The same is observed for rhenium (138 ppb for May 2014 vs 47 ppb for June 2015; Table 1). This difference can be due to many different factors; location, yearly, monthly or daily changes, ocean sediment turbulence, age of the specimen and other present unknown conditions (Lyngby and Brix, 1982; Horta-Puga et al., 2013). Furthermore, to our knowledge the impacts that each specific factor produces to the flux of Re and Os to the nearshore have not been determined. Although the Re and Os abundances are different between the samples collected in May 2014 and June 2015, the $^{187}Re/^{188}Os$ compositions are similar (~30,558 ± 2046 (May 2014) vs ~34,794 ± 2074 (June 2015). The $^{187}Os/^{188}Os$ compositions are slightly different (0.75 ± 0.05 (May 2014) vs 0.91 ± 0.07 (June 2015); Table 2), which likely reflects their geographic positions. For example, the June 2015 samples are taken from within the Harbour at the mouth of Staithes Beck, whereas the May 2014 samples are seaward of the Harbour wall (see Section 4.2).

The tips of the *F. vesiculosus* collected in June 2015 were used for the culture experiments. For all the culture experiments the Re abundance of the tips (~67–79 ppb) is greater than that from specimen tips analysed directly from the ocean (~47 ppb) (Table 1). We note that the only Re present in the culture media is that present in the natural

Table 2
Osmium (ppt) and $^{187}Os/^{188}Os$ compositions in the culture media and in *F. vesiculosus*.

Sample	Seawater [Os] (ppt)	$^{187}Os/^{188}Os$ of seawater culture media	Measured $^{187}Os/^{188}Os$ of seaweed after culture growth	% of Os transferred from seawater culture media into the seaweed
Natural seawater[1]	0.0156	0.94 ± 0.04		
3x seawater	0.05	0.38 ± 0.02	0.35 ± 0.02	17,4
6x seawater	0.1	0.29 ± 0.01	0.28 ± 0.01	16,8
200x seawater	3	0.18 ± 0.01	0.18 ± 0.00	16,9

[1] Measured seawater from Staithes – see Table 1.

seawater (~8 pg/g; Table 1) because the Re abundance in the Os solution (DROsS) used to dope the natural seawater is negligible (e.g., 1 pg/g Os solution contains $\sim 7e^{-6}$ fg/g Re (Nowell et al., 2008). The Re abundance of the cultured tips shows a decrease from ~79 ppb for the 3× experiment, to ~71 ppb for the 6× experiment, and ~67 ppb for the 200× experiment (Table 1).

For osmium, the abundance increases proportionally to the amount of Os doped in the seawater (3× = ~20 ppt, 6× = ~30 ppt, 200× = ~200 ppt; Table 1; Fig. 4). Coupled with this increase in Os abundance is a trend to less radiogenic $^{187}Os/^{188}Os$ compositions (3× = 0.35 ± 0.02, 6× = 0.28 ± 0.01, 200× = 0.18 ± 0.00; Table 1; Fig. 4). Additionally, as a direct result of the overall increase of Os in the cultured tips with a relatively similar Re abundance, the $^{187}Re/^{188}Os$ composition significantly decreases (natural sample = ~32,000; 3× = ~18,000, 6× = ~12,000, 200× = ~1600; Table 1).

4. DISCUSSION AND IMPLICATIONS

4.1. Localization and uptake of Os within *F. vesiculosus*

Five types of cells can be distinguished in brown macroalgae: epidermal cells, primary cortical cells, secondary cortical cells, medullary cells and hyphae (Davy de Virville and Feldmann, 1961). A previous study identified that Re accumulation in *F. vesiculosus* is variable across the structural components (holdfast, blade, stipe, tips) of the macroalgae, indicating that there were some cells/structures more specialized for the uptake of Re (Racionero-Gómez et al., 2016). In the case of Os, its abundance does not significantly vary between structures, with the exception of the holdfast, suggesting that there is no specific cell specialization for the uptake of Os (Fig. 1; Table 1). The holdfast does not serve as the primary organ for water or nutrient uptake, instead it serves to anchor the macroalgae to the substrate. Therefore, lower Os abundances in the holdfast are expected. Moreover, it is suggested that Re could be biologically influenced (Racionero-Gómez et al., 2016), with uptake controlled by the growing season, as observed for zinc, lead and copper (Fuge and James, 1973; Riget et al., 1995). As such, this may also be the case for Os, however we cannot conclusively state that Os uptake is biologically controlled, because our samples were collected principally during the same growing season. Although, this may explain, in part, the variability in Re and Os abundance between the May 2014 and June 2015 samples as noted above. Nevertheless, the uptake of Os by *F. vesiculosus* is similar to that of Re, in the sense that, it is currently known to have no biological role. Further, the difference in Os isotopic composition between each structure cannot be considered significant given that all values overlap within uncertainty, with the exception of the holdfast (see Table 1).

The measured Os abundance in the cultured *F. vesiculosus* tips show a positive correlation with the concentration of Os doped seawater (see Tables 1 and 2; Fig. 4). The culture experiment with the highest Os concentration (200× (3 ppt Os) seawater), resulted in tips possessing an Os abundance of ~194 ppt, which is ~25 times higher than the background concentration of Os in the specimens collected (Table 1).

Using the $^{187}Os/^{188}Os$ composition of the Staithes seawater (0.94 ± 0.04), together with the background Os abundance in the tips of the June 2015 collection (~8 ppt; Table 1), with the concentration of the doped seawater and cultured tips and their $^{187}Os/^{188}Os$ composition, we observe that the percentage of Os that has been transferred from seawater to the algae is about 17% (Table 2).

Coincident with the increase in Os abundance within the culture experiments is the decrease in Re (Table 1), indicating possible competition between similar cell binding sites or uptake pathways between Re and Os, both forming oxoanions in seawater. However, the uptake pathways and binding sites of Re have not yet been identified, thus it is currently not known where Os accumulates in *F. vesiculosus*.

4.2. Implications of the $^{187}Os/^{188}Os$ isotope composition of *F. vesiculosus*

The $^{187}Os/^{188}Os$ composition of *F. vesiculosus* in a natural setting from the harbour at Staithes is 0.91 ± 0.07 (Table 1; Fig. 4) based on results from specimens collected in June 2015, which is within uncertainty to that of the seawater from the same location (0.94 ± 0.04) (Table 1). The agreement of the *F. vesiculosus* and seawater $^{187}Os/^{188}Os$ compositions would imply that macroalgae records the $^{187}Os/^{188}Os$ composition of the watermass it is living in. This is further supported by the culture experiments. For each culture experiment the measured $^{187}Os/^{188}Os$ composition of the tips coincides with the $^{187}Os/^{188}Os$ composition of doped seawater (Table 2; Fig. 4). This indicates that the

$^{187}Os/^{188}Os$ composition of seaweed reflects the media in which it grows, and thus directly supports the use of *F. vesiculosus* (and macroalgae) as a biological proxy for the $^{187}Os/^{188}Os$ composition in seawater (Rooney et al., 2016). For example, the $^{187}Os/^{188}Os$ composition for three floating macroalgae (*Sargassum fluitans* and *Sphaerotilus natans*) collected from three different locations ~300 miles offshore in the Gulf of Mexico (1.05 ± 0.01; Rooney et al., 2016) are coincident with that of the present day open oceanic $^{187}Os/^{188}Os$ value of 1.06 (1.04 for the North Atlantic and Central Pacific; 1.06 for the Eastern Pacific and Indian Ocean) determined from direct analyses of seawater and of hydrogenetic Fe–Mn crusts (see Peucker-Ehrenbrink and Ravizza, 2000 and references therein; Gannoun and Burton, 2014 and references therein). In contrast, macroalgae from the coast of the Disko Bugt and Uummannaq regions of the west coast of Greenland show deviations from the $^{187}Os/^{188}Os$ composition of the open ocean (between 0.9 and 1.9) which directly relate to Os flux (abundance and isotope composition) into the coastal region (Rooney et al., 2016). The latter together with the slightly lower and variable $^{187}Os/^{188}Os$ composition (~0.91 (June 2015 Staithes harbour) vs ~0.81 (Staithes east of the harbour wall); Table 1) of the macroalgae from Staithes in comparison to that of the open sea may suggest that the Os isotope composition of macroalgae is strongly controlled by its proximity to the coast, riverine input and regional variations in the Os flux (i.e., abundance and isotope composition) into the ocean, as also shown along the transects of estuaries (e.g., Levasseur et al., 2000; Martin et al., 2001; Sharma et al., 2007). For example, the Fly River Estuary reflects the input of unradiogenic Os and shows an increasing $^{187}Os/^{188}Os$ composition oceanward from 0.61 to 0.91 (Martin et al., 2001). In contrast, the Lena River Estuary and the Godavari Delta reflects the input of radiogenic Os, with the $^{187}Os/^{188}Os$ value decreasing oceanward from 1.55 to 1.13, and 1.30 to 0.90, respectively (Levasseur et al., 2000; Sharma et al., 2007). Moreover, surface seawater has a distinctly lower $^{187}Os/^{188}Os$ than the deep ocean (Chen and Sharma, 2009; Gannoun and Burton, 2014). Therefore, macroalgae from distinct oceanic settings (e.g., coastal, estuarine vs open ocean) provides the ability to record the $^{187}Os/^{188}Os$ composition of seawater in addition to direct seawater and sediment analysis to further access the factors (e.g., geological and anthroprogenic) controlling the $^{187}Os/^{188}Os$ composition of seawater.

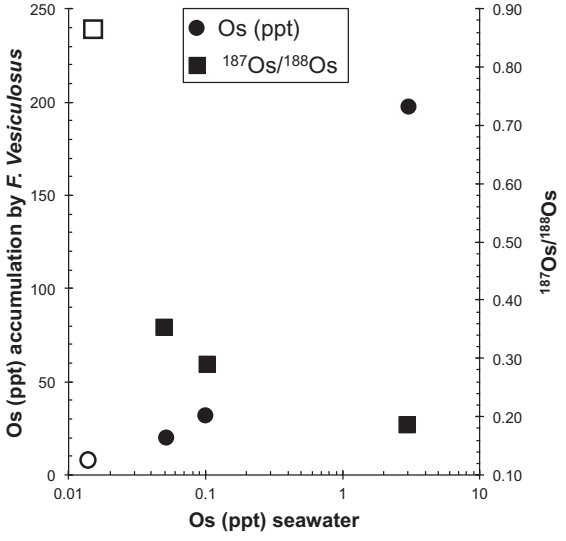

Fig. 4. Osmium (ppt) accumulation (circles) and $^{187}Os/^{188}Os$ compositions (squares) in *F. vesiculosus* under different Os seawater culture media concentrations. The open symbols are for *F. vesiculosus* collected June 2015. See Tables 1 and 2 for data.

4.3. Implications of the $^{187}Re/^{188}Os$ isotope composition of *F. vesiculosus*

In addition to the $^{187}Os/^{188}Os$ composition of macroalgae, the $^{187}Re/^{188}Os$ values of macroalgae (this study; Rooney et al., 2016) may provide insight into the variability of the $^{187}Re/^{188}Os$ in sediments as organic matter. The $^{187}Re/^{188}Os$ values for staithes seawater (2790.6 ± 49.7) falls somewhere between open ocean (4270; Anbar et al., 1992; Colodner et al., 1993a; Sharma et al., 1997; Levasseur et al., 1998; Woodhouse et al., 1999; Peucker-Ehrenbrink and Ravizza, 2000) and riverine (227; Colodner et al., 1993b; Sharma and Wasserburg, 1997; Levassuer et al., 1999; Peucker-Ehrenbrink and Ravizza, 2000) estimates, as expected for estuarine conditions. However, the $^{187}Re/^{188}Os$ values of macroalgae from this study (34794.1 ± 2074.4) are far higher suggesting that the $^{187}Re/^{188}Os$ ratios in macroalgae are not proportional to the seawater in which they live, but controlled by the uptake mechanism(s) of macroalgae that are currently unknown.

To date, it is known that the Re abundance in macroalgae can be highly variable (sub ppb to tens of ppb; Scadden, 1969; Yang, 1991; Mas et al., 2005; Prouty et al., 2014; Racionero-Gómez et al., 2016; Rooney et al., 2016). For osmium, the results thus far also indicate that the Os abundance in macroalgae can also be highly variable (this study; Rooney et al., 2016). Further, in addition to macroalgae that are components of sediment organic matter, microorganisms can also accumulate Re (Mashkani et al., 2009; Ghazvini and Mashkani, 2009; Prouty et al., 2014), although to date, no data exists for osmium. Given the variability of Re and Os uptake by macroalgae, the $^{187}Re/^{188}Os$ composition of macroalgae is seen to range from ~10 to ~35,000 (this study; Rooney et al., 2016). Metabolically inactive (i.e. dead) macroalgae (*F. vesiculosus*) does not appreciably accumulate rhenium (Racionero-Gómez et al., 2016). If Os in metabolically inactive macroalgae and/or microorganisms is not accumulated or released, then the Re and Os abundance, and isotope composition could be dominantly controlled by the abundance, variability, and the structural type of the organisms preserved in a sediment as organic matter rather than purely sequestration at the sediment–water interface (Yamashita et al., 2007 and references therein). As such, organic matter and organic type, in addition to the depositional setting conditions (Yamashita et al., 2007; Georgiev et al., 2011), maybe important factors in controlling Re/Os fractionation observed in organic-rich sediments (Cumming et al., 2012; Harris et al., 2012).

A further implication of the uptake of Re and Os by organisms could be its effect on the Re–Os organic-rich sedimentary geochronology. In addition to the Re–Os isotope system remaining undisturbed and for the samples to possess a range in $^{187}Re/^{188}Os$ values, the stratigraphic interval must possess similar initial $^{187}Os/^{188}Os$ values to provide reliable (accurate and precise) dates of sediment deposition (Cohen et al., 1999; Selby and Creaser, 2003). As such the heterogenous mixing of organisms with variable $^{187}Os/^{188}Os$ compositions in a sedimentary rock could hamper the ability to yield precise Re–Os dates. This could be particularly problematic in nearshore depositional settings of organic-rich sediments. For example, in a estuarine or deltaic sedimentary system the $^{187}Os/^{188}Os$ composition is variable along its transect (Levasseur et al., 2000; Martin et al., 2001; Sharma et al., 2007). Further, macroalgae from Greenland within Disko Bay show a 0.05 difference in their $^{187}Os/^{188}Os$ composition (Rooney et al., 2016). As such, organisms along the transect may also have variable $^{187}Os/^{188}Os$ compositions. Therefore any heterogeneous mixing of organisms that are preserved as organic matter within a sediment with different $^{187}Os/^{188}Os$ compositions could impact on the precision of Re–Os organic-rich sedimentary geochronology.

5. CONCLUSIONS

Culture experiments indicate that macroalgae acquires the $^{187}Os/^{188}Os$ composition of the media in which it grows. As a result this suggests that macroalgae are a viable biological proxy to determine the $^{187}Os/^{188}Os$ composition of seawater in various oceanographic settings. Specifically in coastal settings the $^{187}Os/^{188}Os$ composition of macroalgae could be used to assess the $^{187}Os/^{188}Os$ composition of continental input into the ocean.

ACKNOWLEDGEMENTS

We wish to express special thanks to Dr Joanna Hesselink for technical support and to John Bothwell and the Faculty of Biological Sciences of Durham for the laboratory support. We are very grateful to OEA Labs Ltd for funding the project and DS acknowledges the Total Endowment Fund. Nancy Prouty is thanked for her constructive comments, as are the remarks of two GCA reviewers, which helped improve this manuscript.

REFERENCES

Anbar A. D., Creaser R. A., Papanastassiou D. A. and Wasserburg G. J. (1992) Rhenium in seawater: confirmation of generally conservative behavior. *Geochim. Cosmochim. Acta* **56**, 4099–4103.

Banner J. L. (2004) Radiogenic isotopes: systematics and applications to earth surface processes and chemical stratigraphy. *Earth Sci. Rev.* **65**, 141–194. http://dx.doi.org/10.1016/S0012-8252(03)00086-2.

Birck J. L., Roy-Barman M. and Capmas F. (1997) Re–Os isotopic measurements at the femtomole level in natural samples. *Geostand. Newslett.* **20**, 19–27. http://dx.doi.org/10.1111/j.1751-908X.1997.tb00528.x.

Bryan G. W. (1983) Brown seaweed, *Fucus vesiculosus*, and the gastropod, *Littorina littoralis*, as indicators of trace-metal availability in estuaries. *Sci. Total Environ.* **28**, 91–104. http://dx.doi.org/10.1016/S0048-9697(83)80010-2.

Carlson L. (1991) Seasonal variation in growth, reproduction and nitrogen content of *Fucus vesiculosus* in the Öresund, Southern Sweden. *Bot. Mar.* **34**, 447–453. http://dx.doi.org/10.1515/botm.1991.34.5.447.

Chapman V. and Chapman D. (1980) *Seaweeds and their uses*, 3rd ed., New York.

Chen C. and Sharma M. (2009) High precision and high sensitivity measurements of osmium in seawater. *Anal. Chem.* **81**, 5400–5406. http://dx.doi.org/10.1021/ac900600e.

Cohen A. S., Coe A. L., Barlett J. M. and Hawkesworth C. J. (1999) Precise Re–Os ages of organic-rich mudrocks and the Os isotope composition of Jurassic seawater. *Earth Planet. Sci. Lett.* **167**, 159–173. http://dx.doi.org/10.1016/S0012-821X(99)00026-6.

Cohen A. S., Coe A. L., Harding S. M. and Schwark L. (2003) Osmium isotope evidence for the regulation of atmospheric CO_2 by continental weathering. *Geol. Soc. Am.* **32**, 157–160. http://dx.doi.org/10.1130/G20158.1.

Cohen A. S. and Waters F. C. (1996) Separation of osmium from geological materials by solvent extraction for analysis by thermal ionisation mass spectrometry. *Anal. Chim. Acta* **332**, 269–275. http://dx.doi.org/10.1016/0003-2670(96)00226-7.

Colodner D. C., Boyle E. A. and Edmond J. M. (1993a) Determination of rhenium and platinum in natural waters and sediments, and iridium in sediments by flow injection isotope dilution inductively coupled plasma mass spectrometry. *Anal. Chem.* **65**, 1419–1425.

Colodner D., Sachs J., Ravizza G., Turekian K. K., Edmond J. and Boyle E. (1993b) The geochemical cycle of rhenium: a reconnaissance. *Earth Planet. Sci. Lett.* **117**, 205–221.

Cotton F. G. and Wilkinson G. (1988) *Advanced Inorganic Chemistry*, 5th ed. J. Wiley & Sons.

Creaser R. A., Papanastassiou D. A. and Wasserburg G. J. (1991) Negative thermal ion mass spectrometry of osmium, rhenium and iridium. *Geochim. Cosmochim. Acta* **55**, 397–401. http://dx.doi.org/10.1016/0016-7037(91)90427-7.

Cumming V. M., Selby D. and Lillis P. G. (2012) Re–Os geochronology of lacustrine organic-rich sedimentary rocks: insights into direct depositional dating of lacustrine successions. Re–Os systematics and paleocontinental weathering. *Earth Planet. Sci. Lett.* **359–360**, 194–205. http://dx.doi.org/10.1016/j.epsl.2012.10.012.

Cumming V. M., Poulton S. W., Rooney A. D. and Selby D. (2013) Anoxia in the terrestrial environment during the Late Mesoproterozoic. *Geology*. http://dx.doi.org/10.1130/G34299.1.

Davis T. A., Volesky B. and Mucci A. (2003) A review of the biochemistry of heavy metal biosorption by brown algae. *Water Res.* **37**, 4311–4330. http://dx.doi.org/10.1016/S0043-1354(03)00293-8.

Davy de Virville A. and Feldmann J. (1961) *IV International Symposium on Seaweed*. Pergamon Press, Biarritz.

Fuge R. and James K. H. (1973) Trace metal concentrations in brown seaweeds, Cardigan Bay, Wales. *Mar. Chem.* **1**, 281–293. http://dx.doi.org/10.1016/0304-4203(73)90018-2.

Gannoun A. and Burton K. W. (2014) High precision osmium elemental and isotope measurements of North Atlantic seawater. *J. Anal. Atom. Spectrom.* **29**, 2330–2342. http://dx.doi.org/10.1039/c4ja00265b.

Georgiev S., Stein H. J., Hannah J. L., Bingen B., Weiss H. M. and Piasecki S. (2011) Hot acidic Late Permian seas stifle in record time. *Earth Planet. Sci. Lett.* **310**, 389–400. http://dx.doi.org/10.1016/j.epsl.2011.08.010.

Graham L. E. and Wilcox L. W. (2000) *Algae*. United States of America.

Ghazvini P. T. M. and Mashkani S. G. (2009) Screening of bacterial cells for biosorption of oxyanions: application of micro-PIXE for measurement of biosorption. *Hydrometallurgy* **96**, 246–252. http://dx.doi.org/10.1016/j.hydromet.2008.10.012.

Gustow L., Rahman M. M., Bartl K., Saborowski R., Bartsch I. and Wiencke C. (2014) Ocean acidification affects growth but not nutritional quality of the seaweed *Fucus vesiculosus* (Phaeophyceae, Fucales). *J. Exp. Mar. Biol. Ecol.* **453**, 84–90. http://dx.doi.org/10.1016/j.jembe.2014.01.005.

Harris N. B., Mnich C. A., Selby D. and Korn D. (2012) Minor and trace element and Re–Os chemistry of the upper Devonian woodford shale, permian basin, West Texas: insights into metal abundance and basin processes. *Chem. Geol.* **356**, 76–93. http://dx.doi.org/10.1016/j.chemgeo.2013.07.018.

Hiscock S. (1991) Brown seaweeds. A field key to the British, Shrewsbury, Montford Bridge.

Horta-Puga G., Cházaro-Olvera S., Winfield I., Avila-Romero M. and Moreno-Ramírez M. (2013) Cadmium, copper and lead in macroalgae from Veracruz Reef System, Gulf of Mexico: spatial distribution and rainy season variability. *Mar. Pollut. Bull.* **68**, 127–133. http://dx.doi.org/10.1016/j.marpolbul.2012.12.008.

Karez C. S., Magalhaes V. F., Pfeiffer W. C. and Amado Filho G. M. (1994) Trace metal accumulation by algae in Sepetiba Bay, Brasil. *Environ. Pollut.* **83**, 351–356. http://dx.doi.org/10.1016/0269-7491(94)90157-0.

Levasseur S., Birck J.-L. and Allègre C. J. (1998) Direct measurement of femtomoles of osmium and the $^{187}Os/^{186}Os$ ratio in seawater. *Science* **282**, 272–274. http://dx.doi.org/10.1126/science.282.5387.272.

Levassuer S., Birck J.-L. and Allègre C. J. (1999) The osmium riverine flux and the oceanic mass balance of osmium. *Earth Planet. Sci. Lett.* **174**, 7–23.

Levasseur S., Rachold V., Birck J. L. and Allègre C. J. (2000) Osmium behavior in estuaries: the Lena River example. *Earth Planet. Sci. Lett.* **177**(3–4), 227–235. http://dx.doi.org/10.1016/S0012-821X(00)00049-2.

Lobban C. S. and Harrison P. J. (1994) *Seaweed Ecology and Physiology*. Press Syndicate of the University of Cambridge, Cambridge University.

Lyngby J. E. and Brix H. (1982) Seasonal and environmental variation in cadmium, copper, lead and zinc concentrations in eelgrass (*Zostera marina* L.) in the Limfjor, k Denmark. *Aquat. Bot.* **14**, 59–74. http://dx.doi.org/10.1016/0304-3770(82)90086-9.

Martin C. E., Peucker-Ehrenbrink B., Brunskill G. and Szymczak R. (2001) Osmium isotope geochemistry of a tropical estuary. *Geochim. Cosmochim. Acta* **65**(19), 3193–3200.

Mas J. L., Tagami K. and Uchida S. (2005) Rhenium measurements on North Atlantic seaweed samples by ID-ICP-MS: an observation on the Re concentration factors. *J. Radioanal. Nucl. Chem.* **265**, 361–365. http://dx.doi.org/10.1007/s10967-005-0833-3.

Mashkani S. G., Ghazvini P. T. M. and Aligol D. A. (2009) Uptake of Re(VII) from aqueous solutions by *Bacillus* sp. GT-83-23. *Bioresour. Technol.* **100**, 603–608. http://dx.doi.org/10.1016/j.biortech.2008.06.065.

Morries A. W. and Bale A. J. (1975) The accumulation of cadmium, copper, manganese and zinc by *Fucus vesiculosus* in the Bristol Channel. *Estuar. Coast. Mar. Sci.* **3**, 153–163. http://dx.doi.org/10.1016/0302-3524(75)90018-3.

Nowell G. M., Luguet A., Pearson D. G. and Horstwood M. A. (2008) Precise and accurate $^{186}Os/^{188}Os$ and $^{187}Os/^{188}Os$ measurements by multi-collector plasma ionisation mass spectrometry (MC-ICP-MS) part I: solution analyses. *Chem. Geol.* **248**, 363–393. http://dx.doi.org/10.1016/j.chemgeo.2007.10.020.

Palmer M. R., Falkner K. K., Turekian K. K. and Calvert S. E. (1988) Sources of osmium isotopes in manganese nodules. *Geochim. Cosmochim. Acta* **52**, 1197–1202. http://dx.doi.org/10.1016/0016-7037(88)90274-8.

Peucker-Ehrenbrink B. and Ravizza G. (2000) The marine osmium isotope record. *Terra Nova* **12**, 205–219. http://dx.doi.org/10.1046/j.1365-3121.2000.00295.x.

Peucker-Ehrenbrink B. and Jahn B.-M. (2001) Rhenium–osmium isotope systematics and platinum group element concentrations: loess and the upper continental crust. *Geochem. Geophys. Geosyst.* **2**, Paper number 2001GC000172.

Prouty N. G., Roark E. B., Koenig A., Demopoulos A. W., Batista F. C., Kocar B. D., Selby D., McCarthy M. D. and Mienis F. (2014) Deep-sea coral record of human impact on watershed quality in the Mississippi River Basin. *Global Biochem. Cycles* **28**. http://dx.doi.org/10.1002/2013GB004754.

Racionero-Gómez B., Sproson A. D., Selby D., Gröcke D. R., Redden H. and Greenwell H. C. (2016) Rhenium uptake and distribution in Phaeophyceae macroalgae, *Fucus vesiculosus*. *R. J. Interface: R. Soc. Open Sci.* **3**, 160161. http://dx.doi.org/10.1098/rsos.160161.

Ragan M. A., Smidsrod O. and Larsen B. (1979) Chelation of divalent metal ions by brown algal polyphenols. *Mar. Chem.* **7**, 265–271. http://dx.doi.org/10.1016/0304-4203(79)90043-4.

Rainbow P. S. and Phillips D. J. H. (1993) Cosmopolitan biomonitors of trace metals. *Mar. Pollut. Bull.* **26**, 593–601. http://dx.doi.org/10.1016/0025-326X(93)90497-8.

Raize O., Argaman Y. and Yannai S. (2004) Mechanisms of biosorption of different heavy metals by brown marine macroalgae. *Biotechnol. Bioeng.* **87**, 451–458. http://dx.doi.org/10.1002/bit.20136.

Rawson P. F. and Wright J. K. (2000) The Yorkshire Coast. Geologists' Association Guide No. 34. The Geologists' Association, Burlington House, Piccadilly, London. 130pp. With contributions by Starmer I.C. Whitham F. and Hemingway J.E. The Third Revised Edition, edited by Greensmith J.T.

Riget F., Johansen P. and Asmund G. (1995) Natural seasonal variation of vadmium, copper, lead and zinc in brown seaweed (*Fucus vesiculosus*). *Mar. Pollut. Bull.* **30**, 409–413. http://dx.doi.org/10.1016/0025-326X(95)99847-W.

Rooney A. D., Selby D., Lloyd J. M., Roberts D. H., Lückge A., Sageman B. B. and Prouty N. G. (2016) Tracking millennial-scale Holocene glacial advance and retreat using osmium isotopes: insights from the Greenland Ice Sheet. *Quatern. Sci. Rev.* **138**, 49–61. http://dx.doi.org/10.1016/j.quascirev.2016.02.021.

Scadden E. M. (1969) Rhenium: its concentration in Pacific Ocean surface waters. *Geochim. Cosmochim. Acta* **33**(5), 633–637. http://dx.doi.org/10.1016/0016-7037(69)90019-2.

Selby D. and Creaser R. A. (2003) Re–Os geochronology of organic rich sediments: an evaluation of organic matter analysis methods. *Chem. Geol.* **200**, 225–240. http://dx.doi.org/10.1016/S0009-2541(03)00199-2.

Sharma M., Papanastassiou D. A. and Wasserbug G. J. (1997) The concentration and isotopic composition of osmium in the oceans. *Geochim. Cosmochim. Acta* **61**, 3287–3299. http://dx.doi.org/10.1016/S0016-7037(97)00210-X.

Sharma M. and Wasserburg G. J. (1997) Osmium in the rivers. *Geochim. Cosmochim. Acta* **6**, 5411–5416.

Sharma M., Balakrishna K., Hofmann A. W. and Shankar R. (2007) The transport of osmium and strontium isotopes through a tropical estuary. *Geochim. Cosmochim. Acta* **71**, 4856–4867. http://dx.doi.org/10.1016/j.gca.2007.08.004.

Sharma M., Chen C. and Blazina T. (2012) Osmium contamination of seawater samples stored in polyethylene bottles. *Limnol. Oceanogr. Methods* **10**, 618–630. http://dx.doi.org/10.4319/lom.2012.10.618.

Strömgren T. (1977) Short-term effect of temperature upon the growth of intertidal Fucales. *J. Exp. Mar. Biol. Ecol.* **29**. http://dx.doi.org/10.1016/0022-0981(77)90047-8.

Völkening J., Walczyk T. and Heumann K. G. (1991) Osmium isotope ratio determinations by negative thermal ion mass spectrometry. *Int. J. Mass Spectrom.* **105**, 147–159.

Wedepohl K. H. (1995) The composition of the continental crust. *Geochim. Cosmochim. Acta* **59**, 1217–1232. http://dx.doi.org/10.1016/0016-7037(95)00038-2.

White N. (2008) *Fucus vesiculosus*. Bladder wrack. In *Plymouth: Marine Biological Association of the United Kingdom* (eds. M.L. I.N.B.a.S.K.I.S.-p.) (on-line).

Woodhouse O. B., Ravizza G., Kenison Falker K., Statham P. J. and Peucker-Ehrenbrik B. (1999) Osmium in seawater: vertical profiles of concentration and isotopic composition in the eastern Pacific Ocean. *Earth Planet. Sci. Lett.* **173**, 223–233.

Yang J. S. (1991) High rhenium enrichment in brown algae: a biological sink of rhenium in the sea? *Hydrobiologia* **211**, 165–170. http://dx.doi.org/10.1007/BF00008532.

Yamashita Y., Takahashi Y., Haba H., Enomoto S. and Shimizu H. (2007) Comparison of reductive accumulation of Re and Os in seawater–sediment systems. *Geochim. Cosmochim. Acta* **71**, 3458–3475. http://dx.doi.org/10.1016/j.gca.2007.05.003.

Associate editor: Richard J. Walker

Journal of Applied Phycology

Monitoring nitrogen pollution using the transplantation of isotopically distinct macroalgae

--Manuscript Draft--

Manuscript Number:	
Full Title:	Monitoring nitrogen pollution using the transplantation of isotopically distinct macroalgae
Article Type:	Original Research
Keywords:	Nitrogen; Isotopes; Pollution; Environmental monitoring; Macroalgae; Seaweed
Corresponding Author:	Darren Richard Gröcke Durham University Durham, County Durham UNITED KINGDOM
Corresponding Author Secondary Information:	
Corresponding Author's Institution:	Durham University
Corresponding Author's Secondary Institution:	
First Author:	Darren Richard Gröcke
First Author Secondary Information:	
Order of Authors:	Darren Richard Gröcke
	Blanca Racionero-Gómez
	James W. Marschalek
	Chris Greenwell
Order of Authors Secondary Information:	
Funding Information:	
Abstract:	Macroalgae (seaweed) has been used as a biomonitor of nitrogen pollution through the use of nitrogen isotope ratios. Due to the complexity of flow patterns and inputs into river and estuarine settings, the use of indigenous macroalgae has proven difficult. In this study, we employed a method of transplanting (i.e. relocating) macroalgae from an isotopically distinct coastal location to the field work area, an industrialized estuary with problematic algae species growth, to determine whether the transplanted macroalgae can record spatial difference in the sources of nitrogen nutrients. In addition, a laboratory-controlled study used the same coastal macroalgae to determine the uptake of nitrate and ammonia under different concentrations. Nitrate, in comparison to ammonia, was taken up more rapidly in the lab experiment in that within 13 days the macroalgae tips were in isotopic equilibrium with the nitrate solution at 500 μM. The transplantation study showed that the nitrogen isotope signature of macroalgae shifted 50% within 7 days, but there were uptake differences depending on the depth at which the macroalgae was placed. This study shows that the transplantation of macroalgae with isotopically distinct signatures can be used as a rapid, cost efficient method for nitrogen biomonitoring in estuary environments.

Monitoring nitrogen pollution using the transplantation of isotopically distinct macroalgae

Darren R. Gröcke • Blanca Racionero-Gómez • James W. Marschalek • H. Chris Greenwell

Department of Earth Sciences, Durham University, Durham, DH1 3LE, UK

d.r.grocke@durham.ac.uk

Abstract Macroalgae (seaweed) has been used as a biomonitor of nitrogen pollution through the use of nitrogen isotope ratios. Due to the complexity of flow patterns and inputs into river and estuarine settings, the use of indigenous macroalgae has proven difficult. In this study, we employed a method of transplanting (i.e. relocating) macroalgae from an isotopically distinct coastal location to the field work area, an industrialized estuary with problematic algae species growth, to determine whether the transplanted macroalgae can record spatial difference in the sources of nitrogen nutrients. In addition, a laboratory-controlled study used the same coastal macroalgae to determine the uptake of nitrate and ammonia under different concentrations. Nitrate, in comparison to ammonia, was taken up more rapidly in the lab experiment in that within 13 days the macroalgae tips were in isotopic equilibrium with the nitrate solution at 500 µM. The transplantation study showed that the nitrogen isotope signature of macroalgae shifted 50% within 7 days, but there were uptake differences depending on the depth at which the macroalgae was placed. This study shows that the transplantation of macroalgae with isotopically distinct signatures can be used as a rapid, cost efficient method for nitrogen biomonitoring in estuary environments.

Keywords Nitrogen • Isotopes • Pollution • Environmental monitoring • Macroalgae • Seaweed

Introduction

Stable isotope ratios are an excellent tool with which to discern or ascertain modern biological, ecological and environmental processes. The modern nitrogen cycle has been heavily influenced by human activity. Industrialization, sewage, groundwater and other wastes are normally more enriched in ^{15}N than seawater (Vizzini and Mazzola, 2004), although agricultural waste products are normally more depleted in ^{15}N (Heaton, 1986). Within a modern environmental setting nitrogen isotope values ($\delta^{15}N$) of marine sediments, marine organisms and macroalgae have been used as a biomonitor of nitrogen pollution/contamination (e.g., McClelland et al. 1997; Savage 2005).

$\delta^{15}N$ can be measured in 'dissolved inorganic nitrogen' (DIN) taken directly from the water (Deutsch et al. 2006; Korth et al. 2014). Unfortunately, in systems such as estuaries with very complex flow regimes, spot sampling does not always represent the true average concentrations as a result of high variability; it is also more time-consuming and costly to do isotopic analysis of DIN. To address this difficulty, nitrogen isotope ratios in macroalgal tissues are often utilised in attempts to discern sources of excess nutrients, assuming that macroalgae integrate a nitrogen signature representative of the external environment through a growing season (Costanzo et al. 2001, 2005; Savage and Elmgren 2004; Derse et al. 2007; Dailer et al. 2012).

When using nitrogen isotopes to monitor anthropogenic pollution, it is often assumed that macroalgae $\delta^{15}N$ values are representative of an integrated $\delta^{15}N$ value of nitrogen inputs over a time period. This implies that the $\delta^{15}N$ values of the source(s) are the sole contributors to the $\delta^{15}N$ of the macroalgae. However, this does not account for the potential for fractionation during nitrogen transformations in the water column, or in the processes of uptake and assimilation. Nitrogen uptake by macroalgae is influenced by morphological factors, metabolism, tissue type,

age and nutrition (e.g., Rosenberg and Ramus 1984; Pedersen 1994; Neori et al. 2004). Nitrogen is transported from the water through the cell membrane and assimilated into organic compounds, such as proteins (McGlathery et al. 1996). The $\delta^{15}N$ values recorded from macroalgae are also significantly altered due to the enrichment of nitrates in a river, as originally documented by Minagawa and Wada (1984), and more recently by Savage and Elmgren (2004), Savage (2005) and Viana et al. (2011). However, to more accurately interpret macroalgae $\delta^{15}N$, a good understanding of the fractionation processes taking place is required (Viana et al. 2011).

It has been suggested that variability in $\delta^{15}N$ due to isotopic fractionation may be an important factor controlling macroalgal tissue $\delta^{15}N$ (e.g., Viana and Bode 2015), as macroalgal $\delta^{15}N$ could be modified by environmental parameters such as oxygen concentration, microbe concentration, pH, temperature, light and DIN concentration (Raimonet et al. 2013; Jona-Lasinio et al. 2015). Furthermore, NH_4^+ is preferred to NO_3^- as a nitrogen source (Cohen and Fong 2005), so macroalgal $\delta^{15}N$ could be strongly influenced by a NH_4^+ signal independent of nitrates such that bacterial populations can affect $\delta^{15}N_{DIN}$ (Korth et al. 2014; Ochoa-Izaguirre and Soto-Jiménez 2015).

Riera (1998) and Riera et al. (2000) report that *Fucus* from natural (uncontaminated) sites have $\delta^{15}N$ values around ~ +6 ‰. Savage and Elmgren (2004) and Savage (2005) reported significant increases in $\delta^{15}N$ (greater than 7 ‰) from *Fucus* that were influenced by sewage pollution. Notwithstanding the subtle difference between each site, this could be explained simply by background oceanographic factors independent of human activity – hence, every site being investigated should be treated independently. Deutsch and Voss (2006) indicated that *in situ* incubation experiments in an unpolluted brackish location could be suitable as a simple monitoring tool, but the data was inconclusive for *Fucus vesiculosus*. Viana et al. (2011)

measured $\delta^{15}N$ in macroalgal tissues in coastal areas between 1990 and 2007 and found a decrease in $\delta^{15}N$ from ~ +8 ‰ to ~+5 ‰, which they related to a reduction in human activities and the level of contamination and/or other environmental factors.

In the present study, we aim to assess the usefulness of $\delta^{15}N$ in the macroalgae, *Fucus vesiculosus* (hereafter, *Fucus*) as a nitrogen pollution biomonitor. We use *Fucus* as it is near ubiquitous in United Kingdom coastal waters, and has been shown to be a macroalgae that show a link between the isotopic composition of the environment to that recorded in macroalgae. In the first instance, laboratory incubation experiments were done on non-fertile *Fucus* tips with different concentrations of nitrate and ammonia to determine the nitrogen isotope response. In addition, this study involved the translocation of non-fertile tips of *Fucus* from one site (Staithes, UK) that has an enriched ^{15}N signature to an industrial site (River Tees, UK), which has depleted ^{15}N signatures. The nitrogen isotope response of non-fertile *Fucus* tips in this case was used to determine whether short-term, or long-term, field experiments are required to assess nitrogen pollution. Overall, we aim to determine whether seaweed can be modified to give a signature significantly shifted from any environment where we may wish to deploy environmental monitoring.

Material and methods

Macroalgae Selection

Fucus belong to the brown macroalgae family Phaeophyceae. *Fucus* is commonly found along sheltered shores of the North Sea, Baltic Sea, Atlantic Ocean and Pacific Ocean. *Fucus* is a tethered macroalgae whose growth rate ranges between 0.05 – 0.8 cm/day and have a life span on the order of 3 – 5 years (Strömgren 1977; Carlson 1991). The species is annually episodic,

98 gonochoristic and highly fecund (i.e., prolific). Gametes are released into the seawater and the
99 eggs are fertilized externally to form a zygote that starts to develop as soon as it settles into a
100 substrate. The gametes are released from receptacles, which are found in the fertile tips of the
101 macroalgae. However, *Fucus* also have non-fertile tips that do not contain these structures and
102 are composed of a parenchymatous thallus (Hiscock 1991). The non-fertile tips of *Fucus* have a
103 significantly greater uptake of nitrogen (Savage and Elmgren 2004; Viana et al. 2015), and hence
104 non-fertile tips of *Fucus vesiculosus* were used in this study.
105
106 **Study Area**
107 Two sites were chosen for this study: Staithes, North Yorkshire, UK (54°33'N 00°47'W) and the
108 River Tees, Borough of Teeside, Middlesbrough, UK (54°35′20″N 1°11′15″W) (Fig. 1). Both
109 locations are affected by eutrophication processes. Staithes was selected as a non-industrial site
110 compared to the River Tees, which has extensive industrialization. The River Tees and estuary
111 have experienced intensive industrialization since the 1830's, predominantly through iron
112 manufacturing, ship building, engineering and, recently, the chemical industries. These factors
113 resulted in the estuary of the River Tees becoming one of the most heavily industrialized regions
114 of Britain. Consequently, the lower river became heavily polluted with excessive growth of
115 certain problem macroalgae (*Ulva* spp.) in specific locations of the river causing sandbar
116 accretion and loss of unique wading habitat. Fortunately, since the 1970's there have been major
117 steps taken to reduce the quantity of pollutants delivered to the river (i.e., a 70% reduction in
118 ammonia), which has resulted in a significant decline of macroalgae blooms.
119 *Fucus* non-fertile tips were collected from Staithes in July, August and September 2015 (Fig.
120 1). A random suite of samples from 2015 were used to culture *in situ* the macroalgae in the River

Tees at four specific sites, and heights in the water column; another part of the sample set were used for *in vitro* culturing using different nitrate and ammonia concentrations, and isotopically measured after three or 13 days. Moreover, in order to generate a background $\delta^{15}N$ value, *Fucus* growing in the River Tees were collected throughout 2015 during low and high tidal periods.

In Vitro Cultures

To investigate nitrogen uptake by *Fucus*, non-fertile tips (length = 1.5 cm; wet weight = 0.12 – 0.15 g) without visible microalgae (i.e., epiphytes) from Staithes were cultured in seawater — modified after Gustow et al. (2014). Ten tips were placed into separate 250 mL glass jars containing two mesh shelves. Four tips were placed in the bottom of the jar and three tips above each mesh layer (Fig. 2). All jars were filled with sterile, filtered (0.7 μm) seawater collected from Staithes. Each set of three jars were doped using a known volume of nitrate (HNO_3) or ammonia (NH_4OH). Doped seawater nitrogen concentrations in the cultures were 10 μM, 50 μM, 100 μM and 500 μM. Although diluting a solution rather than using a salt led to slight differences in salinity and pH, these effects were calculated as small enough to be considered negligible. It was also assumed that no other nutrients or trace metals were limiting, and that the water used had very little nitrogen in it initially. Identical tips incubated in just the filtered seawater were used as a control and record the 0 μM $\delta^{15}N$ values of the macroalgae.

To remove the effects of a closed atmospheric environment, all jars were loosely covered with lids to allow gaseous exchange with the atmosphere. No additional nutrients were added into the seawater, except that naturally occurring through gaseous exchange. The non-fertile tips inside the bottles were transferred into an incubator with a set light/dark rhythm of 16:8 h, light intensity of 125 μmol photons/m^2s^2 and a temperature of 11 ºC. For the ammonia and nitrate

144 solutions, after 3 days had elapsed half the tips were removed, weighed and then analyzed for
145 $\delta^{15}N$, with the remainder were weighed and processed after 13 days of incubation. The pH and
146 salinity of each jar was measured throughout the experiment.
147
148 ***In Situ* Cultures – River Tees**
149 In order to monitor changes in $\delta^{15}N$ in *Fucus* arising due to the industrial processes impacting the
150 estuary, non-fertile tips were collected and transferred from Staithes, where they were cultured *in*
151 *situ* at four buoy locations in the River Tees (Fig. 1). All non-fertile apical thallus tips (the
152 specimens) were kept in a plastic container filled with seawater from Staithes for transportation.
153 A random selection of these non-fertile tips was placed in nylon fruit bags and cable tied. Four
154 navigation buoys were used in this study, and at each buoy a chain weighed down by a 1 kg
155 weight was attached. The fruit bags, containing the non-fertile tips, were attached to the chain at
156 each buoy at two depths – 0.2 m and 1 m below the water surface. Two simultaneous *in situ*
157 experiments were undertaken at the same buoy location and heights, as detailed below.
158 At each depth two fruit bags were attached containing the two types of experiment: (i) a long-
159 term (continuous), denoted Experiment 1, and (ii) a short-term culturing experiment (Experiment
160 2). Experiment 1 used 200 non-fertile tips in total (i.e., 25 tips per fruit bag), with five tips
161 collected every seven days for isotopic analysis. Experiment 2 consisted of a total of 40 non-
162 fertile tips (i.e., five tips per fruit bag). After a week of *in situ* culturing all the tips of Experiment
163 2 were collected and replaced with fresh non-fertile tips collected from Staithes that same
164 morning. At the same time five non-fertile tips were collected from Experiment 1 (long-term) but
165 not replaced with fresh tips.
166

Nitrogen Isotope Analysis

Nitrogen isotope ratios were measured in the Stable Isotope Biogeochemistry Laboratory (SIBL) at Durham University. Each sample was oven-dried at 60 °C for 24 h and ground into a powder with an agate mortar and pestle. Aliquots of the powder, weighing between 1.3 mg and 1.6 mg were placed into tin capsules and stored in a desiccator prior to isotopic analysis. Homogenized non-fertile macroalgae tips were analyzed using a Costech Elemental Analyzer (ECS 4010) connected to a Thermo Scientific Delta V Advantage isotope ratio mass spectrometer. Nitrogen isotope ratios are reported in standard delta (δ) notation in per mil (‰) relative to nitrogen in atmospheric air. Data accuracy is monitored through routine analyses of in-house and international standards: the in-house standards are stringently calibrated against international standards (e.g., USGS 40, IAEA 600, IAEA N1, IAEA N2). Analytical uncertainty for $\delta^{15}N$ measurements is typically ± 0.1 ‰ for replicate analyses of in-house and international standards, and typically < 0.2 ‰ on replicate sample analysis. Total nitrogen was obtained as part of the isotopic analysis using an in-house standard (i.e., Glutamic Acid, 9.52 % N).

Results

In Vitro Cultures From Staithes (Nitrate)

The starting $\delta^{15}N$ value of the *Fucus* non-fertile tips in this experiment was +8.7 ‰ (Table 1). The longer the period of exposure to the introduced nitrate allowed the *Fucus* non-fertile tips to integrate the nitrogen isotope signature of the added solution. After culturing *Fucus* for 13 days under 500 µM of nitrate, the $\delta^{15}N$ values (+6.5 ‰ ± 0.2 ‰) of the tips are statistically similar to the $\delta^{15}N$ value of the nitrate solution used (+7.1 ‰ ± 0.4 ‰) (Fig. 3). Within three days the *Fucus* non-fertile tips only shifted ~ 1 ‰ (~ 50%) under a concentration of 500 µM.

190

191 ***In Vitro* Cultures From Staithes (Ammonia)**

192 The starting $\delta^{15}N$ value of the *Fucus* non-fertile tips in this experiment was +10.6 ‰ ± 0.1 ‰
193 (Table 2). After culturing *Fucus* non-fertile tips for 13 days under 500 µM of ammonia, the $\delta^{15}N$
194 values (+6.8 ‰ ± 0.2 ‰) are significantly different from the initial $\delta^{15}N$ value, but do not reach
195 the $\delta^{15}N$ value of the ammonia solution used (+2.4 ‰ ± 0.5 ‰) (Fig. 3). The 13-day experiment
196 at 500 µM only represents approximately 45% of isotopic exchange with the *Fucus* non-fertile
197 tips.

198

199 ***In Situ* Cultures from Staithes to River Tees (Short-Term and Long-Term Experiments)**

200 *Fucus* $\delta^{15}N$ measurements from Staithes 2015 (n = 27) had an average value of +10.0 ‰ ± 0.5 ‰
201 (Table 3). On the other hand, *Fucus* samples from the River Tees in 2015 (n = 94) samples
202 record an average $\delta^{15}N$ value of –1.7 ‰ ± 4.3 ‰ (Table 4), which is statistically different (p-
203 value < 0.001) to that from Staithes 2015. Dividing the *Fucus* samples into blades (–2.5 ‰ ± 4.2
204 ‰), fertile (–1.2 ‰ ± 3.9 ‰) and non-fertile tips (–1.6 ‰ ± 4.8 ‰) showed no statistically
205 significant difference between macroalgae sub-structures. Moreover, the non-fertile tips that
206 were collected from Staithes are statistically different (p-value < 0.05) from those recovered
207 from the River Tees buoys (short-term experiment, +4.1 ‰ ± 1.3 ‰; long-term experiment, +3.9
208 ‰ ± 1.7 ‰), although they do not reach the background levels of *Fucus* growing in the river (–
209 1.7 ‰) (Fig. 4, 5). The long-term *Fucus* non-fertile tips from Buoy 4 after 21 days reached the
210 closest to the average background $\delta^{15}N$ value of the River Tees. After seven days all the
211 transferred non-fertile tips had significantly depleted $\delta^{15}N$ values compared to their original
212 values from Staithes. Significant differences (p-value < 0.01) were observed for the short-term

Experiment 1 samples, depending on the depth that the macroalgae was placed at each buoy (Fig. 4). Significant differences (p-value < 0.01) were also observed for the long-term experiment depending on sample depth (Figure 5).

Discussion

Assessment of *Fucus* to Incorporate Nitrogen Isotope Sources

Many studies have been designed in order to elucidate if macroalgae $\delta^{15}N$ values are a reliable tracer of nitrogen pollution of the marine environment (Savage and Elmgren 2004; Lapointe and Bedford 2007; Piñón-Gimate et al. 2009; Carballeira et al. 2013; Ochoa-Izaguirre and Soto-Jiménez 2015; Wang et al. 2016). However, the direct link between anthropogenic nitrogen inputs and $\delta^{15}N$ values in macroalgae is still not fully understood. In most cases, macroalgae $\delta^{15}N$ values are inferred to be directly related to inorganic nitrogen inputs. Nevertheless, Viana and Bode (2013) analyzed $\delta^{15}N$ from macroalgae, nitrate and ammonia in different environments and concluded that it was not possible to establish a simple relationship between macroalgae $\delta^{15}N$ with the concentration and $\delta^{15}N$ value of nitrate and/or ammonia. Therefore, it was proposed by Viana and Bode (2013) that due to variability in inorganic nitrogen inputs, local environmental factors and coastal upwelling were all contributing to macroalgae $\delta^{15}N$ values. More recently, Swart et al. (2014) has shown that the concentration of nitrate has significant isotopic fractionation (up to 6 ‰) in a green and rhodophyte algae when on the order of 500 µM.

In this study, we show that *in vitro* cultures of *Fucus* grown under different concentrations of nitrate reach isotopic equilibrium at/or after 13 days (Fig. 3). However, the same experimental procedure with ammonia show that isotopic equilibrium was not reached after 13 days (Fig. 3). Consistent with observations that macroalgae with increased nutrient supply have elevated

uptake rates and increased tissue nutrient contents (Valiela et al. 1997; Fong et al. 2004), the cultures with higher nitrate/ammonium concentrations gained more nitrogen and became isotopically lighter than their lower concentration counterparts. Although this study shows a clear relationship between macroalgae $\delta^{15}N$ and source $\delta^{15}N$, this may not be true in a natural environment, as shown by the high degree of scatter in macroalgae $\delta^{15}N$ from the River Tees background dataset (–1.7 ‰ ± 4.3 ‰, Table 4).

In order to establish whether concentration dependent isotopic fractionation occurs, a simple two end-member mixing model was used as a first order approximation (Kaldy 2011). These end members comprised of the initial algal nitrogen pool ($\delta^{15}N$, depending on date) and the nitrate/ammonium added (with $\delta^{15}N$ values of +7.1 ‰ and +2.4 ‰ respectively). The following equation was used to model the mixing:

$$\delta_{sample} = \delta_{source1} \times f_1 + \delta_{source2} \times f_2$$

where, source 1 is the initial algal pool and source 2 is the added nitrogen source, with their relative fractions f_1 and f_2 such that $f_2 = 1 - f_1$. This was used to model the expected $\delta^{15}N$ of the sample if no fractionation was occurring. f values are calculated from the change in total nitrogen, with growth correction. The deviations from the expected values based on a simple mixing model should theoretically represent fractionation. Assuming this to be correct, the nitrate solutions appear to fractionate considerably, whereas the ammonium solutions appear to fractionate very little, even after 13 days at high concentrations (Fig. 3).

Transplantation of *Fucus* as a Nitrogen Isotope Biomonitor

Natural environments are more complex for identifying and tracing nitrogen pollution sources, depending on the isotopic source of the nitrogen, as well as complex organo-mineral interactions

and chemistry occurring in the water column – especially in a river-estuary setting where the salt-wedge of intruding sea water may result in colloid phenomena, such as flocculation. Since the background levels of $\delta^{15}N$ in *Fucus* are reported to be between +4 ‰ and +6 ‰ (e.g., Riera 1998; Riera et al. 2000; Savage and Elmgren 2004), the values observed in *Fucus* from Staithes (+10.0 ‰) and the River Tees (–1.7 ‰) indicate that different anthropogenic inputs of nitrogen have affected them. The more elevated values in Staithes in 2015 compared to 2014 (~ +8.5 ‰, Gröcke et al. unpublished data) may be related to a reported spillage in August 2015 of sludge from Hinderwell Wastewater Treatment Works into Dales beck at Dalehouse, near Staithes. In fact, the degree of variation (4.3 ‰) in $\delta^{15}N$ *Fucus* from the River Tees suggest that this area is affected by multiple nitrogen sources, which is also evident in the transplantation study discussed subsequently. Conversely, $\delta^{15}N$ values from Staithes *Fucus* are tightly constrained (0.5 ‰), suggesting a consistent nitrogen isotope source during collection in 2015. In areas with high natural variation in $\delta^{15}N$, *in situ* incubation of macroalgae can therefore be considered more representative of $\delta^{15}N_{DIN}$ than native macroalgae. This study therefore provides further support to previous research that has indicated that indigenous macroalgae are unsuitable for retrospective monitoring of nitrogen isotopes for pollution monitoring (Carballeira et al. 2014; Viana et al. 2015).

$\delta^{15}N$ values of *Fucus* samples from Staithes changed significantly within the first week of transplantation to the River Tees (Fig. 4). During the short-term transplantation experiment, nearly all non-fertile tips of *Fucus* isotopically shifted by 50% from the background value for Staithes towards the background value of the River Tees in 2015 (Fig. 4, Table 5). However, there are subtle differences between each week of transplantation and collection, between each buoy, and the depth of the samples in the water column. The *Fucus* bottom samples (1 m) did not

isotopically shift as much as the samples located at the top of the chain suspended from the buoy (20 cm). Overall, the range in isotopic exchange between the Staithes and River Tees background $\delta^{15}N$ values ranges from 30–80% using a simple two end-member mixing model. The depth variation observed in this transplantation study can be explained by:

(a) A depth stratification of nitrogen pollution sources. The River Tees has a tidal range of >5 m. However, compared to macroalgae growing on the banks and sea walls of the River Tees the buoy samples remained at the same water depths during the entire tidal cycle (i.e., 20 cm and 1 m). Therefore, the macroalgae at those depths experienced no periods above sea level, and maintained the same environmental conditions for certain parameters (light, temperature) through 24 h, though the relative depth profiles of fresh and saline water may change. The River Tees $\delta^{15}N$ data would suggest that surface waters were ^{15}N-depleted in comparison to deeper water. This is consistent with major industrial effluent discharges being released with fresh water, giving a relatively buoyant waste field (Warwick et al. 2002).

(b) Isotopic fractionation in macroalgae as a result of varying environmental parameters (e.g., salinity, light, temperature etc.) with depth and at different spatial points (buoys). Although fractionation processes in macroalgae are poorly understood, light levels appear to have the opposite effect to what was observed in the present study (Dudley et al. 2010).

For instance, Kim et al. (2013) suggest that periodically immersed *Porphyra umbilicalis* individuals have a higher $\delta^{15}N$ than ones that are continuously submerged. Furthermore, a drop in light levels could cause the more negative fractionation, especially if the nitrogen source is ammonia (Dudley et al. 2010). Few studies have been performed on the effects of other environmental parameters, but it is possible that these also contribute to the observed trend. Complexity in the system's nitrogen pools would be expected to be exacerbated in intertidal

macroalgae, as these are exposed to atmospheric inputs and other local edge effects Ochoa-Izaguirre and Soto-Jiménez 2015).

In this study area, the background noise in the $\delta^{15}N$ values appears to be very high. Suspending transplanted samples in the water column appears to remove most of this natural variation, allowing greater precision when monitoring pollutants on a small scale. It is also interesting to note that at Staithes, the standard deviation and range of $\delta^{15}N$ in *Fucus* non-fertile tips is small despite the fact that these samples were harvested from different positions on the shore face when exposed to the atmosphere. Combined with findings that sites exposed to higher nutrient levels have a higher seasonal variation, this could suggest that environmental controls on fractionation are far more important when nutrient levels are high (Carballeira et al. 2014; Wang et al. 2016).

A similar $\delta^{15}N$ offset between bottom and top buoy samples was also observed for the long-term transplantation experiment (Fig. 5). In fact, even after 21 days of incubation in the River Tees, the Staithes *Fucus* growing tips also show an isotopic exchange of between 30–80% using a simple two end-member mixing model. This is identical to the short-term transplantation experiment. However, some buoys did show a consistent change throughout the experimental period. For example, the top *Fucus* samples from Buoy 4 record a consistent shift towards the River Tees 2015 background $\delta^{15}N$ value of –1.7 ‰ (see Fig. 5, Table 6): 50 % change in the first 7 days, 20 % from day 7 to day 14; and 10 % from day 14 to day 21.

River Tees Spatial Trends

Due to the complexity of the River Tees with respect to flow patterns, nitrogen stratification and human activity (i.e., dredging) it is difficult to explain why this site (i.e., Buoy 4) and depth (i.e.,

top) is the only place to record a pattern expected through Rayleigh fractionation. Other sites, such as Buoy 1 top show a reverse trend through the 21-day transportation experiment (Figure 5). This suggests that the transplantation of non-fertile *Fucus* tips from Staithes would require longer than 21 days to equilibrate with the ambient $\delta^{15}N$ value for the River Tees. Viana et al. (2015) suggested a period of around 16 days would be required for a complete turnover of nitrogen in *F. vesiculosus*. However, the degree of isotopic change between Staithes and the River Tees are much larger than that applied in Viana et al. (2015), and hence the amount of isotopic change required in this study would be energetically demanding and unlikely to benefit the *Fucus* samples (see Raven 2003). Instead, the majority of the nitrogen transfer seems to have occurred by 7 days between the transplantation and collection (see Fig. 4, 5). This fairly rapid uptake and assimilation of the local nitrogen isotope signature into macroalgae suggests that it can be used as an efficient and cost-effective method to trace and monitor short-term nitrogen pollution sources.

Despite the macroalgal $\delta^{15}N$ being far less variable than in native populations, no clear trends in the $\delta^{15}N$ of transplanted tips are apparent along the river channel (see Fig. 1, 5). The seemingly random differences between buoys and weeks suggests local factors such as fluvial inputs, tides, drainage and upwelling could all be playing a minor role in the $\delta^{15}N$ values measured. Further complications include the positioning in the river; the buoys were on both the left and the right-hand sides of the channel (Fig. 1), thus the location the effluent enters the river and the flow patterns would prove to be very important. The major variation shown in Buoy 3 can be explained by human activity affecting the *Fucus* $\delta^{15}N$ values and the distinction between top and bottom samples is reversed (Fig. 5). During weeks 1 and 2 this part of the River Tees

was being dredged and hence would have well-mixed the water in this region and redistributed bottom-water nitrogen to the surface water.

Conclusions

In this study, we demonstrate that by relocating (transplantation) macroalgae from a site with elevated $\delta^{15}N$ values (i.e., Staithes) to a site that is affected by industrialization (low $\delta^{15}N$ values), the source of the nitrogen can be identified in macroalgae within seven days using nitrogen isotope analysis of non-fertile tips. Due to the rapid incorporation of nitrogen into the cellular structure of *Fucus* non-fertile tips this opens up the possibility for rapidly identifying pollution trends when using isotopically distinct macroalgae samples. This can be achieved using natural macroalgae samples where isotopically distinct samples can be obtained, like in this study, or macroalgae can be harvested from isotopically distinct solutions of nitrate or ammonia and then used in the field. Even though this application is less time consuming and cheaper there are several other aspects that require investigation:

(1) how do tidal cycles within rivers and estuaries affect the nitrogen isotope incorporation of nitrogen signals?

(2) are salt wedges and colloid formation, such as flocculation, important in nitrogen metabolism in macroalgae?

(3) is a 7 to 14-day transplantation study long enough to monitor nitrogen isotope inputs through a large section of a river (especially one that crosses a boundary between different nitrogen pollution inputs)?

ACKNOWLEDGMENTS

We are very grateful to OEA Labs Ltd and Durham University for providing funding to BRG and JWM. This research was kindly funded by a Durham University Seedcorn Fund to HCG (26.14.050200) and an MSc scholarship to BRG from OEA Labs Limited. Teeside Nautical Studies provided boats and assistance with the study and collecting the macroalgae. Special thanks to Trevor Forster (Principal & Advanced Powerboat Instructor at Teeside Nautical Studies), and Andrew Ridley (Conservancy Operations Manager at PD Teesport Ltd).

References

Carballeira C, Rey-Asensio A, Carballeira A (2014) Interannual changes in $\delta^{15}N$ values in *Fucus vesiculosus* L. Mar Poll Bull 85:141–145

Carballeira C, Viana IG, Carballeira A (2013) $\delta^{15}N$ values of macroalgae as an indicator of the potential presence of waste disposal from land-based marine fish farms. J Appl Phycol 25:97–107

Carlson L (1991) Seasonal variation in growth, reproduction and nitrogen content of *Fucus vesiculosus* in the Öresund, Southern Sweden. Bot Marina 34:447–453

Cohen RA, Fong P (2005) Experimental evidence supports the use of $\delta^{15}N$ content of the opportunistic green macroalgae *Enteromorpha intestinalis* (Chlorophyta) to determine nitrogen sources to estuaries. J Phycol 41:287–293

Costanzo SD, O'Donohue MJ, Dennison WC, Loneragan NR, Thomas M (2001) A new approach for detecting and mapping sewage impacts. Mar Poll Bull 42:149–156

Costanzo SD, Udy J, Longstaff B, Jones A (2005) Using nitrogen stable isotope ratios ($\delta^{15}N$) of macroalgae to determine the effectiveness of sewage upgrades: changes in the extent of sewage plumes over four years in Moreton Bay, Australia. Mar Poll Bull 51:212–217

Dailer ML, Smith JE, Smith CM (2012) Responses of bloom forming and non-bloom forming macroalgae to nutrient enrichment in Hawai'i, USA. Harmful Algae 17:111–125

Derse E, Knee KL, Wankel SD, Kendall C, Berg CJ, Paytan A (2007) Identifying sources of nitrogen to Hanalei Bay, Kauai, utilizing the nitrogen isotope signature of macroalgae. Environ Sci Tech 41:5217–5223

401 Deutsch B, Mewes M, Liskow I, Voss M (2006) Quantification of diffuse nitrate inputs to a
402 small river system using stable isotopes of oxygen and nitrogen in nitrate. Org Geochem
403 37:1333–1342

404 Deutsch B, Voss M (2006) Anthropogenic nitrogen input traced by means of $\delta^{15}N$ values in
405 macroalgae: results from in-situ incubation experiments. Sci Total Environ 366:799–808

406 Dudley BD, Barr NG, Shima JS (2010) Influence of light intensity and nutrient source on $\delta^{13}C$
407 and $\delta^{15}N$ signatures in *Ulva pertusa*. Aqua Biol 9:85–93

408 Fong P, Fong JJ, Fong CR (2004) Growth, nutrient storage, and release of dissolved organic
409 nitrogen by *Enteromorpha intestinalis* in response to pulses of nitrogen and phosphorus. Aq
410 Bot 78:83–95

411 Gustow L, Rahman MM, Bartl K, Saborowski R, Bartsch I, Wiencke C (2014) Ocean
412 acidification affects growth but not nutritional quality of the seaweed *Fucus vesiculosus*
413 (Phaeophyceae, Fucales). J Exp Mar Biol Ecol 453:84–90

414 Heaton THE (1986) Isotopic studies of nitrogen pollution in the hydrosphere and atmosphere: a
415 review. Chem Geol 59:87–102

416 Hiscock S (1991) *A Field Key to the British Brown Seaweeds (Phaeophyta)*; Field Studies
417 Council: Shrewsbury, UK

418 Jona-Lasinio G, Costantini ML, Calizza E, Pollice A, Bentivoglio F, Orlandi L, Careddu G,
419 Rossi L (2015) Stable isotope-based statistical tools as ecological indicator of pollution
420 sources in Mediterranean transitional water ecosystems. Ecol Indicat 55:23–31

421 Kaldy J (2011) Using a macroalgal $\delta^{15}N$ bioassay to detect cruise ship waste water effluent
422 inputs. Mar Poll Bull 62:1762–1771

423 Kim JK, Kraemer GP, Yarish C (2013) Emersion induces nitrogen release and alteration of
424 nitrogen metabolism in the intertidal genus Porphyra. PloS One 8:1–14

425 Korth, F.; Deutsch, B.; Frey, C.; Moros, C.; Voss, M. Nitrate source identification in the Baltic
426 Sea using its isotopic ratios in combination with a Bayesian isotope mixing model. *Biogeosci.*
427 **2014**, *11*, 4913–4924

428 Lapointe BE, Bedford BJ (2007) Drift rhodophyte blooms emerge in Lee County, Florida, USA:
429 Evidence of escalating coastal eutrophication. Harmful Algae 6:421–437

430 McClelland JW, Valiela I, Michener RH (1997) Nitrogen-stable isotope signatures in estuarine
431 food webs: A record of increasing urbanization in coastal watersheds. Limnol Oceanogr
432 42:930–937

McGlathery KJ, Pedersen MF, Borum J (1996) Changes in intracellular nitrogen pools and feedback controls on nitrogen uptake in *Chaetomorpha linum* (chlorophyta). J Phycol 32:393–401

Minagawa M, Wada E (1994) Stepwise enrichment of ^{15}N along food chains: further evidence and the relation between $\delta^{15}N$ and animal age. Geochim Cosmochim Acta 48:1135–1140

Neori A, Chopin T, Troell M, Buschmann AH, Kraemer GP, Halling C, Shpigel M, Yarish C (2004) Integrated aquaculture: rationale, evolution and state of the art emphasizing seaweed biofiltration in modem mariculture. Aquaculture 231:361–391

Ochoa-Izaguirre MJ, Soto-Jiménez MF (2015) Variability in nitrogen stable isotope ratios of macroalgae: consequences for the identification of nitrogen sources. J Phycol 51:46–65

Pedersen MF (1994) Transient ammonium uptake in the macroalga *Ulva lactuca* (Chlorophyta): nature, regulation, and the consequences for choice of measuring technique. J Phycol 30:980–986

Piñón-Gimate A, Soto-Jiménez M, Ochoa-Izaguirre MJ, García-Pagés E, Páez-Osuna F (2009) Macroalgae blooms and $\delta^{15}N$ in subtropical coastal lagoons from the Southeastern Gulf of California: discrimination among agricultural, shrimp farm and sewage effluents. Mar Poll 58:1144–1151

Raimonet M, Guillou G, Mornet F, Richard P (2013) Macroalgae $\delta^{15}N$ values in well-mixed estuaries: indicator of anthropogenic nitrogen input or macroalgae metabolism? Estuar Coast Shelf Sci 119:126–138

Raven JA (2003) Long-distance transport in non-vascular plants. Plant Cell Env 26:73–85

Riera P (1998) $\delta^{15}N$ of organic matter sources and benthic invertebrates along an estuarine gradient in Marennes-Oleron Bay (France): implications for the study of the trophic structure. Mar Ecol Prog Ser 166:143–150

Riera P, Stal LJ, Nieuwenhuize J (2000) Heavy $\delta^{15}N$ in intertidal benthic algae and invertebrates in the Scheldt Estuary (The Netherlands): effect of river nitrogen inputs. Estuar Coast Shelf Sci 51:365–372

Rosenberg G, Ramus J (1984) Uptake of inorganic nitrogen and seaweed surface-area-volume ratios. Aqua Bot 19:65–72

Savage C (2005) Tracing the influence of sewage nitrogen in a coastal ecosystem using stable nitrogen isotopes. Ambio 34:145–150

Savage C, Elmgren R (2004) Macroalgal (*Fucus vesiculosus*) $\delta^{15}N$ values trace decrease in sewage influence. Ecol Appl 14:517–526

466 Strömgren T (1977) Short-term effect of temperature upon the growth of intertidal fucales. J Exp
467 Mar Biol Ecol 29:181–195

468 Swart PK, Evans S, Capo T, Altabet MA (2014) The fractionation of nitrogen and oxygen
469 isotopes in macroalgae during the assimilation of nitrate. Biogeosci 11:6147–6157

470 Valiela I, McClelland J, Hauxwell J, Behr PJ, Hersh D, Foreman K (1997) Macroalgal blooms in
471 shallow estuaries: controls and ecophysiological and ecosystem consequences. Limnol
472 Oceanogr 42:1105–1118

473 Viana IG, Bode A (2013) Stable nitrogen isotopes in coastal macroalgae: geographic and
474 anthropogenic variability. Sci Total Env 443:887–895

475 Viana IG, Bode A (2015) Variability in $\delta^{15}N$ of intertidal brown algae along a salinity gradient:
476 Differential impact of nitrogen sources. Sci Total Env 512:167–176

477 Viana IG, Bode A, Bartholomew M, Valiela I (2015) Experimental assessment of the macroalgae
478 *Ascophyllum nodosum* and *Fucus vesiculosus* for monitoring N sources at different time-
479 scales using stable isotope composition. J Exp Mar Biol Ecol 466:24–33

480 Viana IG, Fernandez JA, Aboal JR, Carballeira A (2011) Measurement of $\delta^{15}N$ in macroalgae
481 stored in an environmental specimen bank for regional scale monitoring of eutrophication in
482 coastal areas. Ecol Indic 11:888–895

483 Vizzini S, Mazzola A (2004) Stable isotope evidence for the environmental impact of a land-
484 based fish farm in the western Mediterranean. Mar Poll 49:61–70

485 Wang Y, Liu D, Richard P, Di B (2016) Selection of effective macroalgal species and tracing
486 nitrogen sources on the different part of Yantai coast, China indicated by macroalgal $\delta^{15}N$
487 values. Sci Total Env 542:306–314

488 Warwick RM, Ashman CM, Brown AR, Clarke KR, Dowell B, Hart B, Lewis RE, Shillabeer N,
489 Somerfield PJ, Tapp JF (2002) Inter-annual changes in the biodiversity and community
490 structure of the macrobenthos in Tees Bay and the Tees estuary, UK, associated with local
491 and regional environmental events. Mar Ecol Prog Ser 234:1–13

492

Figure captions

Figure 1 Part map of the United Kingdom showing the two locations discussed in this study, River Tees, Middlesbrough, and Staithes, North Yorkshire.

Figure 2 Experimental set up for the *in vitro* cultures used for nitrate and ammonia solutions and non-fertile macroalgae tips from Staithes, UK.

Figure 3 $\delta^{15}N_{seaweed}$ results from the *in vitro* cultures of nitrate (top) and ammonia (bottom). Dashed grey line represents the $\delta^{15}N$ value of the nitrate and ammonia solutions used.

Figure 4 $\delta^{15}N_{seaweed}$ results from the *in situ* Experiment 1 (short-term) done in the River Tees, Middlesbrough, UK. For Buoy number locations refer back to Fig. 1. Bottom and top refer to the position on the rope at each buoy. The dashed grey line represents the 50:50 mass balance value between the $\delta^{15}N$ background value of *Fucus* non-fertile tips from Staithes and all components from the River Tees.

Figure 5 $\delta^{15}N_{seaweed}$ results from the *in situ* Experiment 2 (long-term) done in the River Tees, Middlesbrough, UK. For Buoy number locations refer back to Fig. 1. Bottom and top refer to the position on the rope at each buoy. The dashed grey line represents the 50:50 mass balance value between the $\delta^{15}N$ background value of *Fucus* non-fertile tips from Staithes and all components from the River Tees.

Figure 1

Click here to download colour figure Fig1_maps copy.tif

Figure 2

Click here to download colour figure Fig2_jars copy.tif

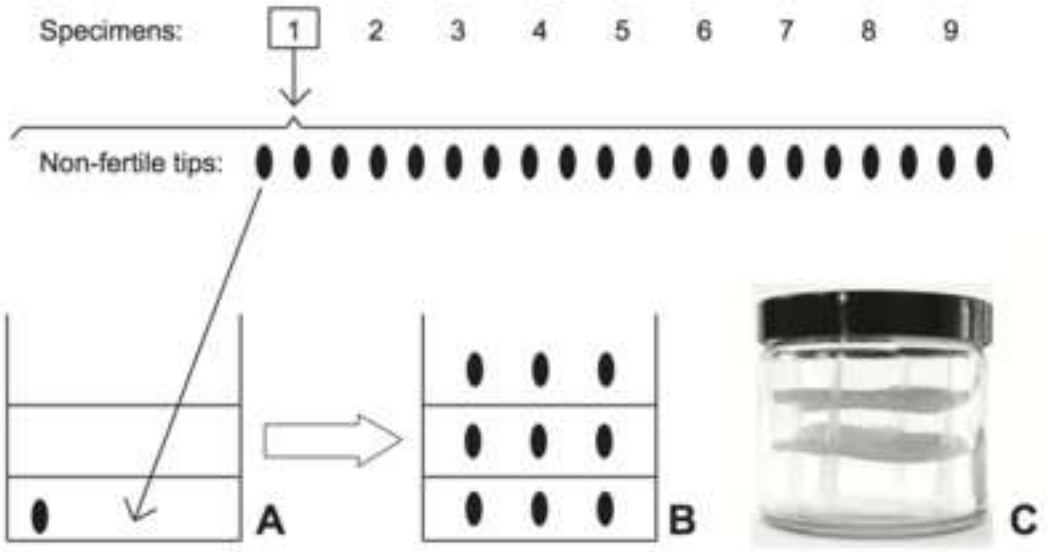

Figure 3

Click here to download colour figure Fig3_nitrate_ammonia copy.tif

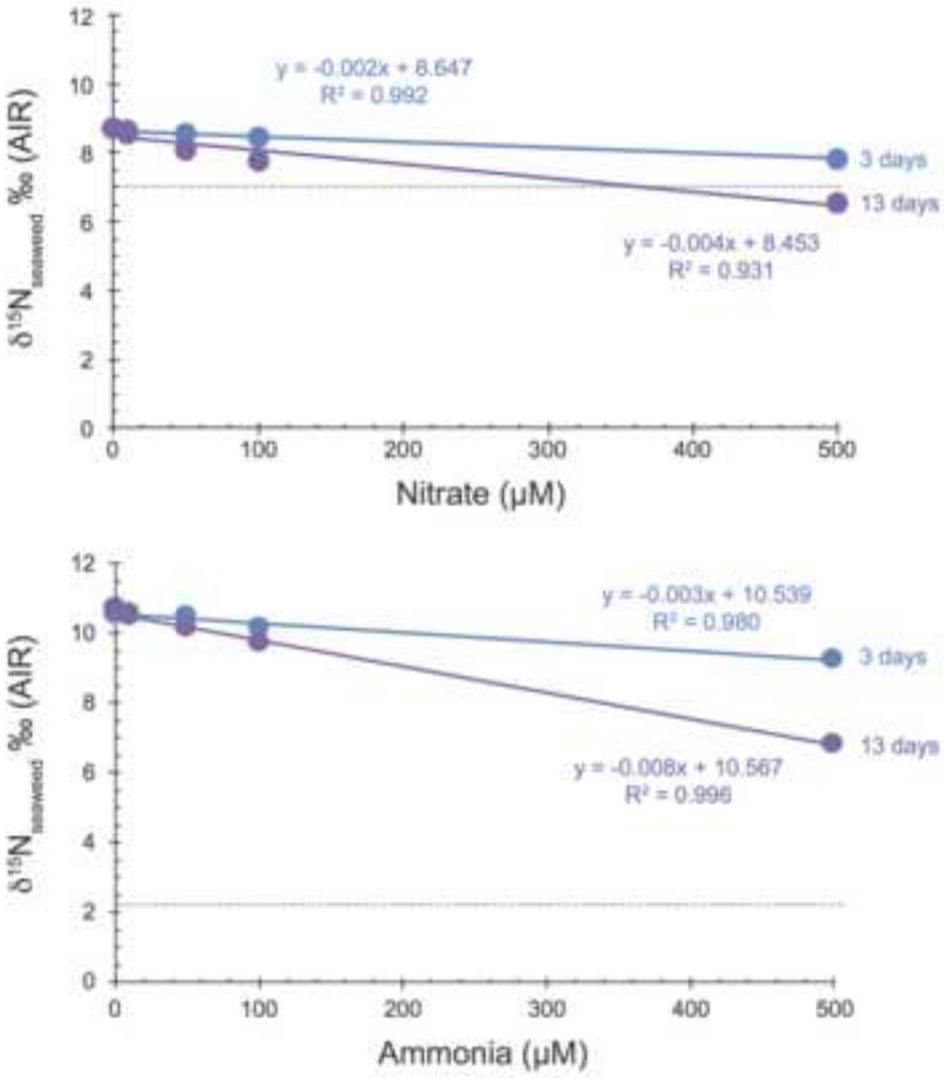

Figure 4

Click here to download colour figure Fig4_short_term copy.tif

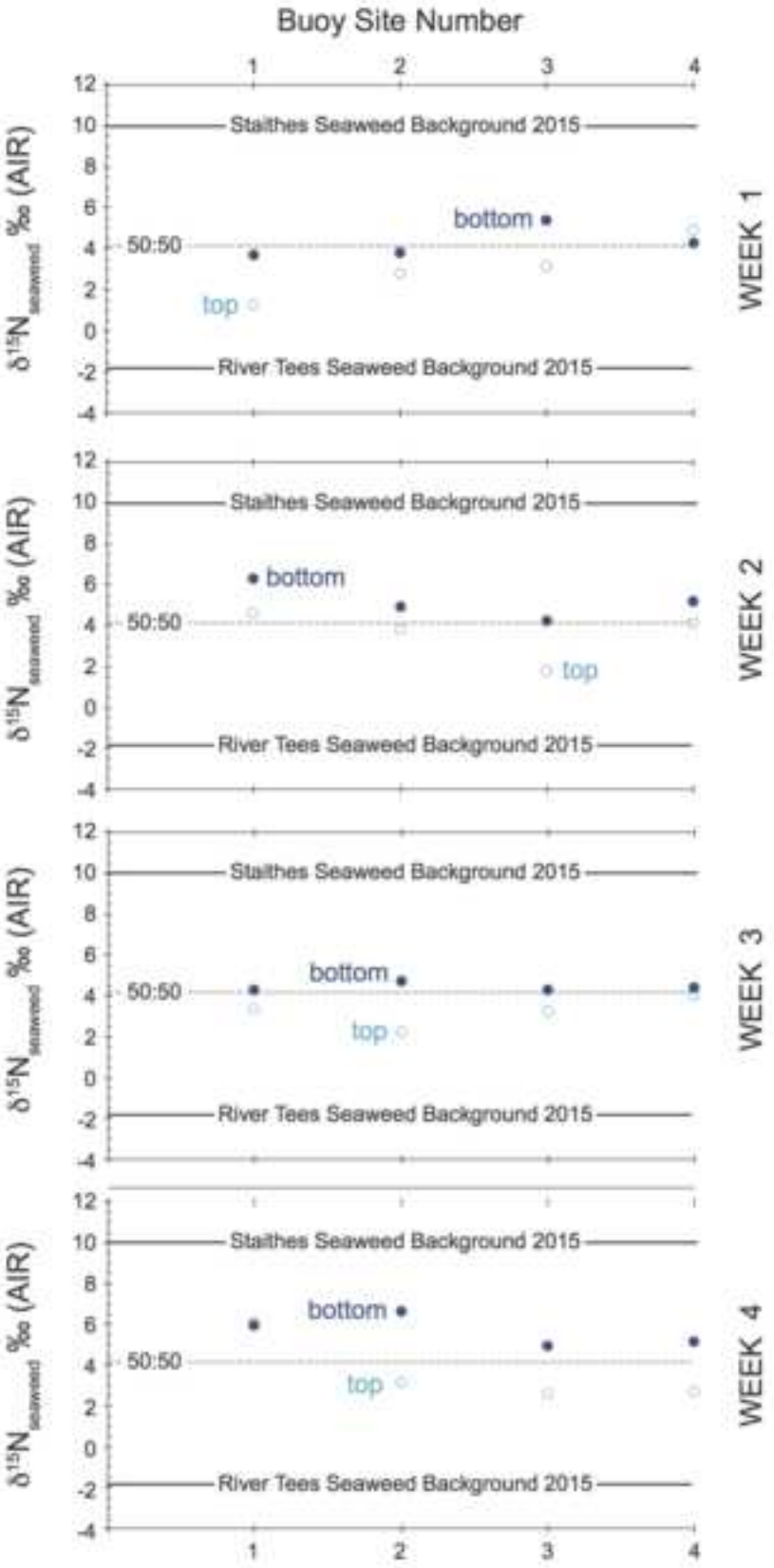

Figure 5

Click here to download colour figure Fig5_long_term copy.tif

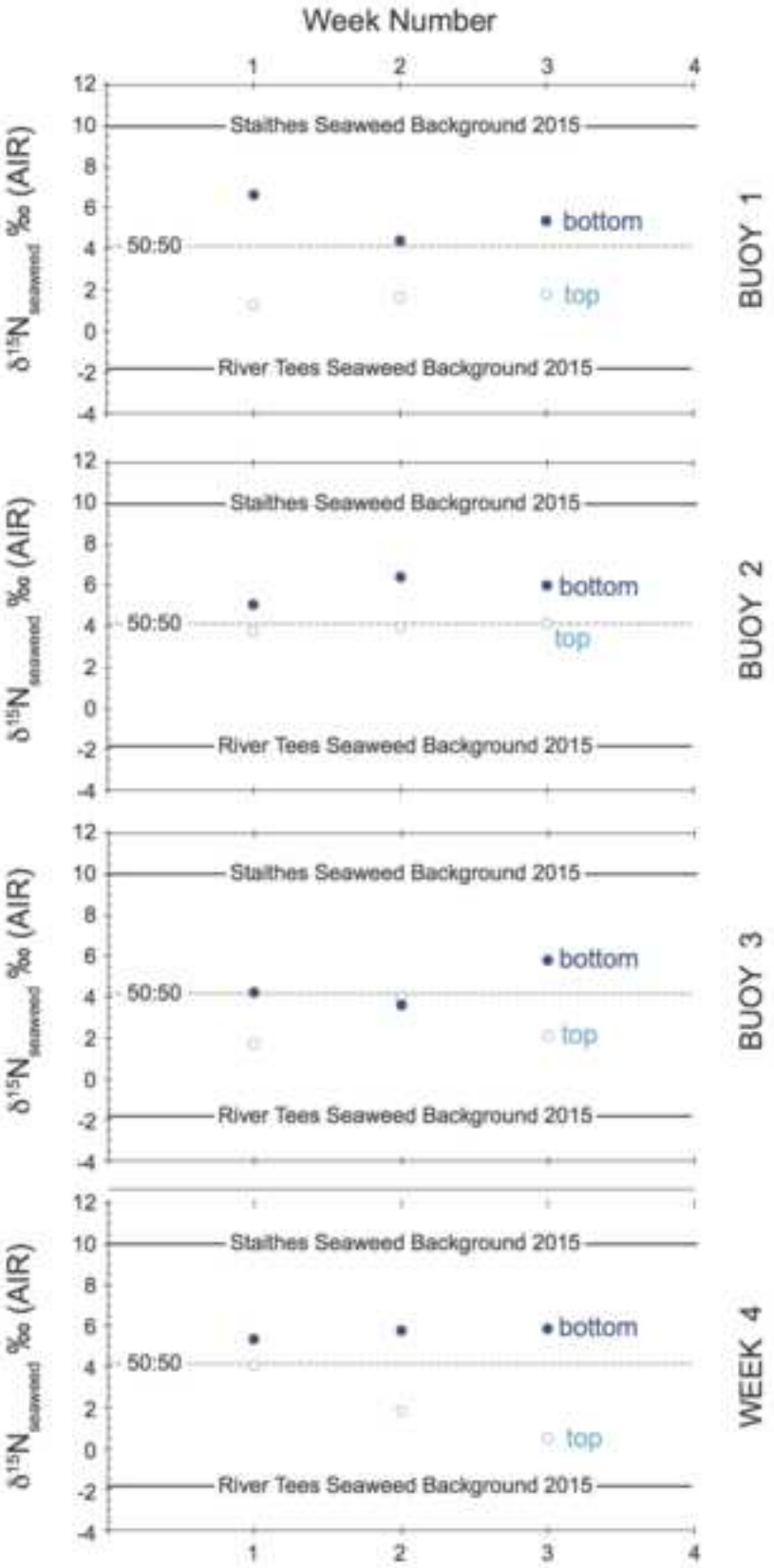

Table 1 $\delta^{15}N$ data from the *in vitro* nitrate lab experiment.

Sample IDs	$\delta^{15}N$ ‰	Sample IDs	$\delta^{15}N$ ‰
3 days		**1 week**	
0 µM		0 µM	
27-07-CONTROL-3-0MN	8.6	*2-1 WEEK 0 MMN*	8.4
27-07-CONTROL-2-0MN	8.7	*3-1 WEEK 0 MMN*	8.8
27-07-CONTROL-1-0MN	8.7	*1-1 WEEK 0 MMN*	8.9
Average (3 days)	8.7	Average (13 days)	8.7
Std dev (3 days)	0.0	Std dev (13 days)	0.2
-		-	
10 µM		10 µM	
27-07-3-10MN	8.7	*1-1 WEEK 10 MMN*	8.6
27-07-2-10MN	8.5	*2-1 WEEK 10 MMN*	8.5
27-07-1-10MN	8.7	*3-1 WEEK 10 MMN*	8.5
Average (3 days)	8.6	Average (13 days)	8.6
Std dev (3 days)	0.1	Std dev (13 days)	0.1
-		-	
50 µM		50 µM	
27-07-3-50MN	8.5	*1-1 WEEK 50 MMN*	8.1
27-07-2-50MN	8.2	*2-1 WEEK 50 MMN*	8.2
27-07-1-50MN	8.9	*3-1 WEEK 50 MMN*	8.0
Average (3 days)	8.5	Average (13 days)	8.1
Std dev (3 days)	0.3	Std dev (13 days)	0.1
-		-	
100 µM		100 µM	
27-07-3-100MN	8.5	*1-1 WEEK 100 MMN*	8.1
27-07-2-100MN	8.4	*2-1 WEEK 100 MMN*	7.5
27-07-1-100MN	8.5	*3-1 WEEK 100 MMN*	7.6
Average (3 days)	8.5	Average (13 days)	7.8
Std dev (3 days)	0.1	Std dev (13 days)	0.2
-		-	
500 µM		500 µM	
27-07-3-500MN	8.0	*1-1 WEEK 500 MMN*	6.3
27-07-2-500MN	7.6	*2-1 WEEK 500 MMN*	6.7
27-07-1-500MN	7.9	*3-1 WEEK 500 MMN*	6.5
Average (3 days)	7.8	Average (13 days)	6.5
Std dev (3 days)	0.1	Std dev (13 days)	0.2

Table 2 $\delta^{15}N$ data from the *in vitro* ammonia lab experiment.

Sample IDs	$\delta^{15}N$ ‰	Sample IDs	$\delta^{15}N$ ‰
3 days		**1 week**	
0 µM		0 µM	
3-0C3D	10.5	*1-0B13D*	10.3
2-0C3D	10.5	*2-0B13D*	10.5
1-0C3D	10.5	*3-0B13D*	11.4
Average (3 days)	10.5	Average (13 days)	10.7
Std dev (3 days)	0.0	Std dev (13 days)	0.5
-		-	
10 µM		10 µM	
3-10C3D	10.8	*1-10B13D*	10.5
2-10C3D	10.3	*2-10B13D*	10.0
1-10C3D	10.6	*3-10B13D*	10.9
Average (3 days)	10.6	Average (13 days)	10.5
Std dev (3 days)	0.2	Std dev (13 days)	0.4
-		-	
50 µM		50 µM	
3-50C3D	10.6	*1-50B13D*	9.6
2-50C3D	11.0	*2-50B13D*	10.9
1-50C3D	9.8	*3-50B13D*	9.9
Average (3 days)	10.5	Average (13 days)	10.1
Std dev (3 days)	0.5	Std dev (13 days)	0.6
-		-	
110 µM		110 µM	
3-100C3D	10.2	*1-100B13D*	9.7
2-100C3D	10.2	*2-100B13D*	9.3
1-100C3D	10.1	*3-100B13D*	10.1
Average (3 days)	10.2	Average (13 days)	9.7
Std dev (3 days)	0.0	Std dev (13 days)	0.3
-		-	
500 µM		500 µM	
3-500C3D	9.3	*1-500B13D*	7.3
2-500C3D	9.2	*2-500B13D*	7.0
1-500C3D	9.3	*3-500B13D*	6.1
Average (3 days)	9.3	Average (13 days)	6.8
Std dev (3 days)	0.1	Std dev (13 days)	0.5

Table 3 $\delta^{15}N$ data from Staithes *Fucus* collected between 27/05/2015 to 25/08/2015.

Sample IDs	$\delta^{15}N$ ‰
STAITHES-18-WHOLE	11.1
STAITHES-17-WHOLE	9.3
STAITHES-16-WHOLE	10.3
STAITHES-15-WHOLE	9.9
STAITHES-14-WHOLE	9.6
STAITHES-13-WHOLE	9.6
STAITHES-12-WHOLE	9.6
STAITHES-11-WHOLE	9.1
STAITHES-10-WHOLE	10.1
STAITHES-9-WHOLE	9.9
22-07-STAITHES-N-Fc	9.5
22-07-STAITHES-N-Fb	9.6
22-07-STAITHES-N-Fa	9.7
28-07-STAITHES	10.2
28-07-STAITHES	10.6
28-07-STAITHES	10.1
03.08A BACKST	10.5
03.08B BACKST	10.7
03.08C BACKST	10.5
11.08A BACKST	10.2
11.08B BACKST	10.1
11.08C BACKST	10.1
11.08D BACKST	10.6
17-08C STAITHES BACK	10.0
17-08A STAITHES BACK	10.1
25-08-BACK-ST-B	9.8
25-08-BACK-ST-A	10.4
Average Staithes ‘15	10.0
Std dev Staithes ‘15	0.5

Table 4 $\delta^{15}N$ data from River Tees *Fucus* collected between 27/05/2015 to 01/07/2015.

Sample IDs	$\delta^{15}N$ ‰	Sample IDs	$\delta^{15}N$ ‰	Sample IDs	$\delta^{15}N$ ‰
Tees seaweed blades		**Tees seaweed fertile tips**		**Tees seaweed non-fertile tips**	
01-07-S11-BLADES	-3.8	*01-07-S11-FERTILE*	-3.9	*01-07-S11-NONFERTILE*	-5.2
01-07-S12-BLADES	-5.3	*01-07-S12-FERTILE*	-4.7	*01-07-S12-NONFERTILE*	-4.2
01-07-S13-BLADES	-1.7	*01-07-S13-FERTILE*	-1.3	*01-07-S13-NONFERTILE*	-1.1
01-07-S15-BLADES	8.6	*01-07-S15-FERTILE*	-3.2	*01-07-S15-NONFERTILE*	10.8
01-07-S2-BLADES	3.8	*01-07-S2-FERTILE*	-5.8	*01-07-S2-NONFERTILE*	-6.3
01-07-S3-BLADES	-8.5	*01-07-S3-FERTILE*	-6.5	*01-07-S3-NONFERTILE*	-9.1
01-07-S5-BLADES	-5.0	*01-07-S5-FERTILE*	-4.4	*01-07-S5-NON-FERTILE*	-5.0
01-07-S6-BLADES	-6.2	*01-07-S6-FERTILE*	-4.9	*01-07-S6-NONFERTILE*	-5.4
01-07-S8-BLADES	-8.1	*01-07-S8-FERTILE*	-6.7	*01-07-S8-NONFERTILE*	-7.8
01-07-S9-BLADES	-2.7	*01-07-S9-FERTILE*	-7.4	*01-07-S9-NONFERTILE*	-2.6
04-06-S11-BLADES	-3.6	*04-06-S11-FERTILE*	-2.8	*04-06-S11-NONFERTILE*	-2.4
04-06-S12-BLADES	-8.1	*04-06-S12-FERTILE*	-5.9	*04-06-S12-NONFERTILE*	-5.5
04-06-S14-BLADES	-4.6	*04-06-S14-FERTILE*	-3.3	*04-06-S14-NONFERTILE*	-1.9
04-06-S15-BLADES	-1.1	*04-06-S15-FERTILE-OLD*	3.1	*04-06-S15-NONFERTILE*	3.2
04-06-S2-BLADES	-4.5	*04-06-S2-FERTILE*	-6.1	*04-06-S2-NONFERTILE*	-8.4
04-06-S3-BLADES	-7.5	*04-06-S3-FERTILE*	-4.8	*04-06-S3-NONFERTILE*	-7.5
04-06-S5-BLADES	-3	*04-06-S5-FERTILE*	-2.6	*04-06-S5-NONFERTILE*	-2.7
04-06-S6-BLADES	-6.4	*04-06-S6-FERTILE*	-5.3	*04-06-S6-NONFERTILE*	-4.4
04-06-S8-BLADES	-4.3	*04-06-S8-FERTILE*	-2.1	*04-06-S8-NONFERTILE*	-2.8
04-06-S9-BLADES	-5.8	*04-06-S9-FERTILE*	-5.9	*04-06-S9-NONFERTILE*	-3.9
27-05-S1-BLADES	2.5	*27-05-S1-FERTILE-OLD*	3.0	*27-05-S1-NON-FERTILE*	4.3
27-05-S10-BLADES	-0.8	*27-05-S1-FERTILE-YOUNG*	4.8	*27-05-S10-NONFERTILE*	0.6
27-05-S13-BLADES	-1.6	*27-05-S10-FERTILE-OLD*	2.4	*27-05-S13-NONFERTILE*	3.4
27-05-S14-BLADES	3.5	*27-05-S10-FERTILE-YOUNG*	-2.3	*27-05-S14-NONFERTILE*	3.9

27-05-S2-BLADES	3.8
27-05-S4-BLADES	0.6
27-05-S5-BLADES	-2.8
27-05-S7-BLADES	1.8
Average blades	-2.5
Std dev blades	4.2

ALL average	-1.7
ALL std dev	4.3

27-05-S13-FERTILE	1.5
27-05-S13-FERTILE-OLD	3.8
27-05-S14-FERTILE	2.4
27-05-S2-FERTILE-OLD	4.2
27-05-S2-FERTILE-YOUNG	4.1
27-05-S4-FERTILE-OLD	2.3
27-05-S5-FERTILE-OLD	-0.5
27-05-S5-FERTILE-YOUNG	-0.6
27-05-S7-FERTILE-OLD	3.7
27-05-S7-FERTILE-YOUNG	3.8
27-05-S8-FERTILE-YOUNG	3.1
27-05-S9-FERTILE-OLD	1.3
27-05-S9-FERTILE-YOUNG	1.7
Average fertile	-1.2
Std dev fertile	3.9

27-05-S2-NONFERTILE	4.5
27-05-S5-NONFERTILE	0.4
27-05-S7-NONFERTILE	4.0
27-05-S8-NONFERTILE	2.9
27-05-S9-NONFERTILE	2.3
Average fertile	-1.6
Std dev fertile	4.8

Table 5 Average $\delta^{15}N$ data from River Tees Experiment 2 (short-term).

	Week 1		Week 2		Week 3		Week 4	
Position	top	bottom	top	bottom	top	bottom	top	bottom
Buoy 1	1.3	3.7	4.6	6.3	3.3	4.3	6.1	5.9
Buoy 2	2.8	3.8	3.8	4.9	2.2	4.7	3.1	6.6
Buoy 3	3.1	5.4	1.8	4.2	3.2	4.3	2.6	4.9
Buoy 4	4.9	4.3	4.1	5.2	4	4.4	2.7	5.1

Table 6 Average $\delta^{15}N$ data from River Tees Experiment 1 (long-term).

	Buoy 1		Buoy 2		Buoy 3		Buoy 4	
Position	top	bottom	top	bottom	top	bottom	top	bottom
Week 1	1.1	6.3	3.8	4.9	1.7	4.2	4.1	5.1
Week 2	1.5	4.5	4	6.1	4	3.6	1.9	5.6
Week 3	1.7	5.3	4.1	6.0	2.2	5.8	0.4	5.7